Validation of HDAC6 and SIRT2 Tubulin Deacetylases as therapeutic targets for Huntington's Disease.

Bobrowska, Anna

Awarding institution:
King's College London

Title: Validation of HDAC6 and SIRT2 Tubulin Deacetylases as therapeutic targets for Huntington's Disease.

Author: Anna Bobrowska

VALIDATION OF HDAC6 AND SIRT2 TUBULIN DEACETYLASES AS THERAPEUTIC TARGETS FOR HUNTINGTON'S DISEASE

By

Anna Bobrowska

Neurogenetics Laboratory

Department of Medical and Molecular Genetics

Division of Genetics and Molecular Medicine

Guy's, King's and St. Thomas' School of Medicine

Guy's Campus, London

A dissertation presented in partial fulfilment for the degree of doctor of philosophy at King's College London, University of London

January 2012

Declaration

I declare that I, Anna Bobrowska, performed all of the experimental work presented in this thesis with the exception of:

Time resolved – Förster resonance energy transfer (TR-FRET) and Mezoscale Discovery (MSD) which were performed by Dr. Andreas Weiss (Neuroscience Discovery, Novartis Institute for Biomedical Research) and are presented in Figure 4.11 and Figure 4.12.

Mouse dosing with CHDI00194500-000-0005, which was performed by Mrs. Hayley Lazell, and subsequent tissue collection which was performed by Miss Agnesska Benjamin, Miss Marie Bondulich, Miss Sophie Franklin and Mrs. Hayley Lazell.

Analysis of CHDI00194500-000-0005 brain penetrance which was performed by BioFocus and is presented in Figure 4.17, and by Pharmidex and is presented in Appendix 2.

Analysis of CHDI00194500-000-0005 SIRT1/SIRT2 IC_{50} properties which was performed by Cerep and is presented in Appendix 2

Abstract

Since the identification of a widespread transcriptional dysregulation that occurs in Huntington's disease (HD), histone deacetylase (HDAC) inhibition has been explored as a possible therapeutic strategy for this devastating disease. Studies using broad-range acting HDAC inhibitors have shown great promise in HD mouse models. Concomitantly, effects of inhibition of individual HDACs have been investigated, however, these experiments have been most frequently performed in worm, fly, and cell and less so in mouse models of HD. Previous reports have demonstrated disease modifying potential for both HDAC6 and SIRT2, which are the only tubulin deacetylases known in mammals. Nevertheless, the therapeutic value of these enzymes has not yet been explored in a complex mammalian system. This work addressed the question of what is the effect of genetically depleting either HDAC6 or SIRT2 in the R6/2 mouse model of HD on disease progression. After thorough characterisation of both *Hdac6*KO and *Sirt2*KO mice and expression of either mutation in the R6/2 mouse, a battery of physiological, behavioural and molecular readouts has clearly demonstrated that previous studies performed in invertebrate or cell culture systems do not translate to the mouse and that, therefore, HDAC6 and SIRT2 inhibition would not be of therapeutic value and should not be prioritised as a therapeutic strategy in HD.

Acknowledgements

First and foremost I would like to thank my supervisor Professor Gillian Bates. Thank you for providing me with the opportunity to pursue this PhD project in your laboratory and all the support and motivation you have given me during the course of this project.

I would like to thank my mother, Iwona Stawicka-Bobrowska, for giving me all her loving support, having faith in me and for always being there when I needed her. Mamo, dziękuję Ci, jesteś najwspanialsza i kocham Cię!

Thank you to my family: Tomasz Bobrowski, Ola Bobrowska, Babcia Lusia Bobrowska, Babcia Ania Zasławska and Grzegorz Murawski. You are amazing and truly great at helping me take a step back, relax and recharge.

Thank you to John Labbadia for all the help and support. I cannot thank you enough for believing in me when I didn't and motivating me when I was down. You are wonderful, I couldn't have done it without you.

Thank you to Maja Uherek, Gosia Skorek, Kamila Kościerzyńska and Asia Jassem. You are the best, most amazing friends I could have and I am grateful for all your support.

Thank you to the members of neurogenetics laboratory who have helped me develop both as a scientist and as a person, in particular to John Labbadia, Christian Landles, Michal Mielcarek and Lara Moumne.

Thank you to Dr. Paolo Paganetti for allowing me to perform TR-FRET experiments in his laboratory and to Barbara Baldo for making my time at Novartis a great experience.

Thank you to John Labbadia and Christian Landles for help in proof-reading of this thesis.

I would also like to express my gratitude to the European Commission and CHDI Foundation for providing the financial support without which this work could not have been undertaken.

Table of contents

List of Figures

List of tables

List of abbreviations

Ac	acetylated
ActB	β-actin
ADP	adenosine diphosphate
AgRP	agouti related peptide
AMPK	adenosine monophosphate activated protein kinase
ANOVA	analysis of variance
ATP	adenosine triphosphate
Atp5b	ATP synthase subunit beta
BAC	bacterial artificial chromosome
BCA	bicinchocinic acid
BDNF	brain derived neurotrophic factor
BLAST	basic local aligmnment search tool
BSA	bovine serum albumin
C	carboxy-
C.elegans	Caenorhabditis elegans
cAMP	cyclic adenosine monophosphate
Canx	calnexin
CB	cannabinoid
CBF	CBAxC57BL/6 F1
CBP	CREB binding protein
Cd	Caudate
CDK	cyclin dependent kinase
CHDI194500	CHDI 00194500-0000-005
CNS	central nervous system
CoA	coenzyme A
Co-REST	co-repressor of REST
CREB	cAMP responsive element binding protein
CtBP	C-terminal binding protein
D.melanogaster	Drosophila melanogaster

Dble	Double mutant *Hdac6*KOxR6/2 mice
DD	deacetylase domain
Dd	double deionised
Dhcr7	dehyrocholesterol reductase 7
DNA	deoxyribonucleic acid
ECL	enhanced chemi-luminescence
EF3	elongation factor 3
EGF	epithelial growth factor
ELISA	enzyme linked immunosorbent assay
ER	endoplasmic reticulum
Fdft1	farnesyl diphosphate farnesyl transferase 1
Fdps	farnesyl diphosphate synthase
GABA	γ-aminobutyric acid
Gapdh	Glyceraldehyde phosphate dehydrogenase
GR	glucocorticoid receptor
h	human
HAP1	huntingtin associated protein 1
HAT	histone acetyltransferase
HD	Huntington's disease
HDAC	histone deacetylase
Hdh	Huntington's disease homologue
HEAT	HTT, EF3, PP2a, TOR1
HEPES	4-(2-hydroxyethyl)-1-piperazineethanesulphonic acid
HET	heterozygous
HIV	human immunodeficiency virus
HMGCoA	4-hydroxy-4-methyl-glutaryl Coenzyme A
Hmgcr	HMGCoA reductase
Hmgcs1	HMGCoA synthase 1
HMGI(Y)	high mobility group protein I(Y)
HPRT	hypoxanthine ribosyltransferase
HRP	horseradish peroxidase

HSF1	heat shock transcription factor 1
HSP90	heat shock protein 90
HSR	heat shock response
HTT	huntingtin
Idi1	isopentenyl diphsphate delta isomerase1
K	lysine
kDa	kilo Dalton
KO	knock-out
LB	Luria-Bethani
LC	liquid chromatography
m	mouse
MEF	myocyte enhancer factor
mGluR	metabotropic glutamate receptor
mHTT	mutant huntingtin
mRNA	messenger RNA
MS	mass spectrometry
MSD	Mezoscale Discovery
MSN	medium sized spiny neurons
N	amino-
NaB	sodium buyrate
NAD	nicotinamide adenine dinucleotide
NAM	nicotinamide
NCoR	nuclear receptor co-repressor
NES	nuclear exclusion signal
NLS	nuclear localisation signal
NMDA	N-methyl-D-aspartate
NMDAR	NMDA receptor
NPY	neuropeptide Y
NRSF	neuronal restrictive silencing factor
NuRD	nuclear remodelling deacetylase
PBS	phosphate buffered saline

PCR	polymerase chain reaction
PD	Parkinson's disease
PEPCK1	phosphoenolpyruvate carboxykinase 1
PGC1α	PPARγ co-activator 1α
PIPES	1,4-piperazinediethanesulphonic acid
polyQ	polyglutamine
POMC	proopiomelanocortin
PP2A	protein phosphatase 2A
PPARγ	peroxisome proliferator activated receptor γ
PSD95	post-synaptic density 95
PTM	post-translational modification
Put	putamen
Q	glutamine
qPCR	quantitative PCR
REST	repressor element 1 silencing transcription factor
RIPA	radioimmunoprecipitation assay
RNA	ribonucleic acid
ROS	reactive oxygen species
Rpl13a	ribosomal protein 13a
rpm	revolutions per minute
rRNA	ribosmal RNA
RT	real time
S	serine
SAHA	suberoylanilide hydroxamic acid
SD	standard deviation
SDS-PAGE	SDS polyacrylamide gel electrophoresis
SE14	serine-glutamate tetradecapeptide
SEM	standard error of the mean
SMRT	silencing ediator for retinoic acid and thyroid hormone receptors
Sp1	specificity protein 1
Sqle	squalene epoxidase

SREBP	sterol regulatory element binding protein
T	threonine
TBP	TATA box binding protein
TBS	Tris buffered saline
TE	Tris-EDTA
TOR1	target of rapamycin 1
TR-FRET	time resolved Förster resonance energy transfer
TSA	Trichostatin A
Ubc	ubiquitin C
UPS	ubiquitin proteasome system
v	volume
VCP	valosin containing protein
Vt	ventricle
w	weight
wk	week
WT	wild type
YAC	yeast artificial chromosome
ZnF-Ub	zinc finger ubiquitin binding

1.0. INTRODUCTION

1.1. Huntington's Disease

Huntington's Disease (HD) is a devastating, autosomal dominant, neurodegenerative disorder. In North America and Western Europe approximately 5-10 people in 100,000 are affected (Warby et al., 2011). The mean age of HD onset is between 35 and 50 years, however, juvenile HD cases where symptoms develop before the age of 20 are also known to occur (Walker, 2007). HD symptoms progress for 15-20 years before death, though juvenile HD patients usually have a more rapid disease progression that is characterised by bradykinesia rather than the typical chorea observed in adult onset HD (Bates et al., 2002; Walker, 2007). Other commonly observed HD symptoms include rapid weight loss, dementia, depression, and cognitive impairment in reasoning, judgement and memory (Novak and Tabrizi, 2010). Therapeutics available to HD patients are directed against primary symptoms like chorea or depression, however, those approaches do not modify disease progression and as such, have limited benefits (Novak and Tabrizi, 2010).

1.1.1. Pathogenesis

At the molecular level HD is caused by the expansion of a CAG tri-nucleotide repeat within exon 1 of the huntingtin gene (*HTT*) (The Huntington's Disease Collaborative Research Group, 1993). Normally, the number of CAG repeats ranges from 6 to 35, however, people who carry 36-39 repeats are at risk of developing HD (Novak and Tabrizi, 2010). Individuals that carry over 39 repeats will develop HD while those with over 60 repeats will most likely develop juvenile HD (Bates et al., 2002). An inverse correlation explaining 40-50% variance exists between the age of onset and CAG repeat length, however, other genetic and environmental factors that influence disease age of onset are currently under investigation (Andrew et al., 1993; Walker, 2007).

HD is primarily a disease of the central nervous system (CNS) as evidenced by the fact that HD patients lose as much as 40% of brain volume compared to non-HD individuals (Bates et al., 2002; Vonsattel et al., 1985). Perhaps the most striking change that takes place in HD is the progressive atrophy of the cerebral cortex and the basal ganglia (Fig. 1.1) (Novak and Tabrizi, 2010; Rosas et al., 2003; Vonsattel et al., 1985). In particular, the caudate nucleus and putamen show dramatic morphological changes, though other regions such as the globulus pallidus, subthalamic nucleus, thalamus, hypothalamus, substantia nigra, white matter and cerebellum are also affected (Politis et al., 2008; Vonsattel and DiFiglia, 1998). It has been reported that atrophy occurs before symptom onset suggesting that the CNS is able to cope with some degree of neuronal damage before any behavioural changes manifest (Rosas et al., 2005).

Outside the CNS, two hallmarks of HD are progressive weight loss and skeletal muscle wasting (Farrer and Meaney, 1985; Sanberg et al., 1981). Impaired glucose tolerance and insulin secretion capacity have also been observed in patients, as well as reduced levels of testosterone, reduced numbers of germ cells and abnormal seminiferous tubule morphology in men (Bacos et al., 2008; Lalic et al., 2008; Markianos et al., 2005; Van Raamsdonk et al., 2007). About 30% of HD patients suffer from cardiac failure compared with 2% in age matched unaffected individuals making it the leading cause of death in HD (Lanska et al., 1988). Though the mechanisms of how these peripheral symptoms arise have not yet been elucidated, there is reason to believe they are not a secondary effect of brain pathology (Saleh et al., 2009).

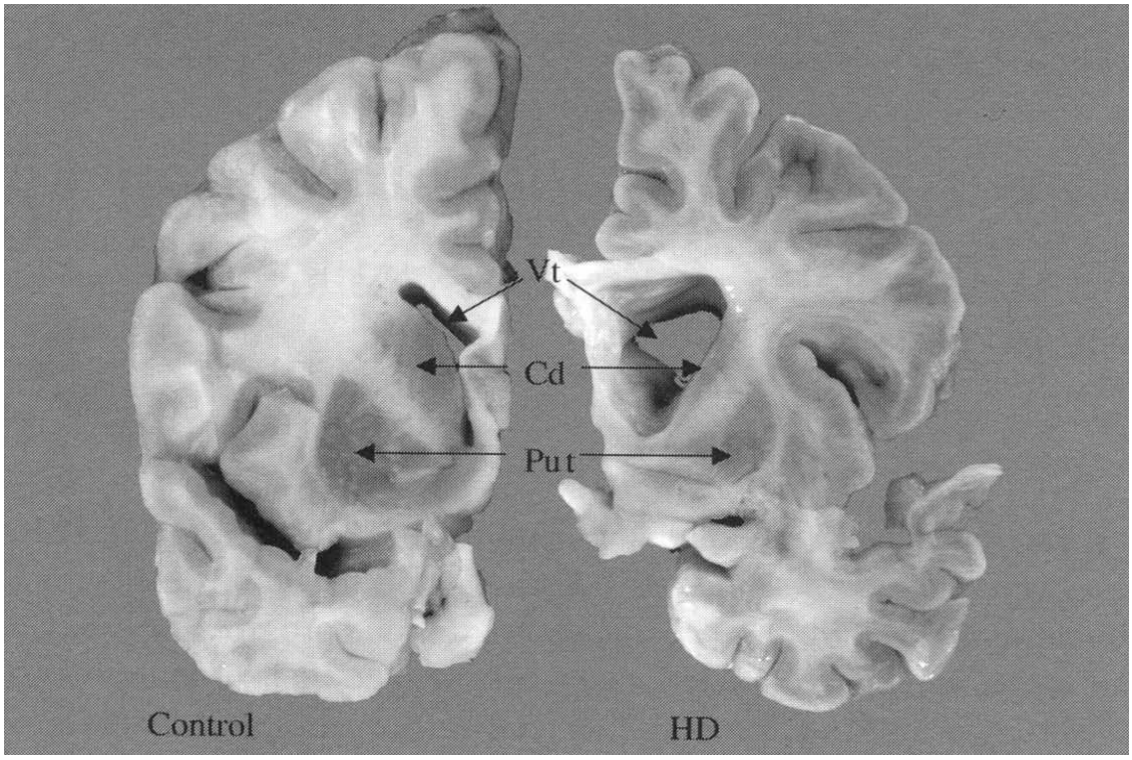

Figure 1.1. Brain atrophy in HD patients.

Comparison of coronal sections of brains from an end stage disease HD and unaffected individual. Note the pronounced atrophy of the cortex, caudate (Cd), and putamen (Put), enlargement of ventricles (Vt) and white matter loss. Reproduced from (Bates et al., 2002), with permission of Oxford University Press.

1.1.2. Huntingtin

The *Huntingtin* gene spans approximately 170 kb, contains 67 exons, and is translated into a 348 kDa protein. The CAG stretch located in exon 1 is translated into a polyglutamine (polyQ) tract starting at the 18th amino acid and is followed by a polyproline stretch that possibly stabilizes the PolyQ tract and maintains its solubility (Steffan et al., 2004). Although huntingtin (HTT) has no sequence homology to any other protein, it does possess four clusters of functional domains called HEAT repeats (from Huntingtin, Elongation factor 3 (EF3), the regulatory A subunit of protein phosphatase 2A (PP2A) and Target of rapamycin 1 (TOR1)) that are involved in protein-protein interactions (Fig. 1.2) (Andrade and Bork, 1995).

1.1.2.1. Post-translational modifications of Huntingtin

It comes as no surprise that a protein as big as HTT contains multiple post-translational modification (PTM) sites, which affect localisation, longevity or toxicity of HTT (Fig. 1.2). For example, there are three lysine (K) residues at the amino(N)-terminus (K6, K9 and K15) that can be either ubiquitinated (promoting HTT degradation) or sumoylated (resulting in HTT nuclear localisation) (Steffan et al., 2004). Phosphorylation of HTT occurs at one threonine (T3) and several serine (S13, S16, S421, S434, S536, S1181, S1201, S2076, S2653 and S2657) residues and its outcome can have variable effects depending on the residue in question, ranging from protection from proteolytic cleavage (S421, S434, S536) (Luo et al., 2005; Schilling et al., 2006; Warby et al., 2009) through proteasomal targeting (S13 and S16)(Thompson et al., 2009) to modulation of vesicle transport (S421) (Zala et al., 2008). Acetylation sites have been identified at K9, K178, K236, K345 and K444 (Cong et al., 2011), and it has been demonstrated that acetylation at K444 promotes targeting of HTT for degradation by autophagy (Jeong et al., 2009). HTT is also palmitoylated at cysteine 214 which is in line with its proposed role in vesicle trafficking (Yanai et al., 2006). Additionally, HTT can be cleaved by calpains, cathepsins, and caspases -2, -3, and -6 and possibly by other proteases such as MMP-10; generating a panel of shorter HTT fragments (Miller et al., 2010). When generated, these fragments can be more toxic than the full length mHTT protein (Graham et al., 2006; Lunkes et al., 2002). As occurrence of these modifications varies between mutant and wild type forms of HTT, strategies that block or enhance their generation are currently under investigation as possible therapeutics for HD.

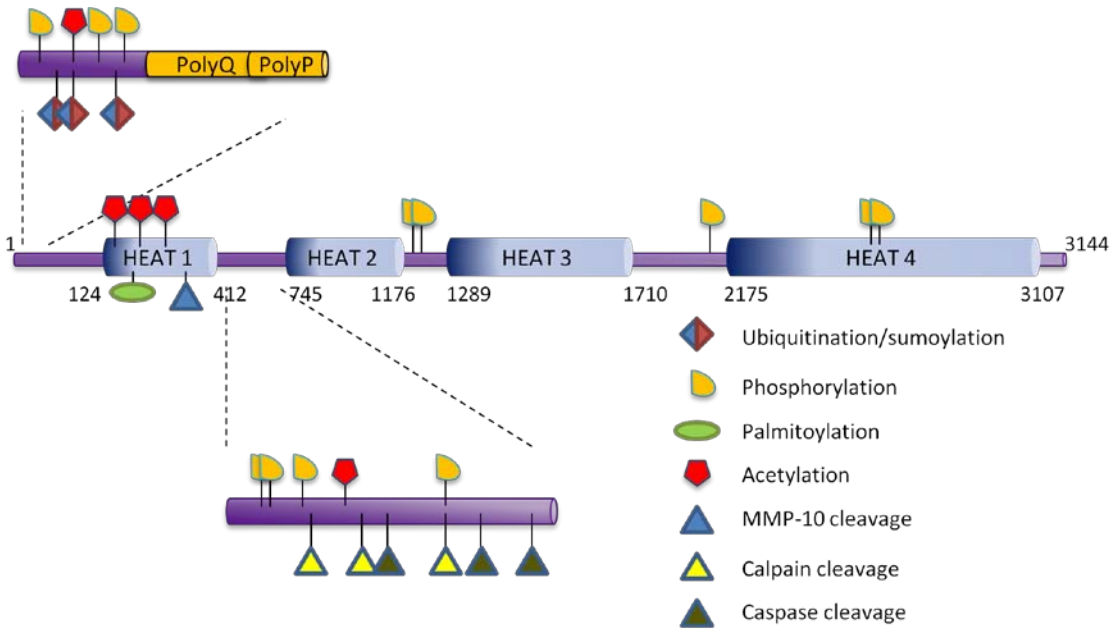

Figure 1.2. Huntingtin post translational modifications.

Huntingtin can become phosphorylated, ubiquitinated, sumoylated, acetylated and palmitoylated, as well as cleaved by proteases. The effect of these modifications on mHTT toxicity and disease pathology is currently being investigated. Modified from (Ehrnhoefer et al., 2011) with permission of SAGE Publications.

1.1.2.2. Huntingtin expression and function

Expression of HTT is ubiquitous in both humans and rodents, though its levels are highest in neurons of the CNS (Li et al., 1993). Inside the cell, HTT can be found in the cytoplasm, often associated with microtubules, the Golgi, the endoplasmic reticulum (ER), and mitochondria (Bhide et al., 1996; Hilditch-Maguire et al., 2000; Panov et al., 2002). HTT can also be found on the membranes of both synaptic and clathrin coated vesicles of the endocytic or secretory pathways (Velier et al., 1998). Although controversial, HTT has also been reported to localise to some neuronal nuclei and nuclear membranes (Hoogeveen et al., 1993; Kegel et al., 2002).

While the exact function of the HTT protein is not clear, it is known that HTT is essential for embryonic development and neurogenesis, as demonstrated by knock-out and knock-down of the *Hdh* (Huntington's Disease Homologue) gene in mice (Duyao et al., 1995; Nasir et al., 1995; White et al., 1997; Zeitlin et al., 1995). In

addition, HTT is anti-apoptotic and protects neurons against excitotoxicity and ischemic injury in adult mouse brains (Leavitt et al., 2006; Rigamonti et al., 2000; Zhang et al., 2003). Furthermore, HTT has been shown to play an important role in regulating neuronal function (Dragatsis et al., 2000). This is achieved by regulating the transcription of neuronal genes via cytoplasmic sequestration of REST/NRSF (Repressor Element 1 Silencing Transcription Factor/Neuronal Restrictive Silencing Factor), and by controlling synaptic transmission and vesicular transport along axons (Gauthier et al., 2004; Zuccato et al., 2003).

Although there are indications that loss of function of wild type HTT contributes to disease progression our current understanding indicates that the pathology observed in HD is a result of a toxic gain of function by mHTT. In order to understand the mechanisms behind HD pathology, numerous models of HD have been created.

1.1.3. HD models

Since the identification of the HD causing mutation, numerous models have been created to study the disease. Though worm, fly and cell culture models are helpful in studying the most basic mechanisms of HD pathogenesis or for screening potential therapeutic compounds, their similarity to the human disease is limited. Placing the mutation in the context of a mammalian organism is essential for proper investigation of the complex disease mechanisms and validation of therapeutic strategies. As such, HD is most commonly modelled in mice, though rat, pig, sheep and monkey models are also used (Crook and Housman, 2011; Jacobsen et al., 2010; von Horsten et al., 2003; Yang et al., 2010; Yang et al., 2008).

1.1.3.1. Mouse models of HD

Mouse models of HD can loosely be divided into 3 categories: transgenic fragment models, transgenic full length models and genetically precise – "knock-in" models. The most commonly used representatives of each group are summarised in Table 1.1.

1.1.3.2. Transgenic fragment models

The first generated and most commonly used mouse model of HD is the R6/2 mouse (Mangiarini et al., 1996). R6/2 mice express a single copy of the first exon of *HTT* under the control of the human HTT promoter that generates a HTT transprotein with 150 – 200 polyQ repeats. These mice develop behavioural abnormalities such as rotarod and grip strength impairments, hypo-activity and deficiencies in learning and memory tasks by 8 weeks of age (Carter et al., 1999; Lione et al., 1999). A concomitant loss of body and brain weight, as well as atrophy of the skeletal muscle and testis is also evident (Mangiarini et al., 1996). R6/2 mice also develop cytoplasmic aggregates and nuclear inclusions in the brain and periphery before symptom onset (Davies et al., 1997; Sathasivam et al., 1999). Although disease progression is very quick and R6/2 mice do not survive for longer than 15 weeks (at King's College London colony), motor impairment and weight loss as well as muscle atrophy and changes to the hypothalamic-endocrine system suggest that the sequence of pathogenic events in these mice is very similar to that seen in humans (Bjorkqvist et al., 2005; Sanberg et al., 1981; Sathasivam et al., 1999).

In addition to R6/2, another commonly used transgenic fragment model is the N171 mouse, which expresses the first 171 amino acids of HTT with 82Q under the control of the mouse prion promoter (Schilling et al., 1999). These mice develop similar behavioural and physiological abnormalities to R6/2, although onset and disease progression is less aggressive than in R6/2 mice. Weight loss begins around 2-3 months of age, rotarod impairment is evident from 4 months onwards and

disease end point occurs at 6 months of age (Schilling et al., 1999). Cytoplasmic and nuclear inclusions are also formed in N171 mice, however, their distribution between brain regions differs from that observed in HD patients and R6/2 mice (Schilling et al., 1999). This may be due to the fact that HTT transprotein expression in N171 mice is under the control of the prion promoter.

1.1.3.3. Transgenic full length models

The two most commonly used full length HD mouse models are the YAC (Yeast Artificial Chromosome) and BAC (Bacterial Artificial Chromosome) HD mice. Both express full length human HTT under the control of its own promoter. YAC mice are available with a polyQ length of 18, 46, 72 and 128 (Hodgson et al., 1999; Slow et al., 2003), and BACHD mice carry 97Q (Gray et al., 2008). In contrast to fragment models, transgenic full length HD mice display a slower disease progression with a normal life span and even exhibit an increase in body weight (Gray et al., 2008; Van Raamsdonk et al., 2005b). However, both YAC128 and BACHD mice develop motor impairment, activity abnormalities and cognitive deficiencies (Gray et al., 2008; Van Raamsdonk et al., 2005b). Equally, both models also suffer from a decrease in brain weight, and cortical and striatal degeneration are evident at 12 months of age (Gray et al., 2008; Slow et al., 2003; Van Raamsdonk et al., 2005a).

Perhaps the greatest difference between fragment and full length transgenic models is in the formation of mHTT aggregates. Large mHTT inclusions are only detected in BAC and YAC mice at 12 months of age, after the appearance of motor symptoms (Gray et al., 2008; Hodgson et al., 1999; Wang et al., 2008a). Equally, large intranuclear and cytoplasmic inclusions are less abundant and a diffuse HTT specific signal and "micro-aggregates" are more commonly found in brain tissue of these full length transgenic mice (Gray et al., 2008; Hodgson et al., 1999; Slow et al., 2003). While full length transgenic mice are useful for studying the mechanisms of HD progression in the context of full length mHTT, they are still not genetically precise and can therefore be limiting in modelling HD.

Table 1.1. Summary of most commonly used HD mouse models.

Model	Genetic basis	Promoter	Repeat length
R6/2	Human *HTT* exon 1	Human *HTT*	200*
N171	Human *HTT* exons 1, 2 and part of 3 (first 171 amino acids)	Prion promoter	82
BACHD	Human *HTT*	Human *HTT*	97
YAC72	Human *HTT*	Human *HTT*	72
YAC128	Human *HTT*	Human *HTT*	128
*Hdh*Q111	Mouse *HTT* homologue (*Hdh*); chimeric human/mouse exon 1	Mouse *HTT* homologue (*Hdh*)	111
CAG140	Mouse *HTT* homologue (*Hdh*); chimeric human/mouse exon 1	Mouse *HTT* homologue (*Hdh*)	140
*Hdh*Q150	Mouse *HTT* homologue (*Hdh*)	Mouse *HTT* homologue (*Hdh*)	150

*Average repeat length of R6/2 mice at the King's College London colony

1.1.3.4. "Knock in" HD mice

The most genetically precise HD models are the “knock in” mice, where the endogenous mouse HD gene (*Hdh)* has been modified to contain an expanded CAG repeat number. Most commonly used are the *Hdh*^{Q111}, CAG140 and *Hdh*Q150 mice, which carry 111, 140 and 150 CAG repeats respectively (Lin et al., 2001; Menalled et al., 2003; Wheeler et al., 1999). Similarly to transgenic full length mice, knock-in mice exhibit slow disease progression. However, certain behaviours such as activity and rearing can be altered as early as 1 month of age in the CAG140 mice, though these mice do not display any overt symptoms such as weight loss, tremor or clasping by 1 year of age (Menalled et al., 2003). *Hdh*Q150 mice do not display physiological abnormalities until 12 months of age with rotarod impairment only becoming pronounced by 18 months of age (Woodman et al., 2007). Nevertheless, these mice form cytoplasmic and nuclear aggregates by 6 months of age and by 21-22 months their pattern of aggregation in both the CNS and peripheral tissues is extremely similar to that of R6/2 mice at 12 weeks of age (Moffitt et al., 2009). At the same time, there are numerous molecular abnormalities that correlate well between HdhQ150, R6/2 and HD patients; an observation which suggests a possible common pathogenic mechanism (Hodges et al., 2006; Kuhn et al., 2007; Labbadia et al., 2011; Landles et al., 2010; Sathasivam et al., 2010). Aggregation is also a feature of disease in the *Hdh*^{Q111} and CAG140 mice, where diffuse nuclear staining can be observed by 1-2 months of age, and nuclear inclusions appear by 6 (CAG140) and 10 months of age (HdhQ111) (Menalled et al., 2003; Wheeler et al., 2000).

The validity and usefulness of HD models has been debated in the context of genetic precision, similarity of symptoms between models and patients, and molecular pathology (Fig 1.3). The rapid disease progression of R6/2 mice allows for efficient compound screening, but the full length or knock in models, with longer “pre-manifest” stage could be more useful for elucidation of subtle molecular changes that occur before symptom onset in an adult organism. Also, some molecular events and their role in HD pathology such as proteolytic cleavage cannot be examined without the context of the full length mutant protein. On the other hand, if toxicity is caused by N-terminal fragments, there is no reason why fragment

models should not be used to study the sequence of pathological events and applicability of therapeutic strategies downstream of HTT cleavage.

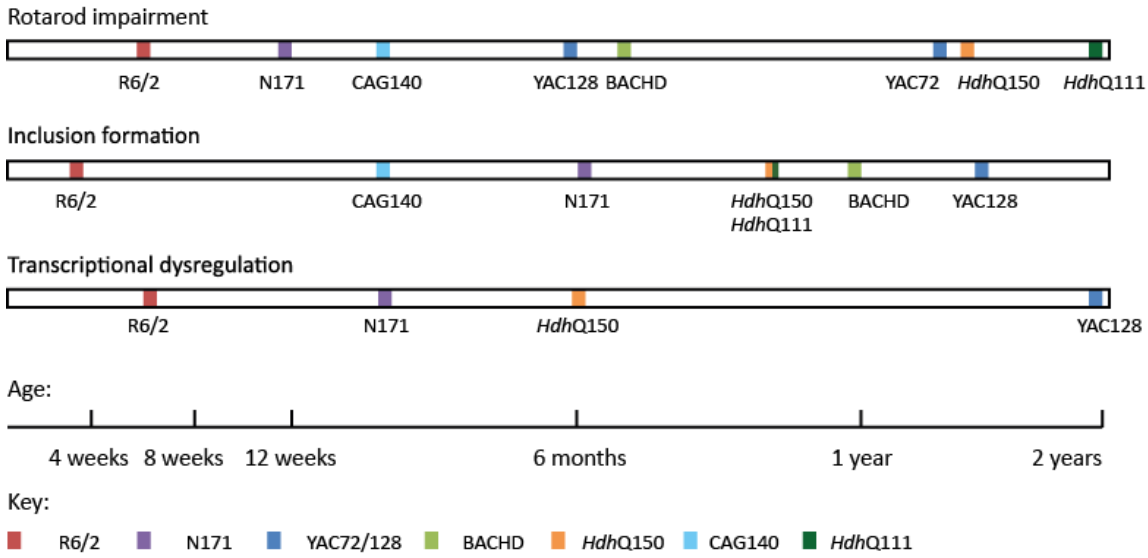

Figure 1.3. Timeline of pathological events in mouse models of HD.

Transgenic fragment (R6/2 and N171) models develop motor dysfunction and molecular pathologies earlier than transgenic full length (BACHD, YAC72 and YAC128) and "knock-in" (*Hdh*Q111, CAG140 and *Hdh*Q150) mice. Modified from (Crook and Housman, 2011) with permission of Elsevier.

1.1.4. Molecular pathogenesis of HD

The events and mechanisms that lead to HD pathology and symptoms have mostly been attributed to a toxic gain of function conferred to mHTT by the expanded polyQ tract. However, several lines of research have also pointed to a contributory effect of a loss of function of HTT through the presence of the HD mutation. The toxic gain of function scenario is supported by the fact that similar symptoms and molecular abnormalities are also displayed by patients and models of other polyQ expansion disorders which are summarized in table 1.2. Although the polyQ expansion occurs in functionally and structurally different proteins, these diseases share common symptomatic and molecular features as well as an inverse correlation between increased polyQ length and disease onset (Williams and Paulson, 2008). Equally, all of the polyQ expanded proteins have a strong propensity for aggregation. Additional evidence comes from a study where a CAG expansion was ectopically inserted into the *Hprt* (hypoxanthine phosphoribosyltransferase) gene. Mice expressing the HPRT protein with an expanded polyQ tract develop a neurological phenotype and neuronal intranuclear inclusions similar to those observed in the nine known polyQ diseases (Ordway et al., 1997). Finally, the severity of symptoms is similar between patients homozygous and heterozygous for the HD mutation (Wexler et al., 1987). At the moment the consensus is that the toxic gain of function in HTT is central to disease pathogenesis, and loss of function of normal HTT has a contributory, rather than causative, toxic effect.

Huntingtin is a protein of many functions with many interacting partners. The expanded polyQ stretch seems to confer additional properties on this already versatile protein. With this in mind it is not surprising that almost every pathway, cycle, cascade or mechanism investigated in HD seems to be affected by the presence of mHTT. The difficulty in elucidating the pathogenic mechanism is disentangling the cause from the effect. However, the main areas in which mHTT appears to play a pivotal role in disease onset and progression include aggregate formation, protein homeostasis, transcriptional dysregulation, neuronal function, and energy homeostasis (Fig. 1.4).

Table 1.2. Summary of polyQ expansion diseases.

Disease	Protein	Size (kDa)	Putative function	Mutation repeat length
HD	Huntingtin	348	Signaling, scaffold, transport, transcription	>39
SBMA	Androgen receptor	99	Steroid hormone receptor	>40
DRPLA	Atrophin-1	125	Transcription	>49
SCA1	Ataxin-1	87	Transcription	>40
SCA2	Ataxin-2	140	RNA metabolism	>32
SCA3	Ataxin-3	42	De-ubiquitination	>52
SCA6	α1A voltage dependent Ca^{2+} channel subunit	282	Ca^{2+} signalling	>20
SCA7	Ataxin-7	95	Transcription	>37
SCA17	TBP	38	Transcription	>47

SBMA – spinal and bulbar muscular atrophy; DRPLA – dentatorubral-pallidoluysian atrophy; SCA – spinocerebellar ataxia, TBP – TATA binding protein

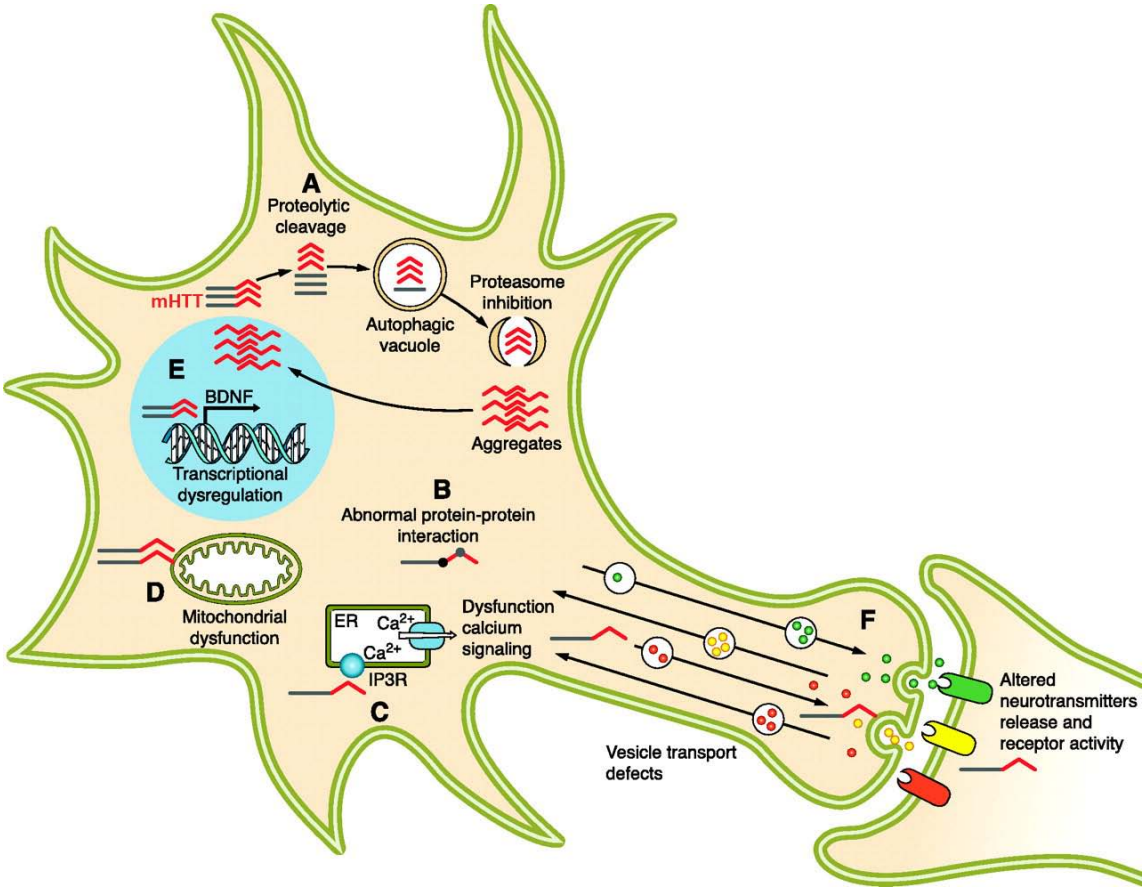

Figure 1.4. Depiction of main events contributing to HD pathogenesis.

Mutant HTT (mHTT) is proteolytically cleaved in the cytoplasm (A). Chaperones attempt to re-fold or target mHTT for proteasomal or autophagic degradation, however, the system is inefficient and mHTT aggregates in the cytoplasm and nucleus. (B) PolyQ expansion enables mHTT and N-terminal fragments to abnormally interact with proteins and organelle membranes, causing defects in Ca^{2+} signalling (C) and mitochondrial dysfunction (D). (E) N-terminal mHTT fragments translocate to the nucleus where they impair transcription and form intranuclear inclusions. (F) mHTT also causes defects in vesicle transport, recycling and neuronal signalling. Reproduced from (Zuccato et al., 2010) with permission of American Physiological Society.

1.1.4.1. Aggregate formation in HD

The presence of mHTT aggregates has been well documented in patients and animal models of HD (Davies et al., 1997; DiFiglia et al., 1997; Gutekunst et al., 1999). The intracellular localisation of aggregates is dependent on the length of the mHTT fragment that is present (Lunkes et al., 2002). The fact that full length mHTT has not been detected in aggregates suggests that cytoplasmic, neuropil, and intranuclear inclusions are formed by shorter N-terminal fragments of mHTT that most likely arise from proteolysis of the full length protein (DiFiglia et al., 1997; Martindale et al., 1998).

Electron microscopy and atomic force microscopy have demonstrated that mHTT forms a spectrum of oligomeric annular, spherical, amorphous, and fibrillar species *in vitro* and *in vivo* in HD mice and HD patients' post mortem brain samples (Fig. 1.5) (Legleiter et al., 2010; Sathasivam et al., 2010; Scherzinger et al., 1997; Wacker et al., 2004). However, the exact mechanisms and kinetics of aggregate formation are still elusive. It is known that the expanded polyQ tract has a propensity to interact with itself and other polyQ tracts to form beta sheet structures termed polar zippers, which could serve as aggregation nuclei (Perutz et al., 1994). Following fast addition of monomers, the oligomers can assemble into protofibrillar species which then form a ribbon like structure with many features of an amyloid such as detergent insolubility, Congo Red staining, birefringence under polarised light and beta sheet structure (Scherzinger et al., 1999).

Aggregate formation is dependent on time, polyQ length and concentration (Scherzinger et al., 1999). It has also been shown that aggregation proceeds faster when fibrillar aggregation nuclei are present (Scherzinger et al., 1999). Additionally, it has been shown that the first 17 amino acids and the polyproline stretch can also influence the aggregation kinetics of HTT exon 1 (Bhattacharyya et al., 2006; Thakur et al., 2009). The polyproline stretch has been predicted to decrease the frequency with which the polyQ tract of mHTT exon 1 forms a beta rich state *in silico* and has been shown to decrease the formation and stability of mHTT exon 1 amyloid formation *in vitro* (Bhattacharyya et al., 2006; Lakhani et al., 2010). In contrast, the

first 17 amino acids of mHTT enhance its propensity for aggregation, as evidenced by *in vitro* and yeast studies (Duennwald et al., 2006; Sivanandam et al., 2011; Thakur et al., 2009). The importance of the region preceding the polyQ expansion in HD pathology is further confirmed by experiments with BACHD mice where mutating serines S13 and S16 to phospho-mimicking aspartate alleviates behavioural symptoms and abolishes aggregation while retaining wild type HTT function (Gu et al., 2009). Given the plethora of aggregate species in HD, it is not surprising that there is great difficulty in determining how each structure contributes to HD pathogenesis.

1.1.4.2. Toxic or protective? Significance of aggregation for HD pathology

While mHTT inclusions can be found in the brains of HD patients and several mouse models (Crook and Housman, 2011; Gutekunst et al., 1999), their contribution to HD pathology is hotly debated within the field. Large mHTT intranuclear inclusions have been shown to sequester vital cellular proteins, including transcription factors and protein quality control components, arguing for their toxic role in HD pathogenesis (Hay et al., 2004; Jiang et al., 2003; Morton and Edwardson, 2001; Steffan et al., 2000). Equally, in at least three studies where motor symptoms were ameliorated in R6/2 mice a concomitant reduction of aggregate load was also observed (Mielcarek et al., unpublished data)(Labbadia et al., 2011; Labbadia et al., 2012).

In contrast, some studies have suggested that inclusion formation is not sufficient to cause cortical or striatal pathology in mice (Gu et al., 2007; Gu et al., 2005). Work in cell culture models has shown that the formation of large nuclear inclusions correlates with survival and that cell death is best predicted by the presence of smaller oligomeric species (Arrasate et al., 2004; Miller et al., 2011). These results have led some to suggest that the detergent soluble oligomeric species could be more reactive and thus more toxic than large insoluble inclusions. In this scenario, cells could be promoting the assembly of small toxic oligomers into large inert inclusions thereby minimising their deleterious effects.

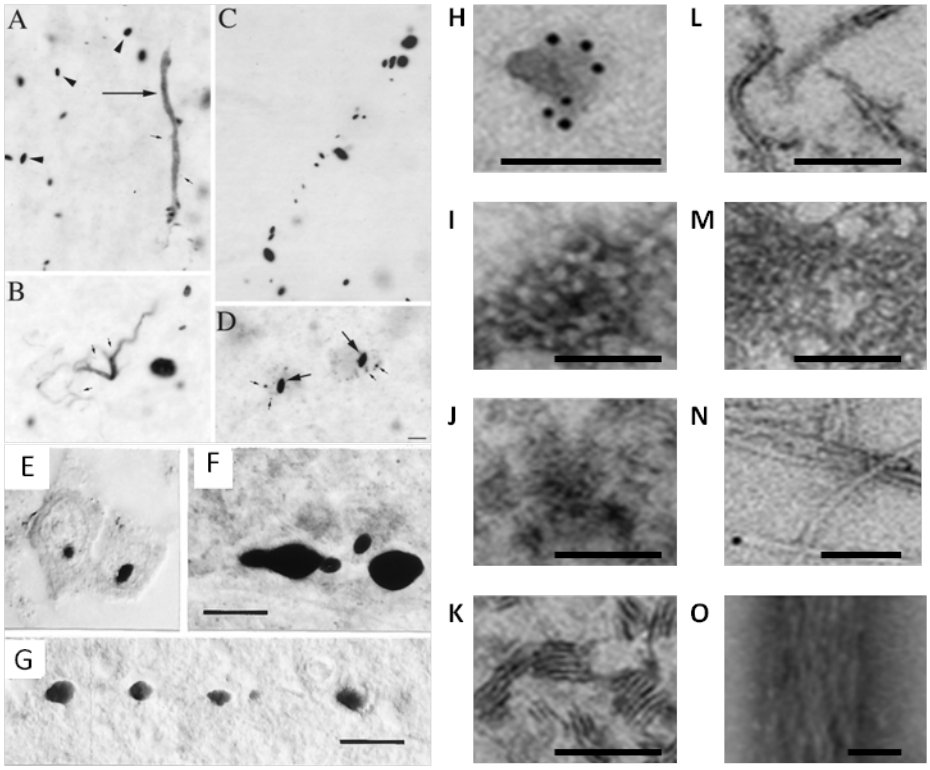

Figure 1.5. N-terminal mHTT forms a spectrum of aggregates in HD patient brains and mouse models.

(A-G) HTT aggregates in the neuropil (A-C, F-G) and nuclei (D-E) of the cortex (A-D, F-G) and striatum (E) of HD patients (A-F) and a pre-symptomatic carrier (G) as revealed under light microscope after staining with huntingtin N-terminal specific antibodies. (H-O) Electron microscopy of aggregated material pulled from R6/2 and *Hdh*Q150 brains with Seprion beads. HTT spherical, amorphous, protofibrillar species can be observed (H-K), as well as immature (L-M) and mature (N-O) fibrils. Scale bar A-D (as shown in D) and E-G (as shown in F and G) = 10 µm, H-O = 100 nm. Reproduced from (Gutekunst et al., 1999) (A-D), (DiFiglia et al., 1997) (E-F) and (Sathasivam et al., 2010) (H-O), with permissions of Society for Neuroscience (A-D), AAAS (E-F) and Oxford University Press (H-O).

1.1.4.3. Mutant huntingtin and protein quality control

The fact that mHTT aggregation only occurs when the polyQ length exceeds a certain threshold indicates that the polyQ expansion confers a conformational change on mHTT that causes it to misfold. Cells are equipped with a network of inducible and constitutively expressed chaperones, and two efficient protein degradation systems that guard against misfolded proteins and eliminate terminally damaged proteins (Muchowski and Wacker, 2005). In theory, misfolding of mHTT into an unfavourable conformation should be recognised by chaperones which then act to neutralize proteotoxicity by re-folding or directing mHTT to the proteasome for degradation. In practice, though there is sufficient evidence that at least the N-terminal part of mHTT becomes misfolded, the widespread toxicity that results from the expression of N-terminal mHTT fragments indicates that the quality control system is not efficient enough in correcting the fault (Gidalevitz et al., 2006).

One possible reason why mHTT is not simply re-folded is that chaperones are not able to perform this task. Their folding capacity could be inefficient, their ability to recognise misfolded mHTT could be compromised or they could be trapped in aggregates. It could also be a question of stoichiometry, where a constant supply of misfolded mHTT, combined with a transcriptional dysregulation resulting in a decrease in chaperone levels, overwhelms the quality control system. Several studies suggest that all of these could be true (Gidalevitz et al., 2006; Hageman et al., 2011; Hay et al., 2004; Zourlidou et al., 2007). Nevertheless, if the load of misfolded mHTT were too great, unfolded protein response or heat shock response (HSR) ought to become activated, increasing the cells' capacity to deal with stress. However, a recent study demonstrated that though fully functional at early disease stage, the HSR is not activated in R6/2 or *Hdh*Q150 mice (Labbadia et al., 2011). Interestingly, the same study demonstrated that pharmacological stimulation of the HSR only transiently improves behavioural phenotypes due to an impairment of the HSR with disease progression (Labbadia et al., 2011).

If mHTT cannot be properly refolded it ought to be eliminated by the ubiquitin – proteasome system (UPS). Current knowledge does not exclude the possibility that some level of mHTT degradation is taking place. Interestingly, ubiquitin has been found tightly associated to a subset of mHTT aggregates, suggesting that the UPS attempts to target mHTT for degradation but fails to execute the final steps (Gutekunst et al., 1999). Whether impairment of the UPS is a part of HD pathology remains debatable – HD post mortem brain samples show decreased proteasome activity and patient fibroblast and other cell culture models confirm this hypothesis (Bence et al., 2001; Bennett et al., 2005; Seo et al., 2004). No overall dysfunction of the proteasome has been found in the brains of R6/2 or R6/1 mice (Bett et al., 2006; Maynard et al., 2009), though one study demonstrated that the proteasome is specifically impaired at the synapse in R6/2 and *Hdh*Q150 mice (Wang et al., 2008b). Equally, it is not clear whether the proteasome is efficient in the degradation of mHTT. Some studies have reported an inability to process the polyQ tract and suggested that mHTT could in fact impair the UPS by physically blocking the proteasome (Holmberg et al., 2004; Venkatraman et al., 2004). Conversely, it has also been shown that the proteasome is capable of processing synthetic polyQ containing peptides (Bennett et al., 2005). More research is needed to determine whether proteasomal targeting of mHTT is possible, feasible and could serve as a therapeutic strategy for HD.

The ubiquitination of HTT aggregates need not necessarily signify a failed attempt at targeting this protein or its fragments to the UPS. Instead, it has been hypothesized that cells could be directing aggregates for bulk degradation by autophagy (Johnston et al., 1998). Evidence for such endeavours comes from observations of increased numbers of autophagic structures in HD post mortem brains, mouse and cell culture models (Kegel et al., 2000; Petersen et al., 2001; Sapp et al., 1997). It has been shown that inhibition of autophagy can cause a neurodegenerative phenotype in mice, whereas chemically or genetically enhancing autophagy is protective in worm, fly and mouse HD models (Jia et al., 2007; Komatsu et al., 2006; Ravikumar et al., 2004). Additionally, it must be noted that a recent study that identified K444 as a site for acetylation on HTT has also

demonstrated that this signal serves for targeting HTT for autophagic degradation (Jeong et al., 2009).

Though it is clear that cells are capable of degrading both soluble and aggregated HTT they appear to be unable to automatically employ these protective strategies. One explanation is that the UPS and autophagic systems are not adequately stimulated; alternatively there could be a malfunction or collapse in their functioning due to direct interference by mHTT, overloading, and/or age related phenomena occurring with disease progression (Ben-Zvi et al., 2009; Cuervo and Dice, 2000; Martinez-Vicente et al., 2010). Therefore, efforts to induce cells to degrade mHTT and eliminate aggregates more efficiently are a promising therapeutic avenue.

1.1.4.4. Transcriptional dysregulation

Evidence for transcriptional dysregulation in HD is overwhelming. Changes to global gene expression levels have been observed in HD patients, mouse and cell culture models (Hodges et al., 2006; Kuhn et al., 2007; Luthi-Carter et al., 2002; Luthi-Carter et al., 2000). Furthermore, the fact that these abnormalities are highly comparable between mouse models and HD patients, occur before symptom onset, and worsen with disease progression strongly indicates that transcriptional dysregulation is a major contributor to HD pathogenesis.

The expression of many neuronal genes is regulated by the cAMP responsive element binding protein (CREB) (Lonze and Ginty, 2002). CREB binding protein (CBP), a transcriptional co-activator with histone acetyltransferase (HAT) activity that links CREB to the basal transcription machinery, is found dysregulated in HD (Nucifora et al., 2001). Mutant HTT interacts with CBP, both through its HAT domain and polyQ tract, which could explain why several (though not all) studies have found CBP in aggregates (Kazantsev et al., 1999; Nucifora et al., 2001).

Other general transcription factors such as Sp1 (specificity protein 1), TBP (TATA-box binding protein) and p53 have all been found to selectively interact with the

expanded polyQ of mHTT thereby making them dysfunctional and dysregulating the genes that they control (Dunah et al., 2002; Li et al., 2002; Schaffar et al., 2004; Steffan et al., 2000). Additionally, mHTT has been found to interact with and disrupt components of the basal transcription machinery such as TFIID, TFIIF and TAFII130, which might explain why most genes dysregulated in HD are down-regulated (Fig. 1.6) (Dunah et al., 2002; Zhai et al., 2005). Evidence supporting the role of mHTT-transcription factor interaction in HD pathogenesis comes from studies where co – expression of Sp1 and TAFII130 or over-expression of a component of TFIID in the context of HD inhibits cellular toxicity (Chen-Plotkin et al., 2006).

There is also evidence of an interaction between mHTT and the nuclear receptor co-repressor (NCoR), which is part of a large repressive complex containing mSin3A and histone deacetylases (HDACs). The localisation of this complex was found to be altered in HD post mortem cortical samples, suggesting that mHTT can also interfere with the regulation of nuclear hormone receptor transcription (Yohrling et al., 2003).

Apart from the altered functioning of transcription factors, there is evidence supporting a significant contribution of abnormal distribution of histone modifications to dysregulated gene expression in HD. Global histone H3 and H4 hypoacetylation as well as histone H3K9 hypermethylation have been observed in HD post mortem brains and mouse models (Ferrante et al., 2003; Gardian et al., 2005; Ryu et al., 2006). Moreover, increased histone H2A ubiquitination, decreased H2B ubiquitination and H3 and H4 hypoacetylation have all been observed at promoters of genes downregulated in HD (Bett et al., 2009; Kim et al., 2008; Labbadia et al., 2011; Sadri-Vakili et al., 2007). Together with the finding that the majority of dysregulated genes in HD are down-regulated, this suggests that there could be a general shift towards a more repressive chromatin state in HD, arising possibly due to lowered HAT and increased HDAC activity (Fig. 1.6). Taken together these findings suggest a central role for transcriptional dysregulation in HD pathogenesis.

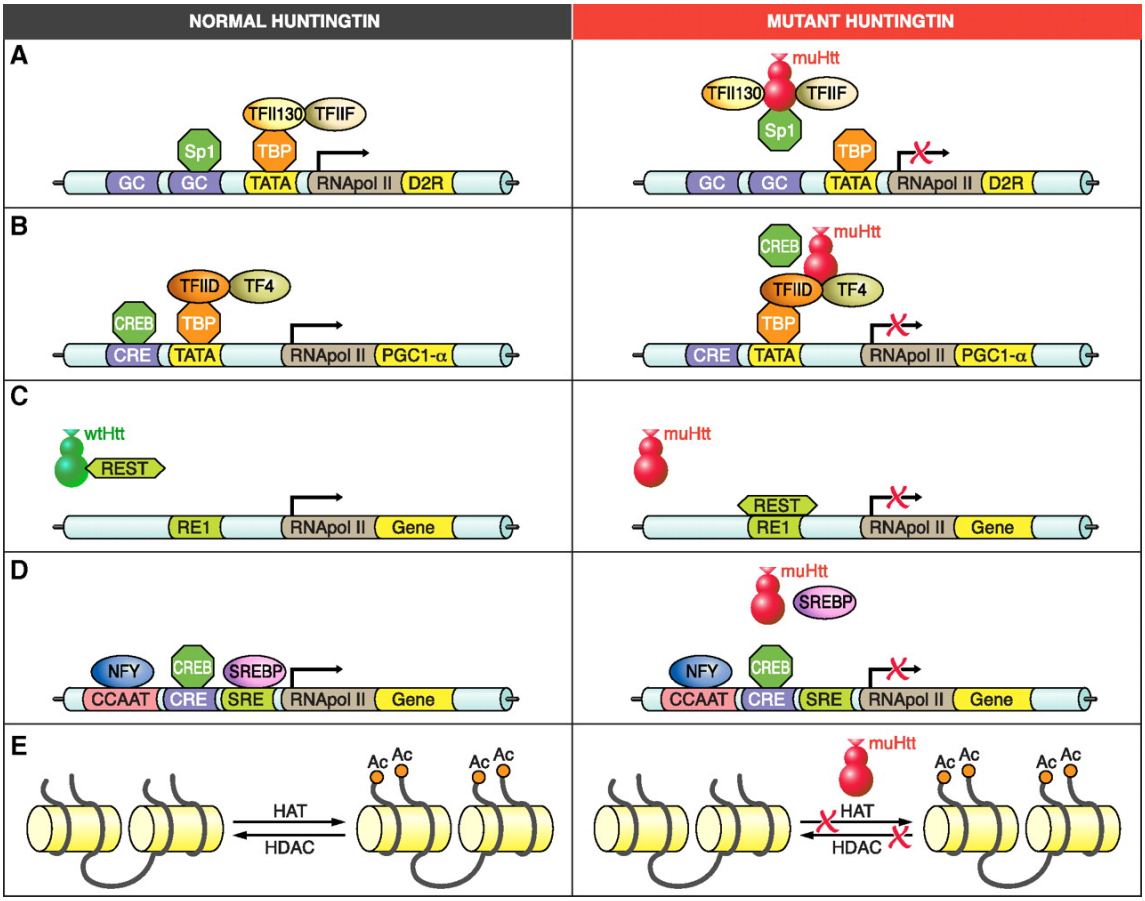

Figure 1.6. Transcriptional dysregulation in HD.

(A) Abnormal interaction of mHTT with Sp1, TFII130 and TFIIF leads to repression of Sp1-dependent promoter repression (e.g. the *D2R* gene). (B) mHTT also disrupts CREB, CBP and TBP regulated transcription of genes such as *PGC1-α*, which itself regulates transcription of many metabolic and mitochondrial genes. Reduced PGC1-α levels lead to down-regulation of its target genes and may contribute to metabolic and mitochondrial dysfunction. (C) Transcription of genes (e.g. *BDNF*) regulated by REST/NRSF is impaired in HD when mHTT fails to sequester REST/NRSF in the cytoplasm. (D) SREBP-2 activation is impaired in the presence of mHTT leading to impairment in the expression of cholesterogenic enzymes. (E) Presence of mHTT leads to an imbalance in HAT and HDAC activities, resulting in abnormal chromatin acetylation, structure and leading to general gene downregulation. Reproduced from (Zuccato et al., 2010) with permission of American Physiological Society.

1.1.4.5. Excitotoxicity

Excitotoxic cell death was one of the first mechanisms proposed to explain the selective vulnerability of medium sized spiny neurons (MSNs) in HD. The first evidence supporting this claim came from the development of similar biochemical and behavioural symptoms in animals injected with the N-methyl – D-aspartate receptor (NMDAR) agonist quinolinic acid (Beal et al., 1991). In contrast to the relatively spared interneurons, MSN's express high levels of NMDARs activated by glutamate and their over-activation can cause an abnormal Ca^{2+} influx that results in apoptosis (Nicholls, 2009). Excitotoxic cell death could result from increased release of glutamate or metabolites such as 3-hydroxykynurenine or quinolinic acid which can activate NMDAR's or cause oxidative stress (Guidetti et al., 2006; Schwarcz et al., 1983). At the same time, removal of glutamate from the synapse is reduced in HD through either reduced levels or abnormal posttratslational modifications of the glutamate transporter in the membranes of glial cells (Fig. 1.7) (Arzberger et al., 1997; Huang et al., 2010; Lievens et al., 2001).

Studies have also demonstrated an enhanced sensitivity of NMDARs in HD models (Cepeda et al., 2001; Zeron et al., 2002). This could be due to an abnormal interaction of mHTT with the post-synaptic density protein 95 (PSD95) which is responsible for proper clustering of NMDARs in lipid rafts at the post-synaptic membrane or to a change in NMDAR subunit composition such that, the presence of the more sensitive NR2B variant is favoured over NR2A (Fig. 1.7) (Milnerwood et al., 2010; Sun et al., 2001).

In addition to glutamate, aberrant adenosine, dopamine and cannabinoid signalling could contribute to excitotoxicity (Dowie et al., 2009; Garrett and Soares-da-Silva, 1992; Glass et al., 1993; Tarditi et al., 2006). Equally, excitotoxicity could be due to disturbances in the proper functioning of cortical neurons and in the downstream signalling cascades in striatal neurons.

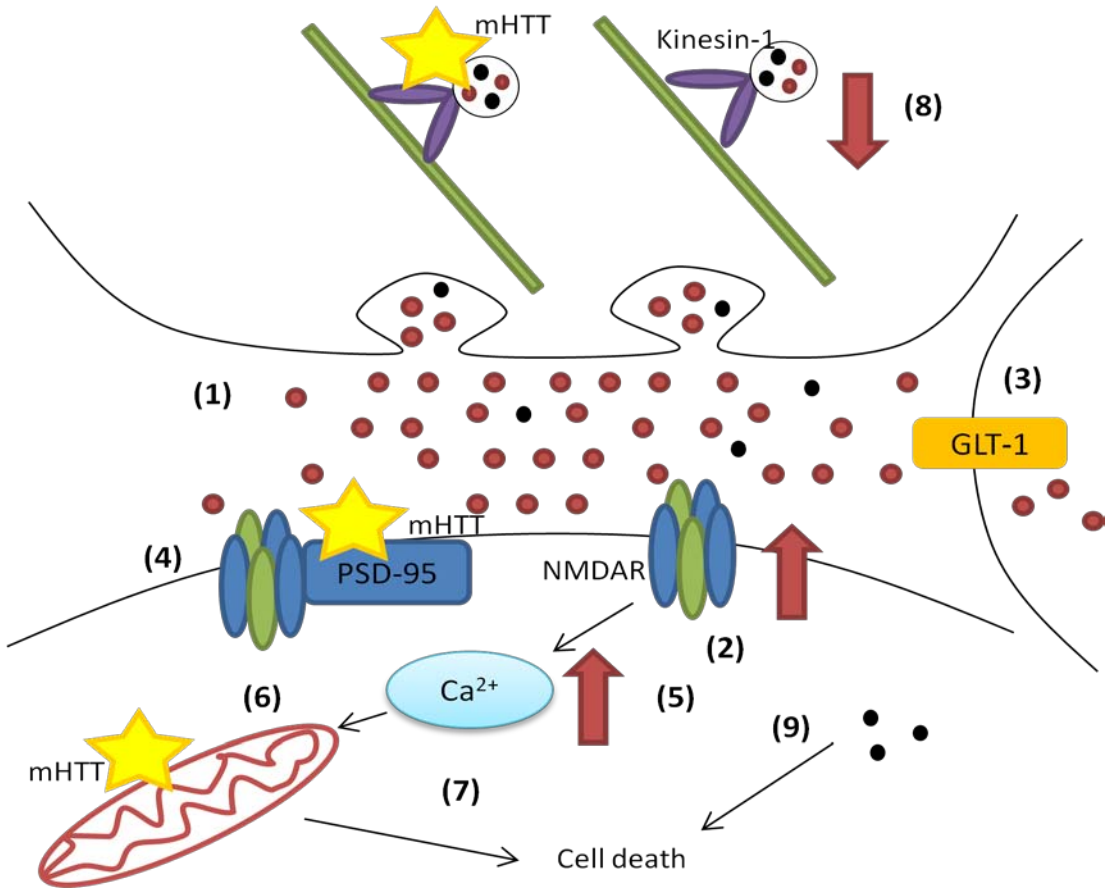

Figure 1.7. Synaptic dusfunction and excitotoxicity in HD.

(1) Altered glutamate release can lead to over-stimulation of NMDA receptors (NMDAR) (2), enhanced by decreased glutamate removal by astrocytes (3) and hypersensitivity of NMDARs due to abnormal clustering by PSD-95 or altered sub-unit composition (4). Hyperactive NMDARs cause increased Ca^{2+} levels (5). Mitochondria are already defective in Ca^{2+} handling and sensitised to depolarisation by presence of mHTT (6). Mitochondrial depolarisation (7) together with defective vesicle transport (8) leading to reduced neurotrophin leves (9) results in excitotoxic cell death.

1.1.4.6. Synaptic function

Alongside excitotoxicity, neurons in HD are affected in many other ways. Firstly, mHTT can alter the availability of molecules involved in synaptic vesicle exocytosis (synaptobrevin-2, rabphilin 3A, complexin II) and recycling (PACSIN/syndapin) (Modregger et al., 2002; Morton and Edwardson, 2001; Morton et al., 2001). Secondly, levels of neurotransmitters such as dopamine, enkephalin, substance P, somatostatin, and corticotrophin releasing hormone, as well as γ-amino-butyric acid (GABA), metabotropic glutamate (mGluR1-3), cannabinoid (CB1), and dopamine receptors are disturbed in HD mice and patients (Augood et al., 1996; Bibb et al., 2000; Cha et al., 1999; Cha et al., 1998; Dowie et al., 2009; Sun et al., 2005). Thirdly, microarray studies have shown abnormal expression levels of genes involved in membrane potential maintenance, intracellular signalling and neuronal differentiation (Luthi-Carter et al., 2000). Finally, studies have shown that microtubule based transport is impaired in HD due to abnormal interaction of mHTT with huntingtin associated protein 1 (HAP1) which prevents it from associating with $p150^{glued}$ – a component of dynein/dynactin motor complex (Gauthier et al., 2004; Gunawardena et al., 2003). Concomitantly, neuropil aggregates may physically impede intracellular trafficking along axons (Li et al., 2001). All these observations imply that the proper functioning of the synapse is impaired on multiple levels which could explain why HD patients display a wide range of behavioural, cognitive and psychiatric disturbances.

1.1.4.6.1. BDNF in Huntington's Disease

Of the four neurotrophins so far identified, Brain Derived Neurotrophic Factor (BDNF) is the best studied in the context of HD. BDNF is implicated in processes such as neurogenesis, neuronal differentiation, neuronal survival and synaptic plasticity (Zuccato and Cattaneo, 2007). Therefore, reductions in the levels of BDNF, which have been observed in both HD post mortem brains as well as mouse models, are very important to consider in terms of both mechanisms of disease pathology as well as therapeutic interventions (Zuccato et al., 2001; Zuccato et al.,

2005; Zuccato et al., 2008). Reduced transcription of *BDNF* is attributed to a loss of wild type HTT function. To achieve BDNF transcription, HTT indirectly interacts with the REST/NRSF complex and prevents it from binding to the *BDNF* promoter and repressing transcription (Zuccato et al., 2003). Mutant HTT is not able to restrict the REST/NRSF complex to its perinuclear localisation and thus, transcription of *BDNF* is repressed (Zuccato et al., 2001).

The major sites of BDNF synthesis are the hippocampus and cortex; the striatum, though containing similar levels of BDNF, has virtually no *BDNF* mRNA and depends mostly on the cortex for the delivery of this trophic factor (Altar et al., 1997). Apart from reduced BDNF synthesis, BDNF cortico-striatal anterograde transport has also been shown to be altered in HD (Gauthier et al., 2004). It is hypothesized that this is due to the modulation of HTT-HAP1 binding upon polyQ expansion in mHTT, which in turn reduces the efficiency of kinesin-1 dependent transport of BDNF containing-vesicles (Gauthier et al., 2004). Another problem that has been suggested to affect the anterograde trafficking of BDNF is a reduced level of acetylated tubulin on the axonal microtubules (Dompierre et al., 2007). Kinesin-1 has been shown to move faster and pause less when tubulin acetylation is higher and one *in vitro* study has demonstrated that increasing tubulin acetylation levels rescued the BDNF transport defect (Dompierre et al., 2007).

Whether the reduced availability of BDNF seen across HD patients and models is indeed responsible for the selective degeneration is still questionable and requires more study. At the same time, it does not explain all the deficits that are occurring in the degenerating brain or in the periphery, such as wide-spread transcriptional dysregulation, disrupted protein homeostasis or defects in metabolism. As such, it is likely that reduced BDNF levels are a contributing factor to, rather than a cause of, HD pathology.

1.1.4.7. Energy homeostasis

Impairment in energy homeostasis has long been recognised as part of disease pathogenesis in HD. Mitochondria isolated from HD patients' lymphoblasts and from YAC72 mouse brain cells have a lower mitochondrial membrane potential that has been attributed to the interaction of mHTT with the outer mitochondrial membrane (Choo et al., 2004; Panov et al., 2002). Data from these and other HD models support the notion that there is an impairment in Ca^{2+} handling by the mitochondria and a higher sensitivity to depolarisation, opening of the mitochondrial permeability transition pore, and collapse of the energy producing electron transport chain (Milakovic et al., 2006). This has also been proposed to result in release of cytochrome c and initiation of apoptosis (Fig. 1.7). At the same time, the transport of mitochondria seems to be impaired by the presence of mHTT aggregates, suggesting that energy dys-homeostasis is affected on many levels (Chang et al., 2006).

Mutant HTT decreases the expression of peroxisome proliferator activated receptor γ coactivator 1 α (PGC1α) - a transcription factor that regulates many genes involved in oxidative phosphorylation, mitochondrial biogenesis, and glucose metabolism (Cui et al., 2006). Furthermore, a reduction in levels of succinate dehydrogenase subunits and lowered activity of the electron transport chain complexes II/III and IV may contribute to disease progression in HD patients (Benchoua et al., 2006; Brennan et al., 1985). Concomitantly, a collapse in oxidative phosphorylation has also been suggested to increase the production of reactive oxygen species (ROS) which in turn severely impairs the mitochondrial enzyme aconitase and could lead to apoptosis (Tabrizi and Schapira, 1999).

1.1.4.7.1. Cholesterol metabolism

The cholesterol synthesis pathway is another important metabolic process that appears to be disrupted in HD. Cholesterol is crucial to the proper functioning of neurons in several ways. Firstly, cholesterol determines the localisation and functioning of ion channels and membrane receptors by acting as a modulator of membrane fluidity and an organiser of lipid rafts (Allen et al., 2007). Secondly, cholesterol is essential for myelination, proper neurite outgrowth and synaptogenesis, and the synthesis of steroid hormones, isoprenoids and ubiquinone (Valenza and Cattaneo, 2011). It is thus conceivable that a disruption in cholesterol levels could contribute to HD pathogenesis.

Several studies have already shown a decrease in expression of cholesterol synthesis enzymes in HD and it has been suggested that this is a result of mHTT perturbing the transcriptional activity of a master regulator of cholesterol synthesis - SREBP-2 (sterol response element binding protein 2) (Fig. 1.6) (Valenza et al., 2005). Decreased activity of 4-hydroxy-4-methyl-glutaryl Coenzyme A (HMGCoA) reductase, that commits HMGCoA to cholesterol synthesis, and reduced brain cholesterol content have also been found in the R6/2, YAC, *Hdh*Q111 and transgenic rat HD models (Valenza et al., 2007a; Valenza et al., 2010; Valenza et al., 2007b). However, other studies have shown increased cholesterol content in YAC72 striata and primary striatal neurons from YAC72 and other mouse models, as well as in the caudate from advanced stage disease post mortem patient samples (del Toro et al., 2010; Trushina et al., 2006). Further studies are required to resolve whether these discrepancies arise from the use of different methods to measure sterol content or from the differences between the different HD models in their response to perturbations in cholesterol homeostasis.

1.1.5. Therapeutic strategies

Although an extensive amount of work has been put into elucidating pathogenic mechanisms, drug discovery and target validation, there is still no disease modifying treatment available for HD. Current therapies are based on treating the symptoms by administration of motor sedatives, cognitive enhancers or antidepressants. The first HD specific symptomatic drug to be approved by the Food and Drug Administration in the USA is tetrabenazine and though it alleviates chorea it can also have devastating side effects. Therefore, strategies targeting specific HD pathogenic mechanisms are currently underway to find a treatment for this debilitating disease.

1.1.5.1. Targeting mutant HTT and protein homeostasis

One obvious way to tackle HD is to specifically rid the organism of mutant HTT, its toxic cleavage products or the aggregates that it forms. Elimination of mHTT could be achieved by targeting it for proteasomal or autophagic degradation. The autophagy inducing drug rapamycin has already shown beneficial effects in *D.melanogaster* and mouse HD models, though there are concerns about its immunosuppressive effect (Ravikumar et al., 2004).

The ambiguous role of aggregates in the pathology of HD caused the search for both targets that inhibit and promote aggregation. Aggregates arise from misfolded proteins, therefore many studies have focused on checking whether chaperones could be used to prevent their formation. Induction of the HSR provided promising results in the R6/2 mouse model, however, this approach may be more complicated than anticipated due to disease related impairment in the HSR (Labbadia et al., 2011).

Another way to tackle aggregation was discovered when it was found that cells sometimes act to concentrate the aggregates into a single peri-nuclear structure termed the aggresome which once formed is degraded by autophagy (Johnston et al., 1998). If such a coping mechanism existed *in vivo*, its upregulation should be of

therapeutic benefit. However, at present the benefits of this approach remain unknown.

1.1.5.2. Improving neuronal function

As excitotoxicity is considered one of the major causes of cell death in HD there are considerable efforts to suppress this pathway. Both memantine and riluzole are drugs directed against glutamate neurotransmission. Though riluzole has shown mild therapeutic effects in R6/2 mice, these findings could not be reproduced when the study was repeated (Hockly et al., 2006; Schiefer et al., 2002). Equally, a meta-analysis of clinical trials performed in HD found no overall beneficial effect of riluzole treatment in HD patients (Mestre et al., 2009). Concomitantly, though memantine has shown some promise in HD mice, its effects in the clinic have only been tested on a small number of patients in an open label trial, and as such, the potential benefit of this drug should be considered with caution (Milnerwood et al., 2010). One promising strategy aimed at reducing excitotoxicity is the inhibition of kynurenine monooxygenase which results in reduced levels of the NMDAR agonist quinolinic acid and increased levels of the NMDAR antagonist kynurenic acid. This intervention has already shown beneficial effects in yeast and mouse HD models (Giorgini et al., 2005; Zwilling et al., 2011). In addition, new approaches that target calcium signalling or specific NMDAR subunits are underway in preclinical studies.

Increasing BDNF is another promising therapeutic strategy. Multiple studies in cell and transgenic animal HD models have shown the potential benefit of this approach. Over-expression of BDNF in the cortex and striatum of R6/1 and YAC128 mice improved motor function, preserved brain weight, restored TrkB signalling in the striatum, and reduced aggregation (Gharami et al., 2008; Xie et al., 2010). Delayed motor impairment and extended survival were also observed in R6/2 mice after intrastriatal adenoviral delivery of BDNF with noggin, a molecule promoting neurogenesis (Cho et al., 2007). Additionally, it has been suggested that rescuing the BDNF transport deficit could be achieved through increasing levels of tubulin

acetylation (Dompierre et al., 2007). Thus far, strategies aimed at increasing striatal BDNF hold great promise for clinical therapies.

1.1.5.3. Targeting transcriptional dysregulation

In theory, alleviating transcriptional dysregulation could have profound effects on many other pathogenic mechanisms that stem from this defect, such as neuronal dysfunction, decreased BDNF levels, energy imbalance, cholesterol metabolism and protein homeostasis. Therapeutic intervention to target transcriptional dysregulation has mainly focused on inhibiting histone deacetylases in an attempt to reduce genome quiescence. While genetic or pharmacological inhibition of HDACs has shown great promise in worm, fly, cell and mouse HD models, broad range HDAC inhibitors have also shown toxicity, thereby warranting a search for specific HDAC targets that can be modulated to achieve therapeutic benefit without adverse effects (Bates et al., 2006; Hockly et al., 2003; Pallos et al., 2008; Steffan et al., 2001).

1.2. Protein deacetylation

Acetylation of the ε-amino group of lysine on histone tails has long been considered to be instrumental in transcriptional control (Allfrey et al., 1964). The observation that euchromatin is heavily acetylated suggests that this post-translational modification (PTM) favours the more open, transcriptionally active DNA conformational state (Lee et al., 1993). Histones bound to promoters of many actively transcribed genes are often acetylated and multiple transcription activating complexes either contain HATs or recruit them to promoters (Nagy and Tora, 2007). At the same time, many transcription factors themselves become acetylated which can either enhance their DNA binding capacity (like for p53) or diminish it (like for HMGI(Y)) (Gu and Roeder, 1997; Munshi et al., 1998). However, the discovery that many proteins that are not involved in transcription are acetylated, suggests that this PTM could have a much broader regulatory role, perhaps similar to that of phosphorylation (Kouzarides, 2000).

Functions outside of direct transcriptional control that have already been demonstrated for acetylation are regulation of protein stability, binding, and activity. Recently, a study has found that the gluconeogenic enzyme phosphoenolpyruvate carboxykinase 1 (PEPCK1) is more readily targeted for proteasomal degradation when acetylated, demonstrating that acetylation regulates protein stability (Jiang et al., 2011). Protein-protein interactions can also be dependent on acetylation as evidenced by the fact that acetylation of α-tubulin enhances the efficiency of kinesin-1 dependent transport or that deacetylation of HSP90 is required for its dissociation from the glucocorticoid receptor (Murphy et al., 2005; Reed et al., 2006). Enzymatic activity can equally be controlled by acetylation, as has been shown for PTEN where acetylation decreases its lipid phosphatase activity (Okumura et al., 2006).

The cells' acetylome is determined by the interplay between HATs and HDACs. Even though it is now well known that these enzymes also act on many non-histone substrates and despite efforts to correct the nomenclature, the groups are still

referred to as HATs and HDACs (Allis et al., 2007). For the purpose of clarity, this convention will be adhered to in this work.

HDAC inhibition has recently emerged as an attractive therapeutic intervention for many complex diseases. Therefore, understanding the biology and effects of inhibition of individual HDACs in the context of mouse models of HD is extremely important in terms of using HDAC inhibitors in disease therapy.

1.2.1. Histone deacetylases general classification

There are altogether 18 mammalian HDACs, divided into four classes depending on their sequence homology to yeast enzymes. Class I includes HDAC1, HDAC2, HDAC3 and HDAC8, which are homologous to the yeast enzyme Rpd3 (de Ruijter et al., 2003). Class IIa encompasses HDAC4, HDAC5, HDAC7 and HDAC9, whereas class IIb contains HDAC6 and HDAC10 (Fig. 1.8) (de Ruijter et al., 2003). All members of class II share most homology with the yeast enzyme Hda1. Sirtuins form the class III deacetylases which contain 7 enzymes that are all similar to the yeast Sir2, thus named SIRT1 through SIRT7 (Fig. 1.9) (Finkel et al., 2009). Class IV's only member is HDAC11, which due to insufficient sequence homology cannot be included in any other class (Gao et al., 2002). Though classes I, II and IV have different sequence homologies, one feature distinguishing them from the sirtuin class III is their mechanism of action.

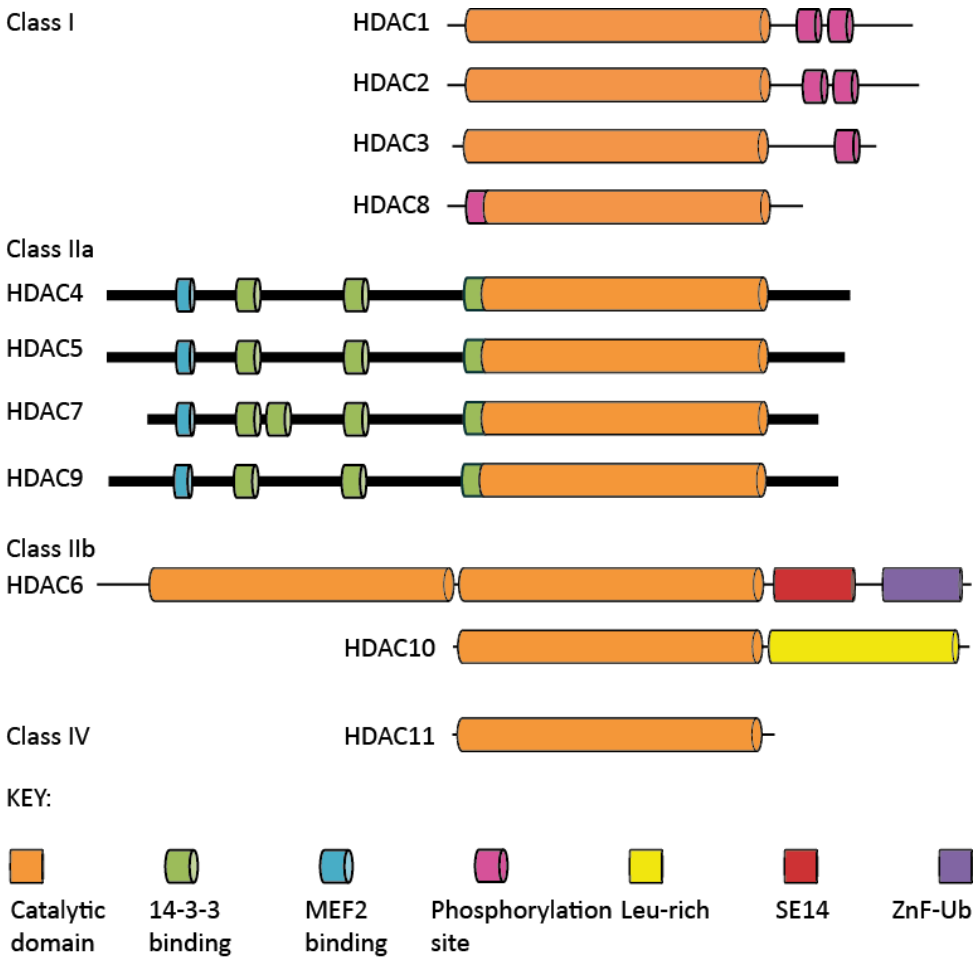

Figure 1.8. Class I, II and IV HDACs - the "conventional" HDAC family.

Though the catalytic mechanism is conserved among HDACs 1-11, regions flanking the catalytic domain (orange) contain sequences for MEF2 (blue), 14-3-3 (green), and ubiquitin binding (purple), a leucine-rich domain (yellow), and phosphorylation sites (pink), and confer specific properties to individual HDACs. Class IIa HDAC N- and C- termini are highly similar (thick black line). MEF2 - myocyte enhancer factor 2; Leu-rich - leucine rich region; SE14 - serine/glutamate tetradecapeptide; ZnF-Ub - zinc finger for ubiquitin binding. Modified from (Yang and Seto, 2008) with permission of Nature Publishing Group.

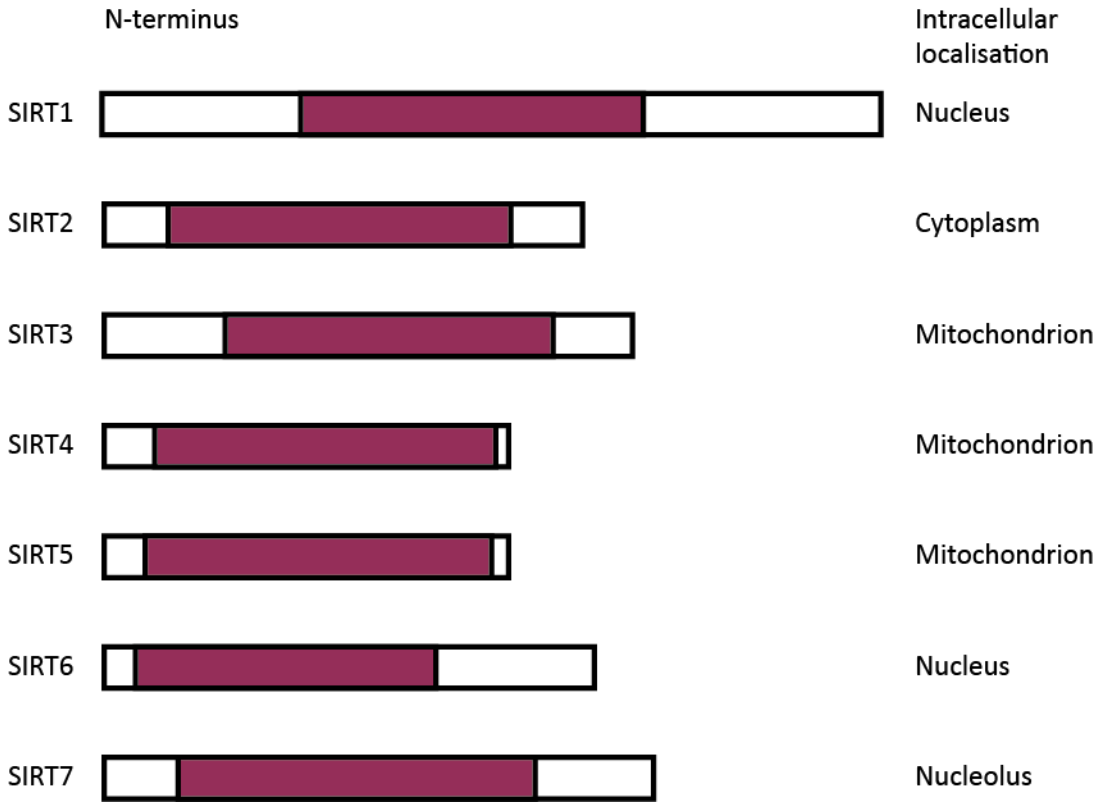

Figure 1.9. Class III HDACs – the mammalian sirtuins.

Catalytic domain (purple) and most prevalent intracellular localisation for SIRT1-7 enzymes. Modified from (Li and Kazgan, 2011) with permission of Ivyspring International Publisher.

1.2.1.1. Reaction mechanisms

HDACs 1 through 11 are all zinc dependent enzymes and share the same reaction mechanism. They rely on a Zn^{2+} ion coordinated by histidine and aspartate residues in a highly conserved catalytic core. Deacetylation occurs by the activation of a water molecule by the zinc cation coupled to the histidine-aspartate charge relay system within the active site (Finnin et al., 1999). The sirtuin reaction mechanism is NAD^{+} (Nicotinamide Adenine Dinucleotide) dependent and proceeds through formation of an oxocarbenium-like transition species and release of nicotinamide (NAM). Upon completion, apart from the deacetylated substrate, 2'-O-acetyl ADP ribose is released (Liang et al., 2010).

1.2.1.2. Expression and functions of HDAC enzymes

Class I HDACs are expressed in a variety of tissues suggesting that they have a general regulatory function in transcription control (Johnstone, 2002). HDAC1 and HDAC2 share 82% sequence homology and are thus far the best characterised HDACs (de Ruijter et al., 2003). They are found exclusively in the nucleus and generally form part of multi-protein transcription modulating complexes such as Sin3, NuRD (nuclear remodelling deacetylase) or Co-REST (co-repressor of REST) (Ahringer, 2000; Humphrey et al., 2001). HDAC3 is the only class I member that in addition to a nuclear localisation signal (NLS) also possesses a nuclear export signal (NES) (Yang et al., 2002). Consistent with this HDAC3 has been detected in both the nucleus and cytoplasm where it is believed to localise to the plasma membrane (Emiliani et al., 1998).

HDAC4, HDAC5, HDAC7 and HDAC9 have their catalytic domain at the C-terminus and an NLS at the N-teminus (Yang and Seto, 2008). However, their N-terminus also has conserved domains for binding the C-terminal binding protein (CtBP), myogenic enhancer factor (MEF2) and 14-3-3 proteins (Yang and Gregoire, 2005). MEF2 is essential for muscle differentiation and inhibited by binding to class IIa HDACs (Verdin et al., 2003). This association is disrupted by CaMK phosphorylation and export of HDACs to the cytoplasm via association with 14-3-3 proteins (McKinsey et al., 2000). HDAC4, HDAC5 and HDAC7 have also been shown to interact with HDAC3 within the N-CoR/SMRT (nuclear co-repressor/silencing mediator for retinoic acid and thyroid hormone receptors) repressive complex (Fischle et al., 2002). In fact, recent data suggests that HDAC4, HDAC5 or HDAC7 might not possess histone deacetylase activity and therefore associate with HDAC3 to achieve transcriptional repression (Fischle et al., 2002).

HDAC6 and HDAC10 are unique in that they have a duplication of the catalytic domain, though the duplicated domain appears to only be functional in HDAC6 (Yang and Seto, 2008). HDAC10, as well as the class IV HDAC11 have only recently been identified and little is known of these two enzymes. HDAC10 has so far been implicated in DNA homologous recombination and 3' pre-mRNA processing and

appears to be vertebrate specific, whereas HDAC 11 is conserved through invertebrates and plants but more investigation is needed to pinpoint its cellular functions (Gao et al., 2002; Kotian et al., 2011; Shimazu et al., 2007; Yang and Seto, 2008).

The sirtuins can be found in the nucleus (SIRT1, SIRT6 and SIRT7), the mitochondrion (SIRT3-5) and in the cytoplasm (SIRT2) (Fig. 1.8) (Finkel et al., 2009). So far, SIRT1 has been most extensively studied, due to its highest homology with the yeast sir2 enzyme and suggested role in mediating lifespan extension (Kaeberlein et al., 1999; Tissenbaum and Guarente, 2001). It has also been implicated in DNA damage response, oxidative stress and heat shock response, cellular differentiation and metabolism (Wang et al., 2008c; Westerheide et al., 2009; Yuan et al., 2007).

Mitochondrial sirtuins have been demonstrated to function as regulators of energy production through concerted action of deacetylation and ADP-ribosylation. SIRT3 can deacetylate Acetyl-CoA synthetase 2, resulting in an increased production of Acetyl-CoA, an intermediate in the Krebs cycle, fatty acid metabolism, and cholesterol synthesis (Hallows et al., 2006). SIRT4 does not seem to have deacetylase activity, but instead uses NAD^+ to ADP-ribosylate glutamate dehydrogenase, inactivating it in the liver and pancreatic β-cells, and regulating gluconeogenesis and insulin secretion in response to glutamine (Haigis et al., 2006). Little is known about SIRT5, though it has recently been demonstrated to deacetylate carbamoyl phosphate synthetase 1, thereby activating it and causing increased urea production in the liver. As SIRT5 mRNA levels are upregulated during fasting, its action on the urea cycle could be protective by increasing the conversion of increased ammonia generated in the process (Ogura et al., 2010).

SIRT6 is another sirtuin without deacetylase but with ADP-ribosylase activity. Its substrates are still unknown but studies from SIRT6 deficient mice indicate a role for this protein in base-excision repair (Mostoslavsky et al., 2006). SIRT7 is a nucleolar enzyme expressed mainly in proliferative tissues such as liver, spleen and testes and with little expression in heart, brain or muscle (Ford et al., 2006). SIRT7

can associate with Pol I and its over-expression increased transcription of rRNA, suggesting that SIRT7 could promote growth by driving ribosome biosynthesis in proliferating cells (Ford et al., 2006).

Similarly to HDAC6, SIRT2 is the only predominantly cytosolic sirtuin. Both are α-tubulin deacetylases and both have been suggested to play a role in Huntington's disease pathogenesis.

1.2.2. HDAC inhibition as therapy for HD

Transcriptional dysregulation in HD has been shown to mostly involve gene downregulation (Luthi-Carter et al., 2000). At the same time, global histone H3 and H4 hypoacetylation has been observed in patients and HD models (Ferrante et al., 2003; Gardian et al., 2005; Ryu et al., 2006). It is therefore of no surprise that HDAC inhibition has emerged as an exciting avenue for therapeutic intervention.

The first indication that HDAC inhibition could correct the transcriptional dysregulation observed in HD emerged in yeast cells where treatment with Trichostatin A (TSA), which inhibits Rpd3 and Hda1, corrected the decrease in transcription caused by expression of an expanded polyQ-GFP directed to the nucleus (Hughes et al., 2001). Subsequently, proof of principle experiments performed with inducible PC12 cells expressing mHTT exon 1 showed a restoration of histone acetylation upon treatment with TSA and other broad range HDAC inhibitors: sodium butyrate (NaB) and suberoylanilide hydroxamic acid (SAHA) (Steffan et al., 2001). The same study also demonstrated that treatment with SAHA or NaB can be neuroprotective in a *D.melanogaster* model of HD (Steffan et al., 2001). These findings were then translated into a mammalian model when R6/2 mice treated with SAHA or NaB showed improved body weight, rotarod performance, survival, and decreased transcriptional dysregulation (Ferrante et al., 2003; Hockly et al., 2003). Sirtuin inhibitors have been less rigorously tested in the context of HD, though two groups found an amelioration of phenotype in

D.melanogaster and mice after nicotinamide administration (Hathorn et al., 2011; Pallos et al., 2008).

However, studies in mice have also identified significant toxicity associated with broad range HDAC inhibitor administration (Hockly et al., 2003). Therefore, efforts to identify the mechanisms mediating the protective HDAC inhibitor effects have been undertaken so that instead of targeting a whole family of HDACs simultaneously, more specific and thus, less toxic inhibitors could be developed.

The search for HDAC targets relevant to HD pathgenesis triggered a cascade of studies in invertebrate HD models. RNAi experiments in *C.elegans* suggested that polyglutamine toxicity could be ameliorated by genetic reduction of *hda-3* which is most homologous to human *HDAC1* (Bates et al., 2006). Concomitantly, reduction of Rpd3, which is equally homologous to human HDAC1, HDAC2 and HDAC3, resulted in neuroprotection in a *D.melanogaster* HD model (Pallos et al., 2008). The same study has also demonstrated a neuroprotective effect of genetic reduction of Sir2 (homologous to SIRT1) and Sirt2 (homologous to SIRT2) in the same model (Pallos et al., 2008). At the same time, over-expression of HDAC6 has been shown to be protective in a *D.melanogaster* model of SBMA with implications that these findings could be translated to HD and other polyglutamine diseases (Pandey et al., 2007b).

However, though invertebrate studies provide important directions for future investigations, little is known about the validity of these targets in mammals. Therefore, this work encompasses the first attempt to validate previous findings from invertebrate and cell polyQ disease models to validate HDAC6 and SIRT2 as therapeutic targets for HD.

1.3. HDAC6 and SIRT2 as therapeutic targets in Huntington's Disease

HDAC6 and SIRT2 are deacetylases from two distinct families, and both are the only representative of each family to reside primarily in the cytoplasm (Bertos et al., 2004; North et al., 2003). They have also both been described primarily as α-tubulin deacetylases and with the exception of H4K16 during cell cycle progression for SIRT2, their targets are non-histone proteins (Hubbert et al., 2002; Vaquero et al., 2006). Thus, in terminally differentiated, non-dividing cell such as neurons, their role in HD pathogenesis would not be expected to be linked to transcriptional dysregulation, but rather depend on their regulation of non-histone targets.

1.3.1. HDAC6

HDAC6 is a class IIb HDAC with most sequence homology to the yeast Hda1 enzyme (Grozinger et al., 1999). It is located on the X-chromosome in both mice and humans and contains two deacetylase domains, though whether they can act independently is a subject of debate (Mahlknecht et al., 2001; Voelter-Mahlknecht and Mahlknecht, 2003; Zhang et al., 2006; Zou et al., 2006). HDAC6 is expressed in several tissues, including heart, brain and liver, with highest levels of expression in the testis (Zhang et al., 2008). A nuclear export signal and additionally in humans, an SE14 (serine-glutamate tetradecapeptide) cytoplasmic anchoring motif cause HDAC6 to be localised to the cytoplasm (Bertos et al., 2004). However, both mouse and human HDAC6 also contain an atypical nuclear localisation signal, which may explain why in some studies HDAC6 has also been detected in the nucleus (Bertos et al., 2004). The linker region between the two catalytic domains could be required for HDAC6 binding to other proteins, such as dynein and $p150^{Glued}$ (Fig.1.9) (Kawaguchi et al., 2003). Finally, the C-terminus of HDAC6 contains a Zn finger ubiquitin binding domain (ZnF-Ub) that is unique amongst HDACs and links HDAC6 to the protein quality control machinery (Boyault et al., 2006; Kawaguchi et al., 2003; Seigneurin-Berny et al., 2001).

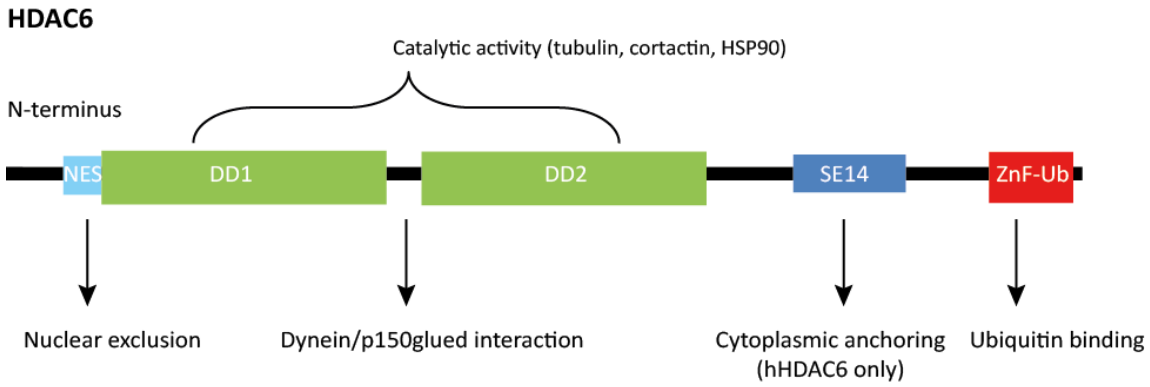

Figure 1.10. Domain organization of the HDAC6 protein.

NES – nuclear export signal; DD – deacetylase domain; SE14 – serine/glutamate tetradecapeptide (only found in hHDAC6); ZnF-Ub – zinc finger for ubiquitin binding; hHDAC6 – human HDAC6.

1.3.1.1. Functions of HDAC6

HDAC6 is a versatile protein implicated in cell motility, signal transduction and protein quality control. Its client proteins include cortactin, HSP90, and β-catenin, but it can also bind mono- and polyubiquitin chains and ubiquitinated proteins with its ZnF-Ub domain (Kovacs et al., 2005; Li et al., 2008; Seigneurin-Berny et al., 2001; Zhang et al., 2007).

Deacetylation of β-catenin in response to epithelial growth factor (EGF) signalling is required for EGF's efficient translocation to the nucleus and induction of *c-myc* expression (Li et al., 2008). At the same time, inhibition of HDAC6 results in a hyper-acetylated form of HSP90 that is defective in binding to the co-chaperone p23 (Kovacs et al., 2005). This compromises maturation of the glucocorticoid receptor and its transcriptional activity upon ligand binding (Kovacs et al., 2005).

Cortactin deacetylation promotes its binding to F-actin and is important for cell motility and angiogenesis (Kaluza et al., 2011). Additionally, deacetylated cortactin is crucial for the autophagosome to lysosome fusion during steady-state macroautophagy (Lee et al., 2010). Interaction with HSP90 also ties HDAC6 to protein homeostasis (Matthias et al., 2008). Though HDAC6 catalytic activity is dispensable for this process, ubiquitin binding induces HDAC6 to facilitate the

dissociation of the HSP90-HSF1 (heat shock transcription factor 1) repressive complex, allowing HSF1 to activate the HSR (Boyault et al., 2007). This shows that HDAC6 is involved in both steady state as well as inducible protein quality control.

1.3.1.1.1. Significance of HDAC6 mediated tubulin deacetylation

Although tubulin deacetylation is the most extensively studied HDAC6 activity, its basic biological significance is still unclear. It has been suggested that tubulin acetylation increases microtubule stability or dynamics (Matsuyama et al., 2002), though these findings are a subject of debate (Palazzo et al., 2003). Protein binding to microtubules, receptor internalization, podosome formation, starvation induced autophagy, dendritic arborisation, immune synapse formation and HIV-1 infection have all been shown to be modulated by HDAC6 mediated changes in tubulin acetylation (Deribe et al., 2009; Destaing et al., 2005; Geeraert et al., 2010; Giustiniani et al., 2009; Ohkawa et al., 2008; Serrador et al., 2004; Valenzuela-Fernandez et al., 2005).

Recently, a novel function for tubulin acetylation has been revealed in intracellular transport. Kinesin-1 dependent transport was enhanced when HDAC6 was inhibited and tubulin acetylation increased (Reed et al., 2006). At the same time, deacetylated tubulin mimicking mutants exhibited slower transport and less kinesin to microtubule binding (Reed et al., 2006). Together with the finding that acetylated microtubules have differential distribution in highly polarised cells such as neurons, one could speculate that the transport of cargoes could be directed to specific cellular locations by alterations of tubulin acetylation levels (Cambray-Deakin and Burgoyne, 1987). Alternatively, acetylation of microtubules could prioritize transporting one cargo over another, as not all kinesin motors respond to tubulin acetylation changes (Reed et al., 2006).

Another interesting role for HDAC6 has been revealed in the formation of stress granules and aggresomes in response to stress (Kawaguchi et al., 2003; Kwon et al., 2007). Stress granules accumulate protein translational machinery, including

mRNAs, initiation factors, ribosomal subunit and proteins involved in RNA remodelling and degradation (Kwon et al., 2007). Aggresomes are perinuclear inclusion bodies of aggregated, ubiquitinated misfolded proteins found to associate with the microtubule organising centre (Johnston et al., 1998). Though a direct involvement of tubulin acetylation has not been demonstrated in the formation of these structures, both aggresomes and stress granules require intact microtubules and a catalytically active HDAC6, again highlighting the role of HDAC6 in protein homeostasis (Kawaguchi et al., 2003; Kwon et al., 2007).

Interestingly, *Tetrahymena thermophila* cells with a deacetylation mimicking mutated tubulin have normal growth and morphology and mice depleted of HDAC6 have highly elevated levels of acetylated tubulin but no obvious phenotypes (Gaertig et al., 1995; Zhang et al., 2008). This strongly suggests that HDAC6 may only become essential in response to stressful stimuli or in a pathogenic context.

1.3.1.2. Therapeutic strategies involving HDAC6

HDAC6 is of particular interest in HD. Firstly, it appears to play a role in protein homeostasis by sensing and responding to ubiquitinated protein accumulation (Matthias et al., 2008). Mutant HTT can become ubiquitinated and has been shown to accumulate in aggresomes in HD cell models (Iwata et al., 2005). HDAC6 participated in aggresome formation by binding ubiquitinated proteins and the retrograde dynein motor (Iwata et al., 2005). Subsequent autophagic degradation of the aggresome was also HDAC6 dependent (Iwata et al., 2005). In addition, it has been demonstrated that in a *D.melanogaster* model of SBMA HDAC6 expression rescued neurodegeneration in an autophagy-dependent manner (Pandey et al., 2007b). Similar results were observed when HDAC6 was overexpressed in *D.melanogaster* models of Alzheimer's Disease and Parkinson's Disease (Pandey et al., 2007a). Taken together with the observation that HDAC6 plays a role in autophagy and heat shock activation these observations indicate that HDAC6 could be protective in a disease where protein homeostasis is disrupted (Boyault et al., 2007; Lee et al., 2010).

In contrast to its role in protein quality control, effects of HDAC6 on tubulin acetylation could be damaging in the context of HD. One study in an HD cell model has indicated that increasing tubulin acetylation by HDAC6 inhibition could rescue the BDNF transport deficit from the cortex to the striatum (Dompierre et al., 2007). This is supported by the fact that BDNF is a cargo of kinesin-1 and tubulin acetylation enhances kinesin-1 dependent transport (Dompierre et al., 2007; Reed et al., 2006).

Taken together, these findings strongly suggest that HDAC6 inhibition should modify HD progression. Based on the previous studies in cell culture and invertebrate models of HD, loss of HDAC6 might be expected to increase aggregate load and exacerbate the phenotype in a mouse model of HD (Iwata et al., 2005; Pandey et al., 2007a; Pandey et al., 2007b). On the other hand, an increase in cortico-striatal BDNF transport might be expected to improve some HD-related phenotypes (Dompierre et al., 2007). In any instance, none of these suggested HDAC6 roles have been tested in a mammalian model.

1.3.2. SIRT2

SIRT2 is a member of class III HDACs also termed sirtuins (Fig. 1.9). SIRT2 contains a catalytic domain and N- and C-terminal extension regions (Fig. 1.11) (Frye, 1999). So far three SIRT2 isoforms, all catalytically active, have been described. Isoform SIRT2.1 is the largest protein produced from full length mRNA containing all 16 exons (Frye, 1999; Maxwell et al., 2011). The two shorter transcripts are generated by skipping exon 2 or exons 2-4, resulting in SIRT2.2 and SIRT2.3 isoforms respectively, both with an altered N-terminus. Little is known of the regulation of SIRT2 through PTMs, except that its deacetylase activity can be inhibited by phosphorylation by various cyclin dependent kinases (CDKs) at its C-terminus (Fig. 1.11) (Pandithage et al., 2008). SIRT2 has also been shown to bind HDAC6 and HOX10a, though the significance of these interactions is currently unknown (Bae et al., 2004; North et al., 2003).

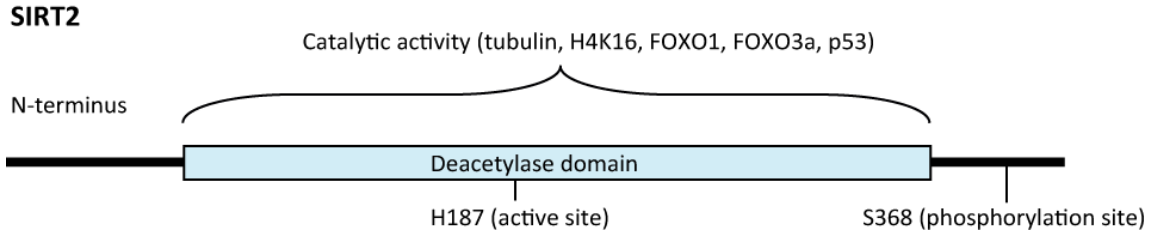

Figure 1.11. Domain organization of the SIRT2 protein.

H4K16 - histone 4 lysine 16; H - histidine; S - serine.

Early data on *SIRT2* expression indicated that it is ubiquitously expressed both in adult and fetal tissue (Afshar and Murnane, 1999). Mouse *Sirt2* however appears to be most highly expressed in the brain, heart, kidney and testis, with less expression in the liver, spleen and skeletal muscle (Yang et al., 2000). Data on *Sirt2* expression in the CNS indicate a peak during postnatal development and a slow reduction in expression with age (Werner et al., 2007). In contrast, recent studies on SIRT2

protein expression levels stipulate that the expression of the SIRT2.3 isoform is increased in the aging mouse brain (Maxwell et al., 2011).

1.3.2.1. Proposed functions of SIRT2

SIRT2 has been implicated in cell cycle progression after the observation that its levels peak during mitosis (Vaquero et al., 2006). Subsequently it was discovered that SIRT2 can deacetylate H4K16-Ac and that global levels of H4K16-Ac decrease during G2/M transition; a period that coincides with SIRT2 localisation to chromatin (Vaquero et al., 2006). Conflicting data exist on the precise role of SIRT2 in cell cycle regulation. While some groups report that SIRT2 is required for efficient G2/M transition, others claim that SIRT2 activity can block mitosis entry upon treatment with compounds that interfere with microtubule assembly (Dryden et al., 2003; Inoue et al., 2007). Yet another study has found no involvement of SIRT2 in mitosis under non-stressful conditions (Pandithage et al., 2008). At the same time the significance of SIRT2 phosphorylation by cyclin dependent kinases 1, 2 and 5 and dephosphorylation by CDC14B is unclear. While one study reported that phosphorylation reduces SIRT2 deacetylase activity another group reported that dephosphorylation targets SIRT2 for proteasomal degradation (Dryden et al., 2003; Pandithage et al., 2008). It seems counterintuitive that both phosphorylation and dephosphorylation would result in reducing a protein's activity. Nevertheless, as these studies have been performed with different cell lines, SIRT2 regulation and its role in cell cycle progression could depend on the tissue under examination and be vastly different between normal and cancerous cells. Evidence in support of a negative role for SIRT2 in cell cycle progression also comes from the fact that expression of SIRT2 is down-regulated in many gliomas (Hiratsuka et al., 2003). Nonetheless, further investigation is required to accurately dissect the function of SIRT2 in cell division.

The growing repertoire of non-histone SIRT2 substrates suggests that this protein could have many functions, some of which could be tissue dependent. In the liver, upon starvation, SIRT2 was found to deacetylate the gluconeogenic enzyme PEPCK1

thus protecting it from proteasomal degradation (Jiang et al., 2011). In kidney and white adipose tissue, levels of SIRT2 are increased upon caloric restriction and in brown adipose tissue upon cold exposure (Wang et al., 2007; Wang and Tong, 2009). Oxidative stress also increased expression of SIRT2 in cells (Wang et al., 2007). Subsequently, it was shown that SIRT2 deacetylates FOXO1 and FOXO3A (Wang and Tong, 2009). Deacetylation increases FOXO1's binding to and inhibition of PPARγ, which results in inhibition of adipocyte differentiation (Wang and Tong, 2009). Deacetylation of FOXO3A increases its transcriptional activity which results in increased expression of MnSOD, $p27^{kip}$ and the pro-apoptotic protein Bim (Wang et al., 2007). Interestingly, these effects are only observed upon low glucose (FOXO1) or oxidative stress (FOXO3A) conditions indicating that SIRT2 might play an important function when challenged with stressful environmental conditions (Wang et al., 2007; Wang and Tong, 2009).

In general, SIRT2 appears to be a pro-survival protein, though some data challenge this assumption. SIRT2 has been suggested to deacetylate p53 thereby down-regulating its transcriptional activity and promoting survival, a theory supported by reports that genetic or pharmacological down-regulation of SIRT2 activity induced apoptosis in cells (Peck et al., 2010). On the other hand, SIRT2 was found to be down-regulated in many gliomas while its ectopic expression reduced glioma proliferation (Hiratsuka et al., 2003). These seemingly contrasting data on SIRT2's role in survival could be a result of differences in SIRT2 function between the periphery and the nervous system.

In the CNS, SIRT2 is expressed in oligodendrocytes and neurons, and possibly in astrocytes (Li et al., 2007; Werner et al., 2007). As SIRT2 levels peak during myelination it has been suggested to function in oligodendrocyte differentiation. Two studies have confirmed this hypothesis, though one showed that SIRT2 is necessary for oligodendrocyte differentiation while the other reported an inhibitory role (Ji et al., 2011; Li et al., 2007). SIRT2 was also suggested to have a function in the mature CNS when it was observed that over-expression of SIRT2 inhibited neurite outgrowth and growth cone collapse in primary hipoccampal neurons (Harting and Knoll, 2010). This indicates that the level of SIRT2 could be a factor

influencing both axonal plasticity and degeneration and that SIRT2 inhibition could prevent neurodegeneration.

1.3.2.2. Therapeutic strategies involving SIRT2

A role for SIRT2 in neurodegeneration is supported by the finding that SIRT2 over-expression promotes axonal degeneration in the slow Wallerian degeneration model, while SIRT2 knock-down protects wild type cerebellar granule cells against axonal degeneration (Suzuki and Koike, 2007). Additionally, in cell models of Parkinson's Disease inhibition of SIRT2 rescued cells from α-synuclein induced toxicity (Outeiro et al., 2007). The same study also found that pharmacological inhibition of SIRT2 protected tyrosine hydroxylase neurons from death in primary midbrain culture and *D.melanogaster* Parkinson's Disease models (Outeiro et al., 2007).

Evidence for a protective role of SIRT2 inhibition in HD came from two important studies. Firstly, genetic knock-down of *Sirt2* to 50% of normal levels prevented photoreceptor neuron degeneration but did not rescue lethality in a HTT exon 1 *D.melanogaster* HD model (Pallos et al., 2008). In a second study, a specific SIRT2 inhibitor was demonstrated to be protective in *D.melanogaster*, *C.elegans* and primary striatal cell fragment models of HD (Luthi-Carter et al., 2010). Though microarray profiling of HD striatal cells showed that SIRT2 inhibition did not correct HD transcriptional dysregulation, it revealed an unanticipated function for SIRT2 in cholesterol biosynthesis. Treatment of striatal cells with the SIRT2 inhibitor AK-1 resulted in a down-regulation of key enzymes in the cholesterol synthesis pathway. Further examination revealed that SIRT2 facilitates the nuclear translocation of SREBP-2 and subsequent activation of the cholesterol synthesis pathway. Inhibition of SIRT2 decreased nuclear SREBP-2, cholesterogenic enzymes' transcript levels and cholesterol levels. It was therefore suggested that the neuroprotective effect observed after treatment with SIRT2 inhibitors was due to reducing the high cholesterol levels observed in the HD striatal cells used (Luthi-Carter et al., 2010).

Taken together these findings strongly indicate that SIRT2 inhibition could be protective in HD. *Sirt2* knock-out (*Sirt2*KO) mice develop normally and do not show any overt phenotypes, supporting a role for SIRT2 only under some, possibly stress related, circumstances. It is conceivable that a normally beneficial stress response of SIRT2 could be deleterious to the cell in a pathological context. Therefore, investigating the effect of *Sirt2* knock-out in a mouse model of HD will be vital to the validation of SIRT2 as a possible therapeutic target in HD.

1.4. Focus of this work

The therapeutic potential of HDAC6 or SIRT2 inhibition for neurodegenerative disease has so far only been tested in cell or invertebrate models of HD. In this study, *Hdac6* and *Sirt2* knock-out mice have been crossed to the R6/2 mouse model of HD and disease progression assessed with physiological, behavioural and molecular readouts. Genetic ablation of either of the two proteins did not modify HD progression, though absence of HDAC6 caused tubulin hyperacetylation throughout the brain. This work provides the first indication that previous findings about the therapeutic potential of HDAC6 or SIRT2 modulation in HD might not translate into a mammalian system.

2.0. MATERIALS AND METHODS

2.1. Materials

2.1.1. Commercial kits

Amersham ECL™ Plus Western Blotting detection kit (GE Healthcare)

BDNF Emax immuno-assay kit (Promega)

Bicinchocinic acid (BCA) Assay (Thermo Scientific)

BigDye Terminator v3.1 Cycle Sequencing kit (Applied Biosystems)

DNase I set (Qiagen)

Qiaquick Gel Extraction Kit (Qiagen)

Qiaprep Spin Miniprep Kit (Qiagen)

QIAzol Lysis reagent (Qiagen)

RNeasy Mini kit (Qiagen)

Seprion ELISA kit (Microsens Technology)

SIRT2 Fluor-de-Lys activity assay (Enzo Life Sciences)

TOPO TA cloning kit (Invitrogen)

Type-it Mutation Detection kit (Qiagen)

Vectastain ABC kit (Vector Labs)

2.1.2. Equipment

7650 accelerating rotarod (Ugo Basile)

96-well transparent polypropylene PCR plates for sequencing (Abgene)

96-well transparent polypropylene PCR plates (Bio-Rad)

96-well white polypropylene PCR plates (Bio-Rad)

96-well clear hard shell polystyrene ELISA plates (Nunc)

ABI 3730xl sequencer (Applied Biosystems)

AM1053 activity cages (Linton Instruments)

Analytical balance (Fisher)

Axiocam camera (Zeiss)

Axioscope 2.0 light microscope (Zeiss)

Bicycle inner tubing (for rotarod) (Evans Cycles)

Biofuge pico centrifuge (Heraeus)

Bio-Rad 680 96-well microplate reader (Bio-Rad)

CFX96 Real-time system thermocycler (Bio-Rad)

Chromo-4 thermo cycler (Bio-Rad)

Dyad thermocycler (Bio-Rad)

Fast-Prep ribolyser (MP Biomedicals)

GD40/50 vacuum gel drier (Life Technologies)

Gel-Doc EQ UV-transilluminator (Bio-Rad)

Grip strength meter (San Diego Instruments)

GS-800 Calibrated Densitometer (Bio-Rad)

Lysing matrix-D tubes (MP Biomedicals)

Nanodrop spectrophotometer (Thermo Scientific)

Omega plate reader (BMG Labtech)

OTF cryostat and 5040 microtome (Bright Instruments)

Polypropylene tubes (1.5 ml) (Eppendorf)

Protean Minigel Western blotting system (Bio-Rad)

PT 1200 homogenizer (Polytron)

Semi-transparent shoebox mouse cage (Techniplast Limited)

Seprion capture buffer (Microsens Technologies)

Seprion coated 96-well plates (Microsens Technologies)

TL-100 ultra-centrifuge (Beckman Coulter)

Transparent activity box (367 × 207 × 140 cm) (Techniplast Limited)

UBD2 heating block (Grant Instruments)

Vibra-Cell sonicator (Sonics and Materials Incorporated)

Xenon lamp envision fluorescent plate reader (Perkin Elmer)

X-ray film developer (Xenograph)

2.1.3. Reagents

2’ – deoxynucelotide triphosphates (dNTPs) (Invitrogen)

2-mercaptoethanol (Sigma)

3,3’diaminobenzidine (DAB) (Sigma)

4-(2-Hydroxyethyl)piperazine-1-ethanesulfonicacid sodium salt (HEPES) (Sigma)

Bacto Agar (BD)

Bacto Tryptone (BD)

Bacto Yeast extract (BD)

Ampicillin (Sigma)

Amplitaq DNA polymerase (Applied Biosystems)

Ammonium persulfate ($(NH_4)_2S_2O_8$) (Sigma)

Bovine serum albumin (BSA) (Sigma)

Bromophenol blue (Sigma)

Brilliant blue – R250 (Pierce)

Calcium chloride ($CaCl_2$) (VWR)

Chloroform (Sigma)

CHDI-001945-0000-005 (Evotec)

Complete protease inhibitor tablets (Roche)

Dimethyl sulphoxide (DMSO) (Sigma)

Dithiothreitol (DTT) (Sigma)

DPX mounting medium (Fluka)

Ethanol (VWR)

Ethidium bromide (Sigma)

Formaldehyde (Sigma)

Glycine (Sigma)

Glycerol (Sigma)

Hidi formamide (Applied Biosystems)

Histoclear (National Diagnostics)

Hydrochloric acid (HCl) (Sigma)

Hyperfilm ECL (Amersham)

Igepal-CA630 (NP-40) (Sigma)

Isopentane (Sigma)

Kanamycin (Sigma)

Lutrol F68 (BASF)

Magnesium chloride ($MgCl_2$) (Sigma)

MegaBACE ET900 size standards (Amersham)

Methanol (VWR)

Moloney murine leukemia virus reverse transcriptase (MMLV-RT) (Invitrogen)

MMLV-RT 1st strand buffer (5x) (Invitrogen)

Nicotinamide (NAM) (Sigma)

Non-fat dry milk powder (Marvel)

Polyethyleneglycol (PEG)-400 (BASF)

Phenyl methane sulphonyl fluoride (PMSF) (Fluka)

Phire Hot Start II Polymerase (New England Biolabs)

PhiX-HindIII Ladder (New England Biolabs)

PIPES (1,4-piperazinediethanesulphonic acid) (Sigma)

Phosphate buffered saline (PBS) tablets (Sigma)

Potassium chloride (VWR)

Potassium di-hydrogen phosphate (Sigma)

Precision mastermix (2x) (Primer Design)

Proteinase K (Fermentas)

Protogel (GeneFlow)

Protogel resolving buffer (GeneFlow)

Protogel stacking buffer (GeneFlow)

Protran nitrocellulose membrane (0.2 µm pore) (Whatman)

Rodent breeding chow (Special Diet Services)

RNasin (Promega)

Sodium dodecyl sulphate (SDS) (Sigma)

SDS-PAGE running buffer (10x) (GeneFlow)

Sodium bicarbonate ($NaHCO_3$)

Sodium carbonate (Na_2CO_3)

Sodium chloride (NaCl) (VWR)

Sodium deoxycholate (Sigma)

Sodium dihydrogen phosphate (NaH_2PO_4)

Sodium fluoride (NaF) (Sigma)

Sodium hydroxide (NaOH) (VWR)

Solutol HS15 (BASF)

Spectra pre-stained protein marker (Fermentas)

Sucrose (VWR)

Tetra methyl ethylene diamine (TEMED) (Sigma)

Thermostart master mix (Thermo Scientific)

TMB plus (Serotec)

Trichostatin A (TSA) (Sigma)

Triethanolamine hydrochloride (Sigma)

Tris Base (Sigma)

Ethylene di-amine tetra-acetic acid (EDTA) (Sigma)

Taq DNA Polymerase from *Thermus aquaticus* (Sigma)

Triton-X100 (Sigma)

Tween-20 (Sigma)

Ultra-pure agarose (Invitrogen)

Ultra-pure water (Sigma)

2.1.4. Antibodies

Table 2.1. Summary of application and dilution of all antibodies used in this thesis

Antibody	Catalogue number	Source	Dilution/ amount	Application
S830	N/A	In House	1:3000	WB
S830	N/A	In House	1:2000	IHC
S829	N/A	In House	1:1000	WB
MW8	N/A	P.Patterson	1:2000	SEP
MW8	N/A	P.Patterson	10 ng in 6µl	TR-FRET
MW8	N/A	P.Patterson	1ng in 6µl	TR-FRET
2B7	N/A	Novartis	10 ng in 6µl	TR-FRET
MW1	N/A	P.Patterson	1ng in 6µl	TR-FRET
HDAC6	N/A	T.Yao	1:250	WB
SIRT2	sc-20966	Santa Cruz	1:1000	WB
SIRT2	S8847	Sigma	1:1000	WB
SIRT1	2028	Cell Signalling	1:1000	WB
SIRT1	S5313	Sigma	1:1000	WB
SIRT1	sc-15404	Santa Cruz	1:1000	WB

Table 2.1 continued

Antibody	Catalogue number	Source	Dilution/ amount	Application
SIRT1	ab12193	Abcam	1:1000	WB
SIRT1	04-1557	Millipore	1:1000	WB
SREBP-2	ab30682	Abcam	1:1000	WB
Ac-FOXO1/3a	sc-49473	Santa Cruz	1:500	WB
Ac-p53	2570	Cell Signalling	1:100	WB
Ac-H4K16	07-329	Millipore	1:1000	WB
Ac-tubulin	T7451	Sigma	1:40 000	WB
Histone H4	04-858	Millipore	1:5000	WB
Histone H3	ab1791	Abcam	1:30 000	WB
α-tubulin	T9026	Sigma	1:30 000	WB
Actin	sc-47778	Sigma	1:40 000	WB
anti-Goat HRP	P044901	Dako	1:5000	WB
anti-Mouse HRP	P0260	Dako	1:5000	WB
anti-Rabbit HRP	32460	Pierce	1:20 000	WB
Anti-Goat biotinylated	BA-9500	Dako	1:2000	IHC
anti-BDNF (monoclonal)	BDNF EMAX kit	Promega	1:500	ELISA
anti-BDNF (polyclonal)	BDNF EMAX kit	Promega	1:1000	ELISA

Key: WB Western blotting, SEP Seprion ligand ELISA for aggregated huntingtin, TR-FRET time resolved Förster resonance energy transfer for soluble huntingtin, IHC immuno-histochemistry, HRP horse radish peroxidise conjugated.

The antibodies MW1 (Ko et al., 2001), MW8 (Ko et al., 2001), 2B7 (Weiss et al., 2009) and HDAC6 (Lee et al., 2010) are not commercially available and were kind gifts as noted in table 2.1. The antibodies S829 and S830 were developed in house by the Scottish Antibody Production Unit (Sathasivam et al., 2001).

2.1.5. Genotyping, sequencing and real time quantitative PCR primers and probes.

Table 2.2 Summary of in house designed primer and probe sequences used in this thesis.

Name	Application	5' – 3' sequence
HTT exon 1 forward	RT-qPCR	GCTGCACCGACCGAGT
HTT exon 1 reverse	RT-qPCR	CGCAGGCTGCAGTTAC
HTT exon 1 probe	RT-qPCR	CAGCTCCCTGTCCCGGCGG
Hdac1 forward	RT-qPCR	TCTGAATACAGCAAGCAGATGCA
Hdac1 reverse	RT-qPCR	ACAGAACTCAAACAAGCCATCAAAC
Hdac1 probe	RT-qPCR	AGATTCAATGTTGGTGAGGACTGTCCGG
Hdac2 forward	RT-qPCR	AGAAGATTGTCCGGTGTTTGATG
Hdac2 reverse	RT-qPCR	CACAGCCCCAGCAACTGAA
Hdac2 probe	RT-qPCR	TTGAGTTTTGTCAGCTCTCCACGGGTG
Hdac3 forward	RT-qPCR	TCAGCCCCACCAATATGCA
Hdac3 reverse	RT-qPCR	GAACTCGAAAAGTCCTGGAAACA
Hdac3 probe	RT-qPCR	CCTTAATGCCTTCAACGTGGGT
Hdac4 forward	RT-qPCR	CTGGCATCCCTGTGTCATTTG
Hdac4 reverse	RT-qPCR	ACACAAGACCTGTGGTGAACCTT
Hdac4 probe	RT-qPCR	CTGCCACCTTCCCCATGTCAGTCC
Hdac5 forward	RT-qPCR	CCAGAGCCGGCATAACT
Hdac5 reverse	RT-qPCR	GCAGGATTTCCAAGATGGTT
Hdac5 probe	RT-qPCR	TCCCAACGAGTCGGATGGCATGT
Hdac6 forward	RT-qPCR	GGAGACAACCCAGTACATGAATGAA
Hdac6 reverse	RT-qPCR	CGGAGGACAGAGCCTGTAG
Hdac6 probe	RT-qPCR	T ATCTGCATCC GAACTCATAT TCCTGTGCCT G
Hdac7 forward	RT-qPCR	CCCACCTGTCAGACCCAAGT
Hdac7 reverse	RT-qPCR	AGTCATAGACCAGCCCTGTAGCA
Hdac7 probe	RT-qPCR	CTCAACAGCTCAGAGACA
Hdac8 forward	RT-qPCR	GGCCCATCCATCCCTGTAG
Hdac8 reverse	RT-qPCR	TTTAGATCGCCGGAGACAGTTT

Table 2.2. Continued.

Name	Application	5' – 3' sequence
Hdac8 probe	RT-qPCR	TGGACGAGGGACCAGG
Hdac9 forward	RT-qPCR	TGGCAGAATCCTCGGTCAGT
Hdac9 reverse	RT-qPCR	CCCAGCAGGGCCATTGT
Hdac9 probe	RT-qPCR	TCTCCAGGGTCAGGTCCCAGTTCACC
Hdac10 forward	RT-qPCR	CCGCTATGAGCATGGAAGCT
Hdac10 reverse	RT-qPCR	CAACTGCATCTGCATCAGACTCT
Hdac10 probe	RT-qPCR	CTGGCCGTTTCTC
Hdac11 forward	RT-qPCR	TGGGCATGAGCGAGACTTC
Hdac11 reverse	RT-qPCR	GCGGTTGTAAACATCCATGATG
Hdac11 probe	RT-qPCR	TGGGTGACAAGCGAG
Sirt1 forward	RT-qPCR	TGTTGGTTGACTTCATCTTCCTT
Sirt1 reverse	RT-qPCR	TCCAATGGCTTTTGAAAACTTTA
Sirt1 probe	RT-qPCR	TTCATTTGTATGATACATTCGTATGTATG
Sirt2 forward	RT-qPCR	TCCTGCAGAAAAGAATACACGAT
Sirt2 reverse	RT-qPCR	CGATATCAGGCTTTACCACACTC
Sirt2 probe	RT-qPCR	AGAGAAGATCTTCTCAGAAGCAACTCC
Sirt3 forward	RT-qPCR	ACAAGAACTGCTGGATCTTATGC
Sirt3 reverse	RT-qPCR	TCTTGCTGGACATAGGATGATCT
Sirt3 probe	RT-qPCR	ACGTGGCAAGCTG GATGGACAGGA
Sirt5 forward	RT-qPCR	CAGAGGCGCTGGAGGTTACTGGAG
Sirt5 reverse	RT-qPCR	CCGGGCTTCACACTGGGCAATGGC
Sirt5 probe	RT-qPCR	AGGCTCAGGACCTGGCAACCCCTCAG
Sirt7 forward	RT-qPCR	GCCTCCCTCTTTCTACTCCTTATC
Sirt7 reverse	RT-qPCR	TGCTCAGACTGGAGGCTTAGTTA
Sirt7 probe	RT-qPCR	TACAAGTGTTCACTTTATAGAAGCCT
Bdnf-b forward	RT-qPCR	CTGGATGCCGCAAACATGTC
Bdnf-b reverse	RT-qPCR	GCAACCGAAGTATGAAATAACCATAG

Table 2.2. Continued.

Name	Application	5' – 3' sequence
Bdnf-b probe	RT-qPCR	TTCCACCAGGTGAGAAGAGTGATGACCAT

KEY: RT-qPCR - real time - quantitative PCR; *Bdnf-b* refers to protein coding exon i.e. *Bdnf* expressed from all promoters); *HTT* exon 1 (Human Huntington's disease transgene), Primer and probe mixes for *ActB, Atp5b*, *Canx*, *Gapdh, Rpl13a* and *Ubc* RT-qPCR assays were purchased from Primer Design. All RT-qPCR probes were labelled 5' with FAM and 3' with TAMRA.

Table 2.3. Primer probe mixes obtained from Primer Design. Forward and reverse primer sequences shown as given by manufacturer. Probe sequences were not disclosed.

Name	Application	5' – 3' sequence
Hmgcr forward	RT-qPCR	CCGAATTGTATGTGGCACTG
Hmgcr reverse	RT-qPCR	TTATCTTTGATCTGTTGTGAACCAT
*Hmgcs1*forward	RT-qPCR	CCTGGACCGCTGCTATTCT
Hmgcs1 reverse	RT-qPCR	CAGTTTACAATATGGTGAGTGAAAGA
Fdft1 forward	RT-qPCR	GGCGGAATTTTATACCCAAGATG
Fdft1 reverse	RT-qPCR	GCTGCGACTGGTCTGATTG
Fdps forward	RT-qPCR	TACAACCGCCTCAAGAGTCT
Fdps reverse	RT-qPCR	GGGGTCACTTTCTCGTTTG
Sqle forward	RT-qPCR	CAGAGCCCAATGTAAAGTTTATAGAA
Sqle reverse	RT-qPCR	CCCAGTCTCCTTGTCCTTGT
Idi1 forward	RT-qPCR	GTTGTTGAGTCCCTAACCCTAAA
Idi1 reverse	RT-qPCR	CGCCATATACTTCCCTATGAAC
Dhcr7 forward	RT-qPCR	CTGCCCTACCTCTACACACT
*Dhcr7*reverse	RT-qPCR	TGGTTGGTCATTCGGAAGATATA

Table 2.3. Continued.

Name	Application	5' – 3' sequence
Sirt4 forward	RT-qPCR	GGAAGAAGGACCAGGCAGAA
Sirt4 reverse	RT-qPCR	GCTTCAGTCAGACACATCCATT
Sirt6 forward	RT-qPCR	ACCCTGCGTGCTAGACAAA
Sirt6 reverse	RT-qPCR	GGGCTTGGACTTATACGAAACA

KEY: RT-qPCR - real time - quantitative PCR; *Hmgcr* – 3-hydroxy-3-methylglutaryl CoA reductase; *Hmgcs1* - 3-hydroxy-3-methylglutaryl Coenzyme A synthase 1; *Fdft1* – farnesyl diphosphate farnesyltransferase 1, *Fdps* – farnesyl diphosphate synthase, *Sqle* – squalene epoxidase, *Dhcr7* – 7-dehydrocholesterol reductase, *Idi1* – isopentenyl diphosphate delta isomerase 1.

Table 2.4. Primers used for genotyping and repeat sizing mice.

Name	Application	5' – 3' sequence
HTT exon 1 forward	Genotyping	CGCAGGCTAGGGCTGTCAATCATGCT
HTT exon1 reverse	Genotyping	GACTCACGGTCGGTGCAGCGGTTCC
Hdac4 forward	Genotyping	CTTGTTGAGAACAAACTCCTGCAGCT
Hdac4 reverse	Genotyping	AGCCCTACACTAGTGTGTGTTACACA
Hdac6 forward	Genotyping	GTACAATGTGGCTCACAGAA
Hdac6 reverse 1	Genotyping	CAACTCTGCCTCTCCTGGAT
Hdac6 reverse 2	Genotyping	CAGGCACAGGAATATGAGTT
Sirt2 forward	Genotyping	CAGGTGTGAGCAGTGTCAGAGTG
Sirt2 reverse KO	Genotyping	GACGTCGAGGTGCCCGAAGGACC
Sirt2 reverse WT	Genotyping	CCAGCCCAGAGTGGACACT
HTT exon 1 forward	Repeat sizing	GAGTCCCTCAAGTCCTTCCAGCA
HTT exon1 reverse	Repeat sizing	GCCCAAACTCACGGTCGGT

KEY: *HTT* exon 1 (Human Huntington's disease transgene).

Table 2.5. Primers used for sequencing the *Sirt2* mutation.

Name	Application	5' – 3' sequence
Sirt2 forward	Sequencing	CAGGTGTGAGCAGTGTCAGAGTG
Sirt2 reverse KO	Sequencing	GACGTCGAGGTGCCCGAAGGACC
Sirt2 reverse WT	Sequencing	CCAGCCCAGAGTGGACACT
Sirt2 forward Seq 2	Sequencing	TCGTGCGCTCCTTTCGGTC
Sirt2 forward Seq 3	Sequencing	TGGCTTCGGTCGGAGCCAT
Sirt2 forward Seq 4	Sequencing	AGATCATCAATTTCGATCCGCTCCT
Sirt2 forward Seq 5	Sequencing	TGTTCAGCAGGGTCGGCGTGTT
Sirt2 forward Seq 6	Sequencing	TCAACTCGGCCATGCGCGGG
Sirt2 forward Seq 7	Sequencing	AGGCCTTCCATCTGTTGCTG
Sirt2 reverse Seq 1	Sequencing	ATGCAGGAGAAGAAGCGCGA
Sirt2 reverse Seq 2	Sequencing	CCAGCCCAGAGTGGACACT

2.1.6. Prepared solutions, buffers, and gels

All solutions, buffers, and gels were prepared with distilled deionized water unless otherwise stated.

Inhibitors added to buffers consisted of:

1 mM PMSF

5 µM TSA

10 mM nicotinamide

Complete protease inhibitor cocktail (1 tablet in 50 mL)

Acid extraction buffer

5% (v/v) Triton X-100

3 mM DTT

1 mM Orthovanadate

5 mM NaF

Inhibitors

Agarose gel for resolution of PCR products (Prepared in 1x TE)

1% (w/v) Ultra-pure agarose

0.1 µg/ml Ethidium bromide

AM buffer

67 mM Tris-HCl pH 8.8

16.6 mM $(NH_4)_2SO4$

2 mM $MgCl_2$

0.17 mg/ml BSA

BDNF ELISA lysis buffer

100 mM PIPES pH 7.0

500 mM NaCl

0.2% (v/v) Triton-X100

0.1% (w/v) NaN_3

2 mM EDTA pH 8.0

2% (w/v) BSA

200 µM PMSF

Complete protease inhibitor cocktail (1 tablet in 50 mL)

Carbonate buffer

25 mM $NaHCO_3$

25 mM Na_2CO_3

Adjusted to pH 9.7 with 1 M HCl/1 M NaOH

Coomassie staining solution

0.25% (w/v) Brilliant blue R-250

50% (v/v) methanol

10% (v/v) acetic acid

Coomassie de-staining solution

16.5% (v/v) methanol

0.5% (v/v) acetic acid

HEPES Buffer

50 mM HEPES pH 7.0

150 mM NaCl

10 mM EDTA

1% NP-40

0.5% sodium deoxycholate

0.1% SDS

Inhibitors

Immuno-peroxidase blocking solution (prepared in TBS)

2% (w/v) BSA

0.1% (v/v) Triton-X100

Immuno-peroxidase staining solution (prepared in TBS)

0.05% (w/v) DAB

100 mM Tris–HCl pH 7.5

0.03% (v/v) H_2O_2 solution

KCl buffer

50 mM Tris–HCl pH 8.0

10% glycerol

5 mM EDTA

150 mM KCl

10 mM DTT

Inhibitors

Laemmli loading buffer (2x)

125 mM Tris–HCl pH 6.8

20% glycerol

4% SDS

0.01% (w/v) bromophenol blue

Luria-Berthani (LB) liquid medium

1% (w/v) Bacto-tryptone

0.5% (w/v) yeast extract

1% (w/v) NaCl

Luria-Berthani (LB) solid medium

1% (w/v) Bacto-tryptone

0.5% (w/v) yeast extract

1% (w/v) NaCl

1.5% (w/v) agar

Phosphate buffered saline (PBS)

137 mM NaCl

2.7 mM KCl

100 mM Na_2HPO_4

2 mM KH_2PO_4

Adjusted pH to 7.4 with HCl

Resolving Gel

20 – 60% (v/v) (for 6-18% arylamide gels) Protogel

25% (v/v) Protogel resolving buffer

1% (w/v) APS

0.1% (v/v) TEMED

RIPA Buffer

150 mM NaCl

1% (v/v) NP-40

0.5% (w/v) Na deoxycholate

0.1% (w/v) SDS

50 mM Tris-HCl pH 8.0

1 mM 2-mercaptoethanol

10 mM DTT

Inhibitors

Seprion ELISA conjugate buffer

150 mM NaCl

4% (w/v) BSA

1% (w/v) non-fat dried milk

0.1% (v/v) Tween-20

Sequencing precipitation solution

120 mM $C_2H_3O_2Na$ (sodium acetate)

Made up in 95% absolute ethanol

Stacking Gel

13% (v/v) Protogel

25% (v/v) Protogel stacking buffer

0.1% (w/v) APS

0.2% (v/v) TEMED

Sucrose buffer

320 mM sucrose

10 mM Tris-HCl pH 7.4

50 mM KCl

1 mM EDTA

5% NP-40

Inhibitors

Sucrose Buffer 1 (for nuclear/cytoplasmic fractionation)

575 mM sucrose

25 mM KCL

50 mM triethanolamine hydrochloride pH 7.5

5 mM $MgCl_2$

1 mM DTT

Inhibitors

Sucrose Buffer 2 (for nuclear/cytoplasmic fractionation)

2.3 M sucrose

2.5 mM KCL

50 mM triethanolamine hydrochloride pH 7.5

2.5 mM $MgCl_2$

1 mM DTT

Inhibitors

Tail lysis buffer (For DNA extraction)

50 mM Tris-HCl pH 8.0

100 mM EDTA

0.5% (w/v) SDS

0.5 mg/ml proteinase K

Tris buffered saline (TBS)

100 mM Tris-HCl pH 7.4

150 mM NaCl

Adjust pH to 7.4 using HCl

Tris buffered saline-Tween 20 (TBST)

20 mM Tris-HCl pH 7.6

150 mM NaCl

0.05% (v/v) Tween 20

Tris-EDTA (TE) (1x)

10 mM Tris-HCl pH 8

0.1 mM EDTA

TR-FRET Antibody master mix buffer

50 mM NaH_2PO_4

400 mM NaF

0.1% (w/v) BSA

0.05% (v/v) Tween 20

"Trottier" buffer

100 mM Tris-HCl pH 9.0

2% SDS

6.7% glycerol

700 mM 2-mercaptoethanol

Inhibitors

TX Buffer

50 mM Tris-HCl pH 7.5

150 mM NaCl

2 mM EDTA

1% (v/v) Triton - X100

Inhibitors

Vehicle for CHDI-001945-0000-005 dosing

30% PEG-400

20% Solutol HS15

0.5% Lutrol F68

Western blotting transfer buffer

25 mM Tris–HCl

192 mM glycine

20% v/v methanol

2.1.7. Computer programs and internet pages

AM logger software (Linton Instruments)

SPSS statistics software (IBM)

Axiovision 4.1 (Zeiss)

Quantity One (Biorad)

Excel (Microsoft)

Opticon 4 (Biorad)

Omega (BMG Labtech)

Gene Mapper v5.2 - 3730xl (Applied Biosystems)

Vector NTI (Invitrogen)

Sequencing Analysis 5.3.1 (Applied Biosystems)

BLAST (NCBI)

2.2. Methods:

2.2.1. Mouse strains

Hemizygous R6/2 mice were maintained by backcrossing R6/2 males to CBAxC57BL/6 F1 (CBF) females (B6CBAF1/OlaHsd, Harlan Olac, UK). *Hdac6* knock-out (*Hdac6*KO) mice were on C57BL/6 background and were backcrossed once to CBF. *Sirt2* knock-out (*Sirt2*KO) mice were on C57BL/6/129Ola background and were backcrossed to CBF three times.

2.2.2. Mouse husbandry

At 4 weeks of age, mice were weaned into cages of 5 or 6 animals (*Sirt2KO*xR6/2 phenotypic assessment study only). For both *Hdac6*KOxR6/2 and *Sirt2*KOxR6/2 phenotypic assessment studies, each cage contained at least one representative of each genotype when available. Animals were housed under 12h light/12h dark cycle, with unlimited access to water and chow (Special Diet Services, Witham, UK). Cages were environmentally enriched with a cardboard tube. R6/2 mice and all mice in phenotypic assessment trials were always given mash food consisting of powdered chow mixed with water from 12 weeks of age until sacrificed. Mice in the *Hdac6*KOxR6/2 phenotypic assessment study were additionally given mash food at 4-6 weeks of age.

All procedures were approved by the King's College London Ethical Review Process and were in accordance with the UK Home Office regulations.

2.2.3. Mouse genotyping and repeat sizing

All mice were genotyped by PCR of tail-tip DNA. Tails were collected at 10-14 days of age or post mortem and incubated at 50°C overnight in lysis buffer. Proteins were precipitated with 300 µL saturated salt solution and spun at 16,200 X *g* for 30 min. The supernatant was decanted into tubes containing 650 µL 100% ethanol and shaken vigorously. The DNA was pelleted by centrifugation at 16,200 X *g* for 15 min. The supernatant was discarded and pellets were washed with 70% ethanol,

spun for 5 min at 16,200 *X g* and the supernatant was removed. Pellets were air dried until all ethanol was evaporated and re-suspended in 250 µL 0.1x TE buffer.

R6/2 mice were genotyped with *HTT* exon 1 forward and reverse primers at 5 µM final concentration. *Hdac4* forward and reverse primers at 10 µM final concentration were included as internal control. All primers were used in a 10 µL reaction also containing 1 µL 100 ng/µL DNA, 5 µL Thermostart Mastermix (2x) and 1 µL DMSO. Cycling conditions were as follows: 94°C for 15 min, (30 s at 94°C; 30 s at 60°C, 60 s at 72°C)x35 and 10 min at 72°C.

For *Hdac6* genotyping, 1 µL of all 3 primers was used at 10 µM in one multiplex 10 µL reaction, also containing 1 µL of 100 ng/µL DNA, 0.8 µL 25 mM $MgCl_2$, 1 µL 2 mM dNTP, 1 µL Sigma 10xPCR buffer and 0.1 µL Sigma Taq Polymerase. Cycling conditions were as follows: 94°C for 5 min, (94°C for 30s, 64°C for 30s and 72°C for 1 min)x40, followed by 10 min at 72°C.

Sirt2 mice were genotyped with all 3 primers at 5 µM final concentration in a 10 µL multiplex reaction also containing 1 µL 100 ng/µL DNA, 1.5 µL 2 mM dNTP, 3 µL Phire reaction buffer (5x) and 0.2 µL Phire Hot Start II Polymerase. Cycling conditions were as follows: 98°C for 30 s, (98°C for 20s, 63°C for 20s and 72°C for 30 min)x35, followed by 1 min at 72°C.

The CAG repeat size was determined using a FAM labelled forward primer and an unlabelled reverse primer, both at 100 mM in a 10 µL reaction also containing 100 ng DNA, 1 µL dNTP's (2 mM), 1 µL DMSO, 1 µL AM buffer, 0.1 µL Amplitaq, with cycling conditions of 94°C for 90 s, (94°C for 30 s, 65°C for 30 s, 72°C for 90 s)x25, followed by 10 min at 72°C. Sequencing reactions containing 1 µL of the FAM labelled PCR product, 0.04 µL of MegaBACE ET900 size standard, and 9 µL of Hidi-formamide were denatured at 94°C for 5 min and analysied with the ABI3730 sequencer. Data was analysed using Gene Mapper software.

2.2.4. Dosing of mice with CHDI-001945-0000-005

CHDI-001945-0000-005 (CHDI194500) SIRT1/SIRT2 inhibitor was obtained from Evotec through the CHDI Foundation. The desired amount of CHDI194500 was prepared freshly before dosing by weighing out the desired amount using an analytical balance and dissolving in "vehicle for CHDI194500 dosing solution". 12 week old wild type and R6/2 mice were weighed and given one acute dose of either vehicle, 1 mg/kg or 3 mg/kg solution of CHDI194500 by oral gavage in the morning and dissected either 4 or 8 hours later. Each treatment group contained age, sex and CAG repeat number matched mice.

2.2.5. Mouse phenotypic assessment

Mice from *Hdac6*KOxR6/2 and *Sirt2*KOxR6/2 crosses were phenotyped using the same procedures. All tests were performed blind to the genotype.

2.2.5.1. Weight/brain weight

Mice were weighed weekly to the nearest 0.01 g. Brains were harvested with optic bulbs and weighed to the nearest 0.001 g immediately after cervical dislocation.

2.2.5.2. Grip strength

Forelimb grip strength was assessed at 4 weeks of age and then weekly from 11 to 14 weeks (*Hdac6*KOxR6/2) or bi-weekly from 7 weeks of age (*Sirt2KO*xR6/2), always prior to rotarod measurements. Mice were gently swung forward to firmly grasp onto the central metal frame and were pulled back until the grip on the metal frame was released, the force exerted measured by the attached force meter. Five measurements were performed for each mouse and the best three were used for statistical analysis.

2.2.5.3. Rotarod

Motor coordination was assessed using an Ugo Basile 7650 rotarod, modified to accelerate from 4 to 44 rpm over 300 s. The ridges of the plastic drums were covered with bicycle inner tubing to provide a smooth slip-free surface. Mice were placed on the rotarod drum for 20 s for acclimatisation before the rotarod was allowed to accelerate. If a mouse fell 3 times before acceleration was switched on, the latency to fall was recorded as 20 s. Mice were measured three times a day for 4 days at 4 weeks of age and three times a day for 3 days at 8, 10, 12 and 14 weeks of age. Data from the first two days (at 4 weeks of age) or first day (all other time points) were not used for statistical analysis.

2.2.5.4. Activity

Spontaneous exploratory motor activity was measured at 5, 7, 9, 11 and 13 weeks of age by placing mice individually in the 1053 activity cages for 30 min during the light phase. Each cage measured 367 x 207 x 140 cm, had a thin layer of wood chippings, 4 food pellets and a water bottle distributed so as not to interfere with the array of infrared beams that measured the mouse activity and mobility. Mice were tested at the same time of day, with male mice always tested before female mice and cages cleaned thoroughly in between the two sexes. Data collection was started immediately after the mouse was placed in the activity cage, by the AM Logger software recording the number of beam breaks occurring in 1 min intervals. Data was then exported to Microsoft Excel and analysed for activity (total number of beam brakes in the lower level), mobility (at least two consecutive beam breaks in the lower level), rearing (beam break in upper level) and centre rearing (beam breaks in upper level away from the cage walls).

2.2.6. Sirt2 KO mutation sequencing

2.2.6.1. PCR and cloning of the product

DNA was isolated from *Sirt2*KO and wild type littermate mice as described above (2.2.3). PCR was performed with Qiagen Type-it Mutation Detection kit using 200 ng DNA in 50 µL reaction containing also 25 µL 2x Master mix, 5 µL forward primer, 5 µL reverse primer and 10 µL Q solution, with cycling conditions of: 95°C for 10 min, (95°C for 30 s, 65°C for 90 s, 72°C for 60 s)x30 and 68°C for 10 min. The product was run on a 1.5% agarose gel and excised under long range UV light (360 nm). The Qiaquick Gel Extraction kit was used according to manufacturer's instructions. Briefly, the gel slice was solubilised at 50°C in 3 volumes of buffer QG (provided with the kit). Before loading onto an anion exchange chromatography column, 1 volume of isopropanol was added. DNA was washed with buffer QG and PE (provided with the kit), eluted with ultra-pure water and quantified using nanodrop.

The purified PCR product was cloned into TOP10 bacteria using the TOPO TA cloning kit according to manufacturer's instructions. Briefly, 1 µL TOPO vector (provided with the kit) was incubated with 1 µL PCR product (50-100 ng DNA) in ligation reaction containing also 1 µL salt solution (provided with the kit) and 1 µL water for 30 min at room temperature. The ligation reaction was then added to TOP10 heat competent bacteria and left for 30 min on ice. Bacteria were heat shocked for 45 s at 42°C, transferred to ice for 5 min, incubated with pre-warmed SOC medium (provided with the kit) for 30 min at 37°C shaking at 200 rpm and streaked onto agar plates with 100 µg/mL of appropriate antibiotic.

2.2.6.2. DNA isolation and sequencing

Bacterial colonies were picked and grown overnight in 3 mL LB medium with 100 µg/mL of appropriate antibiotic at 37°C and shaking at 200 rpm. Plasmid DNA was isolated with Qiaprep Spin Miniprep Kit according to manufacturer's instructions and eluted in ultra-pure water.

Sequencing reactions were carried out in 6.25 µL volume containing 200-500 ng DNA, 0.25 µL BigDye v3.1, 1.25 sequencing buffer (provided with the BigDye kit), 0.25 µL primer (80 ng/µL) under cycling conditions of: 96°C for 2 min, (96°C for 30 s, 50°C for 20 s, 60°C for 1 min)x30. Sequencing PCR products were precipitated with 26 µL sequencing precipitation solution, incubated for 10 min at room temperature and centrifuged at 3,000 X *g* for 20 min. The supernatant was removed with a brief spin (<200 X *g* and less than 5 s) of the plate inverted onto tissue paper. The pellet was washed with 100 µL 70% ethanol, centrifuged at 3,000 X *g* for 20 min, cleared of supernatant as described above and re-suspended in 10 µL Hidi-formamide. The sample was then denatured at 96°C for 2 min and analysed with an ABI3730 sequencer. Sequence traces were analysed with the ABI Sequencing Analysis and Vector NTI programmes.

2.2.7. Tissue preparation

Dissected brain regions or peripheral tissues were snap frozen in liquid nitrogen and stored at -80°C until use. Dissected whole brains were snap frozen in isopentane at -55°C, transferred to 5 mL Bijou tubes and stored at -80°C until used.

2.2.7.1. Nuclear/cytoplasmic fractionation

Whole brains were homogenised in 2 volumes of ice cold sucrose buffer 1 with 10 gentle pestle strokes in a Dounce homogeniser. The homogenates were centrifuged at 500 X *g* for 15 min at 4°C. The supernatant (cytoplasmic fraction) was removed and stored at -80°C. The pellet was re-suspended in 1 mL of ice cold buffer 1 with an additional 10 gentle pestle strokes in the Dounce homogeniser. Two volumes of ice cold sucrose buffer 2 were added to the homogenate and the solution was mixed until uniform. Ultracentrifuge tubes were layered with a 0.5 mL cushion of sucrose buffer 2 and the homogenate was gently layered on top. The tubes were appropriately balanced and spun in pre-cooled SW41 rotor tubes at 124,000 X *g* for

1h at 4°C. Subsequently, the supernatant was removed and the pellet re-suspended in 0.5 mL buffer 1, transferred to fresh 1.5 mL tubes and spun at 800 X *g* for 15 min at 4°C. The supernatant was removed and the pellet was re-suspended in 0.5mL buffer 1, spun at 800 X *g* for 15 min at 4°C twice more before being re-suspended in 50 µL of buffer 1. The nuclear fraction was sonicated on ice for 10s at 80Hz. The protein concentration of both fractions was determined with the BCA assay for each sample.

2.2.7.2. Acid extraction of histone proteins

Tissues were homogenised in 1 volume of acid extraction buffer using a polytron homogenising probe and centrifuged at 800 X *g* for 8 min at 4°C. The supernatant was removed and the pellet washed twice by re-suspending in acid extraction buffer, and centrifuging at 800 X *g* for 8 min at 4°C. The pellet was then re-suspended in 80 µL of 0.2 M HCl and incubated for 3 h at 4°C with constant shaking at 800 rpm. Samples were then centrifuged at 800 X *g* for 8 min at 4°C, the supernatant collected, neutralised with 16 µL of 1 M NaOH, and the protein concentration determined for each sample with the BCA kit.

2.2.7.3. Tissue preparation for SDS PAGE and Western blotting

Unless nuclear/cytoplasmic fractionation, acid extraction or Seprion ELISA were performed, tissue was homogenised in 1 volume of ice cold Hepes, KCl, RIPA, Sucrose, “Trottier” or TX buffer (all buffers – SIRT1 antibody testing; TX – tubulin acetylation, RIPA – all other experiments) with a polytron homogenising probe. Homogenates were sonicated on ice for 10 s at 80 Hz. Lysates were cleared by centrifugation at 16,200 X *g* for 15 min at 4°C. Protein concentration was measured by BCA assay for each sample.

2.2.8. SDS PAGE and Western blotting

Samples were diluted with 2x Laemmli buffer and denatured for 5 min at 95°C. Equal amounts of protein were loaded onto SDS polyacrylamide gel with a size reference. Proteins were transferred onto nitrocellulose membrane at 120 V for 90 min by submerged transfer apparatus in transfer buffer. Membranes were blocked in 5% non-fat dried milk in PBS for at least 1 h. Primary antibodies were applied in 0.02% PBS-Tween 20 (PBST) for 20 min (acetylated α-tubulin; α-tubulin; actin; H3 and H4), 1 hour (S830; SIRT2 (S8847) at room temperature or overnight (HDAC6; SIRT2 (sc-20966); SIRT1 (all), SREBP-2, Acetylated H4K16; Acetylated p53; Acetylated FOXO1) at 4°C. Blots were washed three times for 5 min in 0.2% PBST and incubated with appropriate HRP coupled secondary antibody. For signal detection enhanced chemi-luminescence (ECL) detection system, hyperfilms and Xenograph developer were used according to the manufacturers' instructions. Signals were quantified using GS-800 densitometer.

Antibodies and dilutions at which they were used are presented in Table 2.1.

2.2.8.1. Coomassie staining of polyacrylamide gels

Polyacrylamide gels were stained with Coomassie solution for 30 min with gentle agitation. Gels were then washed several times in ddH_2O and three times for 10 min in de-staining solution. Gels were dried in a vacuum gel drier.

2.2.9. Seprion ELISA

2.5% (w/v) (brain) or 10% (quadriceps muscle) lysates were prepared by homogenising tissue in ice cold RIPA buffer in Lysing Matrix D tubes in a ribolyser. 15 µL of homogenate was mixed in sequential order with 3 µL of 10% SDS, 62 µL of ultra-pure water and 20 µL 5x Seprion capture buffer. Samples was loaded onto Seprion plates and incubated for 1 h at room temperature with gentle shaking.

Samples were removed and the plate was washed 5x with sterile filtered 0.1% PBS-Tween 20 (PBST). Plates were incubated with MW8 antibody diluted in freshly prepared conjugate buffer for 1 h at room temperature with gentle shaking. Primary antibody was removed, plates washed as above, incubated with secondary antibody for 45 min at room temperature with gentle shaking, washed again and incubated for 5-10 min with TMB Plus (in the dark). Signal development was stopped with 0.5 M HCl and absorbance was immediately measured with a microplate reader at 450 nm.

2.2.10. BDNF ELISA

Flat bottom 96-well ELISA plates were coated with BDNF monoclonal antibody diluted in carbonate buffer and incubated overnight at 4°C. Contents were removed and plates were washed 5x with TBST and blocked with Block&Sample buffer (provided with the kit) for 1 h at room temperature without shaking. 2.2% (w/v) lysates were prepared in BDNF ELISA lysis buffer, sonicated briefly on ice (10 pulses at 80 Hz), and cleared by centrifugation at 16,200 X *g* for 15 min at 4°C. After the Block&Sample buffer was removed from the plate, it was washed as above and lysates as well as a series of dilutions of BDNF standard (provided with the kit) were applied to the plate and incubated for 2 h at room temperature with a shaking speed of 400 rpm. Contents were removed, plates washed as above and incubated with anti-human BDNF polyclonal antibody in Block&Sample buffer for 2 h as before. Next, plates were washed, incubated with secondary antibody in Block&Sample buffer for 1 h, washed again, and incubated with 100 µL TMB One for 10 min (in the dark). The reaction was stopped with 1 M HCl and optical density was immediately measured at 450 nm by a 96-well microplate reader.

2.2.11. TR-FRET

Mouse brain and liver tissues were sonicated on ice in 10 volumes of 0.4% PBS-Triton-X100 supplemented with protease inhibitors. Quadriceps muscle was homogenised in 10 volumes of the above buffer by ribolysing in Lysing Matrix D tubes. 1.5 ng/well europium-cryptate and 30 ng/well D2-conjugated antibodies were incubated with 10 µL homogenate in a 384-well microplate overnight at 4°C. Signal was measured after excitation at 320 nm (time delay 100 µs, window 400 µs, 100 flashes/well) with a xenon lamp Envision plate reader. Signal was measured at 680 nm (europium-cryptate background excitation) and at 665 nm (specific excitation of D2 by europium-cryptate). Relative fluorescence of 665/680 nm represented artefact corrected amount of simultaneous binding of both antibodies to huntingtin trans-protein.

2.2.12. RNA extraction

RNA extraction was performed using Qiazol, an RNeasy kit, and Rnase-free DNaseI supplied by Qiagen, according to manufacturer's instructions. All steps were performed at room temperature. Mouse tissue was homogenised in two volumes of Qiazol and snap frozen on dry ice. After thawing, the homogenates were left for 5 min at room temperature. Subsequently, 200 µL of chloroform was added and homogenates were shaken vigorously for 15 s and spun at 16,200 X *g* for 15 min. The aqueous phase was transferred to a fresh tube to which one volume of 70% ethanol was added. The tubes were shaken and the contents were transferred to Qiagen RNeasy kit extraction columns. Binding of the RNA and all subsequent washing steps were achieved by centrifugation for 15 s at 16,200 X *g*. The columns were washed with 350 µL buffer RW1 (provided with kit) and 80 µL of Qiagen RNase-free DNaseI (10 µL DNaseI stock in 70 µL RDD buffer) was applied to the column centre and incubated at room temperature for 30 min. The DNaseI was washed away with 350 µL buffer RW1. Next, the columns were washed twice with 500 µL buffer RPE (provided with kit). Columns were then placed into fresh

collection tubes and spun again to remove any residual buffer. RNA was eluted into new 1.5 mL collection tubes by applying 50-40 µL RNase free water directly to the middle of the column and incubating for 1 min before centrifugation.

2.2.13. cDNA synthesis

RNA concentration and quality were assessed by measuring absorbance at 230 nm and 260 nm by nanodrop spectrophotometer for each sample. 1 µg total RNA was incubated with 9 µL ultra-pure water, 2 µL DTT (0.1 M) and 1 µL random hexamer primers (100 ng/µL) for 2 min at 94°C and cooled on ice for 2 min. To this, 8 µL master mix containing 2 µL dNTPs (10 mM), 4 µL 1^{st} strand buffer (5x), 0.25 µL RNasin, 1 µL MMLV-Reverse transcriptase, and 0.75 µL ultra-pure water was added and the samples were incubated for 10 min at 23°C, 40 min at 37°C and 5 min at 94°C, cooled down to 4°C and subsequently diluted 1:10 with ultra-pure water.

2.2.14. Real Time qPCR

Taqman real time qPCR reactions were performed in triplicate or duplicate (technical replicates) on thermocyclers Chromo4 or CFX96 respectively. For genes where primer/probe mix was available, 3 µL of cDNA was incubated with 0.6 µL primer/probe mix, 6 µL Precision Master Mix (2x) and 2.4 µL water. For other genes, 3 µL of cDNA was combined with 0.45 µL of each primer (100 µM), 0.3 µL of the probe (100 µM), 7.5 µL of Precision Master Mix and 3.3 µL water. The reaction for housekeeping genes was incubated for 10 min at 95°C, followed by 40 cycles of 95°C for 15 s, 50°C for 30 s and then signal reading. The reaction for genes of interest was incubated for 10 min at 95°C, followed by 40 cycles of 95°C for 15 s, 60°C for 30 s and then signal reading. The data was analysed relative to housekeeping genes with the ΔCt method. Samples that did not have two reads less than 0.5 Ct from each other were excluded from analysis.

2.2.15. Immunohistochemistry

Whole brains were cut into 15 µm saggital sections with a Bright instruments cryostat. Sections were incubated briefly in TBS for rehydration, fixed for 15 min in 4% paraformaldehyde in TBS, washed twice in TBS for 15 min and permeabilised in 0.1% TBS-Triton-X100 (v/v) for 15 min. Next, sections were washed twice for 15 min in TBS, incubated for 10 min in 4% hydrogen peroxide, washed in water and blocked in immune-peroxidase blocking solution. S830 primary antibody was diluted in immune-peroxidase solution and incubated with the sections overnight at 4°C. Subsequently, sections were washed twice for 15 min in TBS and incubated for 1 h at room temperature with biotinylated secondary antibody diluted in immune-peroxidase blocking solution. After washing twice with TBS for 15 min, sections were incubated with the ABC-HRP complex from Elite ABC kit according to manufacturer's instructions. Staining solution was then applied, colour allowed to develop for 5 min and sections were washed extensively. Sections were then stained with 20% (v/v) Methyl green, washed and allowed to dry overnight. Further dehydration was achieved by washing with 100% ethanol and histoclear. Slides were mounted with coverslips with DPX mounting media. Images were taken from the Axioscope 2 light microscope with Axiocam camera and Axiovision software.

2.2.16. Statistical Analysis

Statistical analysis was performed with SPSS (two-way ANOVA, repeated measures ANOVA General Linear Model with Greenhouse-Geisser correction for non-sphericity) or Microsoft Excel (Student's t-test) software.

For mouse phenotypic assessment, weight, rotarod and grip strength were analysed with repeated measures ANOVA to determine overall effects of genotype and time and at each time point with two-way ANOVA (*Hdac6*KOxR6/2) or three-way ANOVA (*Sirt2*KOxR6/2) to determine when the effects were occurring. Brain weight was analysed by two-way ANOVA (*Hdac6*KOxR6/2 cross) or three-way ANOVA (*Sirt2*KOxR6/2 cross). Activity was analysed with repeated measures ANOVA at each

time point separately to determine whether there were differences in activity patterns between the genotypes.

For western blotting, ELISA, TR-FRET and qPCR, group means were compared by Student's t-test. When more than two groups were investigated, they were compared by one- or two-way ANOVA. Post-hoc pairwise comparison with Bonferroni correction was used for the analysis of cholesterol genes expression in *Sirt2*KOxR6/2 at 15 weeks of age.

2.2.17. Fluor de Lys SIRT2 activity assay

Tissues were homogenised in Assay Buffer (provided with the kit) supplemented with protease inhibitor cocktail (1 tablet/10 mL), sonicated at 80 Hz for 10 s, and centrifuged at 16,200 X *g* for 15 min at 4°C before protein concentration was determined for each sample with the BCA kit. Lysates were diluted to 0.2 µg/µL, incubated for 10, 20, 40 or 60 min at 37°C, supplemented with DTT to a final concentration of 10 mM, and again incubated for 10 min at 37°C. Samples were loaded onto 96-well plates (provided with the kit) and Fluor-de-Lys acetylated substrate was added to a final concentration of 100 µM with or without 3 mM NAD^+. Reactions were incubated at 37°C for 1 h and stopped by adding 1 volume of Developer (provided with the kit). The plate was incubated for 30 min at room temperature and signal was read (excitation at 355 nm, emission at 460 nm) using an Omega plate reader every 15 min until a plateau was reached.

Results Chapter 3:

Experimental Paper:

Hdac6 Knock-Out Increases Tubulin Acetylation but Does Not Modify Disease Progression in the R6/2 Mouse Model of Huntington's Disease

OPEN ACCESS Freely available online

PLoS one

Hdac6 Knock-Out Increases Tubulin Acetylation but Does Not Modify Disease Progression in the R6/2 Mouse Model of Huntington's Disease

Anna Bobrowska[1], Paolo Paganetti[2¤], Patrick Matthias[3], Gillian P. Bates[1]*

1 Department of Medical and Molecular Genetics, King's College London, London, United Kingdom, **2** Novartis Institutes for BioMedical Research, Neuroscience Discovery, Basel, Switzerland, **3** Friedrich Miescher Institute for Biomedical Research, Novartis Research Foundation, Basel, Switzerland

Abstract

Huntington's disease (HD) is a progressive neurodegenerative disorder for which there is no effective disease modifying treatment. Following-on from studies in HD animal models, histone deacetylase (HDAC) inhibition has emerged as an attractive therapeutic option. In parallel, several reports have demonstrated a role for histone deacetylase 6 (HDAC6) in the modulation of the toxicity caused by the accumulation of misfolded proteins, including that of expanded polyglutamine in an N-terminal huntingtin fragment. An important role for HDAC6 in kinesin-1 dependent transport of brain-derived neurotrophic factor (BDNF) from the cortex to the striatum has also been demonstrated. To elucidate the role that HDAC6 plays in HD progression, we evaluated the effects of the genetic depletion of HDAC6 in the R6/2 mouse model of HD. Loss of HDAC6 resulted in a marked increase in tubulin acetylation throughout the brain. Despite this, there was no effect on the onset and progression of a wide range of behavioural, physiological, molecular and pathological HD-related phenotypes. We observed no change in the aggregate load or in the levels of soluble mutant exon 1 transprotein. HDAC6 genetic depletion did not affect the efficiency of BDNF transport from the cortex to the striatum. Therefore, we conclude that HDAC6 inhibition does not modify disease progression in R6/2 mice and HDAC6 should not be prioritized as a therapeutic target for HD.

Citation: Bobrowska A, Paganetti P, Matthias P, Bates GP (2011) *Hdac6* Knock-Out Increases Tubulin Acetylation but Does Not Modify Disease Progression in the R6/2 Mouse Model of Huntington's Disease. PLoS ONE 6(6): e20696. doi:10.1371/journal.pone.0020696

Editor: Koichi M. Iijima, Thomas Jefferson University, United States of America

Received February 1, 2011; **Accepted** May 6, 2011; **Published** June 3, 2011

Funding: This work was supported by a European Commission Marie Curie Initial Training Network (215618) Fellowship (AB) and the CHDI Foundation. The funders had no role in the study design, data collection and analysis, decision to publish or preparation of the manuscript. At the time that this study was performed, PP was an employee of Novartis Institutes for BioMedical Research and helped with experimental design, data analysis, and reading of the manuscript.

Competing Interests: At the time that this research was performed, PP was an employee of Novartis Institutes for BioMedical Research. There are no patents, products in development, or marketed products to declare. This does not alter the authors' adherence to all the PLoS ONE policies on sharing data and materials, as detailed online in the guide for authors.

* E-mail: gillian.bates@kcl.ac.uk

¤ Current address: AC Immune SA, Lausanne, Switzerland

Introduction

Huntington's disease (HD) is an autosomal dominant progressive neurodegenerative disorder with a mean age of onset of 40 years [1]. The most characteristic features of symptomatic HD patients are motor disorders, cognitive decline, psychiatric disturbances and weight loss. The disease progresses on average for 15–20 years and although the first symptomatic drug has recently been approved by the Federal Drug Administration, there is still no disease modifying treatment available [2]. The cause of HD is the expansion of a CAG trinucleotide repeat in the *HTT* gene, resulting in an expanded polyglutamine (polyQ) tract in the N-terminus of the huntingtin protein [3]. HD pathology is mostly observed in the brain with the striatum displaying pronounced atrophy, although other brain regions are also affected [4,5]. A prominent feature of HD is the presence of mutant huntingtin containing cytoplasmic aggregates and nuclear inclusions that are ubiquitin positive [6]. At the molecular level, many changes have been observed that may contribute to HD pathology including abnormal levels of neurotransmitters and their receptors, mitochondrial dysfunction, metabolic disturbances, transcriptional dysregulation and disruption of microtubule based transport, among others [7].

Histone deacetylases (HDACs) have been proposed as possible therapeutic targets for HD [8]. There are altogether 18 mammalian HDAC's, divided into four classes depending on their homology to yeast enzymes. Class I and II enzymes have Zn^{2+} dependent catalytic domains and are homologous to yeast Rpd3 and Hda1, respectively. HDAC11 is also Zn^{2+} dependent but has been placed in a separate category (class IV) due to a lack of sufficient sequence similarity to any other group [9]. Sirtuins (class III) are homologous to yeast Sir2 and use a different mechanism requiring NAD^{+} as a co-factor [10]. Studies on HDAC inhibition have shown promising results in fly, worm and mouse models of HD [11,12,13,14].

HDAC6 is a target of some of the broad range HDAC inhibitors including suberoyl anilide hydroxamic acid (SAHA) and trichostatin A (TSA) [15]. It is a particularly interesting protein, in that it is the only known HDAC with two catalytically active deacetylase domains and a ubiquitin interacting domain [16,17]. Moreover,

its main activity appears to be in the cytoplasm, where it has been shown to deacetylate α-tubulin, HSP90 and cortactin, among others [18,19,20,21]. HDAC6 is also of particular interest in HD. In cell models, HDAC6 has been shown to act against protein misfolding toxicity by taking part in the formation of a juxtanuclear structure termed the aggresome, a microtubule dependent inclusion body to which dispersed aggregates are targeted and transported by the dynein motor [22]. HDAC6 is required for the targeting of ubiquitinated aggregates to the aggresome, thought to serve as an adaptor protein by binding both poly-ubiquitin chains and the dynein motor. Interestingly, deacetylase activity and intact microtubules are essential to this process implying that aggresome formation depends on tubulin acetylation status [23]. Similarly, it has been shown that HDAC6 is critical for the formation of stress granules [24]. In addition, it has recently been shown that in the case of proteasome overload, aggresome formation might provide the means by which the cell removes accumulated misfolded proteins by autophagy and that HDAC6 is essential for this pathway [25]. In a *Drosophila melanogaster* model of spinal and bulbar muscular atrophy (SBMA) HDAC6 expression rescued neurodegeneration in an autophagy-dependent manner [26]. In fact, HDAC6 has also recently been shown to be involved in ubiquitin selective quality control autophagy by regulating the lysosome to autophagosome fusion [27]. On the other hand, a study in an HD cell model has indicated that increasing tubulin acetylation by HDAC6 inhibition could rescue the brain-derived neurotrophic factor (BDNF) transport deficit from the cortex to the striatum [28]. Taken together, these findings strongly suggest that HDAC6 inhibition should modify HD progression.

Based on the previous studies in cell culture models of HD, we might expect that loss of HDAC6 would increase aggregate load and exacerbate the phenotype in a mouse model of HD. On the other hand, an increase in cortico-striatal BDNF transport might be expected to improve some HD-related phenotypes. To determine whether HDAC6 regulates aggregate formation and turnover and/or plays a role in BDNF transport in a mouse model of HD, we crossed the R6/2 transgene onto an *Hdac6* knock-out background. As *Hdac6* is located on the X-chromosome, hemizygous male mice are nullizygous for *Hdac6* [29]. The R6/2 mouse has an early onset and rapid phenotype progression [30] and at late stage disease expresses HD-related phenotypes that are extremely similar to those that develop in the *Hdh*Q150 knock-in model of HD [31,32,33,34,35]. We showed that in the absence of HDAC6, levels of tubulin acetylation were increased throughout the brain. However, this had no effect on R6/2 readouts in a battery of physiological and behavioural assessments. We also found no difference in levels of soluble or aggregated huntingtin trans-protein upon ablation of HDAC6. Our data thus suggest that HDAC6 is not important for aggregate clearance in a mouse model of HD. Finally, we established that increased tubulin acetylation did not affect levels of BDNF in the striatum. We conclude that inhibition of HDAC6 should not be pursued as a high priority therapeutic target for HD.

Results

Hdac6 knock-out mice (*Hdac6*KO) are viable and fertile, and do not show any overt phenotypes [36]. Before analysing the effect of the genetic depletion of HDAC6 on phenotype progression in the R6/2 mice, we wanted to verify that these mice do not express HDAC6 at the mRNA or protein level. cDNA was prepared from cortex, striatum, cerebellum, muscle and liver from 4 week old wild type (WT) and *Hdac*6KO mice and analysed by real-time quantitative RT-PCR (qPCR). *Hdac6* was not expressed in tissue from *Hdac6*KO mice (Fig. 1A). HDAC6 protein could not be detected in brain or testes by western blot analysis (Fig. 1B). Consistent with previous reports, HDAC6 levels were higher in testes than in brain [36]. R6/2 mice in our colony reach end-stage disease at 15 weeks of age. In order to determine whether *Hdac6* is stably expressed during this disease time-frame, we compared the levels of *Hdac6* mRNA in WT mice at 4, 9 and 15 weeks of age. We established that *Hdac6* is expressed at relatively stable levels in WT mice from 4 to 15 weeks of age, with only a 15% reduction being detected in the cortex at 9 weeks as compared to 4 weeks of age (Fig. 1C). Transcriptional dysregulation is a hallmark of the molecular pathogenesis of HD and is recapitulated by the R6/2 mouse model [37]. Thus, to ensure that *Hdac6* is not dysregulated in R6/2 mice, we measured *Hdac6* expression levels in R6/2 mice at 4, 9 and 15 weeks of age in cortex, striatum and cerebellum and compared them to those observed in WT mice. *Hdac6* levels were unchanged between WT and R6/2 mice (Fig. 1D) indicating that there was no effect of disease progression on the expression of *Hdac6*.

Tubulin is hyperacetylated upon genetic depletion of HDAC6 but is not altered by the presence of the R6/2 transgene

As HDAC6 is an α-tubulin deacetylase, depletion of HDAC6 should result in tubulin hyper-acetylation. It has been previously reported that the *Hdac6*KO line of mice used in this study, has elevated levels of acetylated tubulin in peripheral tissue but not in brain [36]. However, increased tubulin acetylation has been shown to occur in brain as a consequence of HDAC6 depletion in an alternative *Hdac6* knock-out mouse [38]. To resolve this discrepancy, we analysed tubulin acetylation in our *Hdac6*KO mice by western blotting, normalising levels of acetylated tubulin to those of total α–tubulin. We found that tubulin is hyperacetylated in the cortex, striatum and cerebellum of *Hdac6*KO mice at 4, 9 and 15 weeks of age as compared to WT littermates (Fig. 2A and C). The extent of hyperacetylation in *Hdac6*KO mice became less pronounced with age in the cortex and cerebellum, perhaps explaining the earlier results.

Acetylation of lysine 40 on α-tubulin has been demonstrated to increase the binding of certain molecular motor proteins to microtubules, thus modulating intracellular transport dynamics [39]. Impairment of intracellular transport has been suggested to contribute to the molecular pathology of HD [40]. Therefore, we investigated whether tubulin acetylation is altered by the presence of the R6/2 transgene. Our results indicate that there is no difference in tubulin acetylation between R6/2 and WT mice in cortex, striatum and cerebellum at 4, 9 or 15 weeks of age (Fig. 2B and D). This is consistent with the fact that there is no difference in the expression of *Hdac6* between WT and R6/2 mice in the same tissues throughout disease progression (Fig. 1D).

Genetic Depletion of HDAC6 does not modify HD physiological and behavioural phenotypes in R6/2 mice

Previous studies have indicated that both over-expression and depletion of HDAC6 could ameliorate HD phenotypes in cell culture [25,28]. Here, we investigate whether HD-related phenotypes are modulated by the genetic depletion of HDAC6 in an HD mouse model. R6/2 males were bred to *Hdac6*KO heterozygous females and a longitudinal phenotyping study was performed to compare *Hdac6*KOxR6/2 double mutant (Dble) mice to WT, *Hdac6*KO and R6/2 littermates. As *Hdac6* is an X-linked gene [29], males carrying the mutant allele are effectively nullizygous for *Hdac6* (Fig. 1A–B). We obtained at least 16 males for each genotype and the R6/2 and Dble groups were well matched for their CAG repeat size ($p = 0.338$) (Fig. 3A).

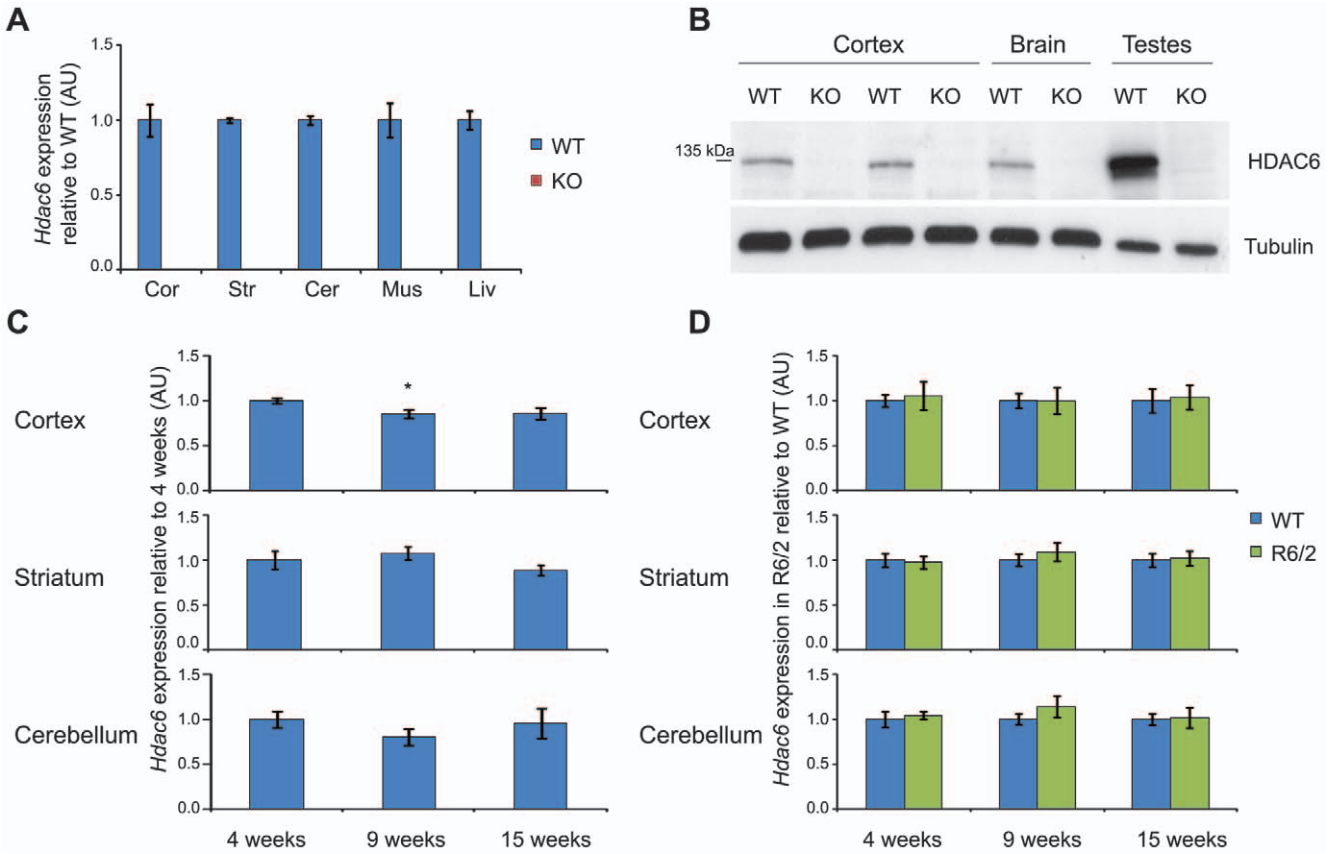

Figure 1. HDAC6 expression in *Hdac6*KO, WT and R6/2 mice. (**A**) Taqman qPCR assay showing absence of *Hdac6* mRNA expression in *Hdac6*KO mice as compared to WT; n = 3/genotype. Data normalised to *Atp5b* and expressed as fold change of WT for each tissue. (**B**) Western blot showing absence of HDAC6 protein expression in *Hdac6*KO mice as compared to WT. (**C**) Taqman qPCR assay showing that *Hdac6* mRNA expression does not change with age in WT mice in cortex, striatum and cerebellum; n = 8/genotype, data normalised to *Atp5b and Rpl13a* (cortex), *Gapdh* (striatum) and 18S RNA (cerebellum) and expressed as fold change of 4 weeks. (**D**) Taqman qPCR assay showing no difference in *Hdac6* mRNA expression between WT and R6/2 mice in cortex, striatum and cerebellum at 4, 9 and 15 weeks; n≥6/genotype, data normalised to WT for each time point and brain region. Error bars represent SEM. * $p<0.05$ as compared to 4 weeks. KO – *Hdac6* knock out, WT – wild type, Cor - cortex, Str - striatum, Cer - cerebellum, Mus - muscle, Liv - liver.
doi:10.1371/journal.pone.0020696.g001

Mice were weighed weekly to the nearest 0.1 g from 4 weeks of age onwards (Fig. 3B). R6/2 mice weighed significantly less than WT mice overall ($F_{(1,64)} = 14.28$, $p<0.001$) and gained weight at a significantly slower rate ($F_{(2,640)} = 55.99$, $p<0.001$). HDAC6 depletion by itself had no impact on the weight ($F_{(1,64)} = 0.567$, $p = 0.454$) and weight gain ($F_{(2,640)} = 0.247$, $p = 0.741$) when compared to WT mice. Absence of HDAC6 did not affect the loss of weight in R6/2 ($F_{(1,64)} = 0.007$, $p = 0.931$) or the decreased rate in weight gain ($F_{(2,640)} = 0.512$, $p = 0.567$). These data indicate that depletion of HDAC6 does not affect weight loss in the R6/2 mice (Fig. 3B).

RotaRod measures motor coordination and balance, both of which become significantly impaired in R6/2 mice. Here the animals were subjected to RotaRod analysis at 4, 8, 10, 12 and 14 weeks of age (Fig. 3C). As expected, R6/2 mice performed worse than WT mice ($F_{(1,71)} = 39.74$, $p<0.001$) and that performance deteriorated over the course of the study ($F_{(3,1420)} = 18.23$, $p<0.001$). The performance of *Hdac6*KO mice was similar to WT ($F_{(1,71)} = 0.32$, $p = 0.573$) but the variability in their performance over time was significantly different to that of WT mice ($F_{(3,1420)} = 3.53$, $p = 0.020$). Nevertheless, the *Hdac6* knock-out genotype did not modify the performance of R6/2 mice overall ($F_{(1,71)} = 0.40$, $p = 0.529$) or with age ($F_{(3,1420)} = 1.09$, $p = 0.352$).

Forelimb grip strength was measured at 4 weeks of age and weekly from 11 to 14 weeks of age (Fig. 3D). As expected, the overall grip strength of R6/2 mice was worse than that of WT ($F_{(1,67)} = 142.41$, $p<0.001$) and deteriorated over time ($F_{(3,536)} = 50.69$, $p<0.001$). The grip strength of *Hdac6*KO mice was no different from WT mice either overall ($F_{(1,67)} = 0.621$, $p = 0.434$) or with time ($F_{(3,536)} = 1.97$, $p = 0.121$). Nullizygosity for *Hdac6* did not have an effect on the overall grip strength of R6/2 mice ($F_{(1,67)} = 3.17$, $p = 0.081$) nor did it influence the deterioration in grip strength over the course of the experiment ($F_{(3,536)} = 0.856$, $p = 0.463$). Therefore, genetic depletion of HDAC6 does not modify loss of forelimb muscle strength in R6/2 mice.

Spontaneous motor activity was recorded for each mouse for 30 min in an infrared activity monitoring cage bi-weekly from 5 weeks of age onwards (Fig. 3E and Fig. S1). Data were analysed by repeated measures general linear model ANOVA and *p*-values are presented in Table S1. At 5 weeks of age, levels of activity between mice of all genotypes were comparable (Fig. 3E and Table S1: R6/2 Genotype and *Hdac6*KO Genotype), but a significant difference in the pattern of activity over time was already evident for activity ($p = 0.011$) and rearing ($p = 0.016$) for mice carrying the R6/2 transgene. At 7 weeks of age the R6/2 genotype significantly affected the activity and mobility ($p<0.001$) of the mice. A clear

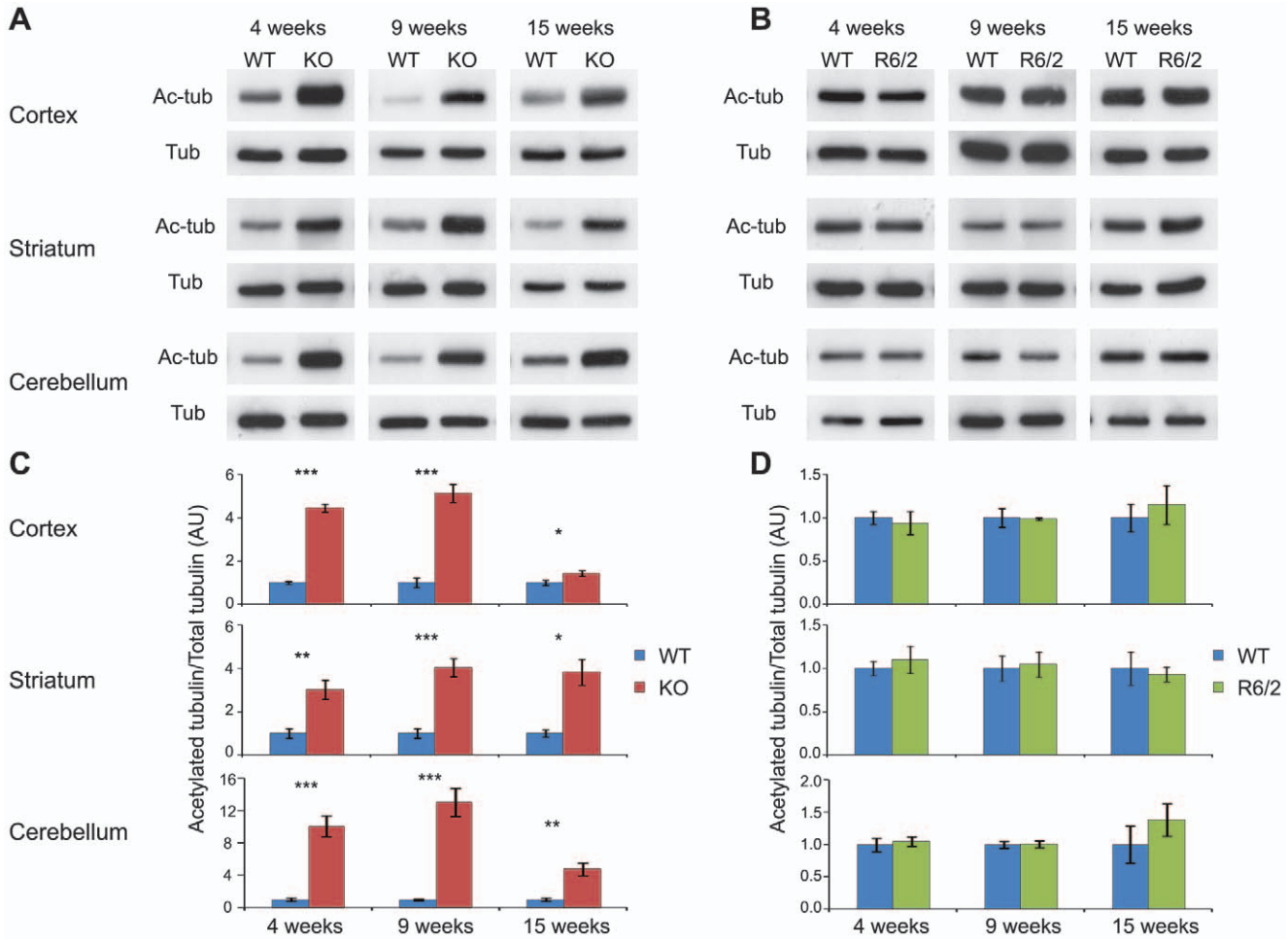

Figure 2. Tubulin acetylation in the brains of *Hdac6*KO and R6/2 mice compared to WT. (**A–B**) Representative western blots showing acetylated tubulin (Ac-tub) between *Hdac6*KO and WT mice (A) and R6/2 and WT mice (B) at 4, 9 and 15 weeks in cortex, striatum and cerebellum with tubulin (Tub) as a loading control. (**C–D**) Densitometric quantification of western blots represented in (A–B). Acetylated tubulin was normalised to α-tubulin and the relative signal for *Hdac6*KO (C) or R6/2 (D) expressed as fold change compared to WT. Error bars represent SEM. * $p<0.05$, ** $p<0.01$, *** $p<0.001$; $n\geq4$/genotype. KO – *Hdac6* knock out, WT – wild type.
doi:10.1371/journal.pone.0020696.g002

hypoactivity was evident in both the R6/2 and Dble mice at 9, 11 and 13 weeks of age (Fig. 3E and Table S1, R6/2 Genotype). *Hdac6*KO mice were comparable to WT and the Dble mutant mice to R6/2 at almost all time points indicating that depletion of HDAC6 had no influence on the R6/2 hypoactivity phenotype.

Mice were sacrificed at 15 weeks of age and brains weighed to the nearest 0.001 g (Fig. 3F). As expected, R6/2 mice had a significantly lower brain weight than WT mice ($p<0.001$). The weight of *Hdac6*KO brains was similar to WT ($p<0.057$) and that of the Dble mutant mice was similar to R6/2 ($p=0.784$). Thus, absence of HDAC6 does not modify the loss in brain weight exhibited by the R6/2 mice at end-stage disease.

Genetic Depletion of HDAC6 does not modify huntingtin aggregation

Aggregation of mutant huntingtin is a prominent feature of HD neuropathology and occurs in all of the HD rodent models that have thus far been developed. Aggregates in the R6/2 mouse appear prior to the onset of behavioural symptoms and continue to accumulate throughout the course of the disease. At the same time, a steady decrease in the levels of soluble transprotein can be observed. In cells, HDAC6 acts as a linker between ubiquitinated protein and/or aggregates and the dynein/dynactin motor complex enabling their transport to the aggresome for autophagic degradation [23]. If this phenomenon is relevant to the mammalian brain, an absence of HDAC6 should result in an increase in aggregate load [25].

We measured the amount of SDS insoluble aggregates by the Seprion ligand ELISA [34] and found no difference in aggregate load between R6/2 and Dble mice at 4, 9 and 15 weeks of age in cortex, hippocampus and brain stem (Fig. 4A and Fig. S2A), or at 9 and 15 weeks in quadriceps muscle (Fig. S2E). The corresponding levels of soluble transprotein were measured in these tissues by means of TR-FRET (Fig. 4B and Fig. S2D–E), similarly, no difference between R6/2 and Dble mice was detected. These results were confirmed by a TR-FRET aggregation assay (Fig. S2D) and by western blotting of SDS-PAGE resolved lysates with an antibody that detects soluble and aggregated huntingtin (S830) (Fig. 4C and Fig. S2B).

Our data show that HDAC6 ablation does not influence aggregate load or levels of soluble mutant huntingtin in the cortex, hippocampus or brain stem at 4, 9 or 15 weeks of age (Fig. 4, Fig. S2A–C) or in quadriceps muscle at 9 and 15 weeks of age (Fig. S2E). In support of this, we did not detect any obvious differences in the level or distribution of aggregates between R6/2 and Dble

A

Genotype	Number of mice	Repeat Size
Wild type	16	
Hdac6KO	19	
R6/2	17	199 (SD 5.66)
R6/2xHdac6KO(Dble)	16	201 (SD 3.52)
Total mice used	68	

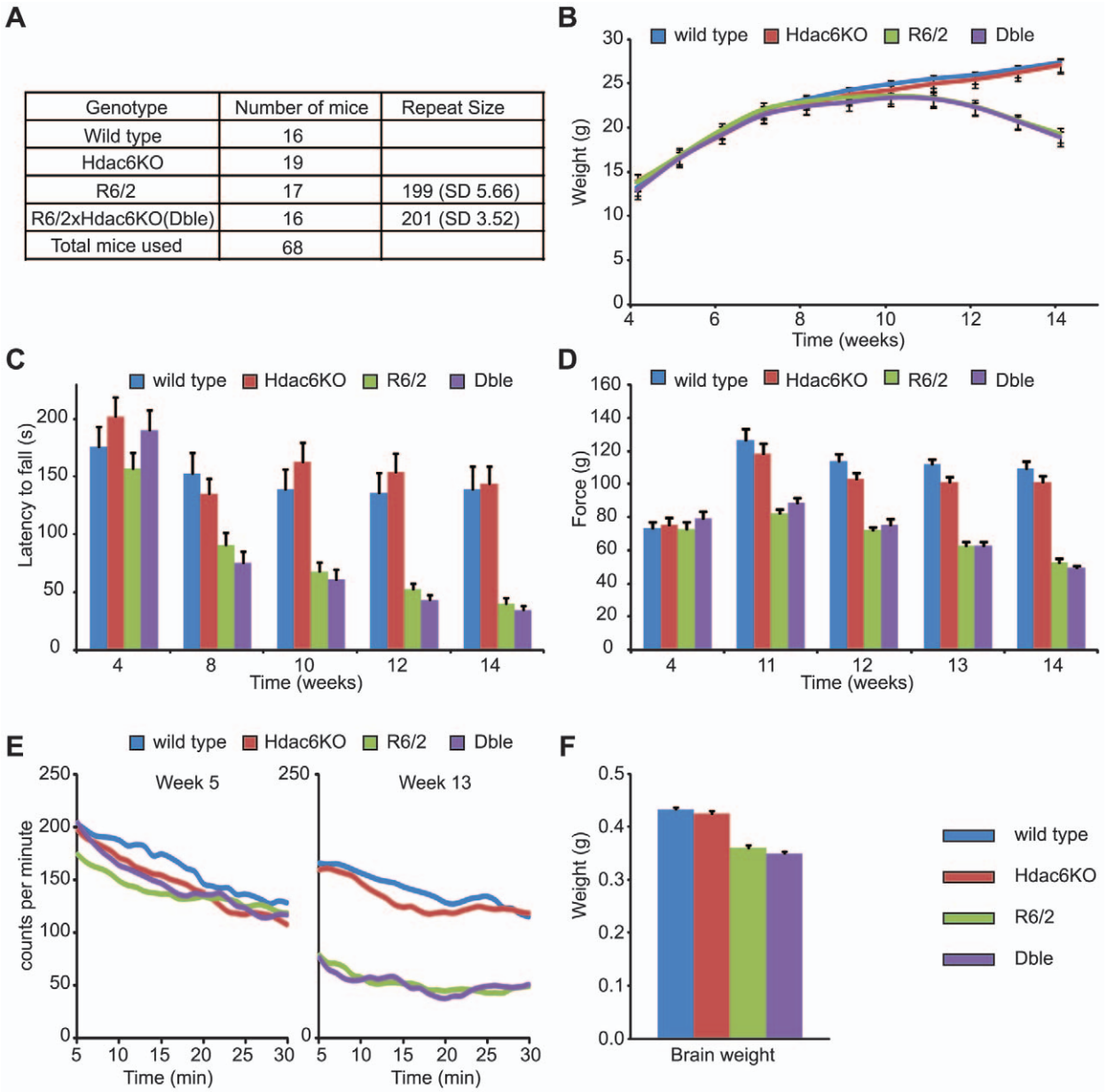

Figure 3. Behavioural and physiological phenotypes in the absence of HDAC6. (**A**) The number of male mice analysed per genotype with the mean CAG repeat size for the groups carrying the R6/2 transgene (SD-standard deviation). (**B**) Body weight (**C**) Time spent on RotaRod (**D**) Forelimb grip strength (**E**) Spontaneous motor activity recorded at the beginning (week 5) and end (week 13) of the study. Graphs were created by plotting 5 min moving averages (**F**) Brain weight measured at week 15. Error bars represent SEM.
doi:10.1371/journal.pone.0020696.g003

striata at 9 weeks of age by immunohistochemistry (Fig. 4D). Although a significant decrease in soluble cortical transprotein levels was detected by TR-FRET in the Dble as compared to the R6/2 mice at 9 weeks of age, further analysis by western blot has shown that this difference, if real, is not large (Fig. 4B–C). At the same age, there was no difference in the cortical aggregate load measured by either Seprion ELISA or TR-FRET (Fig. 4A and Fig. S2D).

Genetic Depletion of HDAC6 results in tubulin hyperacetylation in the brains of R6/2 mice

We have found that the absence of HDAC6 has no effect on R6/2 behavioural phenotypes or on the accumulation of aggregated transprotein in these animals. It is possible that the presence of the R6/2 transgene prevented the hyperacetylation of tubulin from occurring in response to HDAC6 depletion. Therefore, we compared the levels of acetylated tubulin between R6/2 and Dble mice at 4, 9 and 15 weeks of age in the cortex, striatum and cerebellum. We found that HDAC6 depletion resulted in a pronounced increase in tubulin acetylation in R6/2 mice in all brain regions and at all time-points studied (Fig. 5). The increase in tubulin acetylation was comparable between *Hdac6*KO and Dble mutant mice (Fig. S3). We conclude that the substantial increase in tubulin acetylation levels throughout the brain has no consequence on HD-related phenotypes in the R6/2 mouse.

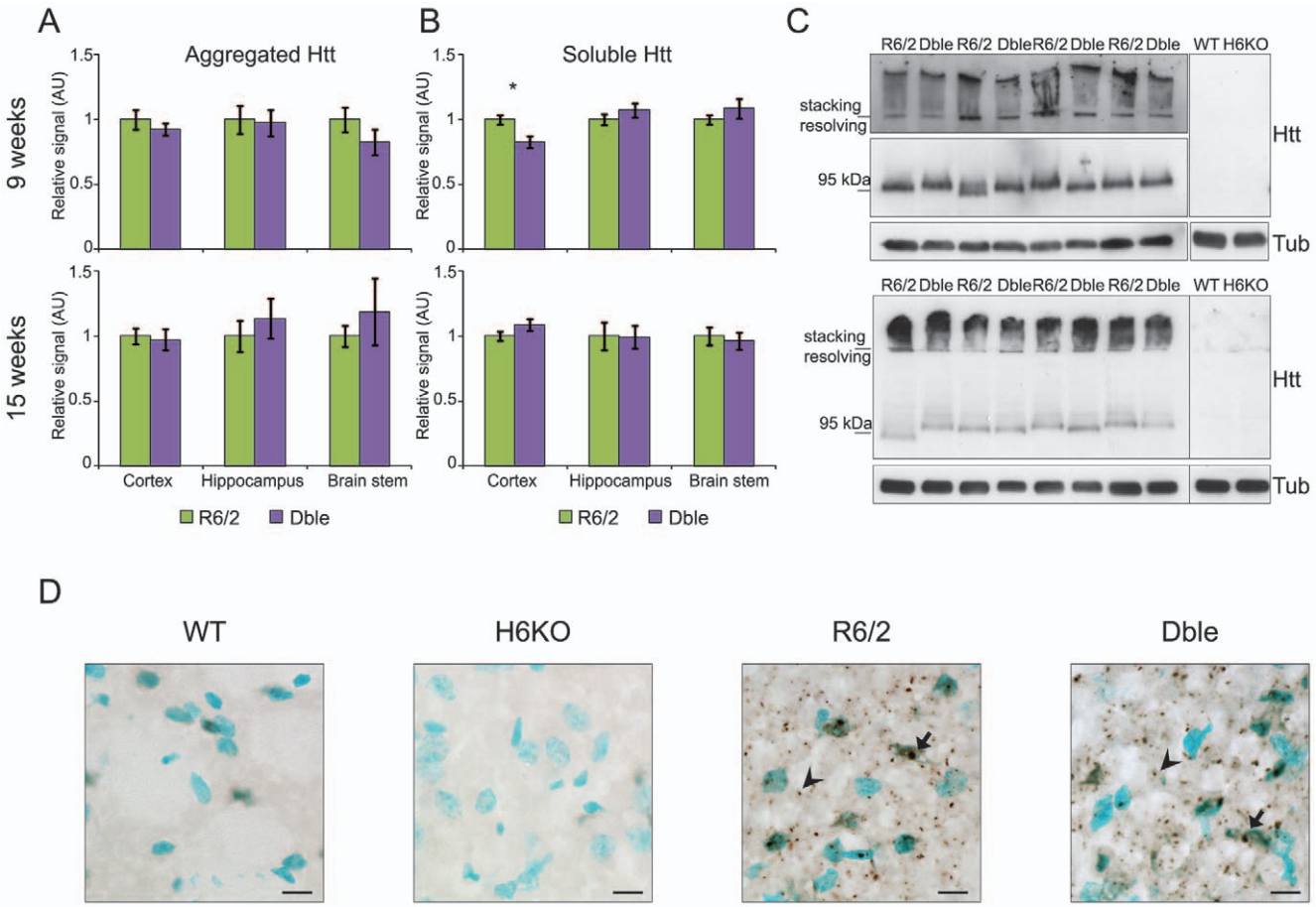

Figure 4. No effect of *Hdac6* knock-out on aggregate load or soluble transprotein levels. (**A**) Aggregate load was measured by Seprion ligand ELISA (MW8 antibody) and (**B**) soluble transprotein levels were measured by TR-FRET (2B7-MW1 antibodies) in the cortex, hippocampus and brain stem of R6/2 and Dble mice at 9 and 15 weeks. The average of the WT and *Hdac6*KO background signal was subtracted from both R6/2 and Dble signals. The Dble signal is expressed as fold change of the R6/2 signal. * $p<0.05$; $n\geq8$/genotype. (**C**) Representative western blots with S830 anti-huntingtin antibody showing aggregated and soluble transprotein (Htt) in the cortex at 9 (upper panel) and 15 (lower panel) weeks. α-tubulin (Tub) was used as a loading control. Specificity of S830 staining is confirmed by lack of signal in WT and *Hdac6*KO cortices. (**D**) Representative sagittal sections from 9 week old mice showing the striatum immunostained with S830 antibody. Nuclei are counterstained with methyl green. Scale bar = 10 μm. Arrow = nuclear inclusion, arrowhead = cytoplasmic aggregate. Error bars represent SEM.
doi:10.1371/journal.pone.0020696.g004

Genetic Depletion of HDAC6 does not modify BDNF content in the striatum

Cell culture studies have shown that an increase in tubulin acetylation increases the transport of BDNF from the cortex to the striatum in the context of both WT and HD [28]. In accordance with previous data [41], we found that *Bdnf* mRNA expression is lower in the cortex of R6/2 mice at 9 weeks of age and that this phenotype is not altered by HDAC6 depletion (Fig. 6A). However, at the same age, levels of BDNF protein in the cortex as measured by ELISA were comparable between mice of all four genotypes (Fig. 6B). Equally, BDNF protein levels in the striatum of *Hdac6*KO, R6/2 and Dble mice were not different from those of WT mice (Fig. 6C). Therefore, the decrease in *Bdnf* mRNA did not translate to a reduction in BDNF protein. As *Bdnf* is expressed in the striatum at a very low level (Fig. S4A) and it has been published that most striatal BDNF protein originates in the cortex [42], we conclude that there is no effect of HDAC6 ablation on the transport efficiency of BDNF from the cortex to the striatum in either WT or R6/2 mice.

Discussion

Previous studies in cell culture models of HD have shown that modulation of HDAC6 levels alters HD-related phenotypes [25,28]. To extend this analysis to a mouse model, we investigated the effects of HDAC6 genetic depletion in the R6/2 mouse. We showed that *Hdac6* knock-out mice (*Hdac6*KO) do not express HDAC6 at the mRNA or protein levels and have hyperacetylated tubulin in the cortex, striatum and cerebellum from 4 to 15 weeks of age. We show that in the presence of the polyQ expanded R6/2 transprotein, levels of acetylated tubulin do not differ from that in wild type animals and similarly, the HD mutation does not interfere with the effect that HDAC6 ablation has on tubulin hyperacetylation. We found that depletion of HDAC6 had no effect on the aggregate load or BDNF levels in the R6/2 brain and did not modify physiological or behavioural HD-related phenotypes in R6/2 mice.

In this study, we have used mice in which the endogenous *Hdac6* gene has been disrupted [36]. One possible concern with using mice that do not express HDAC6 throughout development is that

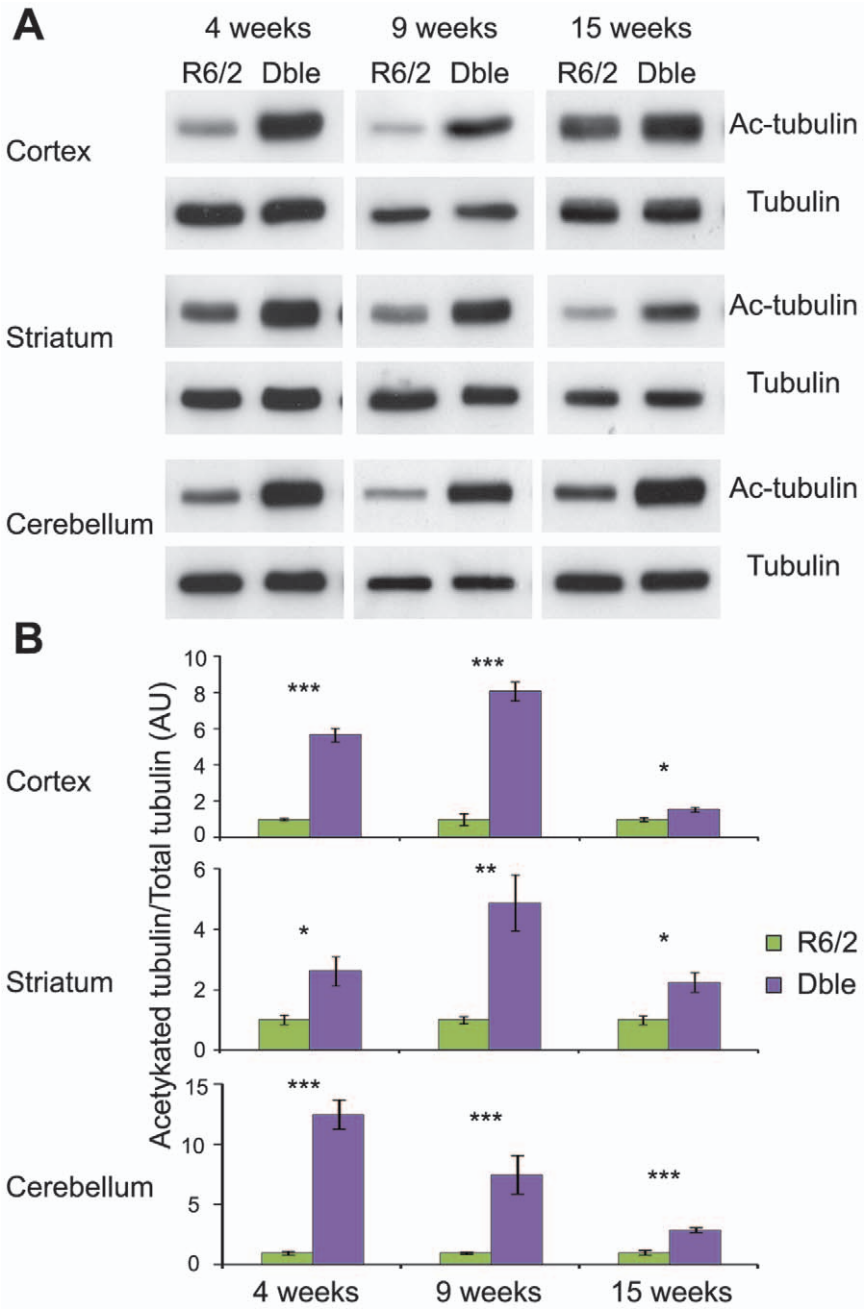

Figure 5. Tubulin acetylation in the brains of Dble as compared to R6/2 mice. (**A**) Representative western blots showing acetylated tubulin in Dble and R6/2 mice at 4, 9 and 15 weeks in cortex, striatum and cerebellum with α-tubulin as a loading control. (**B**) Densitometric quantification of western blots presented in (A). Acetylated tubulin was normalised to α-tubulin and the relative signal for Dble mice expressed as fold change to R6/2. Error bars represent SEM. * $p<0.05$, ** $p<0.01$, ***$p<0.001$; $n\geq4$/genotype.
doi:10.1371/journal.pone.0020696.g005

the expression of other genes will adjust to compensate for the deficit. The HDAC6 mechanisms of action under investigation here are based on HDAC6-tubulin interactions. Our demonstration that tubulin acetylation is increased in the brain from 4 to 15 weeks of age indicates that compensation has not occurred for the HDAC6 target in which we are primarily interested and that the constitutive *Hdac6* knock-out mice used here are a suitable model. There are numerous mouse models of HD, which include mice transgenic for an N-terminal fragment of *HTT*, YAC and BAC mice that are transgenic for full-length *HTT* gene and knock-in mice in which an expanded CAG repeat has been introduced into the mouse *Hdh* gene [43]. The HD cell culture model used by Iwata and colleagues [25] to show that HDAC6 is required for aggresome formation expressed an exon 1 huntingtin transprotein. The R6/2 mice express an exon 1 N-terminal fragment of mutant huntingtin [30] and therefore, they represent an appropriate model with which to first follow-up on their findings. Also, recent analysis has shown that the R6/2 mice develop HD-related phenotypes that are highly comparable to a genetically accurate knock-in mouse model of HD [31,33,34,35] and that, in these knock-in mice, mutant huntingtin is processed to generate N-terminal fragments [32]. Despite this, analysing the effects of the

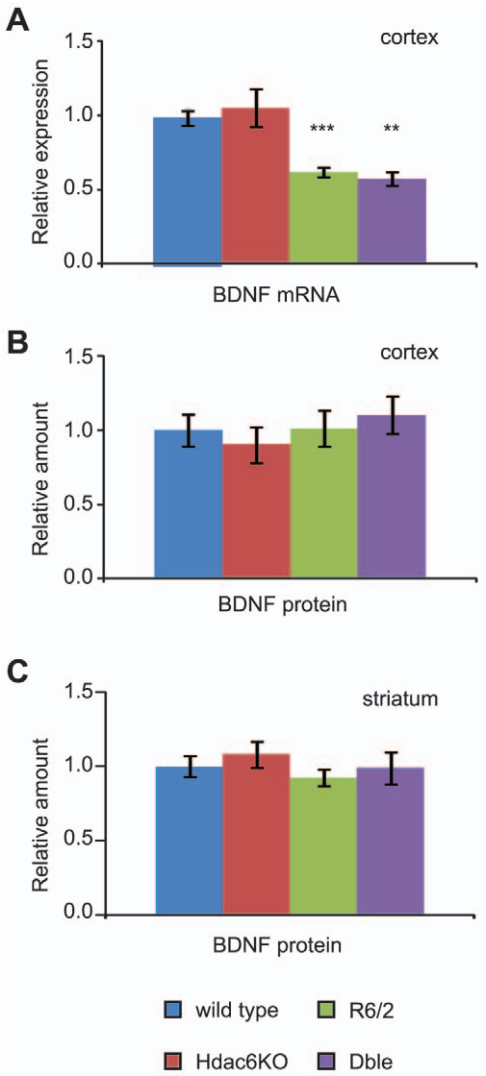

Figure 6. Influence of *Hdac6* knock-out on *Bdnf* mRNA and protein levels. (**A**) Taqman qPCR assay showing a significant down-regulation of *Bdnf* coding region mRNA expression in cortex of mice carrying the R6/2 transgene. Data normalised to WT. ** $p<0.01$ (to *Hdac6KO*), ***$p<0.001$ (to WT); $n\geq4$/genotype. (**B–C**) BDNF protein content in the cortex (B) and striatum (C) measured by ELISA. Data normalised to WT. $n\geq3$/genotype in (B) and $n\geq4$/genotype in (C). Error bars represent SEM.
doi:10.1371/journal.pone.0020696.g006

modulation of *Hdac*6 levels on HD phenotypes in these more genetically precise models might be considered important. However, before embarking on such a project, it would be wise to determine whether a reduction in HDAC6 levels has an effect in cell culture models expressing a mutant version of full-length huntingtin.

HDAC6 has been extensively characterised as being required for the formation and subsequent autophagic degradation of the aggresome [23,25,27]. In an HD cell culture model, HDAC6 was required for aggresome formation and an increase in aggregate load was observed upon HDAC6 knock-down [25]. Proteasome inhibition resulted in an increase in ubiquitin positive aggregates in *Hdac6*KO mouse embryonic fibroblasts as compared to wild type cells indicating that HDAC6 is important for autophagy [44]. HDAC6 knock-down in a *Drosophila melanogaster* model of SBMA exacerbated retinal degeneration and overexpression of HDAC6 decreased aggregate load and ameliorated retinal degeneration, effects that required HDAC6 catalytic activity [26]. In keeping with a role for HDAC6 in protein homeostasis, ubiquitin positive aggregates have been reported to accumulate in the brains of another strain of *Hdac6*KO mice by 6 months of age [27]. Given that an increase in aggregation was not detected in R6/2 mice that lack HDAC6, we conclude that either quality-control autophagy is not important for the clearance of polyQ aggregates or that HDAC6 is not essential for this process in the R6/2 mouse brain. It is possible that the mechanism of aggregate handling could differ between lower organisms/cell culture models and HD mice.

In cultured cells, an increase in tubulin acetylation has been shown to enhance kinesin-1 binding and microtubule-based transport [39]. BDNF is a kinesin-1 cargoe [28], which is actively transported from the cortex to the striatum [42]. A recent study in cells has shown that by increasing tubulin acetylation one can increase BDNF cortico-striatal transport and that this is an HDAC6 dependent process [28]. In HD there is a well documented decrease in cortical *BDNF* mRNA expression [41] and we have confirmed that R6/2 mice at 9 weeks of age recapitulate this phenotype, regardless of presence or absence of HDAC6. However, this did not translate into a reduction in BDNF in either the cortex or the striatum in accordance with some, but not all previously published data [45,46,47], suggesting that R6/2 mice at 9 weeks do not display a deficit in BDNF transport. If HDAC6 depletion increases BDNF transport independent of the presence of the huntingtin mutation, as has been reported [28], we would expect to see an increase in striatal BDNF protein levels in both *Hdac6*KO and double mutant mice. We did not observe any change in BDNF levels. Strategies that increase BDNF levels have been shown to be beneficial in R6/2 mice and other N-terminal fragment models [45,48,49,50]. If small changes had occurred, that were beyond the sensitivity of our detection method, they were not sufficient to improve the phenotype of R6/2 mice.

There has been an increased focus on HDAC6 in neurodegenerative disease. In addition to the polyglutamine diseases, overexpression of HDAC6 was protective in *Drosophila melanogaster* models of Parkinson's disease [51] and Alzheimer's disease [52]. HDAC6 has also been found to localise to Lewy bodies in Parkinson's disease patient brains [23] and there is also evidence supporting a role for HDAC6 in Alzheimer's disease via its association with tau [53]. Our finding that the knock-out of HDAC6 does not affect the phenotype, aggregate load or BDNF transport in R6/2 mice was very surprising. This study underlines the importance of validating pathogenic mechanisms and therapeutic targets in mammalian models. At the same time, our findings indicate that the protective effect of broad range HDAC inhibitors that has been observed in invertebrate and mouse HD models [8] is not predominantly mediated via inhibition of HDAC6. The current study is part of a wider project to investigate the effects of the genetic depletion (knock-out or knock-down) of specific HDACs on HD-related phenotypes in the R6/2 mouse. Genetic reduction of *Hdacs3*, *5*, *7* and *9* have not resulted in a phenotypic improvement ([54] and unpublished data) whereas knock-down of *Hdac4* has shown beneficial effects (unpublished data). Based on our data, we can conclude that HDAC6 inhibition would not be a valid therapeutic strategy for HD.

Materials and Methods

Ethics statement

All experimental procedures performed on mice were approved by the King's College London Ethical Review Process Committee and carried out under the UK Home Office License 70/6545.

Mouse strains and husbandry

Hemizygous R6/2 mice were maintained by backcrossing R6/2 males to CBAxC57BL/6 F1 (CBF) females (B6CBAF1/OlaHsd, Harlan Olac, UK) [30]. *Hdac6* knock-out (*Hdac6*KO) mice [36] on C57BL/6 background were backcrossed once to CBF. For the R6/2x*Hdac6*KO genetic cross, R6/2 males were bred to *Hdac6* heterozygous females. At 4 weeks of age, mice were weaned into cages of 5, each containing at least one representative of each genotype. Animals were housed under 12 h light/12 h dark cycle, with unlimited access to water and chow (Special Diet Services, Witham, UK). Cages were environmentally enriched as described [55]. Mice from the R6/2x*Hdac6*KO cross were given mash food consisting of powdered chow mixed with water during 4–6 and 12–15 weeks of age and sacrificed at 15 weeks.

Genotyping

Mice were genotyped by PCR of tail-tip DNA. R6/2 mice were genotyped and their repeat sizes determined as described [34]. For the *Hdac6* genotyping, the primers were forward: 5′-GTACAATGTGGCTCACAGAA, reverse wt: 5′-CAGGCACAGGAATATGAGTT and reverse KO: 5′-CAACTCTGCCTCTCCTGG each used 1 µL at 10 µM in one multiplex 10 µL reaction, containing also 1 µL of 100 ng/µL DNA, 0.8 µL 25 mM $MgCl_2$, 1 µL 2 mM dNTP, 1 µL Sigma 10×PCR buffer and 0.1 µL Sigma Taq Polymerase (D4545, Sigma). Cycling conditions were as follows: 94°C for 5 min, (94°C for 30 s, 64°C for 30 s and 72°C for 1 min)×40 followed by 10 min at 72°C.

Phenotypic assessment

The phenotypes of the mice from the R6/2x*Hdac6*KO cross were assessed blind to genotype. Mice were weighed weekly to the nearest 0.1 g. RotaRod performance was measured at 4 weeks of age for 4 consecutive days, 3 runs a day and after that at 8, 10, 12 and 14 weeks of age for 3 consecutive days, 3 runs a day, using an accelerating (4–44 rpm in 5 min) Ugo Basile 7650 Rotarod, (Linton Instrumentation, UK) modified as described [55]. Exploratory, spontaneous motor activity was recorded at 5, 7, 9, 11 and 13 weeks of age by placing mice in AM1053 activity cages for 30 min during the day, as described previously [56]. Activity was the total number of lower level beam breaks. Mobility was the number of at least two consecutive beam breaks occurring in the lower level. Rearing was the number of rearing beam breaks and centre rearing was the number of rearing beam breaks occurring away from the cage walls. Forelimb grip strength was assessed at 4 weeks of age and then weekly from 11 to 14 weeks, always prior to RotaRod measurements, with San Diego Instruments Grip Strength Meter (San Diego, CA, USA) as described previously [55]. Mice were sacrificed at 15 weeks of age and brains were weighed to the nearest 0.001 g.

Antibodies

The HDAC6 antibody was a kind gift from Dr. Tso-Pang Yao [38]. Acetylated α-tubulin (6-11B-1, T7451) and α-tubulin (DM1A, T9026) antibodies were purchased from Sigma. S830 is a sheep polyclonal antibody raised against a GST tagged huntingtin exon 1 with 53 glutamines, characterized elsewhere [57] and was generated at Scottish Antibody Production Unit. MW8, MW1 [58] and 2B7 [59] were obtained from Novartis, Basel. Secondary peroxidase coupled antibodies were purchased from Dako (anti-goat, anti-mouse), Pierce (anti-rabbit) or KPL (anti-mouse for Seprion).

Sample preparation

For tubulin acetylation analysis, tissues were homogenised using 1% Triton X-100 buffer with 50 mM Tris-HCl pH 7.5, 150 mM NaCl, 2 mM EDTA, 5 µM TSA (Trichostatin A, Sigma) and 10 mM nicotinamide (Sigma), supplemented with protease inhibitor cocktail (Roche). For HDAC6 immuno-detection, tissues were homogenised in RIPA buffer (1% NP-40, 0.5% Deoxycholate, 0.1% SDS, 50 mM Tris-HCl pH 8, 150 mM NaCl, 1 mM β-mercaptoethanol, 100 µM PMSF, 1 mM DTT) supplemented with protease inhibitor cocktail (Roche). Samples were sonicated on ice for 10 s at 80 Hz (Vibracell Sonicator). Lysates were cleared by centrifugation at 16 200 rcf for 15 min at 4°C. Protein concentration was measured with Pierce BCA assay kit (Thermo Scientific). Samples were diluted with 2× protein Laemmli buffer (1 M Tris-HCl pH 6.8, 2.3% SDS, 4.5% glycerol, 10% β-mercaptoethanol, 0.001 g/mL bromophenol blue) and denatured for 5 min at 95°C.

Western blotting

Equal amounts of protein were loaded onto SDS polyacrylamide gel with a size reference (Broad Range Protein Marker, Cell Signalling or Spectra Broad Range Protein Ladder, Fermentas). Proteins were transferred onto Protran nitrocellulose membrane (Whatman) at 120 V for 90 min by submerged transfer apparatus (Bio-Rad) in transfer buffer (20% v/v methanol, 25 mM Tris, 192 mM glycine). Membranes were blocked in 5% non-fat dried milk in PBS for at least 1 hour. Primary antibodies were applied in 0.02% PBS-Tween 20 (PBST) for 20 min (1:40000 acetylated α-tubulin; 1:30000 α-tubulin) or 1 hour (1:5000 S830) at room temperature or overnight (1:250 HDAC6) at 4°C. Blots were washed thrice for 5 min in 0.2% PBST and incubated with appropriate HRP coupled secondary antibody (all 1:5000 except anti-rabbit 1:20000). For signal detection, GE Healthcare Enhanced Chemiluminescence detection system and Amersham Hyperfilms (both GE Healthcare) were used according to the manufacturer's instructions. Signals were quantified using a GS-800 densitometer (Bio-Rad).

Aggregate detection with Seprion ligand ELISA

For aggregate detection 2.5% lysates (w/v) were prepared by homogenising tissue in RIPA. Aggregate capture and detection were performed in Seprion ligand coated plates (Microsens) as described [34].

TR-FRET

Time resolved - Förster resonance energy transfer experiments (TR-FRET) were performed as described [60].

BDNF ELISA

BDNF protein content was measured by the commercially available ELISA kit (Promega) according to manufacturer's instructions modified as described [61]. Lysates were prepared at 2.2% dilution (w/v) and were not acid treated.

Taqman real time quantitative PCR

RNA extraction, cDNA synthesis, Taqman RT-qPCR and ΔCt analysis were performed as described previously [62]. Housekeeping genes (primer and probe mix purchased from Primer Design) were chosen appropriate to the brain region analysed. For time-course or across tissue analysis, several housekeeping genes were tested and the most stable ones chosen. Primers for *Hdac6* expression analysis were forward: 5′ - GGAGACAACCCAGTACATGAATGAA; reverse: 5′ - CGGAGGACAGAGCCTGTAG and the probe was 5′-FAM-TATCTGCATCCGAACTCATATTCCTGTGCCTG-TAMRA. Primers for *Bdnf* coding region were forward: 5′ - GGGTCACAGCGGCAGATAAA; reverse: 5′ - GCCTTTGGATACCGGGACTT; and the probe was: 5′ - FAM - TCTGGCGGGACGGTCACAGTCC - TAMRA.

Immunohistochemistry

Whole brains were snap frozen in isopentane at −50°C. Immunohistochemistry was performed as described [31].

Statistical Analysis

Data from the R6/2x*Hdac6*KO cross were analysed with SPSS using one way ANOVA or General Linear Model ANOVA with Greenhouse-Geisser correction for non-sphericity. Data from qPCR and tubulin acetylation assay were analysed with Microsoft Excel using Student's *t*-test (two tailed).

Supporting Information

Figure S1 *Hdac6* knock-out has no effect on spontaneous motor activity in WT or R6/2 mice. Five minute moving averages for Activity, Mobility, Rearing and Centre rearing at 5, 7, 9, 11 and 13 weeks of age for WT, *Hdac6KO*, R6/2 and Dble mice. n≥16/genotype (as shown in Fig. 3A).
(TIF)

Figure S2 *Hdac6* knock-out does not change aggregate load in the brain or muscle. (**A**) Aggregate load was measured by Seprion ligand ELISA with the MW8 antibody in the cortex, hippocampus and brain stem of R6/2 and Dble mice at 4 weeks. n≥5/genotype. (**B**) Representative western blot with S830 anti-huntingtin antibody showing aggregated and soluble transprotein (Htt) in the cortex at 4 weeks. α-tubulin (Tub) was used as a loading control. Specificity of S830 staining is confirmed by lack of signal in WT and *Hdac6*KO cortices. (**C**) Densitometric quantification of soluble Htt from western blots shown in (A) and Fig. 4C. Htt signal was normalised to α-tubulin and the relative signal for Dble mice expressed as fold change to R6/2 for each time point. (**D**) Soluble (2B7-MW1 antibodies, upper panel) and aggregated (MW8-MW8 antibodies, lower panel) transprotein levels were measured by TR-FRET in the cortex at 9 and 15 weeks. Data normalised to R6/2 at 9 weeks. * $p<0.05$; n≥8/genotype. (**E**) Aggregate load was measured by Seprion ligand ELISA with the MW8 antibody and soluble transprotein levels were measured by TR-FRET (2B7-MW1 antibodies) in the quadriceps muscle at 9 and 15 weeks. Data normalised to R6/2 at each time point. n≥7/genotype. Error bars represent SEM.
(TIF)

Figure S3 The increase in tubulin acetylation in brain is comparable between Hdac6KO and Dble mice. (**A**) Representative western blots showing acetylated tubulin (Ac-tub) in Dble and *Hdac6*KO mice at 4, 9 and 15 weeks in cortex, striatum and cerebellum with α-tubulin (Tub) as a loading control. There was insufficient tissue to perform the analysis on striatum at 9 and 15 weeks. (**B**) Densitometric quantification of western blots presented in (A). Acetylated tubulin was normalised to α-tubulin and the relative signal for Dble mice expressed as fold change to *Hdac6*KO. Error bars represent SEM. KO - *Hdac6*KO, Dble - *Hdac6*KOxR6/2; n≥3/genotype.
(TIF)

Figure S4 Similar levels of BDNF protein in striatum, cortex and hippocampus despite very low *Bdnf* mRNA striatal expression. (**A**) *Bdnf* mRNA coding region expression in WT mice at 9 weeks between cortex, striatum and hippocampus. Data normalised to *Ubc* and expressed as fold change of cortex. n≥3/genotype. ** $p<0.01$ (to cortex) *** $p<0.001$ (to cortex and to hippocampus) (**B**) BDNF protein content measured by ELISA in cortex, striatum, hippocampus and liver in WT mice at 9 weeks of age. Data normalised to cortex. * $p<0.05$; n = 3/genotype. Error bars represent SEM.
(TIF)

Table S1 Statistical analysis of the influence of time (30 min duration) and genotype(s) on the spontaneous motor activity parameters: activity, mobility, rearing and centre rearing presented as *p* - values calculated via ANOVA General Linear Model with Greenhouse-Geisser correction.
(DOC)

Acknowledgments

We thank Tso-Pang Yao for the HDAC6 antibody, and members of the Neurogenetics Laboratory for the provision of R6/2 males for breeding.

Author Contributions

Conceived and designed the experiments: AB PP PM GPB. Performed the experiments: AB. Analyzed the data: AB GPB. Contributed reagents/materials/analysis tools: PP PM GPB. Wrote the paper: AB GPB. Proofread the manuscript: PP PM.

References

1. Bates G, Harper PS, Jones L (2002) Huntington's disease. Oxford: Oxford University Press. xvi558 p.
2. Novak MJ, Tabrizi SJ (2010) Huntington's disease. BMJ 340: c3109.
3. The Huntington's Disease Collaborative Research Group (1993) A novel gene containing a trinucleotide repeat that is expanded and unstable on Huntington's disease chromosomes. Cell 72: 971–983.
4. Tabrizi SJ, Langbehn DR, Leavitt BR, Roos RAC, Durr A, et al. (2009) Biological and clinical manifestations of Huntington's disease in the longitudinal TRACK-HD study: cross-sectional analysis of baseline data. The Lancet Neurology 8: 791–801.
5. Tabrizi SJ, Scahill RI, Durr A, Roos RAC, Leavitt BR, et al. (2011) Biological and clinical changes in premanifest and early stage Huntington's disease in the TRACK-HD study: the 12-month longitudinal analysis. The Lancet Neurology 10: 31–42.
6. DiFiglia M, Sapp E, Chase KO, Davies SW, Bates GP, et al. (1997) Aggregation of huntingtin in neuronal intranuclear inclusions and dystrophic neurites in brain. Science 277: 1990–1993.
7. Zuccato C, Valenza M, Cattaneo E (2010) Molecular mechanisms and potential therapeutical targets in Huntington's disease. Physiol Rev 90: 905–981.
8. Butler R, Bates GP (2006) Histone deacetylase inhibitors as therapeutics for polyglutamine disorders. Nat Rev Neurosci 7: 784–796.
9. de Ruijter AJ, van Gennip AH, Caron HN, Kemp S, van Kuilenburg AB (2003) Histone deacetylases (HDACs): characterization of the classical HDAC family. Biochem J 370: 737–749.
10. Finkel T, Deng CX, Mostoslavsky R (2009) Recent progress in the biology and physiology of sirtuins. Nature 460: 587–591.
11. Bates EA, Victor M, Jones AK, Shi Y, Hart AC (2006) Differential contributions of Caenorhabditis elegans histone deacetylases to Huntingtin polyglutamine toxicity. Journal of Neuroscience 26: 2830–2838.
12. Hockly E, Richon VM, Woodman B, Smith DL, Zhou X, et al. (2003) Suberoylanilide hydroxamic acid, a histone deacetylase inhibitor, ameliorates motor deficits in a mouse model of Huntington's disease. Proc Natl Acad Sci U S A 100: 2041–2046.
13. Steffan JS, Bodai L, Pallos J, Poelman M, McCampbell A, et al. (2001) Histone deacetylase inhibitors arrest polyglutamine-dependent neurodegeneration in Drosophila. Nature 413: 739–743.
14. Pallos J, Bodai L, Lukacsovich T, Purcell JM, Steffan JS, et al. (2008) Inhibition of specific HDACs and sirtuins suppresses pathogenesis in a Drosophila model of Huntington's disease. Hum Mol Genet 17: 3767–3775.
15. Khan N, Jeffers M, Kumar S, Hackett C, Boldog F, et al. (2008) Determination of the class and isoform selectivity of small-molecule histone deacetylase inhibitors. Biochem J 409: 581–589.
16. Grozinger CM, Hassig CA, Schreiber SL (1999) Three proteins define a class of human histone deacetylases related to yeast Hda1p. Proc Natl Acad Sci U S A 96: 4868–4873.
17. Seigneurin-Berny D, Verdel A, Curtet S, Lemercier C, Garin J, et al. (2001) Identification of components of the murine histone deacetylase 6 complex: link between acetylation and ubiquitination signaling pathways. Mol Cell Biol 21: 8035–8044.
18. Zhang Y, Li N, Caron C, Matthias G, Hess D, et al. (2003) HDAC-6 interacts with and deacetylates tubulin and microtubules in vivo. EMBO J 22: 1168–1179.
19. Hubbert C, Guardiola A, Shao R, Kawaguchi Y, Ito A, et al. (2002) HDAC6 is a microtubule-associated deacetylase. Nature 417: 455–458.
20. Kovacs JJ, Murphy PJ, Gaillard S, Zhao X, Wu JT, et al. (2005) HDAC6 regulates Hsp90 acetylation and chaperone-dependent activation of glucocorticoid receptor. Mol Cell 18: 601–607.

21. Zhang X, Yuan Z, Zhang Y, Yong S, Salas-Burgos A, et al. (2007) HDAC6 modulates cell motility by altering the acetylation level of cortactin. Mol Cell 27: 197–213.
22. Kopito RR (2000) Aggresomes, inclusion bodies and protein aggregation. Trends in Cell Biology 10: 524–530.
23. Kawaguchi Y, Kovacs JJ, McLaurin A, Vance JM, Ito A, et al. (2003) The deacetylase HDAC6 regulates aggresome formation and cell viability in response to misfolded protein stress. Cell 115: 727–738.
24. Kwon S, Zhang Y, Matthias P (2007) The deacetylase HDAC6 is a novel critical component of stress granules involved in the stress response. Genes Dev 21: 3381–3394.
25. Iwata A, Riley BE, Johnston JA, Kopito RR (2005) HDAC6 and microtubules are required for autophagic degradation of aggregated huntingtin. J Biol Chem 280: 40282–40292.
26. Pandey UB, Nie Z, Batlevi Y, McCray BA, Ritson GP, et al. (2007) HDAC6 rescues neurodegeneration and provides an essential link between autophagy and the UPS. Nature 447: 859–863.
27. Lee JY, Koga H, Kawaguchi Y, Tang W, Wong E, et al. (2010) HDAC6 controls autophagosome maturation essential for ubiquitin-selective quality-control autophagy. EMBO J 29: 969–980.
28. Dompierre JP, Godin JD, Charrin BC, Cordelieres FP, King SJ, et al. (2007) Histone deacetylase 6 inhibition compensates for the transport deficit in Huntington's disease by increasing tubulin acetylation. J Neurosci 27: 3571–3583.
29. Mahlknecht U, Schnittger S, Landgraf F, Schoch C, Ottmann OG, et al. (2001) Assignment of the human histone deacetylase 6 gene (HDAC6) to X chromosome p11.23 by in situ hybridization. Cytogenet Cell Genet 93: 135–136.
30. Mangiarini L, Sathasivam K, Seller M, Cozens B, Harper A, et al. (1996) Exon 1 of the HD gene with an expanded CAG repeat is sufficient to cause a progressive neurological phenotype in transgenic mice. Cell 87: 493–506.
31. Moffitt H, McPhail GD, Woodman B, Hobbs C, Bates GP (2009) Formation of polyglutamine inclusions in a wide range of non-CNS tissues in the HdhQ150 knock-in mouse model of Huntington's disease. PLoS One 4: e8025.
32. Landles C, Sathasivam K, Weiss A, Woodman B, Moffitt H, et al. (2010) Proteolysis of Mutant Huntingtin Produces an Exon 1 Fragment That Accumulates as an Aggregated Protein in Neuronal Nuclei in Huntington Disease. Journal of Biological Chemistry 285: 8808–8823.
33. Woodman B, Butler R, Landles C, Lupton MK, Tse J, et al. (2007) The Hdh(Q150/Q150) knock-in mouse model of HD and the R6/2 exon 1 model develop comparable and widespread molecular phenotypes. Brain Res Bull 72: 83–97.
34. Sathasivam K, Lane A, Legleiter J, Warley A, Woodman B, et al. (2010) Identical oligomeric and fibrillar structures captured from the brains of R6/2 and knock-in mouse models of Huntington's disease. Hum Mol Genet 19: 65–78.
35. Kuhn A, Goldstein DR, Hodges A, Strand AD, Sengstag T, et al. (2007) Mutant huntingtin's effects on striatal gene expression in mice recapitulate changes observed in human Huntington's disease brain and do not differ with mutant huntingtin length or wild-type huntingtin dosage. Human Molecular Genetics 16: 1845–1861.
36. Zhang Y, Kwon S, Yamaguchi T, Cubizolles F, Rousseaux S, et al. (2008) Mice lacking histone deacetylase 6 have hyperacetylated tubulin but are viable and develop normally. Mol Cell Biol 28: 1688–1701.
37. Luthi-Carter R, Hanson SA, Strand AD, Bergstrom DA, Chun W, et al. (2002) Dysregulation of gene expression in the R6/2 model of polyglutamine disease: parallel changes in muscle and brain. Human Molecular Genetics 11: 1911–1926.
38. Gao YS, Hubbert CC, Lu J, Lee YS, Lee JY, et al. (2007) Histone deacetylase 6 regulates growth factor-induced actin remodeling and endocytosis. Mol Cell Biol 27: 8637–8647.
39. Reed NA, Cai D, Blasius TL, Jih GT, Meyhofer E, et al. (2006) Microtubule acetylation promotes kinesin-1 binding and transport. Curr Biol 16: 2166–2172.
40. Gauthier LR, Charrin BC, Borrell-Pages M, Dompierre JP, Rangone H, et al. (2004) Huntingtin controls neurotrophic support and survival of neurons by enhancing BDNF vesicular transport along microtubules. Cell 118: 127–138.
41. Zuccato C, Cattaneo E (2009) Brain-derived neurotrophic factor in neurodegenerative diseases. Nat Rev Neurol 5: 311–322.
42. Altar CA, Cai N, Bliven T, Juhasz M, Conner JM, et al. (1997) Anterograde transport of brain-derived neurotrophic factor and its role in the brain. Nature 389: 856–860.
43. Crook ZR, Housman D (2011) Huntington's Disease: Can Mice Lead the Way to Treatment? Neuron 69: 423–435.
44. Martin EJ, Kim M, Velier J, Sapp E, Lee HS, et al. (1999) Analysis of Huntingtin-associated protein 1 in mouse brain and immortalized striatal neurons. J Comp Neurol 403: 421–430.
45. Apostol BL, Simmons DA, Zuccato C, Illes K, Pallos J, et al. (2008) CEP-1347 reduces mutant huntingtin-associated neurotoxicity and restores BDNF levels in R6/2 mice. Mol Cell Neurosci 39: 8–20.
46. Cepeda C, Cummings DM, Hickey MA, Kleiman-Weiner M, Chen JY, et al. (2010) Rescuing the Corticostriatal Synaptic Disconnection in the R6/2 Mouse Model of Huntington's Disease: Exercise, Adenosine Receptors and Ampakines. PLoS Curr 2.
47. Seo H, Kim W, Isacson O (2008) Compensatory changes in the ubiquitin-proteasome system, brain-derived neurotrophic factor and mitochondrial complex II/III in YAC72 and R6/2 transgenic mice partially model Huntington's disease patients. Hum Mol Genet 17: 3144–3153.
48. Cho S-R, Benraiss A, Chmielnicki E, Samdani A, Economides A, et al. (2007) Induction of neostriatal neurogenesis slows disease progression in a transgenic murine model of Huntington disease. The Journal of Clinical Investigation 117: 2889–2902.
49. Canals JM, Pineda JR, Torres-Peraza JF, Bosch M, Martin-Ibanez R, et al. (2004) Brain-derived neurotrophic factor regulates the onset and severity of motor dysfunction associated with enkephalinergic neuronal degeneration in Huntington's disease. J Neurosci 24: 7727–7739.
50. Gharami K, Xie Y, An JJ, Tonegawa S, Xu B (2008) Brain-derived neurotrophic factor over-expression in the forebrain ameliorates Huntington's disease phenotypes in mice. J Neurochem 105: 369–379.
51. Du G, Liu X, Chen X, Song M, Yan Y, et al. (2010) Drosophila histone deacetylase 6 protects dopaminergic neurons against {alpha}-synuclein toxicity by promoting inclusion formation. Mol Biol Cell 21: 2128–2137.
52. Pandey UB, Batlevi Y, Baehrecke EH, Taylor JP (2007) HDAC6 at the intersection of autophagy, the ubiquitin-proteasome system and neurodegeneration. Autophagy 3: 643–645.
53. Ding H, Dolan PJ, Johnson GV (2008) Histone deacetylase 6 interacts with the microtubule-associated protein tau. J Neurochem 106: 2119–2130.
54. Benn CL, Butler R, Mariner L, Nixon J, Moffitt H, et al. (2009) Genetic knock-down of HDAC7 does not ameliorate disease pathogenesis in the R6/2 mouse model of Huntington's disease. PLoS One 4: e5747.
55. Hockly E, Woodman B, Mahal A, Lewis CM, Bates G (2003) Standardization and statistical approaches to therapeutic trials in the R6/2 mouse. Brain Res Bull 61: 469–479.
56. Hockly E, Tse J, Barker AL, Moolman DL, Beunard JL, et al. (2006) Evaluation of the benzothiazole aggregation inhibitors riluzole and PGL-135 as therapeutics for Huntington's disease. Neurobiol Dis 21: 228–236.
57. Sathasivam K, Woodman B, Mahal A, Bertaux F, Wanker EE, et al. (2001) Centrosome disorganization in fibroblast cultures derived from R6/2 Huntington's disease (HD) transgenic mice and HD patients. Hum Mol Genet 10: 2425–2435.
58. Ko J, Ou S, Patterson PH (2001) New anti-huntingtin monoclonal antibodies: implications for huntingtin conformation and its binding proteins. Brain Research Bulletin 56: 319–329.
59. Weiss A, Roscic A, Paganetti P (2009) Inducible mutant huntingtin expression in HN10 cells reproduces Huntington's disease-like neuronal dysfunction. Mol Neurodegener 4: 11.
60. Weiss A, Abramowski D, Bibel M, Bodner R, Chopra V, et al. (2009) Single-step detection of mutant huntingtin in animal and human tissues: a bioassay for Huntington's disease. Anal Biochem 395: 8–15.
61. Szapacs ME, Mathews TA, Tessarollo L, Ernest Lyons W, Mamounas LA, et al. (2004) Exploring the relationship between serotonin and brain-derived neurotrophic factor: analysis of BDNF protein and extraneuronal 5-HT in mice with reduced serotonin transporter or BDNF expression. Journal of Neuroscience Methods 140: 81–92.
62. Benn CL, Fox H, Bates GP (2008) Optimisation of region-specific reference gene selection and relative gene expression analysis methods for pre-clinical trials of Huntington's disease. Mol Neurodegener 3: 17.

Experimental Paper - Supporting Information

Table S1.

Statistical analysis of the influence of time (30 min duration) and genotype(s) on the spontaneous motor activity parameters: activity, mobility, rearing and centre rearing presented as *p* - values calculated via ANOVA General Linear Model with Greenhouse-Geisser correction

	Week	Activity	Mobility	Rearing	Centre Rearing	P = < 0.001
Time	**5**	<0.001	<0.001	<0.001	<0.001	P = < 0.01
	7	<0.001	<0.001	0.001	0.008	P = < 0.05
	9	<0.001	<0.001	<0.001	0.010	
	11	<0.001	<0.001	0.019	0.038	
	13	<0.001	<0.001	0.045	0.054	
R6/2 Genotype	**5**	0.254	0.064	0.241	0.428	
	7	<0.001	<0.001	0.527	0.338	
	9	<0.001	<0.001	<0.001	<0.001	
	11	<0.001	<0.001	<0.001	<0.001	
	13	<0.001	<0.001	<0.001	<0.001	
Time*R6/2 Genotype	**5**	0.011	0.078	0.016	0.091	
	7	<0.001	<0.001	<0.001	0.002	
	9	<0.001	<0.001	0.001	0.071	
	11	<0.001	<0.001	0.001	0.138	
	13	0.009	<0.001	0.063	0.171	
***Hdac6KO* Genotype**	**5**	0.771	0.946	0.421	0.380	
	7	0.204	0.411	0.297	0.452	
	9	0.511	0.906	0.447	0.563	
	11	0.272	0.378	0.876	0.781	
	13	0.557	0.908	0.795	0.765	
Time****Hdac6KO* Genotype**	**5**	0.053	0.070	0.815	0.515	
	7	0.330	0.083	0.449	0.262	
	9	0.401	0.371	0.225	0.229	
	11	0.808	0.747	0.133	0.192	
	13	0.704	0.705	0.726	0.339	
R6/2 Genotype****Hdac6KO* Genotype**	**5**	0.201	0.357	0.950	0.635	
	7	0.718	0.701	0.490	0.891	
	9	0.907	0.746	0.032	0.091	
	11	0.542	0.488	0.638	0.922	
	13	0.587	0.610	0.443	0.499	
Time*R6/2****Hdac6KO***	**5**	0.160	0.481	0.184	0.315	
	7	0.019	0.022	0.167	0.325	
	9	0.263	0.206	0.270	0.559	
	11	0.304	0.495	0.822	0.739	
	13	0.189	0.490	0.556	0.493	

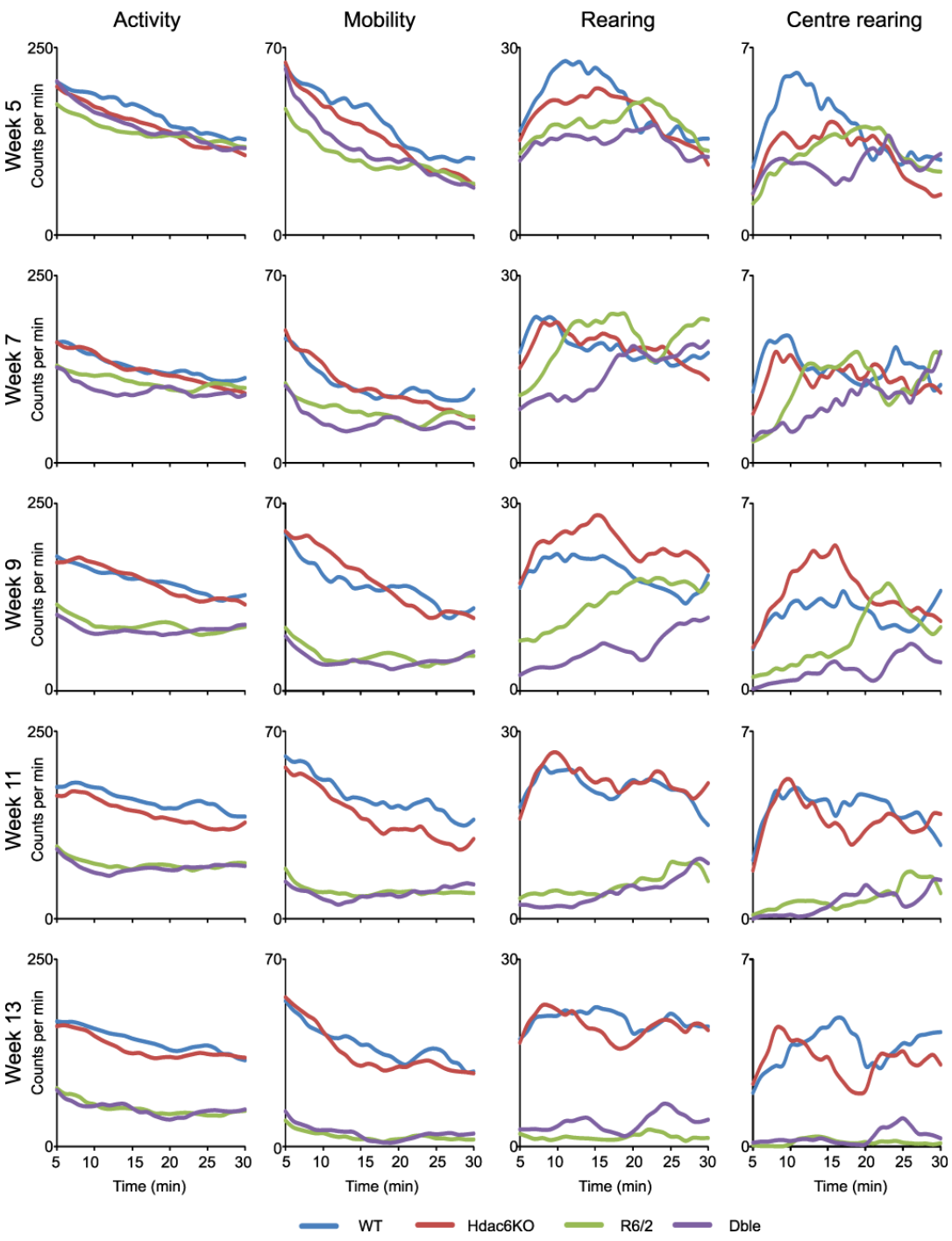

Figure S1. *Hdac6* knock-out has no effect on spontaneous motor activity in WT or R6/2 mice.

Five minute moving averages for Activity, Mobility, Rearing and Centre rearing at 5, 7, 9, 11 and 13 weeks of age for WT, *Hdac6KO*, R6/2 and Dble mice≥ n 16/genotype (as shown in Fig. 3A).

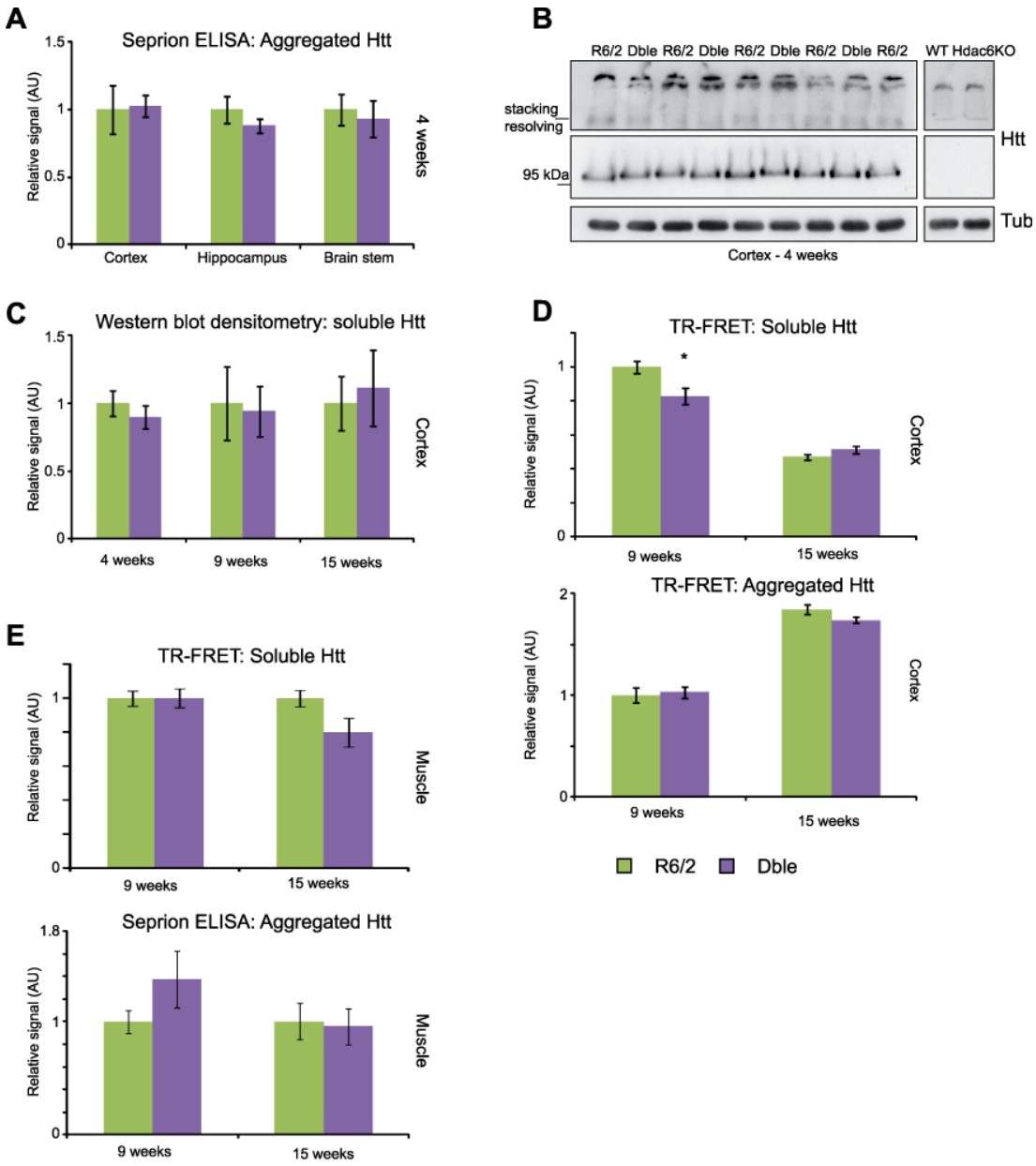

Figure S2. *Hdac6* knock-out does not change aggregate load in the brain or muscle.

(A) Aggregate load was measured by Seprion ligand ELISA with the MW8 antibody in the cortex, hippocampus and brain stem of R6/2 and Dble mice at 4 weeks≥n 5/genotype. **(B)** Representative western blot with S830 anti-huntingtin antibody showing aggregated and soluble transprotein (Htt) in the cortex at 4 weeks. α-tubulin (Tub) was used as a loading control. Specificity of S830 staining is confirmed by lack of signal in WT and *Hdac6*KO cortices. **(C)** Densitometric quantification of soluble Htt from western blots shown in (A) and Fig. 4C. Htt signal was normalised to α-tubulin and the relative signal for Dble mice expressed as fold change to R6/2 for each time point. **(D)** Soluble (2B7-MW1 antibodies, upper panel) and aggregated (MW8-MW8 antibodies, lower panel) transprotein levels were measured by TR-FRET in the cortex at 9 and 15 weeks. Data normalised to R6/2 at 9 weeks. * $p<0.05$; n≥ 8/genotype. **(E)** Aggregate load was measured by Seprion

ligand ELISA with the MW8 antibody and soluble transprotein levels were measured by TR-FRET (2B7-MW1 antibodies) in the quadriceps muscle at 9 and 15 weeks. Data normalised to R6/2 at each time point. ≥ 7/genotype. Error bars represent SEM.

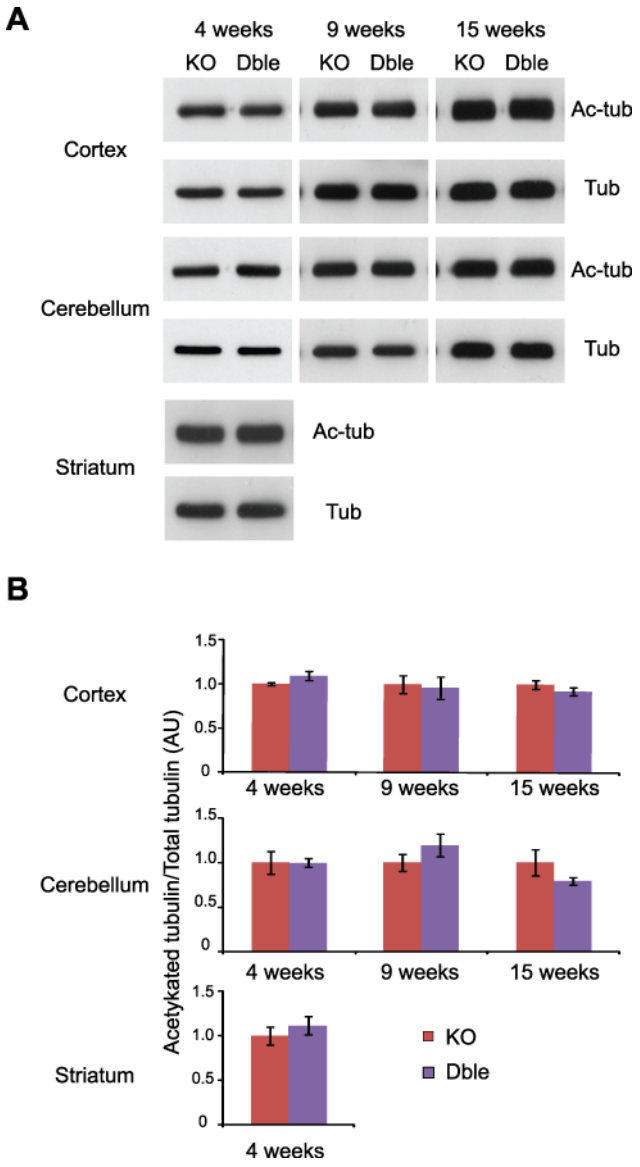

Figure S3. The increase in tubulin acetylation in brain is comparable between *Hdac6*KO and Dble mice.

(A) Representative western blots showing acetylated tubulin (Ac-tub) in Dble and *Hdac6*KO mice at 4, 9 and 15 weeks in cortex, striatum and cerebellum with α-tubulin (Tub) as a loading control. There was insufficient tissue to perform the analysis on striatum at 9 and 15 weeks. **(B)** Densitometric quantification of western blots presented in (A). Acetylated tubulin was normalised to α-tubulin and the relative signal for Dble mice expressed as fold change to *Hdac6*KO. Error bars represent SEM. KO - *Hdac6*KO, Dble - *Hdac6*KOxR6/2; n ≥ 3/genotype.

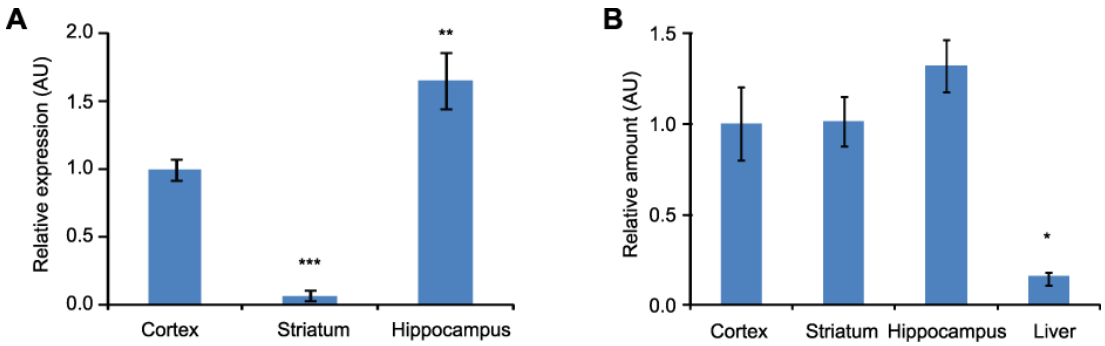

Figure S4. Similar levels of BDNF protein in striatum, cortex and hippocampus despite very low *Bdnf* mRNA striatal expression.

(A) *Bdnf* mRNA coding region expression in WT mice at 9 weeks between cortex, striatum and hippocampus. Data normalised to *Ubc* and expressed as fold change of cortex. n≥ 3/genotype. ** $p<0.01$ (to cortex) *** $p<0.001$ (to cortex and to hippocampus) **(B)** BDNF protein content measured by ELISA in cortex, striatum, hippocampus and liver in WT mice at 9 weeks of age. Data normalised to cortex. * $p<0.05$; n = 3/genotype. Error bars represent SEM.

4.0. RESULTS CHAPTER 4 - GENETIC REDUCTION OF SIRT2 IN R6/2 MICE

4.1. Reducing levels of SIRT2 does not modify disease progression in R6/2 mice

Studies in worms, flies and cells have demonstrated that SIRT2 inhibition could be beneficial in HD by acting to correct cholesterol dys-homeostasis (Luthi-Carter et al., 2010). However, whether this effect translates to an *in vivo* mammalian system remains unknown. To address this question, *Sirt2* was genetically depleted in the R6/2 mouse model of HD and the effects on behaviour, mutant huntingtin (mHTT) aggregation and expression of cholesterogenic enzymes were assessed.

4.2. *Sirt2* knock-out mice express *Sirt2* mRNA, but not SIRT2 protein

Sirt2 knock-out (*Sirt2*KO) mice (a kind gift from Prof. Leonard Guarente) were generated by targeted insertion of a puromycin resistance gene into exon 11 of the *Sirt2* locus. However, the specific position, length and sequence of the insertion were unknown.

4.2.1. Sequencing the *Sirt2* knock-out mutation

To sequence the insertion that disrupts the *Sirt2* gene in *Sirt2*KO mice (Fig. 4.1 A), genotyping primers (primers 1 and A in Fig. 4.1 A) were used to obtain a DNA fragment that contained a part of the *Sirt2* gene and a part of the insertion. Sequencing this product facilitated the design of additional primers that were then used to amplify a second DNA fragment covering the remaining part of the insertion (primers 2-5 in Fig. 4.1 A). As the sequencing reaction was not efficient enough to cover the whole length of the second DNA fragment (with primers 2-5 and B-C in Fig. 4.1 A), more primers were designed to amplify the remainder of the insertion based on the sequence obtained (primers 6 and 7 in Fig. 4.1 A). BLAST analysis of the sequence obtained confirmed that the insertion contains a puromycin resistance gene countersense to the *Sirt2* gene and revealed sequences of at least 3 different vector backbones (Fig. 4.2 A). Further analysis showed that although the insertion does not result in a frameshift in the downstream part of the *Sirt2* gene,

the mutation introduces a stop codon that should result in nonsense-mediated decay of the *Sirt2* mRNA (full sequence of the insertion and its position within the *Sirt2* gene can be found in the Appendix 1).

4.2.2. *Sirt2* knock-out mice express *Sirt2* mRNA at 60% of wild type levels, but lack SIRT2 protein

To investigate how the insertion in the *Sirt2* gene affects *Sirt2* expression, RNA was extracted and cDNA prepared from cortices of *Sirt2*KO, *Sirt2*HET (*Sirt2* heterozygous) and wild type (WT) mice at 4 weeks of age. Levels of total *Sirt2* mRNA were measured by real-time qPCR with primers binding upstream of the insertion. *Sirt2*HET and *Sirt2*KO mice were found to express 80% and 60% of *Sirt2* mRNA as compared to WT levels respectively (Fig. 4.1 B). To investigate whether the mRNA produced in the presence of the insertion is translated, western blotting was performed on brain lysates from 4 week old *Sirt2*KO, *Sirt2*HET and WT mice. Antibodies directed against the N-terminus (Santa Cruz H-95) or the C-terminus (Sigma S8447) of SIRT2 revealed two bands, the lower of which is a doublet. The 3 bands detected correspond to the predicted molecular weight of the three SIRT2 isoforms (43, 37 and 34 kDa) (Fig. 4.1 C) (Maxwell et al., 2011). This signal was absent in *Sirt2*KO samples indicating that no SIRT2 protein is produced in these mice. At the same time, *Sirt2*HET mice were shown to express 55% of SIRT2 levels of WT mice (Fig 4.1 C). Equally, no shorter N-terminal fragment were observed specifically in HET or KO samples with the Santa Cruz H-95 antibody. Though both antibodies detected non-specific bands on western blot, the signal obtained with the S8447 antibody had a lower background and was therefore used for all subsequent experiments.

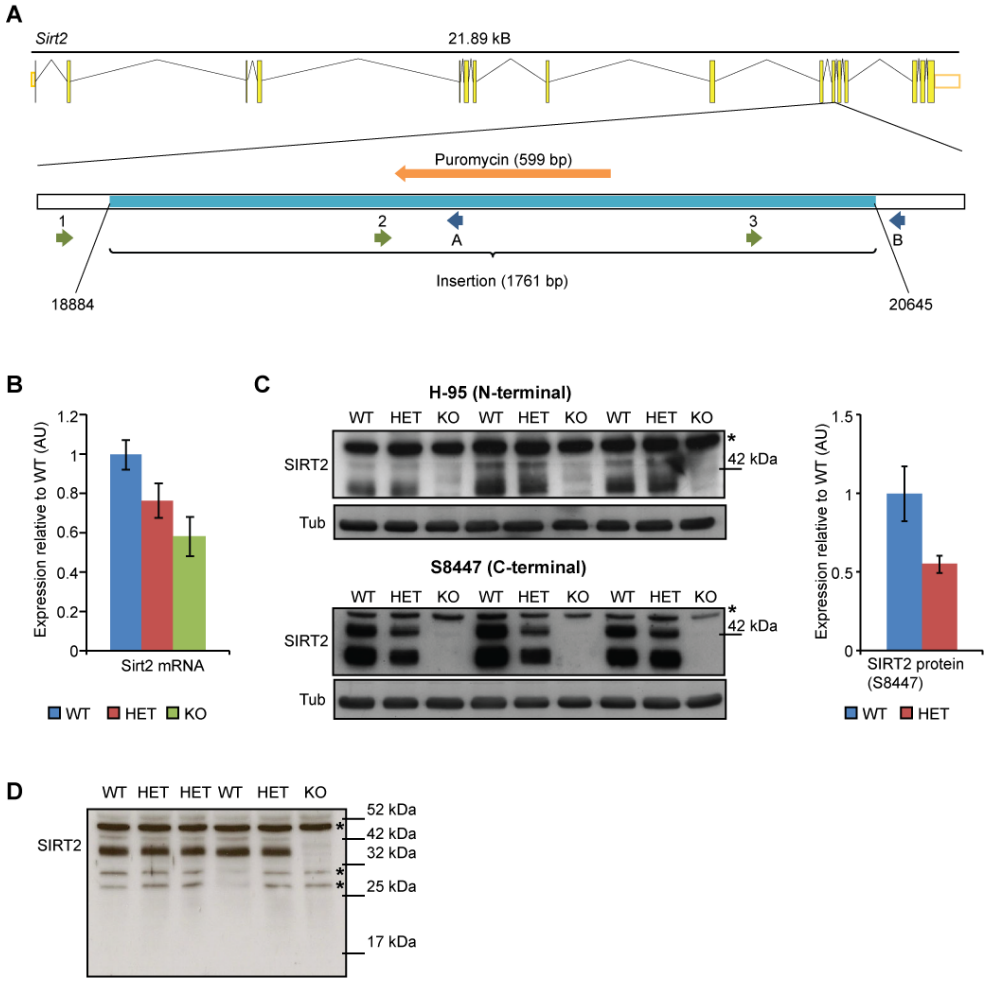

Figure 4.1. The *Sirt2* knock-out mutation results in reduced *Sirt2* mRNA production and an absence of SIRT2 protein.

(A) Exon-intron structure of the *Sirt2* gene in mouse and the location of the insertion (light blue) in exon 11 (after the 18883rd nucleotide) in *Sirt2*KO mice. Positions of genotyping and sequencing forward (green arrows) and reverse (dark blue arrows) primers are shown. 1-*Sirt2*For, 2-*Sirt2*ForSeq2, 3-*Sirt2*ForSeq3, 4-*Sirt2*ForSeq4, 5-*Sirt2*ForSeq5, 6-*Sirt2*ForSeq6, 7-*Sirt2*ForSeq7, A-*Sirt2*RevKO, B-*Sirt2*RevSeq2, C-*Sirt2*RevSeq3, D-*Sirt2*RevWT. **(B)** *Sirt2* mRNA levels in 4 week old cortex from *Sirt2*KO (KO), *Sirt2*HET (HET) and wild type (WT) mice. Expression levels were normalised to the housekeeping genes *Atp5b* and *Canx* and expressed as fold change of WT levels ±SEM. n=8/genotype. **(C)** Western blotting of *Sirt2*KO (KO), *Sirt2*HET (HET) and wild type (WT) brain lysates with SantaCruz H-95 (upper panel) and Sigma S8447 (lower panel) antibodies. The S8447 probed blot was used to quantify SIRT2 levels (both bands) between HET and WT (right panel). Values were normalised to α-tubulin (Tub) and expressed as fold change of WT ±SEM. **(D)** Western blotting of KO, HET and WT brain lysates with SantaCruz H-95 antibody (long exposure) showing no short N-terminal fragments are produced as a result of the *Sirt2* disrupting mutation. * denotes a non-specific bands.

4.3. Characterisation of SIRT2 expression, sub-cellular localisation and effects of SIRT2 reduction on acetylation of tubulin and H4K16

4.3.1. SIRT2 expression between 4 and 15 weeks in mouse brain

At 4 weeks of age R6/2 mice are generally indistinguishable from their wild type littermates by rotarod, grip strength or spontaneous exploratory activity tests (Benn et al., 2009; Hockly et al., 2002). However, disease progression in R6/2 is rapid and mice from the King's College London colony generally do not survive longer than 15 weeks. To investigate the levels of SIRT2 expression in the brain over this time frame, proteins were extracted from cortex, striatum, hippocampus, cerebellum, brain stem and "rest of brain" (what remained after dissecting the 5 regions) from 4 and 15 week old wild type mice. Western blotting revealed that the highest levels of SIRT2 expression are observed in the brain stem (Fig 4.2 A - B). SIRT2 expression was comparable in cortex, striatum, hippocampus and cerebellum with levels between 0.5 and 1.5 times less than that in brain stem. Although levels of SIRT2 were slightly decreased in 15 week brain tissues, the regional distribution of SIRT2 expression remained unchanged (Fig. 4.2 A - B).

4.3.2. Genetic reduction of SIRT2 has no effect on its sub-cellular localisation

The sub-cellular localisation of SIRT2 has previously been reported to be cytoplasmic, with the exception of during cell division, when SIRT2 is reported to translocate to the nucleus (North et al., 2003; North and Verdin, 2007). To ascertain whether this is the case in the mouse brain and whether knock-down of *Sirt2* affects its sub-cellular localisation, nuclear and cytoplasmic fractions were prepared from whole brains of 4 week old *Sirt2*HET and WT mice. Western blotting against actin (cytoplasmic marker) and histone H3 (nuclear marker) revealed minimal cross-contamination of the fractions (Fig. 4.2 C), thereby confirming their purity. Consistent with previous reports, the SIRT2 signal was found predominantly in the cytoplasm. Additionally, the cytoplasmic localisation of SIRT2 was found to be unaltered in the *Sirt2*HET mice, which confirms that SIRT2 reduction does not affect its sub-cellular localisation.

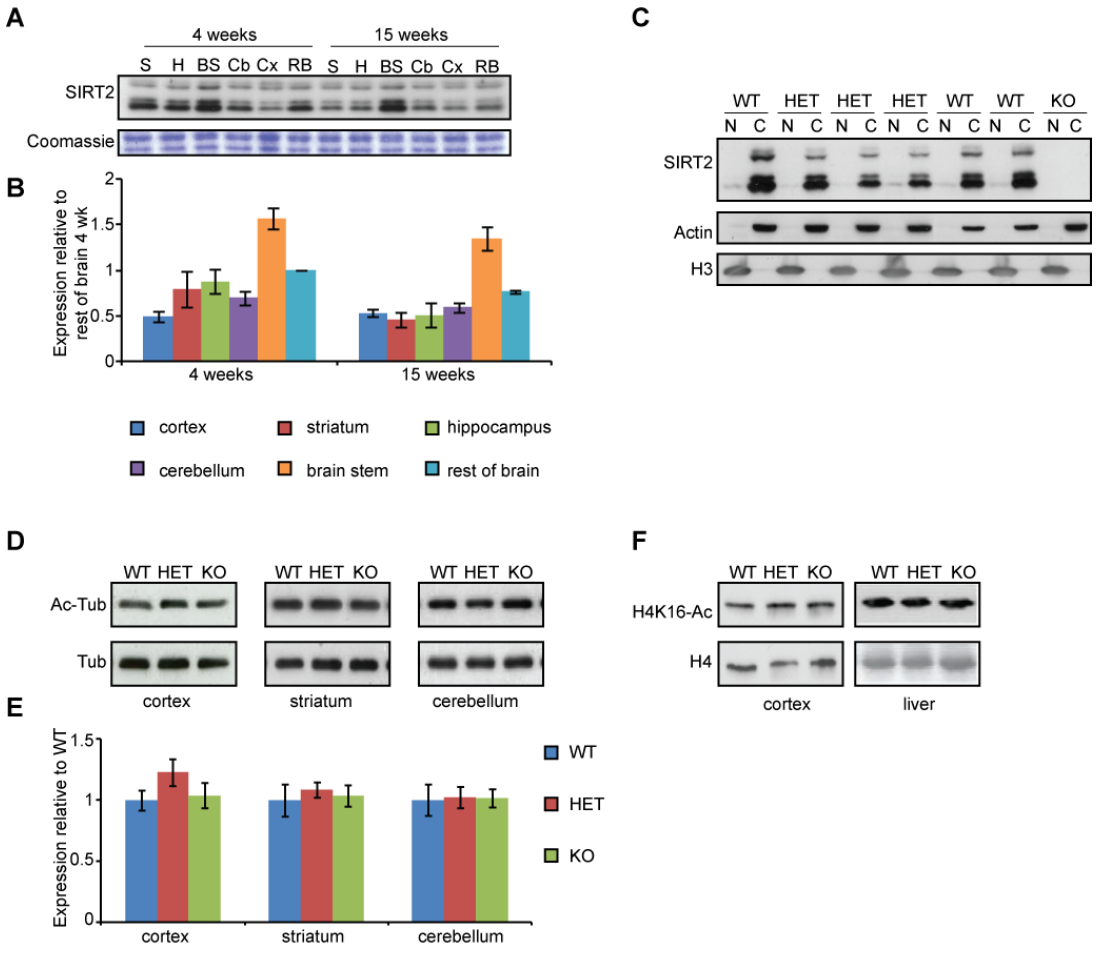

Figure 4.2. SIRT2 is expressed most highly in the brain stem, localised cytoplasmatically and its depletion does not affect tubulin or H4K16 acetylation levels.

(A) Representative western blot showing SIRT2 expression in different brain regions at 4 and 15 weeks of age. **(B)**The signal for SIRT2 was normalised to total protein loaded (Coomasie stain) and expressed as fold change of rest of brain (Rb)(containing all regions except cortex (Cx), striatum (S), hippocampus (H), cerebellum (Cb) and brain stem (BS)) ± SEM. n=4/brain region/time point. **(C)** SIRT2 is localised to the cytoplasm. Purity of fractions was determined by measuring the expression of actin (C-cytoplasm) and H3 (N-nucleus). **(D)** Representative western blots of acetylated tubulin (Ac-Tub) at 4 weeks of age in the cortex, striatum and cerebellum of WT, HET and KO mice and their quantification **(E)**. Signal was normalised to the level of total tubulin (Tub) and expressed as fold change of WT ± SEM. n=4/genotype. **(F)** Representative western blots of acetylated H4K16 (H4K16-Ac) and total H4 (H4) at 4 weeks of age in the cortex and liver of WT, HET and KO mice. n=3/genotype (cortex) and n=6/genotype (liver). WT – wild type, HET – *Sirt2*HET, KO – *Sirt2*KO

4.3.3. No changes in acetylation of tubulin or H4K16 can be detected upon SIRT2 genetic reduction

The first two proposed SIRT2 deacetylation substrates were lysine (K) 40 of α-tubulin and K16 of histone 4 (H4) (North et al., 2003; Vaquero et al., 2006). It has already been shown that knock-out of another tubulin deacetylase, HDAC6, causes tubulin hyperacetylation across the brain (Results Chapter 3 – Experimental Paper, Fig. 2 A). To verify whether a similar effect would be observed after SIRT2 genetic depletion, western blotting was performed on cortical, striatal and cerebellar samples obtained from 4 week old WT, *Sirt2*HET and *Sirt2*KO mice. Interestingly, no differences were observed between WT, HET and KO mice in the levels of acetylated tubulin, indicating that HDAC6, not SIRT2, is the major tubulin deacetylase in the brain (Fig. 4.2 D - E). To check the effect of *Sirt2* knock-out and knock-down on the levels of H4K16 acetylation, histones were enriched by acid extraction from cortices and livers of 4 week old mice. No genotype specific differences could be detected in the levels of acetylated H4K16 in the tissues examined (Fig. 4.2 F).

4.4. Reduction or elimination of SIRT2 has no effect on the expression levels of cholesterol biosynthesis enzymes

Previous studies using mRNA microarray analysis suggested that inhibition of SIRT2 results in a decrease in the expression of enzymes that take part in cholesterol synthesis (Luthi-Carter et al., 2010). To verify whether genetic depletion of SIRT2 causes a reduction in the expression of cholesterogenic enzymes, 7 genes were chosen for analysis on the basis of previously published microarray data (Luthi-Carter et al., 2010). RNA was extracted and cDNA prepared from cortices of 4 week old WT, *Sirt2*HET and *Sirt2*KO mice, an age when SIRT2 levels are highest in the brain. Surprisingly, the expression of cholesterogenic enzymes was not modified by SIRT2 reduction or ablation (Fig. 4.3 A). To ascertain that this effect was not masked by focusing on a specific time point, gene expression was also measured in cortices from 9 week old mice. However, no difference between WT, *Sirt2*HET and *Sirt2*KO

mice could be detected (Fig. 4.3 B). As the expression of SIRT2 is lowest in the cortex but highest in the brain stem at 4 weeks of age (Fig. 4.2 A), there was a possibility that the reduction in SIRT2 levels could only have a detectable effect on cholesterogenic enzymes in brain regions where the reduction of SIRT2 is more dramatic (Fig.4.3 A). Therefore, the effect of SIRT2 depletion on the expression of cholesterol synthesis enzymes was analysed in the brain stem. Nevertheless, the expression levels of cholesterogenic enzymes were unchanged in *Sirt2*HET and *Sirt2*KO mice as compared to WT mice in the brain stem at 4 weeks of age (Fig. 4.3 C). In a final attempt to determine whether *Sirt2* knock-down or knock-out on has an effect on cholesterol synthesis, levels of cholesterogenic enzymes were measured in the liver of 4 week old mice. However, consistent with observations in brain tissue, reduction or ablation of SIRT2 did not produce a detectable change in the levels of cholesterogenic enzymes' mRNA (Fig. 4.3 D). Taken together these results suggest that the expression of enzymes responsible for cholesterol synthesis are not affected in *Sirt2*HET or *Sirt2*KO mice. This may be due to an absence of a role for SIRT2 in the regulation of cholesterol synthesis, or a compensation that occurs when the mammals are faced with a chronic reduction in SIRT2 levels, as is the case in *Sirt2*KO mice.

The mechanism by which SIRT2 was proposed to modulate the expression of cholesterogenic enzymes was that SIRT2 controls the sub-cellular localisation of the transcription factor SREBP-2, a master regulator of cholesterol enzymes' expression (Luthi-Carter et al., 2010). SREBP-2 is synthesised as an inactive, 120 kDa precursor and resides in the cytoplasm, bound to the ER membrane (Eberle et al., 2004). When cholesterol levels are low, SREBP-2 is cleaved into an active, 60 kDa form and translocates to the nucleus to activate transcription of cholesterogenic enzymes (Eberle et al., 2004). To investigate whether compensation in *Sirt2*HET/KO mice occurred downstream of SREBP-2 nuclear translocation, cytoplasmic and nuclear fractions previously used to investigate SIRT2 sub-cellular localisation (Fig. 4.2 B) were used to determine the sub-cellular localisation of SREBP-2. Only a faint 60 kDa signal could be seen in the nuclear fractions and there was no genotype dependent change in the intensity of bands detected, suggesting that if compensation for the

absence of SIRT2 occurs, it is prior to SREBP-2 activation and nuclear translocation (Fig. 4.3 E).

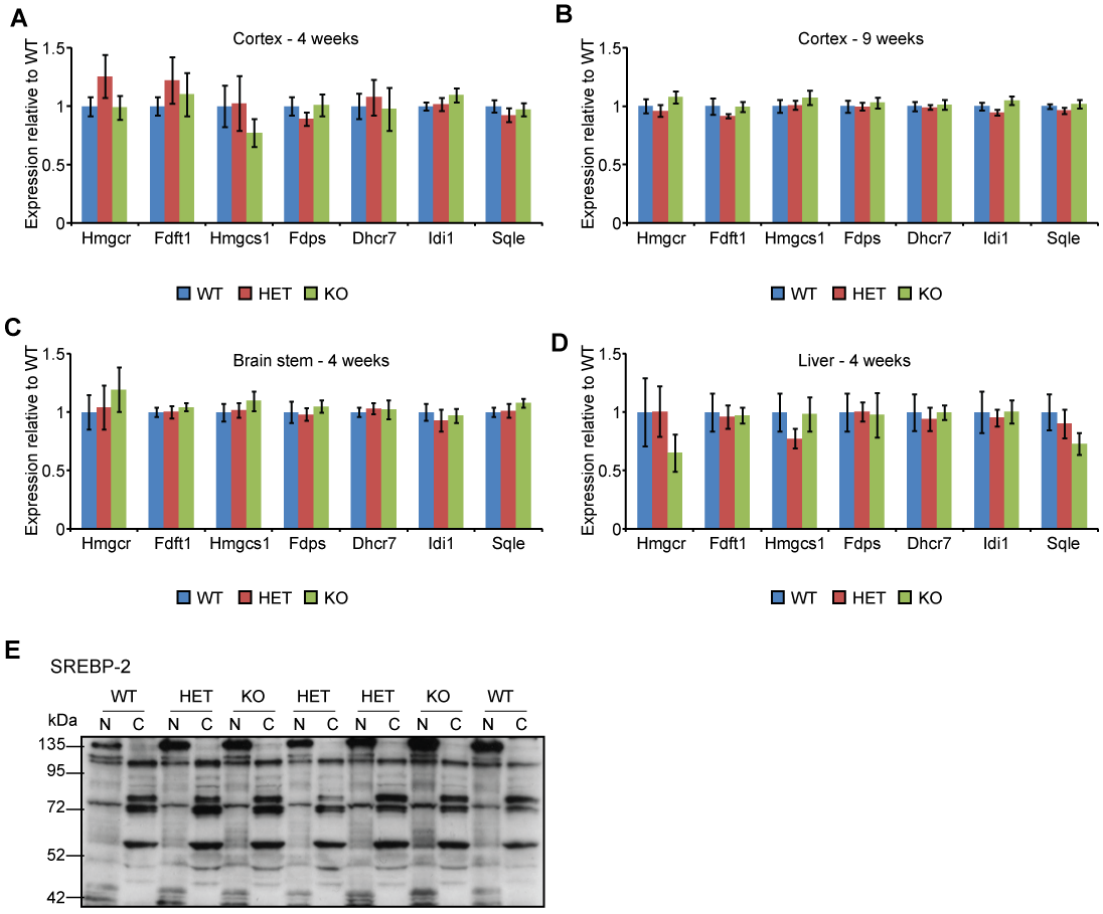

Figure 4.3. Expression of cholesterogenic enzymes is not affected in *Sirt2*HET or *Sirt2*KO mice.

(A - D) The mRNA expression levels of 7 cholesterogenic enzymes were determined by Taqman qPCR in the cortex at **(A)** 4 and **(B)** 9 weeks of age and in the **(C)** brain stem and **(D)** liver at 4 weeks of age between wild type (WT), *Sirt2*HET (HET) and *Sirt2*KO (KO) mice. n ≥ 6/genotype. Expression was normalised to the housekeeping genes *Atp5b* (4 and 9 wk cortex and brain stem), *Canx* (4 and 9 week cortex and liver), *Gapdh* (brain stem and liver), and *ActB* (liver) and expressed as fold change of WT ± SEM. **(E)** Representative immunoblot for SREBP-2 in whole brains of 4 week old wild type (WT), *Sirt2*HET (HET) and *Sirt2*KO (KO) mice. The active form of SREBP-2 was expected to migrate at 60 kDa in the nuclear (N) fractions, the precursor of SREBP-2 was expected to migrate at 120 kDa in the cytoplasmic (C) fractions. n=4/genotype.

4.5. Expression of histone deacetylases is not altered in *Sirt2*KO mice and the expression of *Sirt2* is not affected by disease progression in R6/2 mice

As *Sirt2*HET/KO mice do not show any overt phenotypes or changes in the levels of acetylated tubulin, acetylated H4K16 or cholesterogenic enzyme expression, there was a possibility that other deacetylases are up-regulated to compensate for SIRT2 loss. To investigate this possibility, the mRNA expression level of all 18 HDACs was assessed in cortices from 4 week old WT, *Sirt2*HET and *Sirt2*KO mice. Interestingly, the expression levels of none of the HDACs other than *Sirt2* were changed upon *Sirt2* knock-down or knock-out (Fig. 4.4 A-B).

SIRT1 is the closest SIRT2 homologue in mammals and shares at least 3 common substrates with SIRT2 (p53, FOXO1 and FOXO3a) (Peck et al., 2010; Wang et al., 2011; Wang and Tong, 2009; Yang et al., 2005). At the same time, it has recently been reported that SIRT1 deacetylates SREBP-1, a homologue of SREBP-2 and a master regulator of fatty acid synthesis, making SIRT1 the most likely candidate to compensate for SIRT2 loss (Ponugoti et al., 2010). To find the best antibody with which to assess SIRT1 levels in *Sirt2*KO mice, 5 commercially available SIRT1 antibodies were tested in 6 different buffers. Western blotting of brain lysates from 4 week old WT mice revealed that 4 out of 5 antibodies could detect the same 3 bands roughly corresponding to the predicted SIRT1 size of 110 kDa, whereas the antibody from Millipore did not produce any signal of the expected size (Fig. 4.4 C). Of the 5 antibodies tested, the Cell Signalling antibody proved to be the cleanest, only detecting 3 bands at the expected SIRT1 size. SIRT1 has at least 2 isoforms, therefore there is a strong possibility that at least 2 out of the 3 bands observed with all four antibodies are SIRT1 specific. In any case, when lysates prepared from cortices from 4 week old *Sirt2*KO and WT mice were probed with the Cell Signalling SIRT1 antibody, none of the 3 bands detected displayed a change in intensity which suggests that SIRT1 is not up-regulated upon genetic depletion of SIRT2. However, the addition of reliable positive and negative controls is required to be certain of this result.

Surprising as it was to find that neither knock-down nor knock-out of SIRT2 elicited any changes in tubulin or H4K16 acetylation, or cholesterol enzyme expression, and that there was no compensatory up-regulation in the expression of any other HDACs, it is possible that SIRT2 is only required when cells are faced with stressful or toxic conditions.

In HD, cells are confronted with an overload of toxic misfolded mutant huntingtin (mHTT) that causes widespread dysregulation to a number of pathways including cholesterol synthesis (Valenza et al., 2005). It is thus possible that an effect of SIRT2 genetic reduction would only be evident once the knock-out or knock-down of SIRT2 is placed in the context of the disease. Before embarking on a full scale phenotyping study, it was first necessary to verify that levels of *Sirt2* are not affected by the widespread transcriptional dysregulation that occurs in HD. Interestingly, no differences were found in the cortex, striatum and cerebellum from 4 and 15 weeks old mice in *Sirt2* mRNA levels between WT and R6/2 mice, indicating that *Sirt2* expression does not change with disease progression (Fig. 4.4 E).

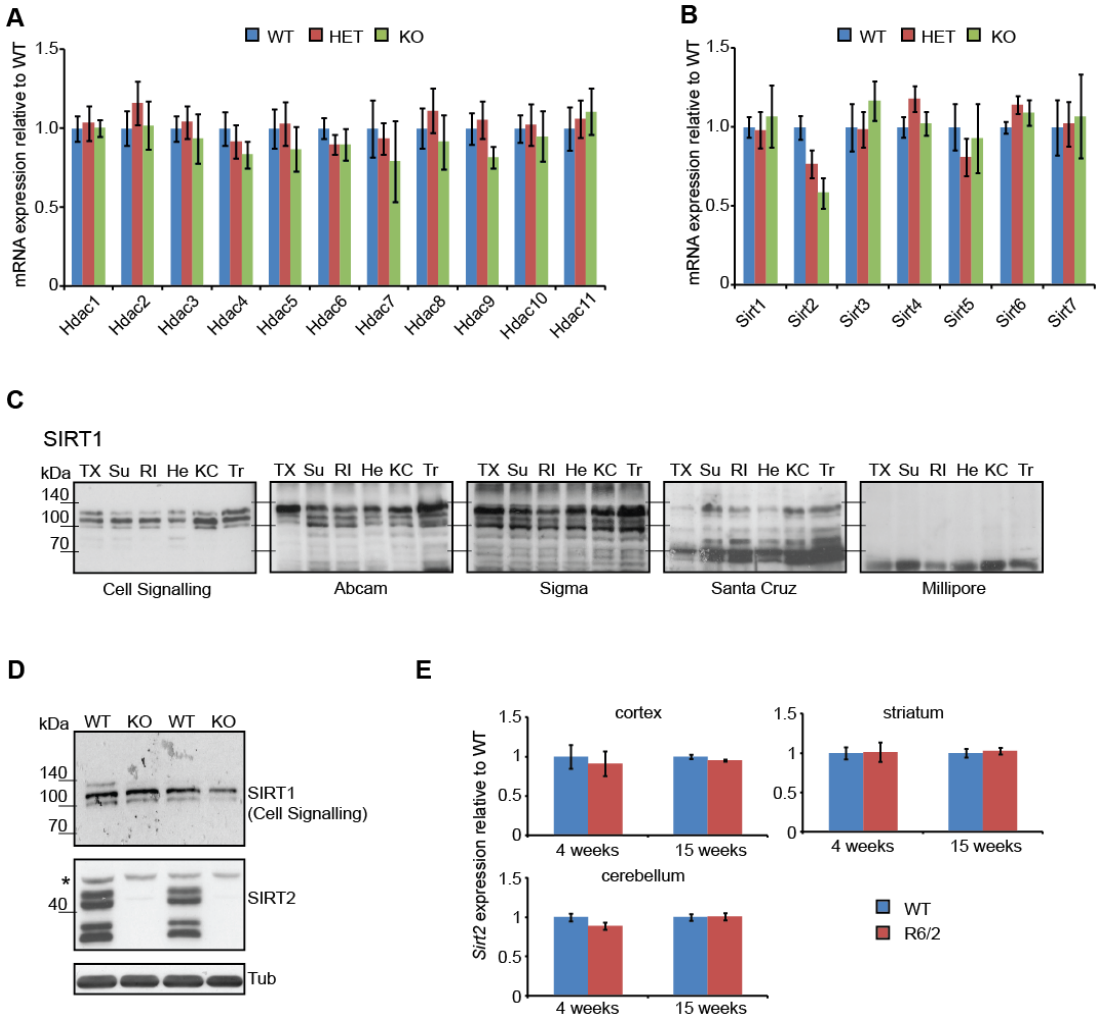

Figure 4.4. Expression of *Hdacs 1-11*, *Sirt1*, SIRT1 and *Sirt3-7* is not affected by genetic reduction of SIRT2 and *Sirt2* expression is not affected by HD progression in R6/2 mice.

(A-B) Taqman qPCR assays measuring the mRNA expression of all known deacetylases in the cortex of 4 week old wild type (WT), *Sirt2*HET (HET) and *Sirt2*KO (KO) mice. Expression was normalised to the housekeeping genes *Atp5b* and *Canx* and expressed as fold change of WT ± SEM. n≥6/genotype. **(C)** Western blots probed with 5 SIRT1 antibodies tested on brain lysates from 4 week old wild type mice extracted with 6 different buffers: TX, sucrose buffer (Su), RIPA (RI), Hepes (He), KCl (KC) and "Trottier" (Tr – high pH buffer). **(D)** Representative western blot probed with SIRT1 Cell Signalling antibody showing SIRT1 expression between wild type (WT) and *Sirt2*KO (KO) brain lysates extracted from cortices of 9 week old mice in RIPA buffer. * denotes a non-specific band. Tubulin (Tub) was used as loading control. n≥3/genotype. **(E)** Taqman qPCR assay measuring levels of *Sirt2* mRNA between wild type (WT) and R6/2 mice at 4 and 15 weeks of age in cortex, striatum and cerebellum. Expression was normalised to the housekeeping genes *Atp5b* and *Canx*, and expressed as fold change of WT ± SEM. n≥6/genotype.

4.6. SIRT2 genetic ablation does not improve phenotypes in the R6/2 mouse model of HD

The potential therapeutic nature of SIRT2 inhibition has not yet been tested in a complex mammalian system. To address this, the *Sirt2* gene disrupting insertion was crossed into the R6/2 mouse model of HD, by breeding *Sirt2*HET females to R6/2 males and subsequently, breeding *Sirt2*HETxR6/2 males to another cohort of *Sirt2*HET females. The progeny, consisting of wild type (WT), *Sirt2*HET (WT HET), *Sirt2*KO (WT KO), R6/2, *Sirt2*HETxR6/2 (R6/2 HET) and *Sirt2*KOxR6/2 (R6/2 KO) mice (Table 4.1), were monitored in a phenotyping study from 4 to 14 weeks of age and sacrificed at 15 weeks of age.

4.6.1. Repeat size was well matched between groups

As the CAG repeat size is intimately linked to age of onset and mHTT toxicity (Andrew et al., 1993), it was ascertained that mice of different genotypes were well matched for the CAG repeat number. Table 4.1 shows the number of mice used in the phenotyping study and their mean CAG repeat length.

Table 4.1 Numbers and CAG repeat sizes of mice used in the *Sirt2*KOxR6/2 phenotyping study.

Genotype	WT	WT HET	WT KO	R6/2	R6/2 HET	R6/2 KO
Males	9	11	11	9	10	6
Females	9	10	5	9	9	9
Total	18	21	16	18	19	15
Mean CAG repeat size ± SD	N/A	N/A	N/A	213 ± 3.14	214 ± 3.94	212 ± 3.58

KEY: WT – wild type, WT HET – *Sirt2*HET, WT KO – *Sirt2*KO, R6/2 HET – *Sirt2*HETxR6/2, R6/2 KO – *Sirt2*KOxR6/2. N/A – not applicable, SD – standard deviation.

4.6.2. SIRT2 reduction increases body weight independently of HD progression

Mice were weighed weekly from 4 until 14 weeks of age. As the gender significantly affected the weight ($F_{(1,96)}$=110.329, p<0.0005) and weight gain ($F_{(3,282)}$=32.704, p<0.0005), male and female weights were depicted separately (Fig. 4.5 A-B). R6/2 mice weighed significantly less than WT mice overall ($F_{(1,96)}$=10.655, p=0.002) and gained weight at a significantly slower rate ($F_{(3,282)}$=61.278, p<0.0005). Weight loss in R6/2 mice started at 9 weeks of age ($F_{(1,96)}$=4.458, p=0.037) and increased with disease progression. Interestingly, *Sirt2*HET and *Sirt2*KO mice had significantly increased weight ($F_{(2,96)}$=4.668, p=0.012) (Fig. 4.5 A-B), starting at 7 weeks of age ($F_{(2,96)}$=3.152,p=0.047). This phenomenon showed a trend to become significant with time ($F_{(6,282)}$=2.131, p=0.051). However, the *Sirt2* mutation had no overall effect on R6/2 weight loss ($F_{(2,96)}$=0.087, p=0.917) or on the decrease in weight in R6/2 over time ($F_{(6,282)}$=1.902, p=0.082), suggesting that if the *Sirt2* mutation modifies weight, it does so independently of HD progression.

The effect of the *Sirt2* genotype did not differ between males and females, ($F_{(1,96)}$=0.739, p=392 for R6/2, and $F_{(2,96)}$=0.13, p=878 for *Sirt2*) but the rate of weight loss was significantly different between male and female R6/2 mice ($F_{(3,282)}$=18.833, p<0.0005), with weight loss being quicker and more pronounced in males (Fig. 4.5 A-B).

4.6.3. Grip strength is not modified by a loss of SIRT2 in mice

Grip strength was measured in mice at 4 weeks of age and bi-weekly from 7 to 13 weeks of age. As there was a significant gender difference in overall grip strength performance ($F_{(1,96)}$=108.4, p<0.0005), the average grip strength of male and female mice is presented separately (Fig. 4.5 C-D).

R6/2 mice had reduced grip strength compared to WT mice ($F_{(1,96)}$=66.79, p<0.0005). This deficit appeared by 11 weeks of age ($F_{(1,96)}$=54.462, p<0.0005) and deteriorated over time ($F_{(3,308)}$=78.857, p<0.0005) (Fig. 4.5 C-D). Weaker grip strength was more evident ($F_{(1,96)}$=6.887, p=0.01) and the time dependent

deterioration was more pronounced ($F_{(3,308)}$=16.308, p<0.0005) in male mice expressing the R6/2 transgene, which is in line with an earlier and more pronounced weight loss in males (Fig. 4.5 C-D).

Grip strength was not altered in mice where SIRT2 was either reduced (*Sirt2*HET) or absent (*Sirt2*KO) overall ($F_{(2,96)}$=0.654, p=0.522) or with time ($F_{(6,308)}$=0.355, p=0.916) and there was no significant effect of modulation of SIRT2 levels on the worse grip strength performance observed in R6/2 mice either overall ($F_{(2,96)}$=0.116, p=0.891), or with time ($F_{(6,308)}$=0.9, p=0.5) (Fig. 4.5 C-D). These findings strongly suggest that reducing or ablating SIRT2 does not affect the grip strength in R6/2 mice.

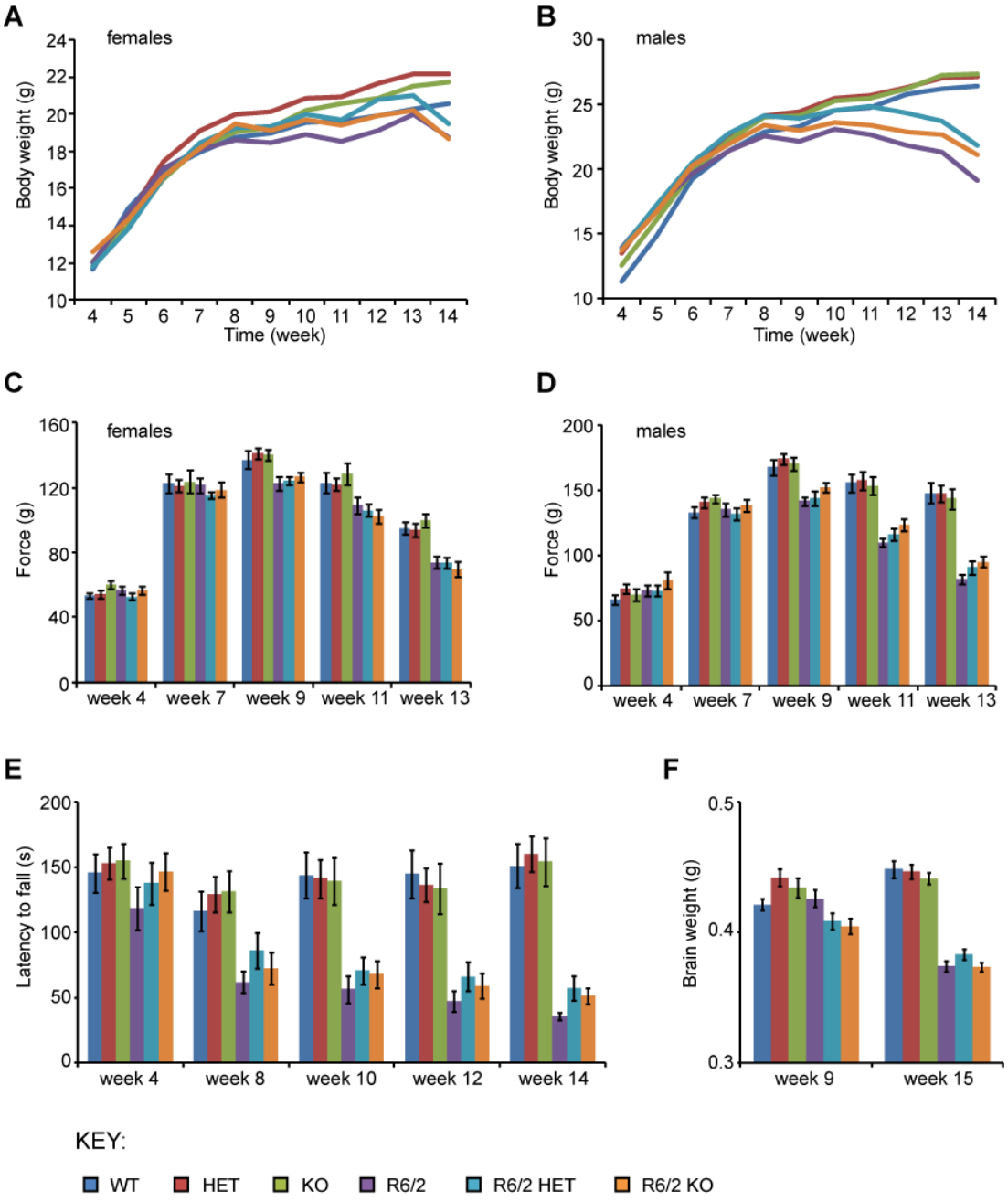

Figure 4.5. Behavioural and physiological phenotypes elicited by *Sirt2* knock-down and knock-out in R6/2 mice.

(A-B) Mean body weight measurements in (A) female and (B) male mice. **(C-D)** Grip strength in (C) female and (D) male mice. **(E)** Rotarod performance. **(F)** Brain weight measured at 9 and 15 weeks of age. Error bars represent SEM. WT – wild type, HET – *Sirt2*HET, KO – *Sirt2*KO, R6/2 HET – *Sirt2*HETxR6/2, R6/2 KO – *Sirt2*KOxR6/2.

4.6.4. Neither SIRT2 reduction nor depletion affect rotarod performance in mice

Rotarod performance is a robust measure of motor coordination and was assessed at 4 weeks of age and bi-weekly from 8 to 14 weeks of age (Fig. 4.5 E). No gender effects were observed ($F_{(1,95)}$=0.765, p=0.384) and thus rotarod performance of males and females was not analysed separately. In line with previous observations, R6/2 mice were indistinguishable from their WT littermates at 4 weeks of age ($F_{(1,95)}$=2.128, p=0.148) (Hockly et al., 2002), but their performance deteriorated over time ($F_{(3,237)}$=23.792, p<0.0005) starting at 8 weeks of age ($F_{(1,95)}$=22.537, p<0.0005) (Fig. 4.5 E). *Sirt2*HET and *Sirt2*KO mice did not perform differently from WT mice overall ($F_{(2,95)}$=0.23, p=0.795) or with time ($F_{(5,237)}$=1.118, p=0.351) and down-regulation or ablation of SIRT2 had no effect on the rotarod performance of R6/2 mice ($F_{(2,95)}$=0.634, p=532) or its deterioration over time ($F_{(5,237)}$=0.376, p=0.865) (Fig. 4.5 E). Therefore, it was concluded that neither SIRT2 reduction nor depletion affect rotarod performance in WT or R6/2 mice.

4.6.5. Reduced brain weight in R6/2 mice is not altered by genetic depletion of SIRT2

Brains were harvested at 9 and 15 weeks of age and weighed to the nearest 0.001 g. As expected, R6/2 brains weighed significantly less than those of WT mice ($F_{(1,41)}$=17.197, p<0.0005 for 9 weeks and $F_{(1,96)}$=268.291, p<0.0005 for 15 weeks) (Fig 4.5 F). Genetic modulation of *Sirt2* on its own had no effect on brain weight ($F_{(2,41)}$=0.734, p=0.486 at 9 weeks and $F_{(2,96)}$=1.107, p=0.335 at 15 weeks). Interestingly, statistical analysis revealed a significant effect of the *Sirt2* genotype on the R6/2 genotype at 9 weeks of age ($F_{(2,41)}$=7.169, p=0.002). However, this is most likely due to the fact that WT *Sirt2*HET and *Sirt2*KO mice had a slightly higher brain weight than WT mice, whereas R6/2 *Sirt2*HET and *Sirt2*KO mice had a slightly lower brain weight than R6/2 mice (Fig. 4.5 F).

4.6.6. SIRT2 genetic reduction does not influence hypo-activity of R6/2 mice

Spontaneous motor activity was measured bi-weekly from 5 to 13 weeks of age. Data were analysed with General Linear Model repeated measures ANOVA and *p*-values are presented in Table 4.2. Figures 4.6 and 4.7 depict 5 min moving averages plotted separately for males and females for activity, mobility (Fig. 4.6), rearing and centre rearing (Fig. 4.7).

The activity, mobility, rearing and centre rearing pattern of activity changed for all mice over the 30 min measurement window at all ages recorded (Table 4.2, Time), with highest levels of activity generally occurring in the first 15 min. Gender had no overall effect on any of the parameters at any time point (Table 4.2 Sex), though males and females had a different pattern of exploration over time at 5 (rearing and centre rearing) and 7 (Activity and mobility) weeks of age.

Deficits in mobility were already apparent in R6/2 mice at 5 weeks of age. Although no hypoactivity was observed in the Hdac6KOxR6/2 phenotyping study at 5 weeks of age (Results Chapter 3 - Experimental Paper, Fig. S1 and Table S1), reduced hypoactivity of R6/2 mice can occur as early as 4 weeks of age (Hockly et al., 2006). These discrepancies are most likely due to phenotype onset and disease progression being modestly variable between the different generations and cohorts of mice studied. Hypoactivity became evident at 7 weeks of age, decreased centre rearing and rearing was detected at 11 and 13 weeks of age respectively (Table 4.2 R6/2 Genotype). There was a pronounced gender difference in the effect of R6/2 genotype only between 9 and 11 weeks of age and that was detected in all parameters (Table 4.2 Sex*R6/2). This was most likely due to the quicker deterioration of the R6/2 males as compared to R6/2 females, which had also been observed for weight and grip strength (Fig. 4.5 A-D) and is visualised in the moving averages (Fig. 4.6 and 4.7).

Reduction or ablation of SIRT2 had no effect on any of the parameters at any age tested, did not modify the pattern of exploration over time and did not affect the hypoactivity of R6/2 mice (Table 4.2 *Sirt2*KO Genotype, Time**Sirt2*KO, R6/2**Sirt2*KO). Nevertheless, there was a *Sirt2* Genotype dependent change in the

pattern of activity, mobility and rearing over time at 7 weeks of age that was different between WT and R6/2 mice. However, this effect is most likely caused by the WT female group that was slightly hyperactive in the first 10 min of the test (Fig. 4.6) and the fact that, the R6/2 KO mice were the most active in rearing group amongst females, whereas the R6/2 mice were more active in rearing amongst males (Fig 4.7). These data imply that *Sirt2* knock-out or knock-down does not modify spontaneous motor activity in mice between 5 and 13 weeks of age and has no effect on the hypoactivity of R6/2 mice.

Table 4.2. Summary of *p*-values obtained from the statistical analysis of exploratory motor activity.

	Week	Activity	Mobility	Rearing	Centre Rearing
Time	**5**	<0.001	<0.001	<0.001	<0.001
	7	<0.001	<0.001	<0.001	<0.001
	9	<0.001	<0.001	<0.001	<0.001
	11	<0.001	<0.001	0.008	0.006
	13	<0.001	<0.001	0.013	0.004
R6/2 Genotype	**5**	0.212	0.044	0.708	0.655
	7	0.055	0.005	0.061	0.557
	9	<0.001	<0.001	0.487	0.910
	11	<0.001	<0.001	0.147	0.004
	13	<0.001	<0.001	<0.001	<0.001
Time*R6/2	**5**	0.041	0.043	0.134	0.025
	7	0.012	0.058	0.167	0.243
	9	0.697	0.561	0.036	0.158
	11	0.078	0.039	0.352	0.464
	13	0.248	0.300	0.060	0.375
***Sirt2*KO Genotype**	**5**	0.651	0.685	0.160	0.314
	7	0.663	0.766	0.669	0.874
	9	0.133	0.243	0.158	0.216
	11	0.660	0.565	0.954	0.136
	13	0.938	0.933	0.195	0.168
TimeSirt2*KO**	**5**	0.143	0.293	0.054	0.063
	7	0.607	0.545	0.366	0.094
	9	0.735	0.756	0.763	0.794
	11	0.469	0.240	0.222	0.271
	13	0.204	0.350	0.191	0.395
Sex	**5**	0.536	0.556	0.129	0.166
	7	0.598	0.381	0.059	0.117
	9	0.185	0.161	0.081	0.496
	11	0.090	0.406	0.309	0.165
	13	0.346	0.423	0.535	0.726
Time*Sex	**5**	0.110	0.166	0.004	0.025
	7	<0.001	<0.001	0.276	0.138
	9	0.654	0.469	0.648	0.579
	11	0.088	0.123	0.836	0.765
	13	0.559	0.494	0.199	0.240
Sex*R6/2	**5**	0.846	0.952	0.865	0.670
	7	0.277	0.569	0.518	0.783
	9	0.298	0.755	0.043	0.009
	11	0.012	0.032	0.007	0.001
	13	0.194	0.319	0.071	0.165

Key: Blue – $p<0.05$, Orange – $p<0.01$, Pink – $p<0.001$

Table 4.2 - Continued

	Week	Activity	Mobility	Rearing	Centre Rearing
Sex*_Sirt2_KO	**5**	0.071	0.147	0.004	0.056
	7	0.395	0.440	0.477	0.803
	9	0.496	0.575	0.645	0.286
	11	0.209	0.209	0.055	0.040
	13	0.909	0.836	0.094	0.206
Sex*R6/2*_Sirt2_KO	**5**	0.908	0.904	0.335	0.804
	7	0.706	0.704	0.772	0.575
	9	0.600	0.506	0.449	0.428
	11	0.079	0.078	0.259	0.524
	13	0.423	0.665	0.505	0.683
R6/2*_Sirt2_KO	**5**	0.431	0.391	0.279	0.872
	7	0.836	0.894	0.151	0.201
	9	0.546	0.662	0.640	0.688
	11	0.800	0.648	0.652	0.729
	13	0.934	0.840	0.483	0.855
Time*R6/2*_Sirt2KO_	**5**	0.436	0.640	0.549	0.617
	7	0.008	0.026	0.043	0.064
	9	0.598	0.579	0.282	0.148
	11	0.789	0.890	0.690	0.821
	13	0.812	0.893	0.293	0.632
Time*Sex*R6/2* _Sirt2_KO	**5**	0.660	0.587	0.562	0.186
	7	0.232	0.222	0.225	0.040
	9	0.683	0.554	0.672	0.780
	11	0.516	0.423	0.382	0.849
	13	0.457	0.603	0.422	0.818

Key: Blue – $p<0.05$, Orange – $p<0.01$, Pink – $p<0.001$

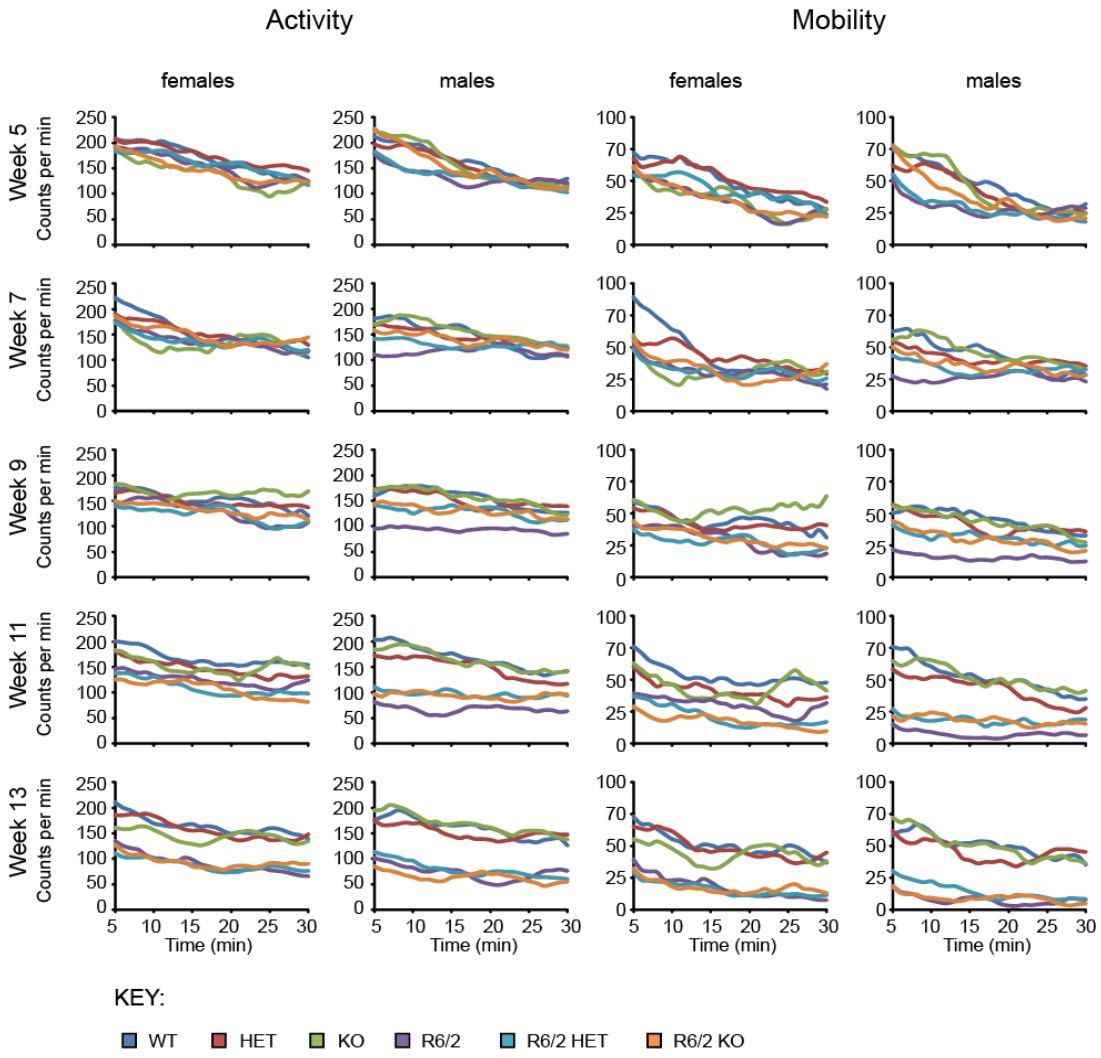

Figure 4.6. Activity and mobility.

Activity and mobility were recorded for wild type (WT), *Sirt2*HET (HET), *Sirt2*KO (KO), R6/2, *Sirt2*HETxR6/2 (R6/2 HET) and *Sirt2*KOxR6/2 (R6/2 KO) mice over the course of 30 min at 5, 7, 9, 11, and 13 weeks of age. Activity parameters measurements were visualised by plotting 5 min moving averages.

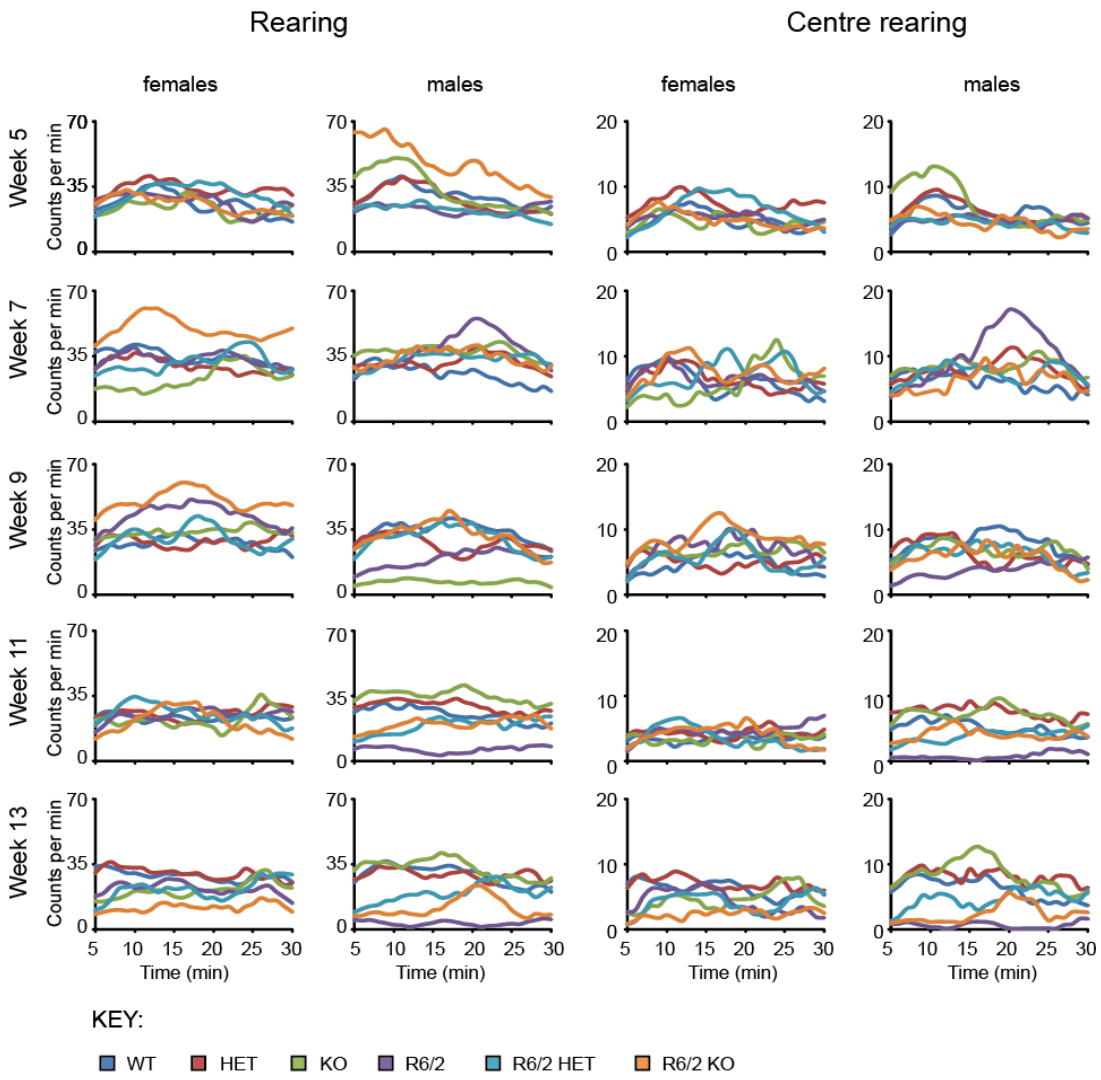

Figure 4.7. Rearing and centre rearing.

Rearing and centre rearing were recorded for wild type (WT), *Sirt2*HET (HET), *Sirt2*KO (KO), R6/2, *Sirt2*HETxR6/2 (R6/2 HET) and *Sirt2*KOxR6/2 (R6/2 KO) mice over the course of 30 min at 5, 7, 9, 11, and 13 weeks of age. Activity parameters measurements were visualised by plotting 5 min moving averages.

4.7. SIRT2 knock-down and knock-out do not affect aggregate load or levels of soluble mHTT in R6/2 mice

Although genetic ablation of SIRT2 had no discernible disease modifying effect on the HD related behavioural and physiological phenotypes in R6/2 mice, it remained possible that SIRT2 depletion elicited more subtle molecular changes. Mutant HTT aggregates are formed in HD patients and all known mouse models and correlate with disease progression (Crook and Housman, 2011; DiFiglia et al., 1997). To investigate whether SIRT2 genetic depletion modified levels of soluble or aggregated mHTT, Seprion ELISA, time resolved – Förster energy transfer (TR-FRET) and Mezoscale Discovery (MSD) were performed on the cortex, hippocampus, brain stem and cerebellum from 4, 9 and 15 week old R6/2, R6/2 HET and R6/2 KO mice.

As has been observed previously, the aggregate load in R6/2 mice was highest in the cortex and hippocampus and much lower in the brain stem (Fig. 4.8-10 C) (Sathasivam et al., 2010). WT, *Sirt2*HET and *Sirt2*KO mouse tissues did not give any signal above background for aggregated or soluble HTT in any brain region or at any age tested (Fig. 4.8-10 B).

Interestingly, Seprion ELISA did not detect any changes in aggregation in the cortex, hippocampus or brain stem at 4, 9 or 15 weeks of age between R6/2, R6/2 HET or R6/2 KO mice. To confirm this finding, samples were separated by SDS-PAGE and immunoblotted with an anti-HTT antibody (S829) (Fig. 4.8-10 A-B). Large SDS-insoluble aggregates are unable to move into the resolving gel and can be only detected in the stacking gel. In contrast, the soluble mHTT transprotein is readily detected at a size of about 90 kDa (SDS-PAGE mobility of the monomeric transprotein is distorted due to its high glutamine content). No aggregated or soluble mHTT could be detected by western blot in any of the WT, *Sirt2*HET or *Sirt2*KO tissues at 4, 9 or 15 weeks of age (Fig. 4.8-10 B). At 9 and 15 weeks of age, aggregates could readily be detected in all brain regions examined, though no genotype specific difference could be observed. Interestingly, at 4 weeks of age aggregates could only be detected in the cortex, which is surprising, given that the Seprion ELISA assay revealed that levels of aggregated mHTT in the cortex were

comparable with those of hippocampus. However, cortical and hipoccampal lysates were run on separate gels and thus, signals obtained after immunodetection are not directly comparable as they depend on factors such as efficiency in protein transfer to nitrocellulose membrane or effectiveness of antibody incubation.

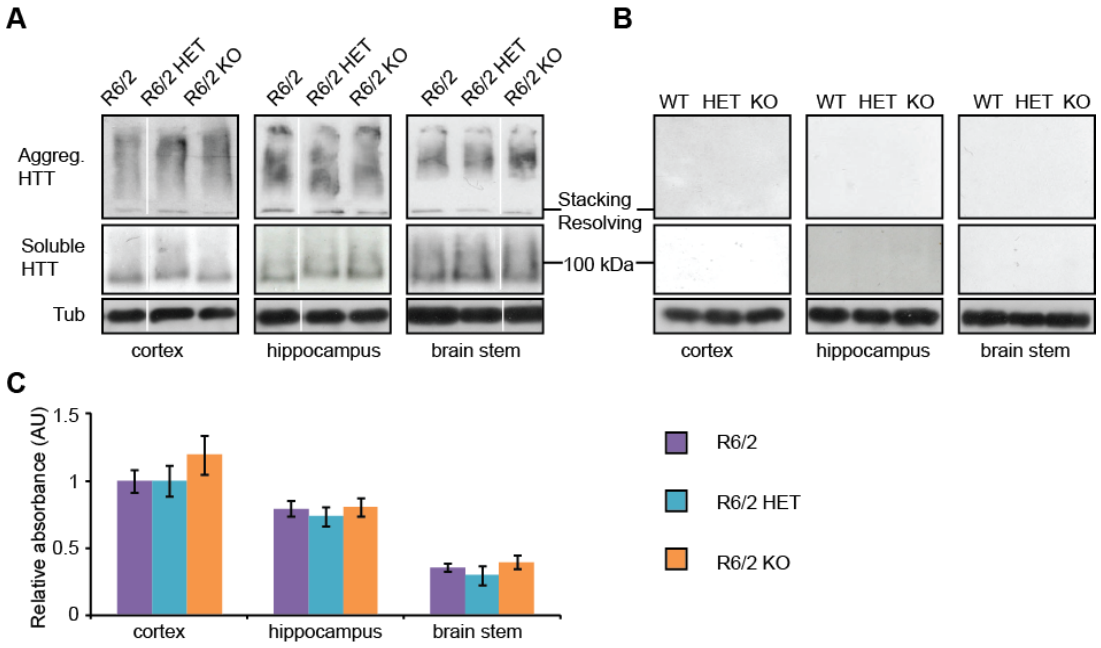

Figure 4.8. Aggregate load in cortex, hippocampus and brain stem at 15 weeks of age.

(A-B) Representative western blots from cortex, hippocampus and brain stem of 15 week old wild type (WT), *Sirt2*HET (HET), *Sirt2*KO (KO), R6/2, *Sirt2*HETxR6/2 (R6/2 HET) and *Sirt2*KOxR6/2 (R6/2 KO) mice probed with an anti-HTT antibody (S829) and tubulin (Tub) as loading control. Both soluble mHTT transprotein and aggregates stuck in the stacking gel can only be detected in mice expressing the R6/2 transgene (A-B). All samples were run on the same gel. White lines indicate where lanes are not contiguous. **(C)** Aggregate load as measured by Seprion ELISA with the MW8 antibody. The average signal for WT, HET and KO values was subtracted from each reading and expressed as fold change of R6/2 cortex ± SEM. n=6/genotype(R6/2, R6/2 HET and R6/2 KO) or n=3/genotype (WT, HET, KO).

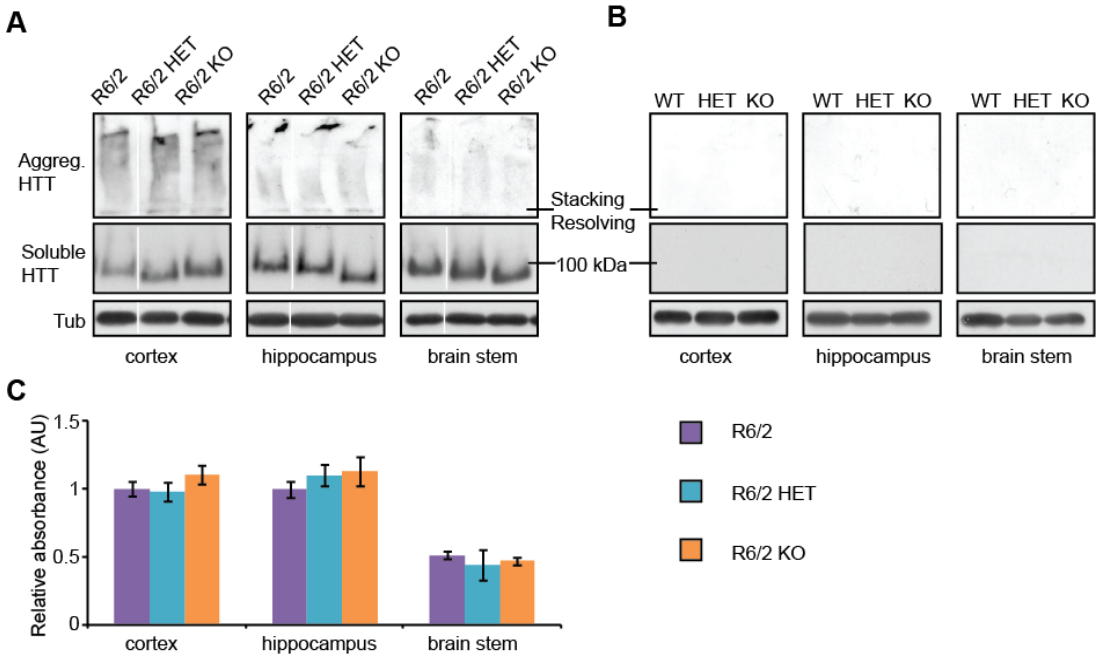

Figure 4.9. Aggregate load in cortex, hippocampus and brain stem at 9 weeks of age.

(A-B) Representative western blots from cortex, hippocampus and brain stem of 9 week old wild type (WT), *Sirt2*HET (HET), *Sirt2*KO (KO), R6/2, *Sirt2*HETxR6/2 (R6/2 HET) and *Sirt2*KOxR6/2 (R6/2 KO) mice probed with an anti-HTT antibody (S829) and tubulin (Tub) as loading control. Both soluble mHTT transprotein and aggregates stuck in the stacking gel can only be detected in mice expressing the R6/2 transgene (A-B). All samples were run on the same gel. White lines indicate where lanes are not contiguous. **(C)** Aggregate load as measured by Seprion ELISA with the MW8 antibody. The average signal for WT, HET and KO values was subtracted from each reading and expressed as fold change of R6/2 cortex ± SEM. n=6/genotype(R6/2, R6/2 HET and R6/2 KO) or n=3/genotype (WT, HET, KO).

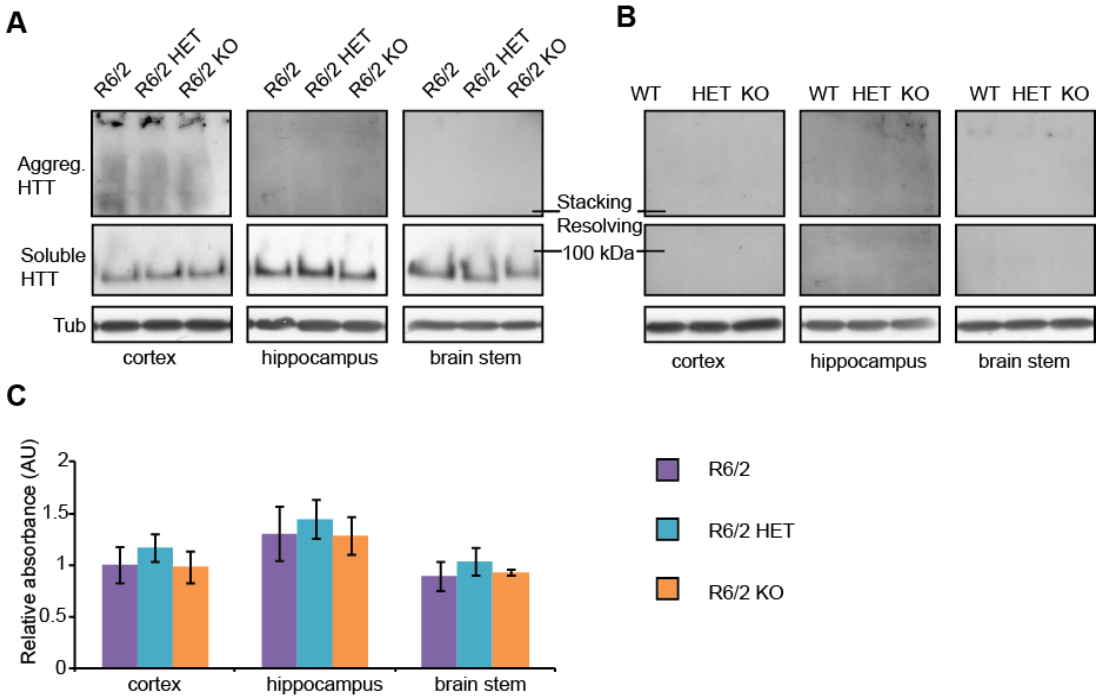

Figure 4.10. Aggregate load in cortex, hippocampus and brain stem at 4 weeks of age.

(A-B) Representative western blots from cortex, hippocampus and brain stem of 4 week old wild type (WT), *Sirt2*HET (HET), *Sirt2*KO (KO), R6/2, *Sirt2*HETxR6/2 (R6/2 HET) and *Sirt2*KOxR6/2 (R6/2 KO) mice probed with an anti-HTT antibody (S829) and tubulin (Tub) as loading control. Soluble mHTT transprotein can only be detected in mice expressing the R6/2 transgene (A-B). Aggregates were only detectable in the cortex. **(C)** Aggregate load as measured by Seprion ELISA with the MW8 antibody. The average signal for WT, HET and KO values was subtracted from each reading and expressed as fold change of R6/2 cortex ± SEM. n=6/genotype(R6/2 and R6/2 HET) or n=3/genotype (WT, HET, KO, R6/2 KO).

TR-FRET analysis revealed no differences in the levels of soluble mHTT between R6/2, R6/2 HET and R6/2 KO brains at any of the ages tested in any tissue examined (Fig 4.11). These results were also confirmed by western blotting. As expected, levels of soluble mHTT are significantly decreased between 4 and 15 weeks of age in all brain regions tested. However, the rate at which levels of soluble mHTT decrease with disease progression varies greatly between different brain regions (Fig. 4.11 A – D). In the cortex, mHTT levels steadily decrease from 4 to 15 weeks of age. In contrast, levels of soluble mHTT in the hippocampus and brain stem exhibit dramatic decreases from 9 to 15, and 4 to 9, weeks of age respectively (Fig. 4.11 B -

C). Furthermore, in the cerebellum, the reduction of soluble mHTT, occurs gradually and, is not as pronounced as in the other brain regions (Fig. 4.11 D).

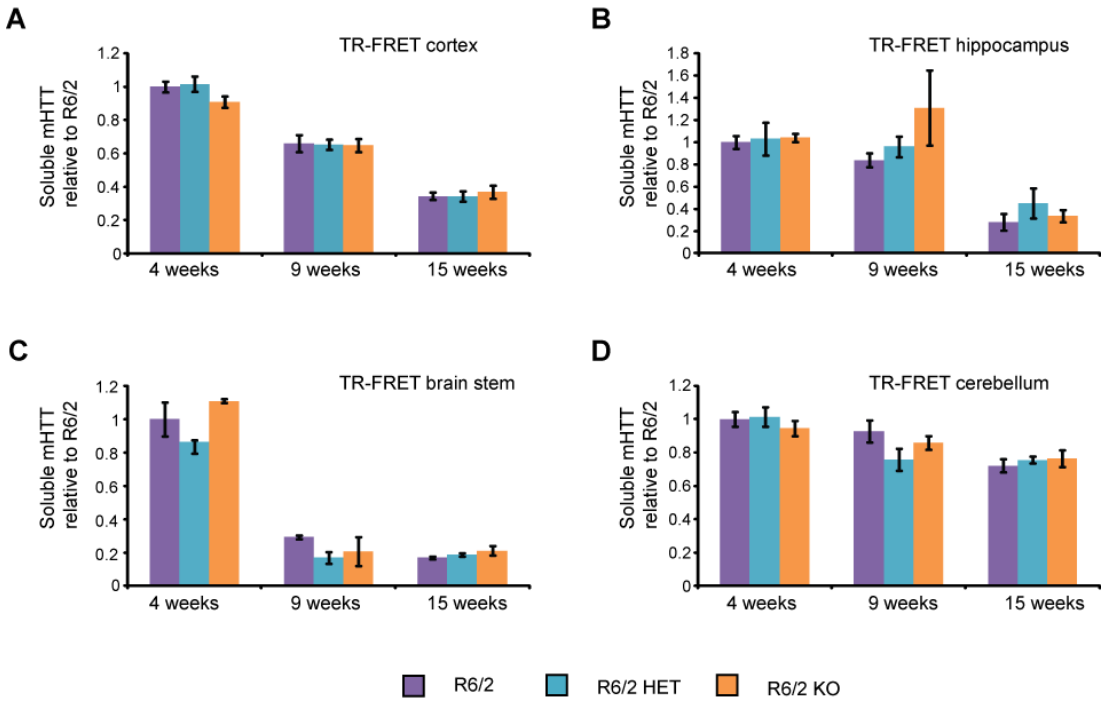

Figure 4.11. Soluble mHTT in the cortex, hippocampus, brain stem and cerebellum at 4, 9 and 15 weeks of age.

Levels of soluble mHTT as measured by TR-FRET with 2B7-MW1 antibodies in the (A) cortex, (B) hippocampus (C) brain stem and (D) cerebellum at 4, 9 and 15 weeks of age in R6/2, Sirt2HETxR6/2 (R6/2 HET) and Sirt2KOxR6/2 (R6/2 KO) mice. The signal for each tissue was expressed as fold change of R6/2 at 4 weeks. No signal above background was observed for mice without the R6/2 transgene. n≥4/genotype/tissue/time point (except for R6/2 KO at 4 weeks where n=3). Error bars represent SEM.

These findings were confirmed by MSD assay (Fig. 4.12). Importantly, the profiles obtained for the decrease in soluble mHTT for each brain region were very similar to those seen by TR-FRET. Interestingly, the aggregate load is progressively increased between 4 and 15 weeks of age in every brain region examined (Fig. 4.12). At first glance this appears contradictory to the soluble mHTT profiles obtained for hippocampus and brain stem. However, this could be explained by the

existence of a population of oligomeric mHTT that is undetected by either of the two antibody combinations in the assays amployed.

Although a significant decrease in the aggregate load in R6/2 HET and R6/2 KO mice was detected in the cortex at 15 weeks of age, these differences were not observed by Seprion ELISA or western blot (Fig. 4.8 A, C and Fig. 4.12 A). At the same time, the *Sirt2* genotype appears to significantly increase levels of soluble mHTT in the hippocampus at 4 weeks and in the brain stem at 15 weeks of age (Fig. 4.12 B – C), findings that were also not reproduced by TR-FRET or western blotting (Fig. 4.8 A, C; Fig. 4.10 A, C and Fig. 4.11 B – C). However, both TR-FRET and MSD assays have been performed on the same lysates and therefore, it is highly likely that any changes that reach statistical significance are a result of the large number of comparisons performed rather than a real biological effect. Taken together, these data demonstrate that genetic ablation of SIRT2 does not alter the dynamics of mHTT aggregation between 4 and 15 weeks of age in brain tissues from R6/2 mice. Furthermore, these results imply that the mechanisms or kinetics of aggregation vary between different brain regions in R6/2 mice and are therefore likely to be dependent on expression levels of mHTT and/or other factors specific to these brain regions.

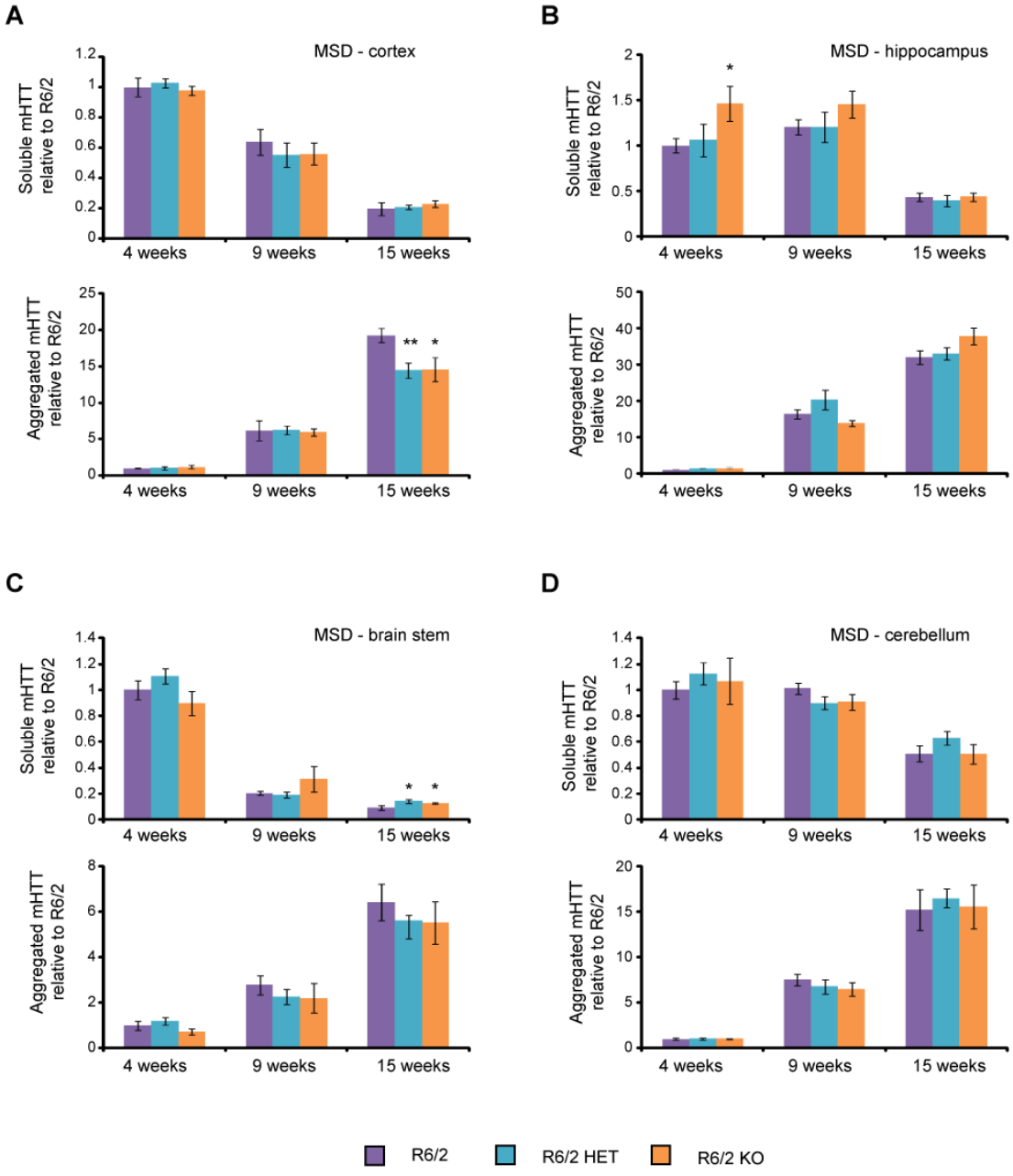

Figure 4.12. Soluble and aggregated mHTT in the cortex, hippocampus, brain stem and cerebellum at 4, 9 and 15 weeks of age as measured by Mezoscale Discovery.

Levels of soluble (upper panels) and aggregated (lower panels) mHTT as measured by Mezoscale Discovery (MSD) in (A) cortex, (B) hippocampus, (C) brain stem, and (D) cerebellum at 4, 9 and 15 weeks of age in R6/2, Sirt2HETxR6/2 (R6/2 HET) and Sirt2KOxR6/2 (R6/2 KO) mice. Soluble mHTT was measured with 2B7-MW1 and aggregated mHTT with MW8-MW8 antibodies combination. The signal for each tissue was expressed as fold change of R6/2 at 4 weeks. No signal above background was observed for mice without the R6/2 transgene. n≥4/genotype/tissue/time point (except for R6/2 KO at 4 weeks where n=3). Error bars represent SEM. *$p \leq 0.05$, **$p \leq 0.01$ (to the R6/2 at the respective time point).

4.8. Cholesterogenic enzyme dys-homeostasis is not corrected by the genetic depletion of SIRT2

Levels of cholesterol biosynthesis enzymes have been reported to be decreased in R6/2 mice (Valenza et al., 2007). SIRT2 genetic ablation had no effect on the expression of cholesterogenic enzymes in WT mice, however, it was possible that SIRT2 deletion effects would only be apparent in the context of HD pathogenesis. To verify if that is the case, RNA was extracted and cDNA prepared from the cortices of 15 week old WT, HET, KO, R6/2, R6/2 HET and R6/2 KO mice.

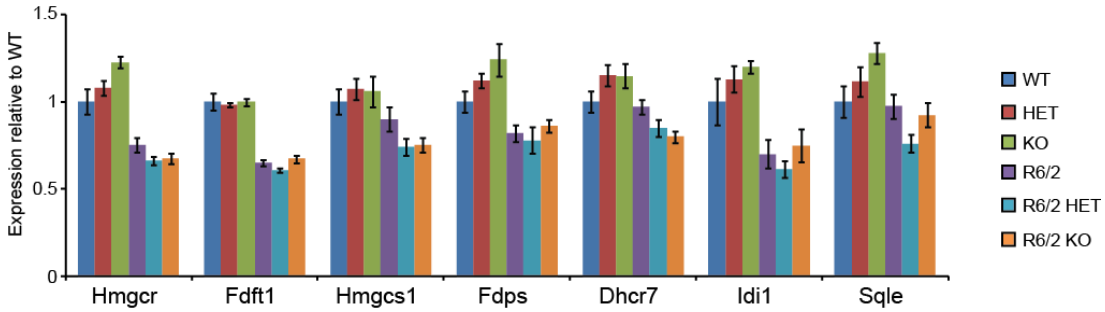

Figure 4.13. Expression of cholesterogenic enzymes at 15 week of age.

Taqman qPCR assay was used to measure cholesterogenic enzymes' mRNA expression in the cortex of 15 week old wild type (WT), *Sirt2*HET (HET), *Sirt2*KO (KO), R6/2, *Sirt2*HETxR6/2 (R6/2 HET) and *Sirt2*KOxR6/2 (R6/2 KO) mice. Values were normalised to the housekeeping genes *Atp5b* and *Canx* and expressed as fold change of WT ± SEM. n≥7/genotype.

The expression of cholesterogenic enzymes was measured by Taqman qPCR assays and data were analysed by two-way ANOVA. The R6/2 genotype had a statistically significant effect on the expression of all cholesterogenic enzymes examined (Fig. 4.13). However, post-hoc pairwise comparison with Bonferroni correction revealed that there is no difference between WT and R6/2 groups in the expression of *Hmgcs1* (p=1), *Fdps* (p=1), *Dhcr7* (p=1), *Idi1* (p=0.278) and *Sqle* (p=1) and the statistical significance obtained from ANOVA is derived from inclusion of *Sirt2*HET and *Sirt2*KO groups with higher than WT values, as well as R6/2 HET and R6/2 KO

groups with lower than R6/2 values. Taken together these data suggest that the expression of *Hmgcs1, Fdps, Dhcr7, Idi1* and *Sqle*, is affected by R6/2 transgene only in the presence of SIRT2 genetic reduction or depletion.

The *Sirt2* genotype alone had no significant effect on the expression of any of the cholesterogenic enzymes. Surprisingly, however, *Sirt2* genotype significantly modified the effect of the R6/2 genotype on the expression of *Hmgcr* ($F_{(2,33)}$=6.03, p=0.006) , *Dhcr7* ($F_{(2,36)}$=5.14, p=0.011) and *Sqle* ($F_{(2,36)}$=3.38, p=0.045). These changes could signify that *Sirt2*KO has a late stage disease-specific effect on the expression of some cholesterol biosynthesis genes. On the other hand, it is possible that statistical significance results from the fact that HET and KO values tend to be higher than WT, whereas R6/2 HET and R6/2 KO values appear to be lower than those of R6/2. If these results are depicting a real effect of SIRT2 deletion, it would appear that SIRT2 is positively regulating cholesterol gene expression in R6/2 mice, but inhibiting the expression of the same genes in WT mice, which is extremely unlikely. In any case, the mechanism proposed for SIRT2 regulation of cholesterol synthesis assumed SIRT2 increasing SREBP-2 nuclear translocation (Luthi-Carter et al., 2010). All of the tested cholesterogenic enzymes are targets of SREBP-2, therefore, if SIRT2 ablation was causing a decrease in nuclear shift of SREBP-2, KO mice should display lowered cholesterogenic enzyme expression levels as compared to WT and the effect ought to be detected in all 7 of the enzymes tested. As this was not the case, the observed statistical differences are more likely a result of biological variability than a depiction of the effect of SIRT2 depletion.

4.9. Acute inhibition of SIRT2 has no effect on the levels of cholesterol biosynthesis enzymes in WT or R6/2 mice

The lack of effect of SIRT2 knock-out on tubulin and H4K16 acetylation, and on cholesterogenic enzyme expression could be due to compensation. With a traditional knock-out, as is the case here, SIRT2 protein is constantly reduced or absent from *Sirt2*HET or *Sirt2*KO mice, respectively, allowing the organism time to adjust and compensate. In contrast, previous studies were performed in a cell

culture setting, where SIRT2 was acutely inhibited, thereby limiting the time for the same compensatory mechanisms to be employed by the system (Luthi-Carter et al., 2010).

To investigate whether the lack of observed effects in the *Sirt2*KO mice could be due to compensation, wild type and R6/2 mice at 12 weeks of age were given a single low (1 mg/kg) or high (3mg/kg) dose of a dual SIRT1/SIRT2 inhibitor CHDI-00194500-0000-0005 (CHDI194500). The doses have been chosen based on pharmacokinetic data and *in vitro* inhibition assays (Appendix 2). Tissues were harvested either 4 or 8 h post dosing. RNA was extracted from the cortex and the expression of cholesterogenic enzymes was measured with Taqman qPCR assays. In line with previous reports and data from this work, expression of all cholesterogenic enzymes was diminished in R6/2 vehicle treated mice as compared to WT vehicle treated mice (Fig 4.14) (Valenza et al., 2007). However, neither dose of CHDI194500 affected the expression of cholesterogenic enzymes at 4 or 8 h post dosing in both WT and R6/2 mice. Although a decrease in the expression of *Hmgcr* can be observed in WT mice 8 h post dosing (Fig. 4.14 B), the fact that none of the other enzymes' expression was changed and that *Hmgcr* expression after 3 mg/kg dose was comparable to vehicle strongly suggests that this observation is a result of experimental variation rather than a real biological effect. These data strongly suggest that either SIRT2 inhibition does not modulate the expression levels of cholesterol biosynthesis enzymes or SIRT2 inhibition was not achieved with CDHI194500.

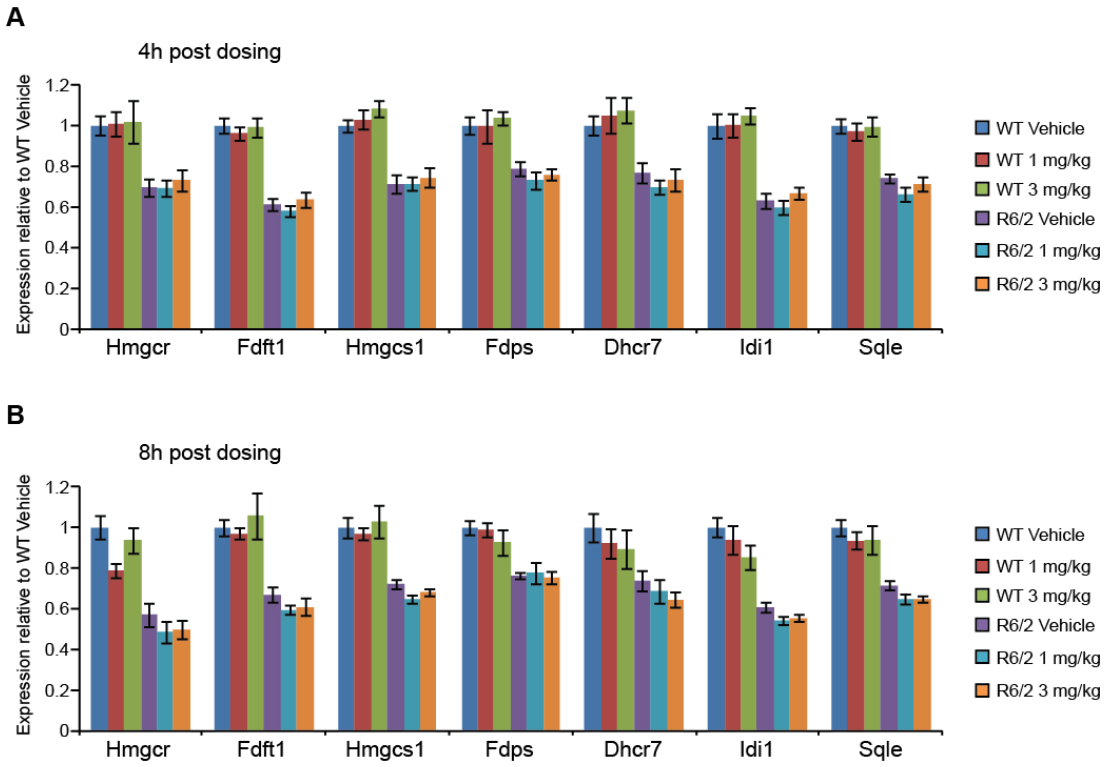

Figure 4.14. Expression of cholesterogenic enzymes in wild type and R6/2 mice after an acute dose of CHDI194500 SIRT1/SIRT2 inhibitor.

Expression of cholesterogenic enzymes in the cortex of 12 week old wild type (WT) and R6/2 mice **(A)** 4 h and **(B)** 8h after an acute dose of the CHDI194500 SIRT1/SIRT2 inhibitor or vehicle. Values were normalised to the housekeeping genes *Atp5b* and *Canx* and expressed as fold change of WT Vehicle ± SEM. n≥7/genotype/treatment group.

4.9.1. Measurement of SIRT2 activity with Fluor de Lys assay

In order to measure the activity of SIRT2 after inhibition with CHDI194500, it was attempted to adapt the Fluor de Lys SIRT2 *in vitro* activity assay kit to measuring SIRT2 activity in tissue lysates. Firstly, different amounts of total protein extracted in Fluor de Lys Assay Buffer from WT and *Sirt2*KO mouse cortices were incubated with or without the SIRT2 cofactor NAD^+ and the SIRT2 acetylated substrate. The SIRT2 substrate is a tetrapeptide corresponding to amino acids 317-320 of human p53, acetylated at position 320 and modified in such a way that deacetylation sensitizes it to produce a fluorophore when incubated with the Developer solution. The signal detected after incubation with the Developer solution was proportional

to the amount of protein added to the substrate, except for when 100 µg of total protein was used, for which the signal was only slightly higher than with 50 µg of protein (Fig. 4.15 A). This indicates that the substrate was consumed and 100 µg contains an excess of deacetylase. At the same time it was noted that although all samples were pre-incubated at 37°C to allow all internal NAD^+ to be used up, the enzyme activity in the reactions to which no NAD^+ was added was considerable and indistinguishable from reactions with external NAD^+ when 50 or 100 µg of protein were used. The largest difference between signals obtained with and without external NAD^+ was seen with 5 µg of total protein. Most importantly however, no difference in activity between lysates obtained from WT or *Sirt2*KO mice could be detected (Fig. 4.15 A). This was not surprising, given that the acetylated substrate is based on p53, which is also a client of SIRT1 and above all, is an artificial short peptide, and could therefore be deacetylated by any of the other Sirtuins or by a yet unidentified deacetylase.

In order to investigate whether extending the 10 min pre-incubation time at 37°C could decrease the signal obtained from reactions where no external NAD^+ was added, so that concentration of NAD^+ could be controlled better by relying mostly on externally added NAD^+, Fluor de Lys was performed on samples containing 5 µg of total protein that were pre-incubated for 20, 40 or 60 min at 37°C. To find out whether the deacetylase activity observed in the *Sirt2*KO samples arises from nuclear Sirtuins, only cytoplasmic fractions were used. Unfortunately, in this experiment the signal obtained from samples without externally added NAD^+ was stronger for all pre-incubation times tested (Fig. 4.15 B).

There was still no difference in signal between the samples obtained from WT and *Sirt2*KO mice, suggesting, that the activity observed in *Sirt2*KO samples was not due to the presence of nuclei (and therefore SIRT1) in the lysates (Fig. 4.15 B).

Although no differences could be detected with the Flour de Lys assay between WT and *Sirt2*KO tissues, it was still possible that this was due to compensation occurring in the *Sirt2*KO animals. In a final attempt to measure SIRT2 activity using the Fluor de Lys kit, cortical samples from WT mice acutely dosed with CHDI194500

were extracted and examined with the Flour de Lys assay. Unfortunately, the assay did not reveal differences between vehicle, 1 mg/kg and 3 mg/kg treated groups. Equally, there was no effect of adding exogenous NAD^+ to any of the samples (Fig. 4.15 C).

This suggests that either internal NAD^+ was not used up before the assay was commenced or that the enzymatic activity towards the acetylated substrate is NAD^+ independent. In any case, all data points to the acetylated substrate not being specific to SIRT2 and clearly shows that the Flour de Lys SIRT2 activity assay is not an appropriate tool to measure SIRT2 activity in animal tissue lysates.

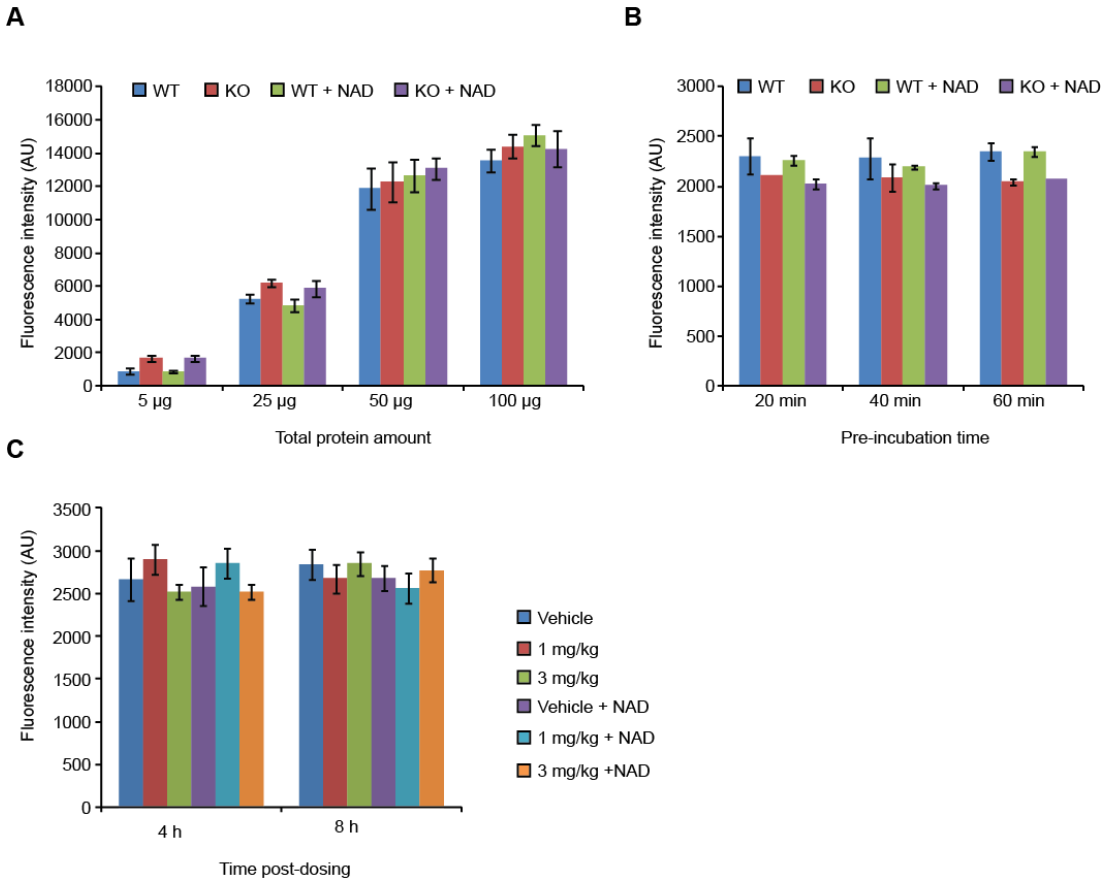

Figure 4.15. Measuring SIRT2 activity with the Flour de Lys SIRT2 activity assay.

(A) Fluorescence signal obtained after different amounts of total protein from wild type (WT) or *Sirt2*KO (KO) mice were incubated with the acetylated substrate and with or without NAD^+(NAD). n=4/genotype, values ± SEM. **(B)** Fluorescence signal obtained after different pre-incubation times were applied to samples from WT or KO mice incubated with the acetylated substrate and with or without NAD^+(NAD). n=3/genotype, values ± SEM (where possible). **(C)** Fluorescence signal obtained from vehicle, 1 mg/kg or 3 mg/kg CHDI194500 treated WT mice dissected 4 or 8 h post-dosing. Samples were incubated with the acetylated substrate and with or without NAD^+(NAD). n=6/treatment group, values ± SEM.

4.9.2. Measurement of the effects of CHDI194500 acute dosing on Ac-p53 and Ac-FOXO1

After efforts to adapt the Flour de Lys SIRT2 activity assay to measure SIRT2 activity in tissue lysates failed, one option to detect a pharmacodynamic effect of CHDI194500 was to assess the levels of acetylated in p53 and FOXO1. These

transcription factors have both been found to be substrates of both SIRT1 and SIRT2 (Peck et al., 2010; Wang et al., 2011). Therefore, as CHDI194500 inhibits both SIRT1 and SIRT2, exposure to CHDI194500 should in theory result in increased levels of acetylated p53 (Ac-p53) and acetylated FOXO1 (Ac-FOXO1). Cortical protein lysates from the acute CHDI194500 dosing study were prepared and western blotted with antibodies against Ac-p53 (expected to resolve at 53 kDa) and Ac-FOXO1 (expected to resolve at 70 kDa). Unfortunately, the antibodies commercially used to detect Ac-p53 and Ac-FOXO1 gave very weak signals even when applied in low dilution (1:100) (Fig. 4.16). Additionally, it was evident that the high amount of protein (60 µg), that was required to detect Ac-p53 and Ac-FOXO1, caused unevenness across the gels during electrophoresis and western transfer. Although it appeared that there was no difference in the acetylation status of either Ac-p53 or Ac-FOXO1 between vehicle, 1 mg/kg or 3 mg/kg dosed mice, the western blotting signal was not quantifiable and therefore, this conclusion cannot be drawn with certainty.

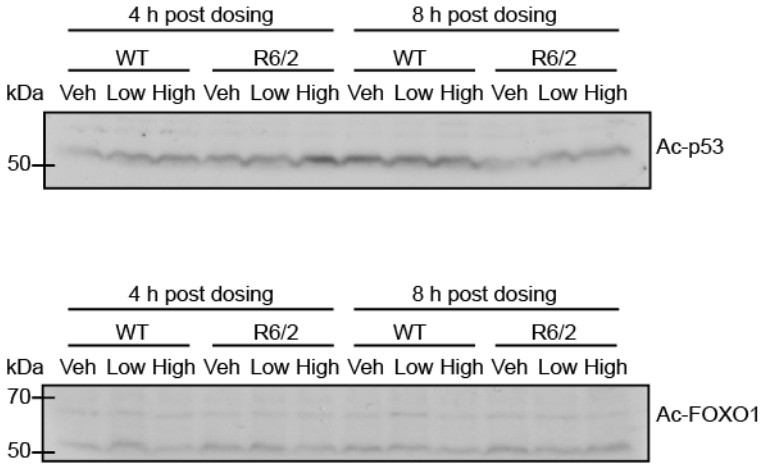

Figure 4.16. Western blotting and immunodetection of Ac-p53 and Ac-FOXO1 in mice acutely dosed with CHDI194500.

Western blots of Ac-p53 (upper panel) or Ac-FOXO1 (lower panel) from cortices of 12 week old wild type (WT) and R6/2 mice acutely dosed with vehicle (Veh), 1 mg/kg (Low) or 3 mg/kg (High) of CHDI194500 and dissected 4 or 8 h post dosing. Image representative of n=4/genotype/treatment group.

4.9.3. Pharmacokinetic analysis reveals presence of CHDI194500 in the brains of dosed mice.

CHDI194500 has already been demonstrated to be brain penetrant (Appendix 2). LC/MS/MS analysis of brain tissue from mice dosed with CHDI194500 revealed that at 4 h post dosing, CHDI194500 was present in both WT and R6/2 mice at concentrations above its IC_{50} for SIRT2 (560 nM) (Fig. 4.17 and Appendix 2). Although at 8 h post dosing the concentration was below the IC_{50} for all groups except WT treated with 3 mg/kg, it could be expected that the downstream effects of SIRT2 inhibition should still be detectable at this time point. Interestingly, a difference in CHDI194500 brain concentration can be observed between WT and R6/2 at 8 h post dosing, indicating that the drug is metabolised quicker in R6/2 mice, a phenomenon not previously reported for these mice. Ultimately however, no differences were found in cholesterol enzyme expression between CHDI194500 and vehicle treated mice in either WT or R6/2 groups at 4 h post-dosing, where the compound was present in both groups at the same level. This suggests that lack of effects in cholesterol biosynthesis pathway observed in SIRT2 knock-out mice is not due to genetic compensation.

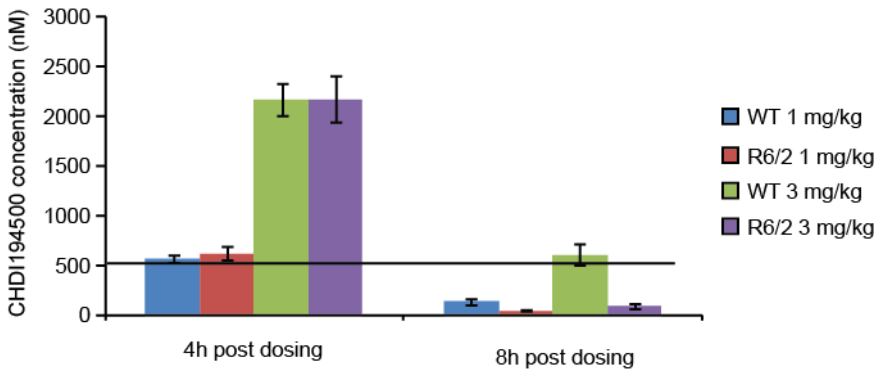

Figure 4.17. CHDI194500 is present in the brain of dosed mice after one acute dose of 1 mg/kg or 3 mg/kg at 4 and 8 hours post dosing

Pharmacokinetic analysis was performed by LC/MS/MS on rest of brain samples (brain except cortex, striatum, hippocampus, cerebellum, and brain stem) from mice dosed with vehicle, 1 mg/kg or 3 mg/kg of CHDI194500. No compound was detected in mice dosed with vehicle alone. Black line denotes the SIRT2 IC_{50} concentration of 560 nM for CHDI194500 as determined in *in vitro* assays (Appendix 2). n≥8/genotype/dose/time point.

4.10. Final conclusions

To conclude, the data presented here show that genetic manipulation causing an approximately 50% reduction in SIRT2 protein levels or total ablation of the SIRT2 protein has no effect on disease progression in the R6/2 mouse. Moreover, reduction or removal of the SIRT2 protein has no effect on the levels of acetylated tubulin, acetylated H4K16 or on the expression of enzymes involved in cholesterol biosynthesis. Additionally, it has been demonstrated that compensation has not occurred in the regulation of the cholesterogenic enzyme expression as no changes have been observed after acute inhibition of SIRT2. Though it was not possible to find an appropriate pharmacodynamic readout of SIRT2 activity after inhibition with CDHI194500, the pharmacokinetic data showed that CHDI194500 was successfully introduced into the brain of dosed mice at 0.5 - 2 μM levels, greater than the IC_{50} of 0.56 μM for SIRT2. Overall, this signifies that the roles of SIRT2 in the regulation of cholesterol biosynthesis and as a possible therapeutic target for HD do not translate to the mammalian system.

5.0. DISCUSSION

5.1. Tubulin hyperacetylation is observed after genetic depletion of HDAC6 but not SIRT2

The significance of tubulin acetylation in cell function and human disease has gradually emerged since the identification of this modification almost 30 years ago (L'Hernault and Rosenbaum, 1983). HDAC6 and SIRT2 are the only known tubulin deacetylating enzymes (Hubbert et al., 2002; North et al., 2003). As acetylation of α-tubulin has been suggested to modify microtubule stability and dynamics (Matsuyama et al., 2002), influence protein-microtubule binding (Giustiniani et al., 2009), and play a role in numerous biological processes (Perdiz et al., 2011), it was surprising to discover that both *Hdac6*KO and *Sirt2*KO mice were viable and did not shown any overt phenotypes. Nevertheless, the observation that *Hdac6*KO mice displayed a deficit in their immunological response to infection (Zhang et al., 2008) argues for the possibility that both *Hdac6*KO and *Sirt2*KO mice could exhibit other subtle phenotypes or alternatively, only present with a phenotype when challenged with stressful conditions.

Thorough investigation of acetylated tubulin levels revealed that tubulin is hyperacetylated throughout the brain of *Hdac6*KO mice (Experimental Paper – Fig. 2 A and C). This finding was surprising as the *Hdac6*KO mice that were used in this study have previously been shown to possess hyperacetylated tubulin in peripheral tissues but not in the brain (Zhang et al., 2008). However, tubulin hyperacetylation has been observed in the brain of a different line of *Hdac6*KO mice (Gao et al., 2007). An absence of tubulin hyperacetylation in brain tissue in the experiments performed by Zhang and colleagues, was attributed to constitutively high levels of acetylated tubulin in the brain of wild type mice (Zhang et al., 2008). This discrepancy may be due to differences in tubulin acetylation within the brain during ageing. Zhang and colleagues characterised mice at 12-26 weeks of age (Zhang et al., 2008), whereas the work presented here was performed in mice that were 15

weeks of age or younger. Interestingly, tubulin hyperacetylation was found to be highest at 4 and 9 weeks of age and decreased by 15 weeks of age in *Hdac6*KO brain tissue. This effect appears to be due to an increase in tubulin acetylation in wild type mice at 15 weeks of age. Given that mice older than 15 weeks have not been examined here and assuming that tubulin acetylation continues to increase with age it is possible that the effects of HDAC6 depletion are not detectable in mice older than 15 weeks. However, as no specification as to the age of mice tested in the study by Zhang et al was given (Zhang et al., 2008), it is not possible to determine if this explanation could apply. A minimal decrease in *Hdac6* mRNA expression level was observed between 4 and 9 weeks of age in the cortex, but not in the striatum or cerebellum of wild type mice (Experimental Paper – Fig. 1C). It is possible that this could account for the increase in tubulin acetylation observed at 15 weeks of age. Alternatively, this phenomenon could be a result of changes in the expression or activity of recently identified tubulin acetylatransferases αTAT (previously MEC-17) and the elongator complex (Akella et al., 2010; Creppe et al., 2009). Although these experiments are beyond the scope of this project, it would be interesting to investigate which factors regulate tubulin acetylation in the brain.

Like HDAC6, SIRT2 has been shown to deacetylate tubulin *in vitro* and in cell culture experiments. Given the dramatic changes in tubulin acetylation in *Hdac6*KO mice, it was expected that a similar change would be observed in *Sirt2*KO mice. Surprisingly, no differences could be observed in the levels of acetylated tubulin between brains of *Sirt2*KO mice and those of wild type mice. It is unlikely that an age related change in SIRT2 levels is the explanation for these observations as SIRT2 levels in the brain were found to be higher at 4 than at 15 weeks of age, which is consistent with previous studies (Werner et al., 2007). The data obtained in this study suggest that either SIRT2 is not critical for tubulin deacetylation or that a chronic loss of SIRT2 is compensated for in *Sirt2*KO mice.

It is possible that SIRT2, though shown to be capable of tubulin deacetylation *in vitro* and in cell culture after acute RNAi mediated SIRT2 knock-down, is not a *bona fide* tubulin deacetylase *in vivo*. Previous studies could not detect changes to levels of acetylated tubulin in mouse embryonic fibroblasts derived from *Sirt2*KO mice

(Zhang et al., 2008). At the same time, double mutant *Hdac6*KOx*Sirt2*KO mice are viable and do not display any overt phenotypes up to 4 weeks of age, arguing for non-redundant roles for HDAC6 and SIRT2 (unpublished observations). Therefore, it is possible that previous findings on the function of SIRT2 as a tubulin deacetylase do not translate to the mammalian system.

Structural and functional similarity implies that increases in either SIRT1 or HDAC6 activity could compensate for SIRT2 loss. However, neither *Hdac6* nor *Sirt1* levels were found to be changed in *Sirt2*KO mice implying that SIRT2 loss is not compensated for by changes in the expression of HDAC6 or SIRT1. Nevertheless, it remains possible that increases in HDAC6 or SIRT1 activity could occur independently of changes in expression upon SIRT2 loss. As such, it would be interesting to investigate whether compensation occurs via changes in enzymatic activity of HDAC6, SIRT1 or another deacetylase. However, the tools required to address this question are not currently available. Though the mechanism regulating tubulin acetylation was not the focus of this work, further investigation assessing the levels and activity of tubulin acetyltrasferases and histone deacetylases upon SIRT2 depletion may be interesting.

5.2. SIRT2 loss does not affect histone 4 lysine 16 acetylation

In addition to tubulin, SIRT2 has been proposed to regulate the acetylation status of several other clients. Although cytoplasmic in nature, SIRT2 has been shown to regulate cell cycle progression through deacetylation of lysine 16 of histone 4 (H4K16) (Vaquero et al., 2006). Interestingly, no change in the levels of acetylated H4K16 were observed in brain and liver tissue from *Sirt2*KO mice.

The absence of change in levels of acetylated H4K16 between wild type and *Sirt2*KO mice was not due to the fact that the brain contains fewer dividing cells than other organs, as the same observation was also made in the liver, which contains a high number of dividing cells. It is equally unlikely that the antibody used in this work was not specific enough to detect changes in this particular modification of H4, as

this antibody has been extensively characterised through the modENCODE project (Egelhofer et al., 2011). Together with the fact that *Sirt2*KO mice develop normally and do not show any phenotypes it appears that cell cycle progression is not impaired in these mice.

In accordance with previously published data (Vaquero et al., 2006), SIRT2 was found to be predominantly cytoplasmic with little SIRT2 being found in nuclear fractions isolated from mouse brain. This could indicate that SIRT2 is only important for cell cycle regulation under specific conditions, as has been suggested by some, but not all, previous studies (Dryden et al., 2003; Inoue et al., 2007; Pandithage et al., 2008; Vaquero et al., 2006). Equally, in addition to its role in cell cycle progression, acetylation of H4K16 has been reported to be important for cellular processes such as maintenance of active chromatin for transcription or DNA repair (Vaquero et al., 2007). Given the fundamental importance of these pathways, it is highly likely that compensatory mechanisms to maintain proper H4K16 acetylation levels exist and could be responsible for the inability to detect differences in H4K16 acetylation between wild type and *Sirt2*KO mice.

5.3. SIRT2 ablation has no effect on the expression of cholesterol biosynthesis enzymes

Cholesterol is vital to the proper functioning of neurons through its involvement in myelin formation, neurite outgrowth, synaptogenesis and proper clustering of membrane proteins such as ion channels and neurotransmitter receptors (Valenza and Cattaneo, 2011). Defects in cholesterol biosynthesis can lead to malfunctioning of the central nervous system, as is the case in Smith-Lemli-Opitz syndrome (Waterham et al., 1998). Changes in cholesterol levels have also been observed in HD patients as well as in all HD models investigated (Valenza and Cattaneo, 2011). However, therapeutic interventions aimed at correcting cholesterol levels in HD

have not yet been investigated in HD mouse models or patients. Equally, as the contribution of cholesterol dys-homeostasis to HD pathology is unknown, finding a strategy for studying the effects of varying cholesterol levels on HD progression might shed light on the potential benefits of this unexplored therapeutic avenue. Consistent with previous reports, the expression of cholesterol enzymes *Hmgcr*, *Hmgcs1*, *Dhcr7*, *Fdft1*, *Fdps*, *Idi1* and *Sqle* was reduced at 12 weeks of age in vehicle treated R6/2 mice that were part of the CHDI 00194500-0000-005 (CHDI194500) acute dosing study. This reduction has been proposed to contribute to altered cholesterol levels in HD and may be due to aberrant interaction of mHTT with SREBP-2 – a transcription factor that controls the expression of cholesterol biosynthesis enzymes. Surprisingly, expression of cholesterol enzymes *Hmgcs1*, *Dhcr7* and *Sqle* was not reduced in R6/2 mice at 15 weeks of age. However, in contrast to the mice treated with CHDI1945 vehicle, these mice were included in the *Sirt2*KOxR6/2 phenotyping study and would have been subjected to forced regular exercise. Though the effect of exercise on brain cholesterol is unknown, physical exercise correlates with changes in cholesterol levels in the liver and in blood. Therefore, differential effects of exercise on the expression of *Hmgcs1*, *Dhcr7* and *Sqle* between wild type and R6/2 mice could explain the discrepancies observed.

A role of SIRT2 in modulation of cholesterol content was suggested after acute inhibition of SIRT2 ameliorated mHTT toxicity in worm, fly and cell culture HD models (Luthi-Carter et al., 2010). This effect was attributed to SIRT2 inhibition decreasing cholesterol synthesis via cytoplasmic retention of SREBP-2 (Luthi-Carter et al., 2010). Therefore, genetically depleting SIRT2 in mice was expected to lead to a decrease in the expression of cholesterol synthesis enzymes that are targets of SREBP-2. Surprisingly, the expression of 7 enzymes of the cholesterol biosynthesis pathway, 6 of which were confirmed targets of SREBP-2 (Horton et al., 2002), was found to be unaltered in *Sirt2*KO mice. Absence of an effect upon SIRT2 depletion was not due to focusing on a specific time point, brain region or tissue as the same observations were made in the cortex at 4 and 9 weeks of age, and in the brain stem and liver at 4 weeks of age. Equally, expression of cholesterogenic enzymes

was not affected by *Sirt2* knock-out at 15 weeks of age, when *Sirt2*HET and *Sirt2*KO mice were included in the analysis of cholesterogenic enzymes expression in double mutant *Sirt2*KOxR6/2 mice.

One straightforward reason for the lack of changes in the expression of cholesterol biosynthesis enzymes detected after SIRT2 depletion is that SIRT2 does not play a role in cholesterol synthesis in the mouse. Previous work linking SIRT2 to cholesterol synthesis was performed with inhibitors that could have multiple off-target effects. Although changes in the expression of *Fdft1*, *Hgmcs1* and *Hmgcr* were also detected after over-expression of a catalytically dead SIRT2 (Luthi-Carter et al., 2010), these changes could be due to viral transduction being stressful to cells.

On the other hand, it is possible that SIRT2 does promote SREBP-2 nuclear localisation and the fact that no changes in the expression of cholesterol biosynthesis enzymes were detected in the brains of *Sirt2*KO mice could be a result of compensatory mechanisms, which may also account for an absence of changes in tubulin and H4K16 acetylation. Therefore, it was important to attempt to verify whether acute SIRT2 inhibition would decrease the expression levels of cholesterol biosynthesis enzymes. The CHDI compound 00194500-0000-005 (CHDI194500) is brain penetrant when administered by gavage and inhibits SIRT1 and SIRT2 in *in vitro* assays (Appendix 2). Unfortunately, attempts in adapting an *in vitro* SIRT2 activity kit to measuring SIRT2 activity in brain lysates were unsuccessful, most likely due to the design of the assay and presence of other proteins with deacetylase activity in the lysate. Future experiments with probes specific for SIRT2 activity would be more apt at answering the question of SIRT2 inhibition.

As it was not feasible to ascertain that SIRT2 activity was reduced after dosing with CHDI194500, there was a possibility that although CHDI1945 was found in the brains of dosed mice, it might not have inhibited SIRT2. Overall, it is not possible to definitely rule out compensatory mechanisms, however, taken together, these data suggest that the changes previously observed upon SIRT2 inhibition in cell culture do not translate to the mammalian brain.

5.4. Tubulin acetylation is not altered in R6/2 brains

Given that histone acetyltransferase and deacetylase activity has been shown to be altered in HD, it was possible that this imbalance could have effects on targets other than histone proteins such as tubulin. On the other hand, neither *Hdac6* nor *Sirt2* expression was found to be dysregulated in R6/2 mice (Experimental Paper – Fig. 1 D). Interestingly, a thorough characterisation of tubulin acetylation levels in R6/2 brain tissue revealed that tubulin acetylation is not affected by disease progression at any age tested (Experimental Paper – Fig. 2 B and D). This is in accordance with another study published during the timeframe of this work, which also found no differences in acetylation of tubulin in the CAG140 knock-in mice or in the cortex from HD patients (Quinti et al., 2010). In contrast, a more limited study using a smaller number of samples reported that tubulin acetylation is reduced in the striatum of HD patient brains (Dompierre et al., 2007). Considering the pronounced variability in tubulin acetylation levels observed in the cortex of HD patients (Quinti et al., 2010), and the fact that only 2 biological replicates were used to measure tubulin acetylation in the striatum (Dompierre et al., 2007), it is possible that this finding is not an accurate reflection of the state of striatal tubulin acetylation in HD. Nevertheless, it would be very interesting to find out whether these findings represent a discrepancy between the methods used to detect tubulin acetylation or a real biological phenomenon, whereby tubulin acetylation is reduced in the striatum, but not in the cortex during HD.

5.5. Knock-out of HDAC6 has no effect on physiological or behavioural phenotypes in R6/2 mice

Previous studies in cell culture and *D.melanogaster* models of polyglutamine disease indicated that modulation of HDAC6 levels could affect polyglutamine-related toxicity (Dompierre et al., 2007; Iwata et al., 2005; Pandey et al., 2007). However, to date only one study has also investigated the effect of HDAC6 genetic

depletion on behavioural phenotypes in the context of neurodegenerative disease. Flies deficient in HDAC6 have been found to have a significantly greater impairment in climbing assay in a *D.melanogaster* model of Parkinson's Disease (PD) (Du et al., 2010). However, the work presented in this thesis showed that the depletion of HDAC6 did not modify the R6/2 phenotype in rotarod performance, grip strength or spontaneous exploratory activity (Experimental Paper – Fig. 3 C-E and Fig. S1). Concomitantly, HDAC6 loss did not affect body or brain weight loss in R6/2 mice at any age tested (Experimental Paper – Fig B and F). The discrepancy between these findings and previous studies can possibly best be explained by the differences in the models used and diseases investigated. Equally, a decrease in polyglutamine mediated toxicity and rescue of neurodegeneration measured with cell viability and ommatidial degeneration assays respectively, might not necessarily translate into changes in behavioural outputs. The data presented here clearly suggest that genetic ablation of HDAC6 has no effect on behavioural or physiological dysfunctions observed in R6/2 mice and previous findings on HDAC6 depletion do not translate to the mammalian system. On the other hand, effects of HDAC6 depletion might only manifest in the context of full length mHTT and/or with age. Nevertheless, though the investigation of the behaviour of *Hdh*Q150 knock-in mice with HDAC6 depletion would be valuable, such an endeavour is very impractical as the end point in these mice is 22 months of age.

Given that HDAC6 has been reported to be necessary for HSP90 mediated glucocorticoid receptor (GR) maturation (Kovacs et al., 2005) and disruptions in GR signalling have been linked to both loss of anxiety and depressive-like behaviours (Urani and Gass, 2003), it was interesting to find that *Hdac6*KO mice showed no change in spontaneous exploratory activity. Nevertheless, it has also been reported that mice with a forebrain specific knock-out of GR in the mature CNS do not display altered anxiety or activity unless placed under stress (Boyle et al., 2006). As the mice examined in this work have not been placed under stressful conditions, it is not possible to determine whether depletion of HDAC6 affects the GR signalling in a manner similar to that observed after GR loss. Equally, although it has been ascertained that compensatory mechanisms in *Hdac6*KO mice did not occur for

tubulin acetylation, the acetylation of HSP90 has not been assessed and therefore further investigation would be required to address the question of the role of HDAC6 in GR mediated anxiety and depressive-like behaviour.

5.6. Knock-out of SIRT2 increases body weight, but has no effect on brain weight or behavioural phenotypes in R6/2 mice

Rescue of mHTT toxicity after genetic knock-down or pharmacological inhibition of SIRT2 has been observed in *D.melanogaster* models of HD and PD (Luthi-Carter et al., 2010; Outeiro et al., 2007; Pallos et al., 2008). Although the question of how SIRT2 inhibition affects behaviour in the context of HD has not been previously addressed, one study demonstrated an improvement in the phenotype of R6/1 mice upon treatment with nicotinamide (NAM), a pan-sirtuin inhibitor (Hathorn et al., 2011). In contrast, thorough phenotypical characterisation performed in this work revealed that SIRT2 genetic depletion did not modulate rotarod performance, grip strength or spontaneous exploratory activity and had no effect on the brain weight in wild type or in R6/2 mice. These data suggest that the use of a pan-sirtuin inhibitor is not directly comparable to a genetic depletion of a single sirtuin. Additionally, off-target effects of NAM, which is an element of cellular energy metabolism and therefore also a possible substrate, activator or inhibitor of other enzymes, cannot be excluded. Equally, although both studies were performed in a fragment HD mouse model, slower disease progression in R6/1 mice could account for manifestation of an effect. Thus, the effects seen in the study of Hathorn and colleagues (Hathorn et al., 2011), are not in conflict with the data presented here, but rather indicate that combinatorial sirtuin inhibition could be a more effective therapeutic strategy for HD.

Interestingly, both reduction and depletion of SIRT2 caused a significant increase in body weight that was observed in both wild type and R6/2 mice, indicating that this effect is independent of disease progression. No effect on body weight was observed when mice were treated with nicotinamide, suggesting that this

phenotype depends not only on loss of SIRT2 activity but also on the activity of other sirtuins (Hathorn et al., 2011). The question of how SIRT2 loss causes body weight gain can be approached from different angles. Firstly, SIRT2 has been shown to inhibit adipocyte differentiation by deacetylation of FOXO1 and by engagement and inhibition of PPARγ controlled promoters (Jing et al., 2007; Wang and Tong, 2009). SIRT2 knock-down causes cytoplasmic retention of FOXO1, and increased adipocyte differentiation (Jing et al., 2007). Therefore, *Sirt2*KO mice could have an increased potential for adipogenesis that could have a significant influence on body weight. Bearing in mind that mice are maintained on a diet enriched in protein and fat, it is plausible to expect that increased adipogenesis could occur and translate into an increased body weight in mice with reduced or depleted SIRT2. Additionally, it has been suggested that knock-down of SIRT2 decreases intracellular ATP levels in PC12 cells (Nie et al., 2011). Although the validity of this observation in the context of the mouse is unknown, decreased ATP levels in *Sirt2*Het or *Sirt2*KO mice could lead to activation of the AMPK (Adenosine monophosphate activated protein kinase) pathway (Hardie, 2007). This in turn has been shown to affect multiple downstream events, including hypothalamic increase in cellular NAD^+ levels and SIRT1 activation, which leads to FOXO1 deacetylation, inhibition of POMC (proopiomelanocortin), activation of NPY (neuropeptide Y)/AgRP (Agouti-related protein) and increase in food intake (Cakir et al., 2009; Canto et al., 2009; Hardie, 2007). A role for SIRT1 in mediating effects of SIRT2 depletion could explain why no changes in body weight were observed upon NAM treatment. Whether any of these speculative explanations could account for the phenotype observed requires further investigation. Nevertheless, it would be very interesting to elucidate the mechanism of the weight gain in *Sirt2*KO mice.

5.7. Knock-out of HDAC6 or SIRT2 does not affect aggregate load or levels of soluble mutant huntingtin

Aggregates of mHTT are formed in HD patient brains and all known mouse models and their appearance correlates with disease progression. Genetic depletion of either HDAC6 or SIRT2 did not affect aggregate load or levels of soluble mHTT in the R6/2 brain at any age examined.

These findings were very surprising given that previous studies have identified HDAC6 as indispensable for the formation of the aggresome and its subsequent autophagic degradation (Iwata et al., 2005). Aggresome formation has been suggested to occur in the context of misfolded protein accumulation, whereby small dispersed aggregates become ubiquitinated, recognised by HDAC6 via its ubiquitin binding domain and transported to a peri-nuclear localisation by dynein, which can also interact with HDAC6 through the $p150^{glued}$ protein (Iwata et al., 2005; Johnston et al., 2002; Johnston et al., 1998; Kawaguchi et al., 2003). This process was hypothesized to result in neuroprotection by allowing cells to dispose of an excess of misfolded proteins. In keeping with that assumption, overexpression of HDAC6 has been demonstrated to rescue neurodegeneration in the *D.melanogaster* SBMA model in an autophagy dependent manner (Pandey et al., 2007). The reason why an absence of HDAC6 does not increase aggregate load in R6/2 mice is unknown but could include compensatory mechanisms, differences in aggregate handling between lower organisms/cell culture systems and mice (as evidenced by differences in disruption to of the UPS in cell and mouse models of HD) or the effects being too subtle to be detected.

Given that impairment of the UPS has been reported to be localised to the synapses in mouse models of HD (Wang et al., 2008), it is unlikely that changes in proteasome function upon HDAC6 depletion account for an absence of detectable changes in aggregate load. However, accumulation of K48 and K63 ubiquitin linked chains has been reported in R6/2 mice (Bennett et al., 2007). It is possible that HDAC6 modulates aggregation through its ubiquitin binding domain and a specific

species of ubiquitin conjugate. Therefore, it is conceivable that a lack of a particular species of ubiquitin such as K63 in R6/2 mice could prevent HDAC6 from affecting aggregate load.

Alternatively, constitutive knock-out of HDAC6 could have allowed compensation to occur during development. However, the fact that both an intact microtubule network and HDAC6 catalytic activity are required for aggresome formation (Iwata et al., 2005), together with the observation that tubulin is hyperacetylated in *Hdac6*KO mice, strongly suggest that compensation has not occurred. On the other hand, it has been suggested that HDAC6 is found in a complex with the p97/VCP (valosin containing protein) chaperone, which possesses segregase activity and has been implicated to be important for proteasomal clearance of ubiquitinated proteins (Richly et al., 2005; Rumpf and Jentsch, 2006; Seigneurin-Berny et al., 2001). Interestingly, it has been shown that the fate of ubiquitinated proteins is determined by the balance between HDAC6 and p97/VCP, whereby an excess of p97/VCP causes dissociation of ubiquitinated proteins from HDAC6 and their subsequent proteasomal degradation, whereas excess of HDAC6 promotes aggresome formation (Boyault et al., 2006). At the same time, p97/VCP has been shown to suppress aggregate formation in a *C.elegans* mHTT exon 1 HD model (Nishikori et al., 2008). It is also possible that in the absence of HDAC6, altered p97/VCP activity, which has been demonstrated to interact with several E3 ubiquitin ligases (Halawani and Latterich, 2006), affects ubiquitination of mHTT. Given that impairment of the proteasome could not be demonstrated in R6/2 mice, it is possible that HDAC6 genetic depletion stimulates compensatory mechanisms that involve p97/VCP and result in an overall comparable level of aggregate load between R6/2 and *Hdac6*KOxR6/2 mice. Further investigation of the activity of p97/VCP and its association with ubiquitinated proteins in R6/2 and *Hdac6*KOxR6/2 mice is necessary to address this issue.

An alternative reason for not observing a change in aggregate load upon HDAC6 ablation is that the effect was too subtle to be detected. With 8 mice, the Seprion ELISA technique has 80% power to detect a 30-50% change between 4 and 8 weeks of age, and a 20-40% change between 4 and 12 weeks of age in the R6/2 brain,

depending on the region examined (Sathasivam et al., 2010). Nevertheless, genetic knock-down of HDAC6 in a mHTT-exon 1 cell culture model of HD led to an approximately 3-fold increase in aggregate load and a 2-fold increase in inclusion number (Iwata et al., 2005). This indicates that even if genetic depletion of HDAC6 leads to a subtle and undetectable increase in aggregate load, handling of misfolded mHTT exon-1 fragment is different between invertebrates/cell culture systems and the mouse brain, as previously discussed (Experimental Paper – Discussion).

Lack of effect of SIRT2 loss on aggregate load or levels of soluble mHTT was equally interesting. SIRT2 pharmacological inhibition was found to reduce mHTT inclusion number in primary striatal neurons, but over-expression of a catalytically dead SIRT2, that was suggested to diminish activity of endogenous SIRT2, had little effect on mHTT inclusion number in the same model (Luthi-Carter et al., 2010). Additionally, SIRT2 knock-down rescued α-synuclein mediated toxicity in human neuroglioma cells but SIRT2 inhibition led to a decrease in number and increase in size of inclusions in the same model of PD (Outeiro et al., 2007). No changes in inclusion size were observed when the same SIRT2 inhibitors were used on primary striatal HD neurons (Luthi-Carter et al., 2010). Interestingly, HDAC6 has also been implicated in the rescue of α-synuclein toxicity by promoting large inclusion formation in a *D.melanogaster* PD model (Du et al., 2010). On the other hand, though not a specific SIRT2 inhibitor, NAM treatment had no effect on inclusion number in R6/1 mice (Hathorn et al., 2011). Considering previously published findings and data obtained in this study it appears that not only could mechanisms of aggregate formation be quite different for α-synuclein and mHTT but also that mHTT aggregate formation and handling is dependent on the cellular and organismal context. Further work that directly compares aggregate formation between different model systems is necessary to shed more light on these intriguing observations.

5.8. Rate of soluble mHTT level reduction but not aggregate load increase during disease progression is not homogeneous throughout the brain

Intriguingly, though aggregated and soluble mHTT levels were unaltered by SIRT2 depletion, TR-FRET and Mezoscale Discovery (MSD) assays revealed that the rate at which soluble mHTT levels decrease is dependent on the brain region examined. On the other hand, the rate of aggregate formation was similar across brain regions, a result that is in accordance with previous observations where aggregate load was measured by Seprion ELISA (Sathasivam et al., 2010). This suggests that aggregation proceeds through the formation of a population of mHTT that is an intermediate between soluble and aggregated mHTT, and which is not detected by either of the two antibody combinations employed in the MSD assay or by TR-FRET analysis. Based on the data obtained, it is also likely that the kinetics and/or mechanisms that govern the formation of such a population depend on the expression of either mHTT or other brain region specific factors. For example, it is well documented that the expression of the proteostasis machinery components, a system with many links to aggregate formation, is not homogeneous throughout the mouse brain (Powers et al., 2009; Tebbenkamp and Borchelt, 2010). The existence of differences in kinetics/mechanisms of mHTT aggregation throughout the brain could account for the fact that some therapeutic interventions are effective at reducing the aggregate load in some brain regions but not others (Mielcarek et al., 2011). Further experiments examining the existence, nature, and mechanisms of formation of this hypothetical mHTT species are required to shed more light on this novel observation.

5.9. HDAC6 depletion has no effect on the efficiency of BDNF cortico-striatal transport

Although several studies have argued for a role of HDAC6 in aggregate clearance, there was also rationale to think that HDAC6 could be beneficial in HD independently of aggregation (Dompierre et al., 2007). Reduced levels of the neurotrophin BDNF have been implicated in HD pathology and increasing levels of BDNF has been proposed to be beneficial in models of HD (Cho et al., 2007; Gharami et al., 2008; Xie et al., 2010). HDAC6 has been proposed to negatively regulate the transport of BDNF from the cortex to the striatum and therefore, inhibition of HDAC6 might be expected to increase striatal BDNF delivery and improve behavioural phenotypes in HD mice (Dompierre et al., 2007). In accordance with previous findings *Bdnf* mRNA was found to be highly expressed in the cortex and hippocampus, but not striatum (Schmidt-Kastner et al., 1996). In contrast, BDNF protein levels between cortex, striatum and hippocampus were highly comparable (Experimental paper - Fig S4). These data are consistent with an existing model whereby BDNF is synthesized in the cortex and then transported to the striatum (Altar et al., 1997). Therefore, measuring BDNF levels in the striatum is a good indicator of the efficiency of BDNF cortico-striatal transport.

Interestingly, although *Bdnf* mRNA expression was found to be decreased in the cortex of 9 week old R6/2 mice, no changes in the levels of BDNF protein could be detected in the cortex or striatum of R6/2 mice at this age. This was especially surprising given that tubulin was hyperacetylated in both the cortex and the striatum at this age, and that the proposed mechanism of increased BDNF cortico-striatal transport involves faster movement of microtubule cargo as a consequence of reduced kinesin-1 pausing on acetylated microtubules (Dompierre et al., 2007; Gauthier et al., 2004; Reed et al., 2006). It is conceivable that the method employed for detection of BDNF protein levels was not sensitive enough to detect subtle changes in BDNF. However, the fact that levels of cortical BDNF were not decreased in R6/2 mice is contrary to some, though not all, previous studies, indicating that sample preparation, mouse husbandry or even the ELISA assay itself could carry

considerable variability between groups (Apostol et al., 2008; Cepeda et al., 2010; Seo et al., 2008). The effects of environmental enrichment on R6/2 phenotype and BDNF levels are well documented (Ickes et al., 2000; Spires et al., 2004; Zhu et al., 2006). Although unable to detect changes in BDNF with disease progression, the method employed was able to detect a significant difference between brain tissues and liver (Experimental Paper – Fig. S4 B) indicating that any dramatic changes in BDNF levels could be identified. Therefore, the data presented here strongly indicate that while HDAC6 depletion induces tubulin hyperacetylation, BDNF cortico-striatal transport efficiency and behavioural phenotypes are unaffected.

5.10. Compensation for HDAC6 or SIRT2 in conventional knock-out mice

Generation and use of constitutive knock-out mice has been instrumental to the elucidation of functional importance of many proteins, including huntingtin. However, this tool has a serious limitation in that both compensatory mechanisms as well as pleiotropic effects resulting from compensation can be mistakenly interpreted as a direct consequence (or lack thereof) of deleting a certain protein (Gerlai, 2001). Examples include lack of phenotype in MyoD knock-out mice that became apparent when double knock-out mice for MyoD and Myf-5 were created (Rudnicki et al., 1993) or up-regulation of HDAC1 in *Hdac2* knock-out mice (unpublished data from our lab).

The finding that *Hdac6*KO mice were viable was surprising, given the multiple proposed roles of HDAC6. Importantly, compensation for HDAC6 has not occurred in the acetylation of tubulin, as these mice show hyperacetylated tubulin throughout the brain and the periphery (Zhang et al., 2008), (Experimental Paper – Fig. 2A and C), suggesting that cells can tolerate high levels of acetylated tubulin. Whether this is because hyperacetylation of tubulin is not detrimental to cellular functions or downstream compensatory mechanisms have occurred remains to be investigated. In any instance, changes to BDNF transport efficiency were reported to be a direct effect of increased tubulin acetylation (Dompierre et al., 2007), and

therefore, *Hdac6*KO mice were the appropriate model with which to investigate this process. At the same time, HDAC6 dependent aggresome formation required both its catalytic activity and ubiquitin binding domain (Kawaguchi et al., 2003). The combination of these two properties has not yet been detected on any other protein. Therefore, if compensatory mechanisms have occurred, they would need to involve at least two proteins, which is possible, although unlikely.

It was even more interesting to find that genetic depletion of SIRT2 did not affect tubulin acetylation or H4K16 acetylation. Both of these substrates have been well characterised in *in vitro* SIRT2 assays and cell culture studies of SIRT2 over-expression, knock-down, or knock-out. It is therefore impossible to quickly determine whether SIRT2 does not deacetylate tubulin or H4K16 *in vivo* or whether compensatory mechanisms have occurred. Although expression of other deacetylases was not modified in *Sirt2*KO mice, compensation could occur on the level of protein expression, its activity or sub-cellular localisation. Unfortunately, though it would be interesting to test all of these possibilities, tools to address these questions are largely unavailable for mouse tissue studies.

The reported role of SIRT2 in cholesterol biosynthesis could also not be reproduced in *Sirt2*KO mice. However, the rationale for a SIRT2 involvement in this process was derived from two studies where SIRT2 was pharmacologically inhibited (Luthi-Carter et al., 2010; Taylor et al., 2011). The on-target effect of the inhibitors used was supported by the observation of reduced levels of *Hmgcr*, *Hmgcs1* and *Fdft1* after the over-expression of a catalytically dead SIRT2 ($SIRT2^{H150Y}$) (Luthi-Carter et al., 2010). Interestingly, in the same study, over-expression of $SIRT2^{H150Y}$ did not have the same effect on mHTT inclusion number reduction as did the SIRT2 inhibitors used (Luthi-Carter et al., 2010). This implies that these results should be approached with caution. Compounds can have many off target effects and the over-expression of a protein can also evoke compensatory mechanisms or aberrant interactions within cells, especially when the expressed protein is a mutant version of the endogenous one. It would have been interesting to examine the effects of shRNA mediated SIRT2 knock-down in the primary striatal cells used in the study by Luthi-Carter and colleagues (Luthi-Carter et al., 2010), to determine whether this

approach complimented their findings from over-expression of SIRT2^{H150Y} and pharmacological inhibition of SIRT2.

No changes in the expression of cholesterol biosynthesis enzymes have been observed in wild type or R6/2 mice after acute inhibition of SIRT2 with the CHDI194500 compound. Although a pharmacodynamic read-out was not available, the potency of CHDI194500 to inhibit SIRT2 in an *in vitro* activity assay and the presence of the drug in the brain of the dosed mice suggests that SIRT2 was inhibited by CHDI194500. Nevertheless, there is a possibility that CHDI194500 was not active in the context of mouse tissue and thus, SIRT2 inhibition was not achieved. Although it would be interesting to directly compare the brain specific effects of CHDI194500 with those of the inhibitors used in primary striatal neurons (Luthi-Carter et al., 2010), the blood-brain-barrier permeability has only so far been established for AK-7, a weak SIRT2 inhibitor (Taylor et al., 2011), which has not been previously examined for the SIRT2 inhibition mediated effect on cholesterol enzyme expression.

Overall, there is strong indication that SIRT2 does not play a role in cholesterol biosynthesis and the previously observed findings are a result of off-target effects of the inhibitors used or of the differences between primary cell culture and mouse models. However, until appropriate tools to confirm SIRT2 inhibition after acute dosing become available, compensatory mechanisms cannot be excluded.

5.11. Limitation in tools for studying protein activity and modification in mouse tissues

Robust molecular read-outs are necessary to ascertain that the intended genetic or pharmacological disruption to the protein's function has taken place. Otherwise, it is impossible to determine whether the intervention was successful. *Hdac6*KO mice have hyperacetylated tubulin throughout the brain, clearly demonstrating that absence of the HDAC6 protein translates into a molecular phenotype. In contrast,

though the SIRT2 protein is absent in *Sirt2*KO mice, they have not displayed any difference in acetylated tubulin or H4K16 levels. Other reported SIRT2 substrates are acetylated p53 (Ac-p53), acetylated FOXO1 (Ac-FOXO1), and acetylated FOXO3a (Ac-FOXO3a) (Peck et al., 2010; Wang et al., 2007; Wang and Tong, 2009). Regrettably, when western blotting against those substrates was attempted, the antibodies against Ac-p53 or Ac-FOXO1 (reported to also cross-react with Ac-FOXO3a) proved to be inadequate for this purpose. Bands corresponding to the expected size of these proteins could not be detected unless a very low dilution of the antibody and a large amount of protein were used in the experiment. Unfortunately, during SDS-PAGE the large protein amount of the protein loaded caused the electrophoresis and the transfer to run unevenly across the gel. The resulting signal was not only weak and hardly detectable, but also impossible to quantify and interpret. It would have been very interesting to be able to accurately measure the levels of Ac-p53, Ac-FOXO1 and Ac-FOXO3a in both the *Sirt2*KO and CHDI194500 treated mice.

The failure to detect differences in SIRT2 activity between wild type and *Sirt2*KO brain lysates with the Fluor de Lys SIRT2 activity assay was perhaps unsurprising. The fluorogenic substrate used in this assay is an acetylated tetrapeptide which in theory could be deacetylated by any of the 17 deacetylases other than SIRT2. Although the Zn^{2+} dependent HDACs were inhibited by Trichostatin A, 6 sirtuins were still present in the *Sirt2*KO brain lysates. At the same time, the finding that the signal detection was not enhanced by addition of extracellular NAD^+ suggests that efforts to deplete intracellular NAD^+ may have been unsuccessful. However, even when conditions well in excess (1h of incubation at 37°C) of those previously reported to be sufficient (10 min of incubation at 37°C) (Escande et al., 2010) were used, no effect of external NAD^+ addition could be observed. Therefore, it is likely that the fluorescent signal detected was due to an NAD^+ independent activity, perhaps not resulting from a deacetylation event but from an unknown mechanism. Overall, it was unfortunate that the Flour de Lys activity assay could not successfully be adapted to measure SIRT2 activity in mouse tissue lysates.

An absence of appropriate molecular tools to measure SIRT2 activity in mouse tissue constituted a major obstacle in determining whether acute treatment of mice with CHDI194500 resulted in SIRT2 inhibition, and in turn, whether a lack of differences in cholesterogenic enzyme expression between vehicle and CHDI194500 treated mice supports data from *Sirt2*KO mice that SIRT2 does not play a role in cholesterol biosynthesis as has been reported previously.

5.12. Genetic depletion of tubulin deacetylases HDAC6 or SIRT2 does not modify disease progression in the R6/2 mouse model of HD

The rapid onset of behavioural, physiological and molecular phenotypes that deteriorate with disease progression makes the R6/2 mouse model a useful tool to study the validity of therapeutic targets and drug treatments. Studies reporting both beneficial and detrimental effects in these mice have been published (Hernandez-Espinosa and Morton, 2006; Labbadia et al., 2011), strongly suggesting that when no effects on phenotype are observed it is not due to an inability of these mice to deteriorate further or to improve.

In this study the R6/2 phenotype was not altered by genetic depletion of either HDAC6 or SIRT2. Compensatory mechanisms have been partly excluded for HDAC6 dependent activities and it can therefore be assumed that HDAC6 inhibition in R6/2 mice would not result in altered phenotype. No changes to HD progression in the R6/2 mice were observed after SIRT2 loss, except for an increase in body weight, which was however, not specific to the HD phenotype. Pharmacological SIRT2 inhibition was only partially confirmed, and though there were no changes to the R6/2 phenotype after chronic treatment with CHDI194500 (unpublished data – CHDI foundation), lack of appropriate pharmacodynamic readouts does not allow for conclusive interpretation of these data. Therefore, though the data presented here do not support SIRT2 as a modifier of R6/2 phenotype, inability to exclude compensatory mechanisms only allows for the conclusion that constitutive knock-out and knock-down of SIRT2 have no effect on disease progression in R6/2 mice.

5.13. Validity of tubulin deacetylases HDAC6 and SIRT2 as therapeutic targets in HD

The finding that depletion of neither HDAC6 nor SIRT2 exerted any changes on HD progression in R6/2 mice was surprising. Previously published reports on the roles of HDAC6 and SIRT2 as modifiers of neurodegenerative disease clearly provided a rationale for conducting a phenotypic study in a mouse model of HD. However, R6/2 mice are not a genetically precise HD model and thus the lack of phenotypic modulation observed could be due to the necessity of placing the knock-out mutations in the context of full length mHTT. On the other hand, involvement of HDAC6 in the aggresome pathway and of SIRT2 in cholesterol biosynthesis were studied in cells expressing N-terminal fragments of mHTT (Iwata et al., 2005; Luthi-Carter et al., 2010), which would suggest that the R6/2 mouse is an ideal system to study those findings in the context of a mammalian brain. Although the role for HDAC6 in modulation of BDNF cortico-striatal transport was elucidated in cells derived from knock-in mice (*Hdh*^{Q109}), this consequence of HDAC6 inhibition was shown to be a direct result of increased tubulin acetylation and reported to be independent of disease context (Dompierre et al., 2007). The finding that an increase in the efficiency of BDNF cortico-striatal transport could not be demonstrated in *Hdac6*KO mice, strongly suggests that this process is regulated differently in the context of the mouse brain than in cell culture. Nevertheless, the short lifespan of R6/2 mice prevents detection of any changes that could be associated with ageing. *Hdh*Q150 mice are not only a genetically precise model of HD, but their normal life-span also allows the study of treatments in the context of an ageing organism. However, given that the rate limiting step in disease progression in knock-in mice is likely to be the formation of an N-terminal fragment of mHTT (Graham et al., 2006; Landles et al., 2010), it is highly unlikely that genetic depletion of HDAC6 and SIRT2 would modify phenotype in the *Hdh*Q150 knock-in mouse model of HD. Moreover, the time and resources required to perform these experiments are considerable and therefore, efforts should be prioritised to address more pertinent questions first.

Given the devastating nature of HD and the lack of disease modifying treatments, considerable effort has been invested in the search for, and validation of, therapeutic strategies. However, the ethical considerations and cost of clinical trials require therapeutic targets to be prioritised according to their probability of yielding promising treatments for HD during pre-clinical assessment. Pan HDAC and sirtuin inhibitors such as SAHA and nicotinamide have been shown to ameliorate disease phenotype in HD mice but are also associated with significant toxic effects. In order to divorce the toxic and beneficial effects of HDAC inhibition, considerable efforts have been made to determine which HDAC(s) and sirtuin(s) are key modifiers of disease progression. Genetic knock-down or knock-out of HDAC3, 5, 7 and 9 has shown no benefit in R6/2 mice whereas genetic knock-down of HDAC4 resulted in a marked improvement in R6/2 behavioural and molecular phenotypes ((Benn et al., 2009) and unpublished data from our lab). This suggests, that the positive effects of general HDAC inhibitors are mediated at least in part through HDAC4 inhibition.

This study demonstrates that like HDAC3,5,7 and 9, HDAC6 and SIRT2 do not modify disease progression in R6/2 mice and should not be prioritised as therapeutic targets in HD. As a consequence, further work should be focused on investigating the effects of the remaining HDACs and sirtuins on disease progression whilst attempting to uncover efficient ways to target and inhibit HDAC4 in mouse brain tissue.

In conclusion, the purpose of this work was to perform a pre-clinical validation of HDAC6 and SIRT2 tubulin deacetylase inhibition as a therapeutic target in HD using the R6/2 mouse model. The data collected strongly suggest that neither HDAC6 nor SIRT2 inhibition would modify HD progression and therefore, HDAC6 and SIRT2 should not be prioritised as therapeutic targets in HD.

6.0. BIBLIOGRAPHY

Afshar, G., and Murnane, J.P. (1999). Characterization of a human gene with sequence homology to Saccharomyces cerevisiae SIR2. Gene *234*, 161-168.

Ahringer, J. (2000). NuRD and SIN3: histone deacetylase complexes in development. Trends in Genetics *16*, 351-356.

Akella, J.S., Wloga, D., Kim, J., Starostina, N.G., Lyons-Abbott, S., Morrissette, N.S., Dougan, S.T., Kipreos, E.T., and Gaertig, J. (2010). MEC-17 is an alpha-tubulin acetyltransferase. Nature *467*, 218-222.

Allen, J.A., Halverson-Tamboli, R.A., and Rasenick, M.M. (2007). Lipid raft microdomains and neurotransmitter signalling. Nat Rev Neurosci *8*, 128-140.

Allfrey, V.G., Faulkner, R., and Mirsky, A.E. (1964). Acetylation and Methylation of Histones and Their Possible Role in the Regulation of Rna Synthesis. Proc Natl Acad Sci U S A *51*, 786-794.

Allis, C.D., Berger, S.L., Cote, J., Dent, S., Jenuwien, T., Kouzarides, T., Pillus, L., Reinberg, D., Shi, Y., Shiekhattar, R.*, et al.* (2007). New nomenclature for chromatin-modifying enzymes. Cell *131*, 633-636.

Altar, C.A., Cai, N., Bliven, T., Juhasz, M., Conner, J.M., Acheson, A.L., Lindsay, R.M., and Wiegand, S.J. (1997). Anterograde transport of brain-derived neurotrophic factor and its role in the brain. Nature *389*, 856-860.

Andrade, M.A., and Bork, P. (1995). HEAT repeats in the Huntington's disease protein. Nat Genet *11*, 115-116.

Andrew, S.E., Goldberg, Y.P., Kremer, B., Telenius, H., Theilmann, J., Adam, S., Starr, E., Squitieri, F., Lin, B., Kalchman, M.A.*, et al.* (1993). The relationship between trinucleotide (CAG) repeat length and clinical features of Huntington's disease. Nat Genet *4*, 398-403.

Apostol, B.L., Simmons, D.A., Zuccato, C., Illes, K., Pallos, J., Casale, M., Conforti, P., Ramos, C., Roarke, M., Kathuria, S.*, et al.* (2008). CEP-1347 reduces mutant huntingtin-associated neurotoxicity and restores BDNF levels in R6/2 mice. Mol Cell Neurosci *39*, 8-20.

Arrasate, M., Mitra, S., Schweitzer, E.S., Segal, M.R., and Finkbeiner, S. (2004). Inclusion body formation reduces levels of mutant huntingtin and the risk of neuronal death. Nature *431*, 805-810.

Arzberger, T., Krampfl, K., Leimgruber, S., and Weindl, A. (1997). Changes of NMDA receptor subunit (NR1, NR2B) and glutamate transporter (GLT1) mRNA expression in Huntington's disease--an in situ hybridization study. J Neuropathol Exp Neurol *56*, 440-454.

Augood, S.J., Faull, R.L., Love, D.R., and Emson, P.C. (1996). Reduction in enkephalin and substance P messenger RNA in the striatum of early grade Huntington's disease: a detailed cellular in situ hybridization study. Neuroscience *72*, 1023-1036.

Bacos, K., Bjorkqvist, M., Petersen, A., Luts, L., Maat-Schieman, M.L., Roos, R.A., Sundler, F., Brundin, P., Mulder, H., and Wierup, N. (2008). Islet beta-cell area and hormone expression are unaltered in Huntington's disease. Histochem Cell Biol *129*, 623-629.

Bae, N.S., Swanson, M.J., Vassilev, A., and Howard, B.H. (2004). Human histone deacetylase SIRT2 interacts with the homeobox transcription factor HOXA10. J Biochem *135*, 695-700.

Bates, E.A., Victor, M., Jones, A.K., Shi, Y., and Hart, A.C. (2006). Differential contributions of Caenorhabditis elegans histone deacetylases to huntingtin polyglutamine toxicity. J Neurosci *26*, 2830-2838.

Bates, G., Harper, P.S., and Jones, L. (2002). Huntington's disease, 3rd ed. / [edited by] Gillian Bates, Peter S. Harper, Lesley Jones. edn (Oxford, Oxford University Press).

Beal, M.F., Ferrante, R.J., Swartz, K.J., and Kowall, N.W. (1991). Chronic quinolinic acid lesions in rats closely resemble Huntington's disease. J Neurosci *11*, 1649-1659.

Ben-Zvi, A., Miller, E.A., and Morimoto, R.I. (2009). Collapse of proteostasis represents an early molecular event in Caenorhabditis elegans aging. Proc Natl Acad Sci U S A *106*, 14914-14919.

Bence, N.F., Sampat, R.M., and Kopito, R.R. (2001). Impairment of the ubiquitin-proteasome system by protein aggregation. Science *292*, 1552-1555.

Benchoua, A., Trioulier, Y., Zala, D., Gaillard, M.C., Lefort, N., Dufour, N., Saudou, F., Elalouf, J.M., Hirsch, E., Hantraye, P.*, et al.* (2006). Involvement of mitochondrial complex II defects in neuronal death produced by N-terminus fragment of mutated huntingtin. Mol Biol Cell *17*, 1652-1663.

Benn, C.L., Butler, R., Mariner, L., Nixon, J., Moffitt, H., Mielcarek, M., Woodman, B., and Bates, G.P. (2009). Genetic knock-down of HDAC7 does not ameliorate disease pathogenesis in the R6/2 mouse model of Huntington's disease. PLoS One *4*, e5747.

Bennett, E.J., Bence, N.F., Jayakumar, R., and Kopito, R.R. (2005). Global impairment of the ubiquitin-proteasome system by nuclear or cytoplasmic protein aggregates precedes inclusion body formation. Mol Cell *17*, 351-365.

Bennett, E.J., Shaler, T.A., Woodman, B., Ryu, K.Y., Zaitseva, T.S., Becker, C.H., Bates, G.P., Schulman, H., and Kopito, R.R. (2007). Global changes to the ubiquitin system in Huntington's disease. Nature *448*, 704-708.

Bertos, N.R., Gilquin, B., Chan, G.K., Yen, T.J., Khochbin, S., and Yang, X.J. (2004). Role of the tetradecapeptide repeat domain of human histone deacetylase 6 in cytoplasmic retention. J Biol Chem *279*, 48246-48254.

Bett, J.S., Benn, C.L., Ryu, K.Y., Kopito, R.R., and Bates, G.P. (2009). The polyubiquitin Ubc gene modulates histone H2A monoubiquitylation in the R6/2 mouse model of Huntington's disease. J Cell Mol Med *13*, 2645-2657.

Bett, J.S., Goellner, G.M., Woodman, B., Pratt, G., Rechsteiner, M., and Bates, G.P. (2006). Proteasome impairment does not contribute to pathogenesis in R6/2 Huntington's disease mice: exclusion of proteasome activator REGgamma as a therapeutic target. Hum Mol Genet *15*, 33-44.

Bhattacharyya, A., Thakur, A.K., Chellgren, V.M., Thiagarajan, G., Williams, A.D., Chellgren, B.W., Creamer, T.P., and Wetzel, R. (2006). Oligoproline effects on polyglutamine conformation and aggregation. J Mol Biol *355*, 524-535.

Bhide, P.G., Day, M., Sapp, E., Schwarz, C., Sheth, A., Kim, J., Young, A.B., Penney, J., Golden, J., Aronin, N.*, et al.* (1996). Expression of normal and mutant huntingtin in the developing brain. J Neurosci *16*, 5523-5535.

Bibb, J.A., Yan, Z., Svenningsson, P., Snyder, G.L., Pieribone, V.A., Horiuchi, A., Nairn, A.C., Messer, A., and Greengard, P. (2000). Severe deficiencies in dopamine signaling in presymptomatic Huntington's disease mice. Proc Natl Acad Sci U S A *97*, 6809-6814.

Bjorkqvist, M., Fex, M., Renstrom, E., Wierup, N., Petersen, A., Gil, J., Bacos, K., Popovic, N., Li, J.Y., Sundler, F.*, et al.* (2005). The R6/2 transgenic mouse model of Huntington's disease develops diabetes due to deficient beta-cell mass and exocytosis. Hum Mol Genet *14*, 565-574.

Boyault, C., Gilquin, B., Zhang, Y., Rybin, V., Garman, E., Meyer-Klaucke, W., Matthias, P., Muller, C.W., and Khochbin, S. (2006). HDAC6-p97/VCP controlled polyubiquitin chain turnover. EMBO J *25*, 3357-3366.

Boyault, C., Zhang, Y., Fritah, S., Caron, C., Gilquin, B., Kwon, S.H., Garrido, C., Yao, T.P., Vourc'h, C., Matthias, P.*, et al.* (2007). HDAC6 controls major cell response pathways to cytotoxic accumulation of protein aggregates. Genes Dev *21*, 2172-2181.

Boyle, M.P., Kolber, B.J., Vogt, S.K., Wozniak, D.F., and Muglia, L.J. (2006). Forebrain Glucocorticoid Receptors Modulate Anxiety-Associated Locomotor Activation and Adrenal Responsiveness. The Journal of Neuroscience *26*, 1971-1978.

Brennan, W.A., Jr., Bird, E.D., and Aprille, J.R. (1985). Regional mitochondrial respiratory activity in Huntington's disease brain. J Neurochem *44*, 1948-1950.

Cakir, I., Perello, M., Lansari, O., Messier, N.J., Vaslet, C.A., and Nillni, E.A. (2009). Hypothalamic Sirt1 regulates food intake in a rodent model system. PLoS One *4*, e8322.

Cambray-Deakin, M.A., and Burgoyne, R.D. (1987). Posttranslational modifications of alpha-tubulin: acetylated and detyrosinated forms in axons of rat cerebellum. The Journal of Cell Biology *104*, 1569-1574.

Canto, C., Gerhart-Hines, Z., Feige, J.N., Lagouge, M., Noriega, L., Milne, J.C., Elliott, P.J., Puigserver, P., and Auwerx, J. (2009). AMPK regulates energy expenditure by modulating NAD+ metabolism and SIRT1 activity. Nature *458*, 1056-1060.

Carter, R.J., Lione, L.A., Humby, T., Mangiarini, L., Mahal, A., Bates, G.P., Dunnett, S.B., and Morton, A.J. (1999). Characterization of progressive motor deficits in mice transgenic for the human Huntington's disease mutation. J Neurosci *19*, 3248-3257.

Cepeda, C., Ariano, M.A., Calvert, C.R., Flores-Hernandez, J., Chandler, S.H., Leavitt, B.R., Hayden, M.R., and Levine, M.S. (2001). NMDA receptor function in mouse models of Huntington disease. J Neurosci Res *66*, 525-539.

Cepeda, C., Cummings, D.M., Hickey, M.A., Kleiman-Weiner, M., Chen, J.Y., Watson, J.B., and Levine, M.S. (2010). Rescuing the Corticostriatal Synaptic Disconnection in the R6/2 Mouse Model of Huntington's Disease: Exercise, Adenosine Receptors and Ampakines. PLoS Curr *2*.

Cha, J.H., Frey, A.S., Alsdorf, S.A., Kerner, J.A., Kosinski, C.M., Mangiarini, L., Penney, J.B., Jr., Davies, S.W., Bates, G.P., and Young, A.B. (1999). Altered neurotransmitter receptor expression in transgenic mouse models of Huntington's disease. Philos Trans R Soc Lond B Biol Sci *354*, 981-989.

Cha, J.H., Kosinski, C.M., Kerner, J.A., Alsdorf, S.A., Mangiarini, L., Davies, S.W., Penney, J.B., Bates, G.P., and Young, A.B. (1998). Altered brain neurotransmitter receptors in transgenic mice expressing a portion of an abnormal human huntington disease gene. Proc Natl Acad Sci U S A *95*, 6480-6485.

Chang, D.T., Rintoul, G.L., Pandipati, S., and Reynolds, I.J. (2006). Mutant huntingtin aggregates impair mitochondrial movement and trafficking in cortical neurons. Neurobiol Dis *22*, 388-400.

Chen-Plotkin, A.S., Sadri-Vakili, G., Yohrling, G.J., Braveman, M.W., Benn, C.L., Glajch, K.E., DiRocco, D.P., Farrell, L.A., Krainc, D., Gines, S*., et al.* (2006). Decreased association of the transcription factor Sp1 with genes downregulated in Huntington's disease. Neurobiol Dis *22*, 233-241.

Cho, S.R., Benraiss, A., Chmielnicki, E., Samdani, A., Economides, A., and Goldman, S.A. (2007). Induction of neostriatal neurogenesis slows disease progression in a transgenic murine model of Huntington disease. J Clin Invest *117*, 2889-2902.

Choo, Y.S., Johnson, G.V., MacDonald, M., Detloff, P.J., and Lesort, M. (2004). Mutant huntingtin directly increases susceptibility of mitochondria to the calcium-induced permeability transition and cytochrome c release. Hum Mol Genet *13*, 1407-1420.

Cong, X., Held, J.M., DeGiacomo, F., Bonner, A., Chen, J.M., Schilling, B., Czerwieniec, G.A., Gibson, B.W., and Ellerby, L.M. (2011). Mass spectrometric identification of novel lysine acetylation sites in huntingtin. Mol Cell Proteomics *10*, M111 009829.

Creppe, C., Malinouskaya, L., Volvert, M.L., Gillard, M., Close, P., Malaise, O., Laguesse, S., Cornez, I., Rahmouni, S., Ormenese, S.*, et al.* (2009). Elongator controls the migration and differentiation of cortical neurons through acetylation of alpha-tubulin. Cell *136*, 551-564.

Crook, Z.R., and Housman, D. (2011). Huntington's disease: can mice lead the way to treatment? Neuron *69*, 423-435.

Cuervo, A.M., and Dice, J.F. (2000). Age-related decline in chaperone-mediated autophagy. J Biol Chem *275*, 31505-31513.

Cui, L., Jeong, H., Borovecki, F., Parkhurst, C.N., Tanese, N., and Krainc, D. (2006). Transcriptional repression of PGC-1alpha by mutant huntingtin leads to mitochondrial dysfunction and neurodegeneration. Cell *127*, 59-69.

Davies, S.W., Turmaine, M., Cozens, B.A., DiFiglia, M., Sharp, A.H., Ross, C.A., Scherzinger, E., Wanker, E.E., Mangiarini, L., and Bates, G.P. (1997). Formation of neuronal intranuclear inclusions underlies the neurological dysfunction in mice transgenic for the HD mutation. Cell *90*, 537-548.

de Ruijter, A.J., van Gennip, A.H., Caron, H.N., Kemp, S., and van Kuilenburg, A.B. (2003). Histone deacetylases (HDACs): characterization of the classical HDAC family. Biochem J *370*, 737-749.

del Toro, D., Xifro, X., Pol, A., Humbert, S., Saudou, F., Canals, J.M., and Alberch, J. (2010). Altered cholesterol homeostasis contributes to enhanced excitotoxicity in Huntington's disease. J Neurochem *115*, 153-167.

Deribe, Y.L., Wild, P., Chandrashaker, A., Curak, J., Schmidt, M.H., Kalaidzidis, Y., Milutinovic, N., Kratchmarova, I., Buerkle, L., Fetchko, M.J.*, et al.* (2009). Regulation of epidermal growth factor receptor trafficking by lysine deacetylase HDAC6. Sci Signal *2*, ra84.

Destaing, O., Saltel, F., Gilquin, B., Chabadel, A., Khochbin, S., Ory, S., and Jurdic, P. (2005). A novel Rho-mDia2-HDAC6 pathway controls podosome patterning through microtubule acetylation in osteoclasts. J Cell Sci *118*, 2901-2911.

DiFiglia, M., Sapp, E., Chase, K.O., Davies, S.W., Bates, G.P., Vonsattel, J.P., and Aronin, N. (1997). Aggregation of huntingtin in neuronal intranuclear inclusions and dystrophic neurites in brain. Science *277*, 1990-1993.

Dompierre, J.P., Godin, J.D., Charrin, B.C., Cordelieres, F.P., King, S.J., Humbert, S., and Saudou, F. (2007). Histone deacetylase 6 inhibition compensates for the transport deficit in Huntington's disease by increasing tubulin acetylation. J Neurosci *27*, 3571-3583.

Dowie, M.J., Bradshaw, H.B., Howard, M.L., Nicholson, L.F., Faull, R.L., Hannan, A.J., and Glass, M. (2009). Altered CB1 receptor and endocannabinoid levels precede motor symptom onset in a transgenic mouse model of Huntington's disease. Neuroscience *163*, 456-465.

Dragatsis, I., Levine, M.S., and Zeitlin, S. (2000). Inactivation of Hdh in the brain and testis results in progressive neurodegeneration and sterility in mice. Nat Genet *26*, 300-306.

Dryden, S.C., Nahhas, F.A., Nowak, J.E., Goustin, A.S., and Tainsky, M.A. (2003). Role for human SIRT2 NAD-dependent deacetylase activity in control of mitotic exit in the cell cycle. Mol Cell Biol *23*, 3173-3185.

Du, G., Liu, X., Chen, X., Song, M., Yan, Y., Jiao, R., and Wang, C.-c. (2010). Drosophila Histone Deacetylase 6 Protects Dopaminergic Neurons against α-Synuclein Toxicity by Promoting Inclusion Formation. Mol Biol Cell *21*, 2128-2137.

Duennwald, M.L., Jagadish, S., Muchowski, P.J., and Lindquist, S. (2006). Flanking sequences profoundly alter polyglutamine toxicity in yeast. Proc Natl Acad Sci U S A *103*, 11045-11050.

Dunah, A.W., Jeong, H., Griffin, A., Kim, Y.M., Standaert, D.G., Hersch, S.M., Mouradian, M.M., Young, A.B., Tanese, N., and Krainc, D. (2002). Sp1 and TAFII130 transcriptional activity disrupted in early Huntington's disease. Science *296*, 2238-2243.

Duyao, M.P., Auerbach, A.B., Ryan, A., Persichetti, F., Barnes, G.T., McNeil, S.M., Ge, P., Vonsattel, J.P., Gusella, J.F., Joyner, A.L.*, et al.* (1995). Inactivation of the mouse Huntington's disease gene homolog Hdh. Science *269*, 407-410.

Eberle, D., Hegarty, B., Bossard, P., Ferre, P., and Foufelle, F. (2004). SREBP transcription factors: master regulators of lipid homeostasis. Biochimie *86*, 839-848.

Egelhofer, T.A., Minoda, A., Klugman, S., Lee, K., Kolasinska-Zwierz, P., Alekseyenko, A.A., Cheung, M.-S., Day, D.S., Gadel, S., Gorchakov, A.A.*, et al.* (2011). An assessment of histone-modification antibody quality. Nat Struct Mol Biol *18*, 91-93.

Ehrnhoefer, D.E., Sutton, L., and Hayden, M.R. (2011). Small changes, big impact: posttranslational modifications and function of huntingtin in Huntington disease. Neuroscientist *17*, 475-492.

Emiliani, S., Fischle, W., Van Lint, C., Al-Abed, Y., and Verdin, E. (1998). Characterization of a human RPD3 ortholog, HDAC3. Proceedings of the National Academy of Sciences *95*, 2795-2800.

Escande, C., Chini, C.C., Nin, V., Dykhouse, K.M., Novak, C.M., Levine, J., van Deursen, J., Gores, G.J., Chen, J., Lou, Z.*, et al.* (2010). Deleted in breast cancer-1 regulates SIRT1 activity and contributes to high-fat diet-induced liver steatosis in mice. J Clin Invest *120*, 545-558.

Farrer, L.A., and Meaney, F.J. (1985). An anthropometric assessment of Huntington's disease patients and families. Am J Phys Anthropol *67*, 185-194.

Ferrante, R.J., Kubilus, J.K., Lee, J., Ryu, H., Beesen, A., Zucker, B., Smith, K., Kowall, N.W., Ratan, R.R., Luthi-Carter, R.*, et al.* (2003). Histone deacetylase inhibition by sodium butyrate chemotherapy ameliorates the neurodegenerative phenotype in Huntington's disease mice. J Neurosci *23*, 9418-9427.

Finkel, T., Deng, C.X., and Mostoslavsky, R. (2009). Recent progress in the biology and physiology of sirtuins. Nature *460*, 587-591.

Finnin, M.S., Donigian, J.R., Cohen, A., Richon, V.M., Rifkind, R.A., Marks, P.A., Breslow, R., and Pavletich, N.P. (1999). Structures of a histone deacetylase homologue bound to the TSA and SAHA inhibitors. Nature *401*, 188-193.

Fischle, W., Dequiedt, F., Hendzel, M.J., Guenther, M.G., Lazar, M.A., Voelter, W., and Verdin, E. (2002). Enzymatic activity associated with class II HDACs is dependent on a multiprotein complex containing HDAC3 and SMRT/N-CoR. Mol Cell *9*, 45-57.

Ford, E., Voit, R., Liszt, G., Magin, C., Grummt, I., and Guarente, L. (2006). Mammalian Sir2 homolog SIRT7 is an activator of RNA polymerase I transcription. Genes Dev *20*, 1075-1080.

Frye, R.A. (1999). Characterization of five human cDNAs with homology to the yeast SIR2 gene: Sir2-like proteins (sirtuins) metabolize NAD and may have protein ADP-ribosyltransferase activity. Biochem Biophys Res Commun *260*, 273-279.

Gaertig, J., Cruz, M.A., Bowen, J., Gu, L., Pennock, D.G., and Gorovsky, M.A. (1995). Acetylation of lysine 40 in alpha-tubulin is not essential in Tetrahymena thermophila. J Cell Biol *129*, 1301-1310.

Gao, L., Cueto, M.A., Asselbergs, F., and Atadja, P. (2002). Cloning and functional characterization of HDAC11, a novel member of the human histone deacetylase family. J Biol Chem *277*, 25748-25755.

Gao, Y.S., Hubbert, C.C., Lu, J., Lee, Y.S., Lee, J.Y., and Yao, T.P. (2007). Histone deacetylase 6 regulates growth factor-induced actin remodeling and endocytosis. Mol Cell Biol *27*, 8637-8647.

Gardian, G., Browne, S.E., Choi, D.K., Klivenyi, P., Gregorio, J., Kubilus, J.K., Ryu, H., Langley, B., Ratan, R.R., Ferrante, R.J.*, et al.* (2005). Neuroprotective effects of phenylbutyrate in the N171-82Q transgenic mouse model of Huntington's disease. J Biol Chem *280*, 556-563.

Garrett, M.C., and Soares-da-Silva, P. (1992). Increased cerebrospinal fluid dopamine and 3,4-dihydroxyphenylacetic acid levels in Huntington's disease: evidence for an overactive dopaminergic brain transmission. J Neurochem *58*, 101-106.

Gauthier, L.R., Charrin, B.C., Borrell-Pages, M., Dompierre, J.P., Rangone, H., Cordelieres, F.P., De Mey, J., MacDonald, M.E., Lessmann, V., Humbert, S.*, et al.* (2004). Huntingtin controls neurotrophic support and survival of neurons by enhancing BDNF vesicular transport along microtubules. Cell *118*, 127-138.

Geeraert, C., Ratier, A., Pfisterer, S.G., Perdiz, D., Cantaloube, I., Rouault, A., Pattingre, S., Proikas-Cezanne, T., Codogno, P., and Pous, C. (2010). Starvation-induced hyperacetylation of tubulin is required for the stimulation of autophagy by nutrient deprivation. J Biol Chem *285*, 24184-24194.

Gerlai, R. (2001). Gene targeting: technical confounds and potential solutions in behavioral brain research. Behavioural Brain Research *125*, 13-21.

Gharami, K., Xie, Y., An, J.J., Tonegawa, S., and Xu, B. (2008). Brain-derived neurotrophic factor over-expression in the forebrain ameliorates Huntington's disease phenotypes in mice. J Neurochem *105*, 369-379.

Gidalevitz, T., Ben-Zvi, A., Ho, K.H., Brignull, H.R., and Morimoto, R.I. (2006). Progressive disruption of cellular protein folding in models of polyglutamine diseases. Science *311*, 1471-1474.

Giorgini, F., Guidetti, P., Nguyen, Q., Bennett, S.C., and Muchowski, P.J. (2005). A genomic screen in yeast implicates kynurenine 3-monooxygenase as a therapeutic target for Huntington disease. Nat Genet *37*, 526-531.

Giustiniani, J., Daire, V., Cantaloube, I., Durand, G., Pous, C., Perdiz, D., and Baillet, A. (2009). Tubulin acetylation favors Hsp90 recruitment to microtubules and stimulates the signaling function of the Hsp90 clients Akt/PKB and p53. Cell Signal *21*, 529-539.

Glass, M., Faull, R.L., and Dragunow, M. (1993). Loss of cannabinoid receptors in the substantia nigra in Huntington's disease. Neuroscience *56*, 523-527.

Graham, R.K., Deng, Y., Slow, E.J., Haigh, B., Bissada, N., Lu, G., Pearson, J., Shehadeh, J., Bertram, L., Murphy, Z.*, et al.* (2006). Cleavage at the caspase-6 site is required for neuronal dysfunction and degeneration due to mutant huntingtin. Cell *125*, 1179-1191.

Gray, M., Shirasaki, D.I., Cepeda, C., Andre, V.M., Wilburn, B., Lu, X.H., Tao, J., Yamazaki, I., Li, S.H., Sun, Y.E.*, et al.* (2008). Full-length human mutant huntingtin with a stable polyglutamine repeat can elicit progressive and selective neuropathogenesis in BACHD mice. J Neurosci *28*, 6182-6195.

Grozinger, C.M., Hassig, C.A., and Schreiber, S.L. (1999). Three proteins define a class of human histone deacetylases related to yeast Hda1p. Proc Natl Acad Sci U S A *96*, 4868-4873.

Gu, W., and Roeder, R.G. (1997). Activation of p53 sequence-specific DNA binding by acetylation of the p53 C-terminal domain. Cell *90*, 595-606.

Gu, X., Andre, V.M., Cepeda, C., Li, S.H., Li, X.J., Levine, M.S., and Yang, X.W. (2007). Pathological cell-cell interactions are necessary for striatal pathogenesis in a conditional mouse model of Huntington's disease. Mol Neurodegener *2*, 8.

Gu, X., Greiner, E.R., Mishra, R., Kodali, R., Osmand, A., Finkbeiner, S., Steffan, J.S., Thompson, L.M., Wetzel, R., and Yang, X.W. (2009). Serines 13 and 16 are critical determinants of full-length human mutant huntingtin induced disease pathogenesis in HD mice. Neuron *64*, 828-840.

Gu, X., Li, C., Wei, W., Lo, V., Gong, S., Li, S.H., Iwasato, T., Itohara, S., Li, X.J., Mody, I.*, et al.* (2005). Pathological cell-cell interactions elicited by a neuropathogenic form of mutant Huntingtin contribute to cortical pathogenesis in HD mice. Neuron *46*, 433-444.

Guidetti, P., Bates, G.P., Graham, R.K., Hayden, M.R., Leavitt, B.R., MacDonald, M.E., Slow, E.J., Wheeler, V.C., Woodman, B., and Schwarcz, R. (2006). Elevated brain 3-hydroxykynurenine and quinolinate levels in Huntington disease mice. Neurobiol Dis *23*, 190-197.

Gunawardena, S., Her, L.S., Brusch, R.G., Laymon, R.A., Niesman, I.R., Gordesky-Gold, B., Sintasath, L., Bonini, N.M., and Goldstein, L.S. (2003). Disruption of axonal transport by loss of huntingtin or expression of pathogenic polyQ proteins in Drosophila. Neuron *40*, 25-40.

Gutekunst, C.A., Li, S.H., Yi, H., Mulroy, J.S., Kuemmerle, S., Jones, R., Rye, D., Ferrante, R.J., Hersch, S.M., and Li, X.J. (1999). Nuclear and neuropil aggregates in Huntington's disease: relationship to neuropathology. J Neurosci *19*, 2522-2534.

Hageman, J., van Waarde, M.A., Zylicz, A., Walerych, D., and Kampinga, H.H. (2011). The diverse members of the mammalian HSP70 machine show distinct chaperone-like activities. Biochem J *435*, 127-142.

Haigis, M.C., Mostoslavsky, R., Haigis, K.M., Fahie, K., Christodoulou, D.C., Murphy, A.J., Valenzuela, D.M., Yancopoulos, G.D., Karow, M., Blander, G.*, et al.* (2006). SIRT4 inhibits glutamate dehydrogenase and opposes the effects of calorie restriction in pancreatic beta cells. Cell *126*, 941-954.

Halawani, D., and Latterich, M. (2006). p97: The cell's molecular purgatory? Mol Cell *22*, 713-717.

Hallows, W.C., Lee, S., and Denu, J.M. (2006). Sirtuins deacetylate and activate mammalian acetyl-CoA synthetases. Proc Natl Acad Sci U S A *103*, 10230-10235.

Hardie, D.G. (2007). AMP-activated/SNF1 protein kinases: conserved guardians of cellular energy. Nat Rev Mol Cell Biol *8*, 774-785.

Harting, K., and Knoll, B. (2010). SIRT2-mediated protein deacetylation: An emerging key regulator in brain physiology and pathology. Eur J Cell Biol *89*, 262-269.

Hathorn, T., Snyder-Keller, A., and Messer, A. (2011). Nicotinamide improves motor deficits and upregulates PGC-1alpha and BDNF gene expression in a mouse model of Huntington's disease. Neurobiol Dis *41*, 43-50.

Hay, D.G., Sathasivam, K., Tobaben, S., Stahl, B., Marber, M., Mestril, R., Mahal, A., Smith, D.L., Woodman, B., and Bates, G.P. (2004). Progressive decrease in chaperone protein levels in a mouse model of Huntington's disease and induction of stress proteins as a therapeutic approach. Hum Mol Genet *13*, 1389-1405.

Hernandez-Espinosa, D., and Morton, A.J. (2006). Calcineurin inhibitors cause an acceleration of the neurological phenotype in a mouse transgenic for the human Huntington's disease mutation. Brain Res Bull *69*, 669-679.

Hilditch-Maguire, P., Trettel, F., Passani, L.A., Auerbach, A., Persichetti, F., and MacDonald, M.E. (2000). Huntingtin: an iron-regulated protein essential for normal nuclear and perinuclear organelles. Hum Mol Genet *9*, 2789-2797.

Hiratsuka, M., Inoue, T., Toda, T., Kimura, N., Shirayoshi, Y., Kamitani, H., Watanabe, T., Ohama, E., Tahimic, C.G., Kurimasa, A.*, et al.* (2003). Proteomics-based identification of differentially expressed genes in human gliomas: down-regulation of SIRT2 gene. Biochem Biophys Res Commun *309*, 558-566.

Hockly, E., Cordery, P.M., Woodman, B., Mahal, A., van Dellen, A., Blakemore, C., Lewis, C.M., Hannan, A.J., and Bates, G.P. (2002). Environmental enrichment slows disease progression in R6/2 Huntington's disease mice. Ann Neurol *51*, 235-242.

Hockly, E., Richon, V.M., Woodman, B., Smith, D.L., Zhou, X., Rosa, E., Sathasivam, K., Ghazi-Noori, S., Mahal, A., Lowden, P.A.*, et al.* (2003). Suberoylanilide hydroxamic acid, a histone deacetylase inhibitor, ameliorates motor deficits in a mouse model of Huntington's disease. Proc Natl Acad Sci U S A *100*, 2041-2046.

Hockly, E., Tse, J., Barker, A.L., Moolman, D.L., Beunard, J.L., Revington, A.P., Holt, K., Sunshine, S., Moffitt, H., Sathasivam, K.*, et al.* (2006). Evaluation of the benzothiazole aggregation inhibitors riluzole and PGL-135 as therapeutics for Huntington's disease. Neurobiol Dis *21*, 228-236.

Hodges, A., Strand, A.D., Aragaki, A.K., Kuhn, A., Sengstag, T., Hughes, G., Elliston, L.A., Hartog, C., Goldstein, D.R., Thu, D.*, et al.* (2006). Regional and cellular gene expression changes in human Huntington's disease brain. Hum Mol Genet *15*, 965-977.

Hodgson, J.G., Agopyan, N., Gutekunst, C.A., Leavitt, B.R., LePiane, F., Singaraja, R., Smith, D.J., Bissada, N., McCutcheon, K., Nasir, J.*, et al.* (1999). A YAC mouse model for Huntington's disease with full-length mutant huntingtin, cytoplasmic toxicity, and selective striatal neurodegeneration. Neuron *23*, 181-192.

Holmberg, C.I., Staniszewski, K.E., Mensah, K.N., Matouschek, A., and Morimoto, R.I. (2004). Inefficient degradation of truncated polyglutamine proteins by the proteasome. EMBO J *23*, 4307-4318.

Hoogeveen, A.T., Willemsen, R., Meyer, N., de Rooij, K.E., Roos, R.A., van Ommen, G.J., and Galjaard, H. (1993). Characterization and localization of the Huntington disease gene product. Hum Mol Genet *2*, 2069-2073.

Horton, J.D., Goldstein, J.L., and Brown, M.S. (2002). SREBPs: activators of the complete program of cholesterol and fatty acid synthesis in the liver. J Clin Invest *109*, 1125-1131.

Huang, K., Kang, M.H., Askew, C., Kang, R., Sanders, S.S., Wan, J., Davis, N.G., and Hayden, M.R. (2010). Palmitoylation and function of glial glutamate transporter-1 is reduced in the YAC128 mouse model of Huntington disease. Neurobiol Dis *40*, 207-215.

Hubbert, C., Guardiola, A., Shao, R., Kawaguchi, Y., Ito, A., Nixon, A., Yoshida, M., Wang, X.F., and Yao, T.P. (2002). HDAC6 is a microtubule-associated deacetylase. Nature *417*, 455-458.

Hughes, R.E., Lo, R.S., Davis, C., Strand, A.D., Neal, C.L., Olson, J.M., and Fields, S. (2001). Altered transcription in yeast expressing expanded polyglutamine. Proc Natl Acad Sci U S A *98*, 13201-13206.

Humphrey, G.W., Wang, Y., Russanova, V.R., Hirai, T., Qin, J., Nakatani, Y., and Howard, B.H. (2001). Stable histone deacetylase complexes distinguished by the presence of SANT domain proteins CoREST/kiaa0071 and Mta-L1. J Biol Chem *276*, 6817-6824.

Ickes, B.R., Pham, T.M., Sanders, L.A., Albeck, D.S., Mohammed, A.H., and Granholm, A.-C. (2000). Long-Term Environmental Enrichment Leads to Regional Increases in Neurotrophin Levels in Rat Brain. Experimental Neurology *164*, 45-52.

Inoue, T., Hiratsuka, M., Osaki, M., Yamada, H., Kishimoto, I., Yamaguchi, S., Nakano, S., Katoh, M., Ito, H., and Oshimura, M. (2007). SIRT2, a tubulin deacetylase, acts to block the entry to chromosome condensation in response to mitotic stress. Oncogene *26*, 945-957.

Iwata, A., Riley, B.E., Johnston, J.A., and Kopito, R.R. (2005). HDAC6 and microtubules are required for autophagic degradation of aggregated huntingtin. J Biol Chem *280*, 40282-40292.

Jacobsen, J.C., Bawden, C.S., Rudiger, S.R., McLaughlan, C.J., Reid, S.J., Waldvogel, H.J., MacDonald, M.E., Gusella, J.F., Walker, S.K., Kelly, J.M.*, et al.* (2010). An ovine transgenic Huntington's disease model. Hum Mol Genet *19*, 1873-1882.

Jeong, H., Then, F., Melia, T.J., Jr., Mazzulli, J.R., Cui, L., Savas, J.N., Voisine, C., Paganetti, P., Tanese, N., Hart, A.C.*, et al.* (2009). Acetylation targets mutant huntingtin to autophagosomes for degradation. Cell *137*, 60-72.

Ji, S., Doucette, J.R., and Nazarali, A.J. (2011). Sirt2 is a novel in vivo downstream target of Nkx2.2 and enhances oligodendroglial cell differentiation. J Mol Cell Biol.

Jia, K., Hart, A.C., and Levine, B. (2007). Autophagy genes protect against disease caused by polyglutamine expansion proteins in Caenorhabditis elegans. Autophagy *3*, 21-25.

Jiang, H., Nucifora, F.C., Jr., Ross, C.A., and DeFranco, D.B. (2003). Cell death triggered by polyglutamine-expanded huntingtin in a neuronal cell line is associated with degradation of CREB-binding protein. Hum Mol Genet *12*, 1-12.

Jiang, W., Wang, S., Xiao, M., Lin, Y., Zhou, L., Lei, Q., Xiong, Y., Guan, K.L., and Zhao, S. (2011). Acetylation regulates gluconeogenesis by promoting PEPCK1 degradation via recruiting the UBR5 ubiquitin ligase. Mol Cell *43*, 33-44.

Jing, E., Gesta, S., and Kahn, C.R. (2007). SIRT2 regulates adipocyte differentiation through FoxO1 acetylation/deacetylation. Cell Metab *6*, 105-114.

Johnston, J.A., Illing, M.E., and Kopito, R.R. (2002). Cytoplasmic dynein/dynactin mediates the assembly of aggresomes. Cell Motil Cytoskeleton *53*, 26-38.

Johnston, J.A., Ward, C.L., and Kopito, R.R. (1998). Aggresomes: a cellular response to misfolded proteins. J Cell Biol *143*, 1883-1898.

Johnstone, R.W. (2002). Histone-deacetylase inhibitors: novel drugs for the treatment of cancer. Nat Rev Drug Discov *1*, 287-299.

Kaeberlein, M., McVey, M., and Guarente, L. (1999). The SIR2/3/4 complex and SIR2 alone promote longevity in Saccharomyces cerevisiae by two different mechanisms. Genes Dev *13*, 2570-2580.

Kaluza, D., Kroll, J., Gesierich, S., Yao, T.P., Boon, R.A., Hergenreider, E., Tjwa, M., Rossig, L., Seto, E., Augustin, H.G.*, et al.* (2011). Class IIb HDAC6 regulates endothelial cell migration and angiogenesis by deacetylation of cortactin. EMBO J *30*, 4142-4156.

Kawaguchi, Y., Kovacs, J.J., McLaurin, A., Vance, J.M., Ito, A., and Yao, T.-P. (2003). The Deacetylase HDAC6 Regulates Aggresome Formation and Cell Viability in Response to Misfolded Protein Stress. Cell *115*, 727-738.

Kazantsev, A., Preisinger, E., Dranovsky, A., Goldgaber, D., and Housman, D. (1999). Insoluble detergent-resistant aggregates form between pathological and nonpathological lengths of polyglutamine in mammalian cells. Proc Natl Acad Sci U S A *96*, 11404-11409.

Kegel, K.B., Kim, M., Sapp, E., McIntyre, C., Castano, J.G., Aronin, N., and DiFiglia, M. (2000). Huntingtin expression stimulates endosomal-lysosomal activity, endosome tubulation, and autophagy. J Neurosci *20*, 7268-7278.

Kegel, K.B., Meloni, A.R., Yi, Y., Kim, Y.J., Doyle, E., Cuiffo, B.G., Sapp, E., Wang, Y., Qin, Z.H., Chen, J.D.*, et al.* (2002). Huntingtin is present in the nucleus, interacts with the transcriptional corepressor C-terminal binding protein, and represses transcription. J Biol Chem *277*, 7466-7476.

Kim, M.O., Chawla, P., Overland, R.P., Xia, E., Sadri-Vakili, G., and Cha, J.H. (2008). Altered histone monoubiquitylation mediated by mutant huntingtin induces transcriptional dysregulation. J Neurosci *28*, 3947-3957.

Ko, J., Ou, S., and Patterson, P.H. (2001). New anti-huntingtin monoclonal antibodies: implications for huntingtin conformation and its binding proteins. Brain Res Bull *56*, 319-329.

Komatsu, M., Waguri, S., Chiba, T., Murata, S., Iwata, J., Tanida, I., Ueno, T., Koike, M., Uchiyama, Y., Kominami, E.*, et al.* (2006). Loss of autophagy in the central nervous system causes neurodegeneration in mice. Nature *441*, 880-884.

Kotian, S., Liyanarachchi, S., Zelent, A., and Parvin, J.D. (2011). Histone deacetylases 9 and 10 are required for homologous recombination. J Biol Chem *286*, 7722-7726.

Kouzarides, T. (2000). Acetylation: a regulatory modification to rival phosphorylation? EMBO J *19*, 1176-1179.

Kovacs, J.J., Murphy, P.J., Gaillard, S., Zhao, X., Wu, J.T., Nicchitta, C.V., Yoshida, M., Toft, D.O., Pratt, W.B., and Yao, T.P. (2005). HDAC6 regulates Hsp90 acetylation and chaperone-dependent activation of glucocorticoid receptor. Mol Cell *18*, 601-607.

Kuhn, A., Goldstein, D.R., Hodges, A., Strand, A.D., Sengstag, T., Kooperberg, C., Becanovic, K., Pouladi, M.A., Sathasivam, K., Cha, J.H.*, et al.* (2007). Mutant huntingtin's effects on striatal gene expression in mice recapitulate changes observed in human Huntington's disease brain and do not differ with mutant huntingtin length or wild-type huntingtin dosage. Hum Mol Genet *16*, 1845-1861.

Kwon, S., Zhang, Y., and Matthias, P. (2007). The deacetylase HDAC6 is a novel critical component of stress granules involved in the stress response. Genes Dev *21*, 3381-3394.

L'Hernault, S.W., and Rosenbaum, J.L. (1983). Chlamydomonas alpha-tubulin is posttranslationally modified in the flagella during flagellar assembly. The Journal of Cell Biology *97*, 258-263.

Labbadia, J., Cunliffe, H., Weiss, A., Katsyuba, E., Sathasivam, K., Seredenina, T., Woodman, B., Moussaoui, S., Frentzel, S., Luthi-Carter, R.*, et al.* (2011). Altered chromatin architecture underlies progressive impairment of the heat shock response in mouse models of Huntington disease. J Clin Invest *121*, 3306-3319.

Labbadia, J., Novoselov, S.S., Bett, J.S., Weiss, A., Paganetti, P., Bates, G.P., and Cheetham, M.E. (2012). Suppression of protein aggregation by chaperone modification of high molecular weight complexes. Brain.

Lakhani, V.V., Ding, F., and Dokholyan, N.V. (2010). Polyglutamine induced misfolding of huntingtin exon1 is modulated by the flanking sequences. PLoS Comput Biol *6*, e1000772.

Lalic, N.M., Maric, J., Svetel, M., Jotic, A., Stefanova, E., Lalic, K., Dragasevic, N., Milicic, T., Lukic, L., and Kostic, V.S. (2008). Glucose homeostasis in Huntington disease: abnormalities in insulin sensitivity and early-phase insulin secretion. Arch Neurol *65*, 476-480.

Landles, C., Sathasivam, K., Weiss, A., Woodman, B., Moffitt, H., Finkbeiner, S., Sun, B., Gafni, J., Ellerby, L.M., Trottier, Y.*, et al.* (2010). Proteolysis of mutant huntingtin produces an exon 1 fragment that accumulates as an aggregated protein in neuronal nuclei in Huntington disease. J Biol Chem *285*, 8808-8823.

Lanska, D.J., Lavine, L., Lanska, M.J., and Schoenberg, B.S. (1988). Huntington's disease mortality in the United States. Neurology *38*, 769-772.

Leavitt, B.R., van Raamsdonk, J.M., Shehadeh, J., Fernandes, H., Murphy, Z., Graham, R.K., Wellington, C.L., Raymond, L.A., and Hayden, M.R. (2006). Wild-type huntingtin protects neurons from excitotoxicity. J Neurochem *96*, 1121-1129.

Lee, D.Y., Hayes, J.J., Pruss, D., and Wolffe, A.P. (1993). A positive role for histone acetylation in transcription factor access to nucleosomal DNA. Cell *72*, 73-84.

Lee, J.Y., Koga, H., Kawaguchi, Y., Tang, W., Wong, E., Gao, Y.S., Pandey, U.B., Kaushik, S., Tresse, E., Lu, J.*, et al.* (2010). HDAC6 controls autophagosome maturation essential for ubiquitin-selective quality-control autophagy. EMBO J *29*, 969-980.

Legleiter, J., Mitchell, E., Lotz, G.P., Sapp, E., Ng, C., DiFiglia, M., Thompson, L.M., and Muchowski, P.J. (2010). Mutant huntingtin fragments form oligomers in a polyglutamine length-dependent manner in vitro and in vivo. J Biol Chem *285*, 14777-14790.

Li, H., Li, S.H., Yu, Z.X., Shelbourne, P., and Li, X.J. (2001). Huntingtin aggregate-associated axonal degeneration is an early pathological event in Huntington's disease mice. J Neurosci *21*, 8473-8481.

Li, S.H., Cheng, A.L., Zhou, H., Lam, S., Rao, M., Li, H., and Li, X.J. (2002). Interaction of Huntington disease protein with transcriptional activator Sp1. Mol Cell Biol *22*, 1277-1287.

Li, S.H., Schilling, G., Young, W.S., 3rd, Li, X.J., Margolis, R.L., Stine, O.C., Wagster, M.V., Abbott, M.H., Franz, M.L., Ranen, N.G.*, et al.* (1993). Huntington's disease gene (IT15) is widely expressed in human and rat tissues. Neuron *11*, 985-993.

Li, W., Zhang, B., Tang, J., Cao, Q., Wu, Y., Wu, C., Guo, J., Ling, E.A., and Liang, F. (2007). Sirtuin 2, a mammalian homolog of yeast silent information regulator-2 longevity regulator, is an oligodendroglial protein that decelerates cell differentiation through deacetylating alpha-tubulin. J Neurosci *27*, 2606-2616.

Li, X., and Kazgan, N. (2011). Mammalian sirtuins and energy metabolism. Int J Biol Sci *7*, 575-587.

Li, Y., Zhang, X., Polakiewicz, R.D., Yao, T.P., and Comb, M.J. (2008). HDAC6 is required for epidermal growth factor-induced beta-catenin nuclear localization. J Biol Chem *283*, 12686-12690.

Liang, Z., Shi, T., Ouyang, S., Li, H., Yu, K., Zhu, W., Luo, C., and Jiang, H. (2010). Investigation of the catalytic mechanism of Sir2 enzyme with QM/MM approach: SN1 vs SN2? J Phys Chem B *114*, 11927-11933.

Lievens, J.C., Woodman, B., Mahal, A., Spasic-Boscovic, O., Samuel, D., Kerkerian-Le Goff, L., and Bates, G.P. (2001). Impaired glutamate uptake in the R6 Huntington's disease transgenic mice. Neurobiol Dis *8*, 807-821.

Lin, C.H., Tallaksen-Greene, S., Chien, W.M., Cearley, J.A., Jackson, W.S., Crouse, A.B., Ren, S., Li, X.J., Albin, R.L., and Detloff, P.J. (2001). Neurological abnormalities in a knock-in mouse model of Huntington's disease. Hum Mol Genet *10*, 137-144.

Lione, L.A., Carter, R.J., Hunt, M.J., Bates, G.P., Morton, A.J., and Dunnett, S.B. (1999). Selective discrimination learning impairments in mice expressing the human Huntington's disease mutation. J Neurosci *19*, 10428-10437.

Lonze, B.E., and Ginty, D.D. (2002). Function and regulation of CREB family transcription factors in the nervous system. Neuron *35*, 605-623.

Lunkes, A., Lindenberg, K.S., Ben-Haiem, L., Weber, C., Devys, D., Landwehrmeyer, G.B., Mandel, J.L., and Trottier, Y. (2002). Proteases acting on mutant huntingtin generate cleaved products that differentially build up cytoplasmic and nuclear inclusions. Mol Cell *10*, 259-269.

Luo, S., Vacher, C., Davies, J.E., and Rubinsztein, D.C. (2005). Cdk5 phosphorylation of huntingtin reduces its cleavage by caspases: implications for mutant huntingtin toxicity. J Cell Biol *169*, 647-656.

Luthi-Carter, R., Hanson, S.A., Strand, A.D., Bergstrom, D.A., Chun, W., Peters, N.L., Woods, A.M., Chan, E.Y., Kooperberg, C., Krainc, D.*, et al.* (2002). Dysregulation of gene expression in the R6/2 model of polyglutamine disease: parallel changes in muscle and brain. Hum Mol Genet *11*, 1911-1926.

Luthi-Carter, R., Strand, A., Peters, N.L., Solano, S.M., Hollingsworth, Z.R., Menon, A.S., Frey, A.S., Spektor, B.S., Penney, E.B., Schilling, G.*, et al.* (2000). Decreased expression of striatal signaling genes in a mouse model of Huntington's disease. Hum Mol Genet *9*, 1259-1271.

Luthi-Carter, R., Taylor, D.M., Pallos, J., Lambert, E., Amore, A., Parker, A., Moffitt, H., Smith, D.L., Runne, H., Gokce, O.*, et al.* (2010). SIRT2 inhibition achieves neuroprotection by decreasing sterol biosynthesis. Proc Natl Acad Sci U S A *107*, 7927-7932.

Mahlknecht, U., Schnittger, S., Landgraf, F., Schoch, C., Ottmann, O.G., Hiddemann, W., and Hoelzer, D. (2001). Assignment of the human histone deacetylase 6 gene (HDAC6) to X chromosome p11.23 by in situ hybridization. Cytogenet Cell Genet *93*, 135-136.

Mangiarini, L., Sathasivam, K., Seller, M., Cozens, B., Harper, A., Hetherington, C., Lawton, M., Trottier, Y., Lehrach, H., Davies, S.W.*, et al.* (1996). Exon 1 of the HD gene with an expanded CAG repeat is sufficient to cause a progressive neurological phenotype in transgenic mice. Cell *87*, 493-506.

Markianos, M., Panas, M., Kalfakis, N., and Vassilopoulos, D. (2005). Plasma testosterone in male patients with Huntington's disease: relations to severity of illness and dementia. Ann Neurol *57*, 520-525.

Martindale, D., Hackam, A., Wieczorek, A., Ellerby, L., Wellington, C., McCutcheon, K., Singaraja, R., Kazemi-Esfarjani, P., Devon, R., Kim, S.U.*, et al.* (1998). Length of huntingtin and its polyglutamine tract influences localization and frequency of intracellular aggregates. Nat Genet *18*, 150-154.

Martinez-Vicente, M., Talloczy, Z., Wong, E., Tang, G., Koga, H., Kaushik, S., de Vries, R., Arias, E., Harris, S., Sulzer, D.*, et al.* (2010). Cargo recognition failure is responsible for inefficient autophagy in Huntington's disease. Nat Neurosci *13*, 567-576.

Matsuyama, A., Shimazu, T., Sumida, Y., Saito, A., Yoshimatsu, Y., Seigneurin-Berny, D., Osada, H., Komatsu, Y., Nishino, N., Khochbin, S.*, et al.* (2002). In vivo destabilization of dynamic microtubules by HDAC6-mediated deacetylation. EMBO J *21*, 6820-6831.

Matthias, P., Yoshida, M., and Khochbin, S. (2008). HDAC6 a new cellular stress surveillance factor. Cell Cycle *7*, 7-10.

Maxwell, M.M., Tomkinson, E.M., Nobles, J., Wizeman, J.W., Amore, A.M., Quinti, L., Chopra, V., Hersch, S.M., and Kazantsev, A.G. (2011). The Sirtuin 2 microtubule deacetylase is an abundant neuronal protein that accumulates in the aging CNS. Hum Mol Genet *20*, 3986-3996.

Maynard, C.J., Bottcher, C., Ortega, Z., Smith, R., Florea, B.I., Diaz-Hernandez, M., Brundin, P., Overkleeft, H.S., Li, J.Y., Lucas, J.J*., et al.* (2009). Accumulation of ubiquitin conjugates in a polyglutamine disease model occurs without global ubiquitin/proteasome system impairment. Proc Natl Acad Sci U S A *106*, 13986-13991.

McKinsey, T.A., Zhang, C.L., and Olson, E.N. (2000). Activation of the myocyte enhancer factor-2 transcription factor by calcium/calmodulin-dependent protein kinase-stimulated binding of 14-3-3 to histone deacetylase 5. Proceedings of the National Academy of Sciences *97*, 14400-14405.

Menalled, L.B., Sison, J.D., Dragatsis, I., Zeitlin, S., and Chesselet, M.F. (2003). Time course of early motor and neuropathological anomalies in a knock-in mouse model of Huntington's disease with 140 CAG repeats. J Comp Neurol *465*, 11-26.

Mestre, T., Ferreira, J., Coelho, M.M., Rosa, M., and Sampaio, C. (2009). Therapeutic interventions for disease progression in Huntington's disease. Cochrane Database Syst Rev, CD006455.

Mielcarek, M., Benn, C.L., Franklin, S.A., Smith, D.L., Woodman, B., Marks, P.A., and Bates, G.P. (2011). SAHA decreases HDAC 2 and 4 levels in vivo and improves molecular phenotypes in the R6/2 mouse model of Huntington's disease. PLoS One *6*, e27746.

Milakovic, T., Quintanilla, R.A., and Johnson, G.V. (2006). Mutant huntingtin expression induces mitochondrial calcium handling defects in clonal striatal cells: functional consequences. J Biol Chem *281*, 34785-34795.

Miller, J., Arrasate, M., Brooks, E., Libeu, C.P., Legleiter, J., Hatters, D., Curtis, J., Cheung, K., Krishnan, P., Mitra, S*., et al.* (2011). Identifying polyglutamine protein species in situ that best predict neurodegeneration. Nat Chem Biol *7*, 925-934.

Miller, J.P., Holcomb, J., Al-Ramahi, I., de Haro, M., Gafni, J., Zhang, N., Kim, E., Sanhueza, M., Torcassi, C., Kwak, S*., et al.* (2010). Matrix metalloproteinases are modifiers of huntingtin proteolysis and toxicity in Huntington's disease. Neuron *67*, 199-212.

Milnerwood, A.J., Gladding, C.M., Pouladi, M.A., Kaufman, A.M., Hines, R.M., Boyd, J.D., Ko, R.W., Vasuta, O.C., Graham, R.K., Hayden, M.R*., et al.* (2010). Early increase in extrasynaptic NMDA receptor signaling and expression contributes to phenotype onset in Huntington's disease mice. Neuron *65*, 178-190.

Modregger, J., DiProspero, N.A., Charles, V., Tagle, D.A., and Plomann, M. (2002). PACSIN 1 interacts with huntingtin and is absent from synaptic varicosities in presymptomatic Huntington's disease brains. Hum Mol Genet *11*, 2547-2558.

Moffitt, H., McPhail, G.D., Woodman, B., Hobbs, C., and Bates, G.P. (2009). Formation of polyglutamine inclusions in a wide range of non-CNS tissues in the HdhQ150 knock-in mouse model of Huntington's disease. PLoS One *4*, e8025.

Morton, A.J., and Edwardson, J.M. (2001). Progressive depletion of complexin II in a transgenic mouse model of Huntington's disease. J Neurochem *76*, 166-172.

Morton, A.J., Faull, R.L., and Edwardson, J.M. (2001). Abnormalities in the synaptic vesicle fusion machinery in Huntington's disease. Brain Res Bull *56*, 111-117.

Mostoslavsky, R., Chua, K.F., Lombard, D.B., Pang, W.W., Fischer, M.R., Gellon, L., Liu, P., Mostoslavsky, G., Franco, S., Murphy, M.M*., et al.* (2006). Genomic instability and aging-like phenotype in the absence of mammalian SIRT6. Cell *124*, 315-329.

Muchowski, P.J., and Wacker, J.L. (2005). Modulation of neurodegeneration by molecular chaperones. Nat Rev Neurosci *6*, 11-22.

Munshi, N., Merika, M., Yie, J., Senger, K., Chen, G., and Thanos, D. (1998). Acetylation of HMG I(Y) by CBP turns off IFN beta expression by disrupting the enhanceosome. Mol Cell *2*, 457-467.

Murphy, P.J., Morishima, Y., Kovacs, J.J., Yao, T.P., and Pratt, W.B. (2005). Regulation of the dynamics of hsp90 action on the glucocorticoid receptor by acetylation/deacetylation of the chaperone. J Biol Chem *280*, 33792-33799.

Nagy, Z., and Tora, L. (2007). Distinct GCN5/PCAF-containing complexes function as co-activators and are involved in transcription factor and global histone acetylation. Oncogene *26*, 5341-5357.

Nasir, J., Floresco, S.B., O'Kusky, J.R., Diewert, V.M., Richman, J.M., Zeisler, J., Borowski, A., Marth, J.D., Phillips, A.G., and Hayden, M.R. (1995). Targeted disruption of the Huntington's disease gene results in embryonic lethality and behavioral and morphological changes in heterozygotes. Cell *81*, 811-823.

Nicholls, D.G. (2009). Mitochondrial calcium function and dysfunction in the central nervous system. Biochim Biophys Acta *1787*, 1416-1424.

Nie, H., Chen, H., Han, J., Hong, Y., Ma, Y., Xia, W., and Ying, W. (2011). Silencing of SIRT2 induces cell death and a decrease in the intracellular ATP level of PC12 cells. Int J Physiol Pathophysiol Pharmacol *3*, 65-70.

Nishikori, S., Yamanaka, K., Sakurai, T., Esaki, M., and Ogura, T. (2008). p97 Homologs from Caenorhabditis elegans, CDC-48.1 and CDC-48.2, suppress the aggregate formation of huntingtin exon1 containing expanded polyQ repeat. Genes Cells *13*, 827-838.

North, B.J., Marshall, B.L., Borra, M.T., Denu, J.M., and Verdin, E. (2003). The human Sir2 ortholog, SIRT2, is an NAD+-dependent tubulin deacetylase. Mol Cell *11*, 437-444.

North, B.J., and Verdin, E. (2007). Interphase nucleo-cytoplasmic shuttling and localization of SIRT2 during mitosis. PLoS One *2*, e784.

Novak, M.J., and Tabrizi, S.J. (2010). Huntington's disease. BMJ *340*, c3109.

Nucifora, F.C., Jr., Sasaki, M., Peters, M.F., Huang, H., Cooper, J.K., Yamada, M., Takahashi, H., Tsuji, S., Troncoso, J., Dawson, V.L.*, et al.* (2001). Interference by huntingtin and atrophin-1 with cbp-mediated transcription leading to cellular toxicity. Science *291*, 2423-2428.

Ogura, M., Nakamura, Y., Tanaka, D., Zhuang, X., Fujita, Y., Obara, A., Hamasaki, A., Hosokawa, M., and Inagaki, N. (2010). Overexpression of SIRT5 confirms its involvement in deacetylation and activation of carbamoyl phosphate synthetase 1. Biochem Biophys Res Commun *393*, 73-78.

Ohkawa, N., Sugisaki, S., Tokunaga, E., Fujitani, K., Hayasaka, T., Setou, M., and Inokuchi, K. (2008). N-acetyltransferase ARD1-NAT1 regulates neuronal dendritic development. Genes Cells *13*, 1171-1183.

Okumura, K., Mendoza, M., Bachoo, R.M., DePinho, R.A., Cavenee, W.K., and Furnari, F.B. (2006). PCAF modulates PTEN activity. J Biol Chem *281*, 26562-26568.

Ordway, J.M., Tallaksen-Greene, S., Gutekunst, C.A., Bernstein, E.M., Cearley, J.A., Wiener, H.W., Dure, L.S.t., Lindsey, R., Hersch, S.M., Jope, R.S*., et al.* (1997). Ectopically expressed CAG repeats cause intranuclear inclusions and a progressive late onset neurological phenotype in the mouse. Cell *91*, 753-763.

Outeiro, T.F., Kontopoulos, E., Altmann, S.M., Kufareva, I., Strathearn, K.E., Amore, A.M., Volk, C.B., Maxwell, M.M., Rochet, J.C., McLean, P.J*., et al.* (2007). Sirtuin 2 inhibitors rescue alpha-synuclein-mediated toxicity in models of Parkinson's disease. Science *317*, 516-519.

Palazzo, A., Ackerman, B., and Gundersen, G.G. (2003). Cell biology: Tubulin acetylation and cell motility. Nature *421*, 230.

Pallos, J., Bodai, L., Lukacsovich, T., Purcell, J.M., Steffan, J.S., Thompson, L.M., and Marsh, J.L. (2008). Inhibition of specific HDACs and sirtuins suppresses pathogenesis in a Drosophila model of Huntington's disease. Hum Mol Genet *17*, 3767-3775.

Pandey, U.B., Batlevi, Y., Baehrecke, E.H., and Taylor, J.P. (2007a). HDAC6 at the intersection of autophagy, the ubiquitin-proteasome system and neurodegeneration. Autophagy *3*, 643-645.

Pandey, U.B., Nie, Z., Batlevi, Y., McCray, B.A., Ritson, G.P., Nedelsky, N.B., Schwartz, S.L., DiProspero, N.A., Knight, M.A., Schuldiner, O*., et al.* (2007b). HDAC6 rescues neurodegeneration and provides an essential link between autophagy and the UPS. Nature *447*, 859-863.

Pandithage, R., Lilischkis, R., Harting, K., Wolf, A., Jedamzik, B., Luscher-Firzlaff, J., Vervoorts, J., Lasonder, E., Kremmer, E., Knoll, B*., et al.* (2008). The regulation of SIRT2 function by cyclin-dependent kinases affects cell motility. J Cell Biol *180*, 915-929.

Panov, A.V., Gutekunst, C.A., Leavitt, B.R., Hayden, M.R., Burke, J.R., Strittmatter, W.J., and Greenamyre, J.T. (2002). Early mitochondrial calcium defects in Huntington's disease are a direct effect of polyglutamines. Nat Neurosci *5*, 731-736.

Peck, B., Chen, C.Y., Ho, K.K., Di Fruscia, P., Myatt, S.S., Coombes, R.C., Fuchter, M.J., Hsiao, C.D., and Lam, E.W. (2010). SIRT inhibitors induce cell death and p53 acetylation through targeting both SIRT1 and SIRT2. Mol Cancer Ther *9*, 844-855.

Perdiz, D., Mackeh, R., Poüs, C., and Baillet, A. (2011). The ins and outs of tubulin acetylation: More than just a post-translational modification? Cell Signal *23*, 763-771.

Perutz, M.F., Johnson, T., Suzuki, M., and Finch, J.T. (1994). Glutamine repeats as polar zippers: their possible role in inherited neurodegenerative diseases. Proc Natl Acad Sci U S A *91*, 5355-5358.

Petersen, A., Larsen, K.E., Behr, G.G., Romero, N., Przedborski, S., Brundin, P., and Sulzer, D. (2001). Expanded CAG repeats in exon 1 of the Huntington's disease gene stimulate dopamine-mediated striatal neuron autophagy and degeneration. Hum Mol Genet *10*, 1243-1254.

Politis, M., Pavese, N., Tai, Y.F., Tabrizi, S.J., Barker, R.A., and Piccini, P. (2008). Hypothalamic involvement in Huntington's disease: an in vivo PET study. Brain *131*, 2860-2869.

Ponugoti, B., Kim, D.H., Xiao, Z., Smith, Z., Miao, J., Zang, M., Wu, S.Y., Chiang, C.M., Veenstra, T.D., and Kemper, J.K. (2010). SIRT1 deacetylates and inhibits SREBP-1C activity in regulation of hepatic lipid metabolism. J Biol Chem *285*, 33959-33970.

Powers, E.T., Morimoto, R.I., Dillin, A., Kelly, J.W., and Balch, W.E. (2009). Biological and chemical approaches to diseases of proteostasis deficiency. Annu Rev Biochem *78*, 959-991.

Quinti, L., Chopra, V., Rotili, D., Valente, S., Amore, A., Franci, G., Meade, S., Valenza, M., Altucci, L., Maxwell, M.M*., et al.* (2010). Evaluation of histone deacetylases as drug targets in Huntington's disease models. Study of HDACs in brain tissues from R6/2 and CAG140 knock-in HD mouse models and human patients and in a neuronal HD cell model. PLoS Curr *2*.

Ravikumar, B., Vacher, C., Berger, Z., Davies, J.E., Luo, S., Oroz, L.G., Scaravilli, F., Easton, D.F., Duden, R., O'Kane, C.J*., et al.* (2004). Inhibition of mTOR induces autophagy and reduces toxicity of polyglutamine expansions in fly and mouse models of Huntington disease. Nat Genet *36*, 585-595.

Reed, N.A., Cai, D., Blasius, T.L., Jih, G.T., Meyhofer, E., Gaertig, J., and Verhey, K.J. (2006). Microtubule acetylation promotes kinesin-1 binding and transport. Curr Biol *16*, 2166-2172.

Richly, H., Rape, M., Braun, S., Rumpf, S., Hoege, C., and Jentsch, S. (2005). A series of ubiquitin binding factors connects CDC48/p97 to substrate multiubiquitylation and proteasomal targeting. Cell *120*, 73-84.

Rigamonti, D., Bauer, J.H., De-Fraja, C., Conti, L., Sipione, S., Sciorati, C., Clementi, E., Hackam, A., Hayden, M.R., Li, Y.*, et al.* (2000). Wild-type huntingtin protects from apoptosis upstream of caspase-3. J Neurosci *20*, 3705-3713.

Rosas, H.D., Hevelone, N.D., Zaleta, A.K., Greve, D.N., Salat, D.H., and Fischl, B. (2005). Regional cortical thinning in preclinical Huntington disease and its relationship to cognition. Neurology *65*, 745-747.

Rosas, H.D., Koroshetz, W.J., Chen, Y.I., Skeuse, C., Vangel, M., Cudkowicz, M.E., Caplan, K., Marek, K., Seidman, L.J., Makris, N.*, et al.* (2003). Evidence for more widespread cerebral pathology in early HD: an MRI-based morphometric analysis. Neurology *60*, 1615-1620.

Rudnicki, M.A., Schnegelsberg, P.N., Stead, R.H., Braun, T., Arnold, H.H., and Jaenisch, R. (1993). MyoD or Myf-5 is required for the formation of skeletal muscle. Cell *75*, 1351-1359.

Rumpf, S., and Jentsch, S. (2006). Functional division of substrate processing cofactors of the ubiquitin-selective Cdc48 chaperone. Mol Cell *21*, 261-269.

Ryu, H., Lee, J., Hagerty, S.W., Soh, B.Y., McAlpin, S.E., Cormier, K.A., Smith, K.M., and Ferrante, R.J. (2006). ESET/SETDB1 gene expression and histone H3 (K9) trimethylation in Huntington's disease. Proc Natl Acad Sci U S A *103*, 19176-19181.

Sadri-Vakili, G., Bouzou, B., Benn, C.L., Kim, M.O., Chawla, P., Overland, R.P., Glajch, K.E., Xia, E., Qiu, Z., Hersch, S.M.*, et al.* (2007). Histones associated with downregulated genes are hypo-acetylated in Huntington's disease models. Hum Mol Genet *16*, 1293-1306.

Saleh, N., Moutereau, S., Durr, A., Krystkowiak, P., Azulay, J.P., Tranchant, C., Broussolle, E., Morin, F., Bachoud-Levi, A.C., and Maison, P. (2009). Neuroendocrine disturbances in Huntington's disease. PLoS One *4*, e4962.

Sanberg, P.R., Fibiger, H.C., and Mark, R.F. (1981). Body weight and dietary factors in Huntington's disease patients compared with matched controls. Med J Aust *1*, 407-409.

Sapp, E., Schwarz, C., Chase, K., Bhide, P.G., Young, A.B., Penney, J., Vonsattel, J.P., Aronin, N., and DiFiglia, M. (1997). Huntingtin localization in brains of normal and Huntington's disease patients. Ann Neurol *42*, 604-612.

Sathasivam, K., Hobbs, C., Turmaine, M., Mangiarini, L., Mahal, A., Bertaux, F., Wanker, E.E., Doherty, P., Davies, S.W., and Bates, G.P. (1999). Formation of polyglutamine inclusions in non-CNS tissue. Hum Mol Genet *8*, 813-822.

Sathasivam, K., Lane, A., Legleiter, J., Warley, A., Woodman, B., Finkbeiner, S., Paganetti, P., Muchowski, P.J., Wilson, S., and Bates, G.P. (2010). Identical oligomeric and fibrillar structures captured from the brains of R6/2 and knock-in mouse models of Huntington's disease. Hum Mol Genet *19*, 65-78.

Sathasivam, K., Woodman, B., Mahal, A., Bertaux, F., Wanker, E.E., Shima, D.T., and Bates, G.P. (2001). Centrosome disorganization in fibroblast cultures derived from R6/2 Huntington's disease (HD) transgenic mice and HD patients. Hum Mol Genet *10*, 2425-2435.

Schaffar, G., Breuer, P., Boteva, R., Behrends, C., Tzvetkov, N., Strippel, N., Sakahira, H., Siegers, K., Hayer-Hartl, M., and Hartl, F.U. (2004). Cellular toxicity of polyglutamine expansion proteins: mechanism of transcription factor deactivation. Mol Cell *15*, 95-105.

Scherzinger, E., Lurz, R., Turmaine, M., Mangiarini, L., Hollenbach, B., Hasenbank, R., Bates, G.P., Davies, S.W., Lehrach, H., and Wanker, E.E. (1997). Huntingtin-encoded polyglutamine expansions form amyloid-like protein aggregates in vitro and in vivo. Cell *90*, 549-558.

Scherzinger, E., Sittler, A., Schweiger, K., Heiser, V., Lurz, R., Hasenbank, R., Bates, G.P., Lehrach, H., and Wanker, E.E. (1999). Self-assembly of polyglutamine-containing huntingtin fragments into amyloid-like fibrils: implications for Huntington's disease pathology. Proc Natl Acad Sci U S A *96*, 4604-4609.

Schiefer, J., Landwehrmeyer, G.B., Luesse, H.G., Sprunken, A., Puls, C., Milkereit, A., Milkereit, E., and Kosinski, C.M. (2002). Riluzole prolongs survival time and alters nuclear inclusion formation in a transgenic mouse model of Huntington's disease. Mov Disord *17*, 748-757.

Schilling, B., Gafni, J., Torcassi, C., Cong, X., Row, R.H., LaFevre-Bernt, M.A., Cusack, M.P., Ratovitski, T., Hirschhorn, R., Ross, C.A.*, et al.* (2006). Huntingtin phosphorylation sites mapped by mass spectrometry. Modulation of cleavage and toxicity. J Biol Chem *281*, 23686-23697.

Schilling, G., Becher, M.W., Sharp, A.H., Jinnah, H.A., Duan, K., Kotzuk, J.A., Slunt, H.H., Ratovitski, T., Cooper, J.K., Jenkins, N.A.*, et al.* (1999). Intranuclear inclusions and neuritic aggregates in transgenic mice expressing a mutant N-terminal fragment of huntingtin. Hum Mol Genet *8*, 397-407.

Schmidt-Kastner, R., Wetmore, C., and Olson, L. (1996). Comparative study of brain-derived neurotrophic factor messenger RNA and protein at the cellular level suggests multiple roles in hippocampus, striatum and cortex. Neuroscience *74*, 161-183.

Schwarcz, R., Whetsell, W.O., Jr., and Mangano, R.M. (1983). Quinolinic acid: an endogenous metabolite that produces axon-sparing lesions in rat brain. Science *219*, 316-318.

Seigneurin-Berny, D., Verdel, A., Curtet, S., Lemercier, C., Garin, J., Rousseaux, S., and Khochbin, S. (2001). Identification of components of the murine histone deacetylase 6 complex: link between acetylation and ubiquitination signaling pathways. Mol Cell Biol *21*, 8035-8044.

Seo, H., Kim, W., and Isacson, O. (2008). Compensatory changes in the ubiquitin-proteasome system, brain-derived neurotrophic factor and mitochondrial complex II/III in YAC72 and R6/2 transgenic mice partially model Huntington's disease patients. Hum Mol Genet *17*, 3144-3153.

Seo, H., Sonntag, K.C., and Isacson, O. (2004). Generalized brain and skin proteasome inhibition in Huntington's disease. Ann Neurol *56*, 319-328.

Serrador, J.M., Cabrero, J.R., Sancho, D., Mittelbrunn, M., Urzainqui, A., and Sanchez-Madrid, F. (2004). HDAC6 deacetylase activity links the tubulin cytoskeleton with immune synapse organization. Immunity *20*, 417-428.

Shimazu, T., Horinouchi, S., and Yoshida, M. (2007). Multiple histone deacetylases and the CREB-binding protein regulate pre-mRNA 3'-end processing. J Biol Chem *282*, 4470-4478.

Sivanandam, V.N., Jayaraman, M., Hoop, C.L., Kodali, R., Wetzel, R., and van der Wel, P.C. (2011). The aggregation-enhancing huntingtin N-terminus is helical in amyloid fibrils. J Am Chem Soc *133*, 4558-4566.

Slow, E.J., van Raamsdonk, J., Rogers, D., Coleman, S.H., Graham, R.K., Deng, Y., Oh, R., Bissada, N., Hossain, S.M., Yang, Y.Z*., et al.* (2003). Selective striatal neuronal loss in a YAC128 mouse model of Huntington disease. Hum Mol Genet *12*, 1555-1567.

Spires, T.L., Grote, H.E., Varshney, N.K., Cordery, P.M., van Dellen, A., Blakemore, C., and Hannan, A.J. (2004). Environmental Enrichment Rescues Protein Deficits in a Mouse Model of Huntington's Disease, Indicating a Possible Disease Mechanism. The Journal of Neuroscience *24*, 2270-2276.

Steffan, J.S., Agrawal, N., Pallos, J., Rockabrand, E., Trotman, L.C., Slepko, N., Illes, K., Lukacsovich, T., Zhu, Y.Z., Cattaneo, E*., et al.* (2004). SUMO modification of Huntingtin and Huntington's disease pathology. Science *304*, 100-104.

Steffan, J.S., Bodai, L., Pallos, J., Poelman, M., McCampbell, A., Apostol, B.L., Kazantsev, A., Schmidt, E., Zhu, Y.Z., Greenwald, M*., et al.* (2001). Histone deacetylase inhibitors arrest polyglutamine-dependent neurodegeneration in Drosophila. Nature *413*, 739-743.

Steffan, J.S., Kazantsev, A., Spasic-Boskovic, O., Greenwald, M., Zhu, Y.Z., Gohler, H., Wanker, E.E., Bates, G.P., Housman, D.E., and Thompson, L.M. (2000). The Huntington's disease protein interacts with p53 and CREB-binding protein and represses transcription. Proc Natl Acad Sci U S A *97*, 6763-6768.

Sun, Y., Savanenin, A., Reddy, P.H., and Liu, Y.F. (2001). Polyglutamine-expanded huntingtin promotes sensitization of N-methyl-D-aspartate receptors via post-synaptic density 95. J Biol Chem *276*, 24713-24718.

Sun, Z., Wang, H.B., Deng, Y.P., Lei, W.L., Xie, J.P., Meade, C.A., Del Mar, N., Goldowitz, D., and Reiner, A. (2005). Increased calbindin-D28k immunoreactivity in striatal projection neurons of R6/2 Huntington's disease transgenic mice. Neurobiol Dis *20*, 907-917.

Suzuki, K., and Koike, T. (2007). Mammalian Sir2-related protein (SIRT) 2-mediated modulation of resistance to axonal degeneration in slow Wallerian degeneration mice: a crucial role of tubulin deacetylation. Neuroscience *147*, 599-612.

Tabrizi, S.J., and Schapira, A.H. (1999). Secondary abnormalities of mitochondrial DNA associated with neurodegeneration. Biochem Soc Symp *66*, 99-110.

Tarditi, A., Camurri, A., Varani, K., Borea, P.A., Woodman, B., Bates, G., Cattaneo, E., and Abbracchio, M.P. (2006). Early and transient alteration of adenosine A2A receptor signaling in a mouse model of Huntington disease. Neurobiol Dis *23*, 44-53.

Taylor, D.M., Balabadra, U., Xiang, Z., Woodman, B., Meade, S., Amore, A., Maxwell, M.M., Reeves, S., Bates, G.P., Luthi-Carter, R.*, et al.* (2011). A Brain-Permeable Small Molecule Reduces Neuronal Cholesterol by Inhibiting Activity of Sirtuin 2 Deacetylase. ACS Chem Biol *6*, 540-546.

Tebbenkamp, A.T., and Borchelt, D.R. (2010). Analysis of chaperone mRNA expression in the adult mouse brain by meta analysis of the Allen Brain Atlas. PLoS One *5*, e13675.

Thakur, A.K., Jayaraman, M., Mishra, R., Thakur, M., Chellgren, V.M., Byeon, I.J., Anjum, D.H., Kodali, R., Creamer, T.P., Conway, J.F.*, et al.* (2009). Polyglutamine disruption of the huntingtin exon 1 N terminus triggers a complex aggregation mechanism. Nat Struct Mol Biol *16*, 380-389.

The Huntington's Disease Collaborative Research Group (1993). A novel gene containing a trinucleotide repeat that is expanded and unstable on Huntington's disease chromosomes. Cell *72*, 971-983.

Thompson, L.M., Aiken, C.T., Kaltenbach, L.S., Agrawal, N., Illes, K., Khoshnan, A., Martinez-Vincente, M., Arrasate, M., O'Rourke, J.G., Khashwji, H.*, et al.* (2009). IKK phosphorylates Huntingtin and targets it for degradation by the proteasome and lysosome. J Cell Biol *187*, 1083-1099.

Tissenbaum, H.A., and Guarente, L. (2001). Increased dosage of a sir-2 gene extends lifespan in Caenorhabditis elegans. Nature *410*, 227-230.

Trushina, E., Singh, R.D., Dyer, R.B., Cao, S., Shah, V.H., Parton, R.G., Pagano, R.E., and McMurray, C.T. (2006). Mutant huntingtin inhibits clathrin-independent endocytosis and causes accumulation of cholesterol in vitro and in vivo. Hum Mol Genet *15*, 3578-3591.

Urani, A., and Gass, P. (2003). Corticosteroid Receptor Transgenic Mice. Ann N Y Acad Sci *1007*, 379-393.

Valenza, M., Carroll, J.B., Leoni, V., Bertram, L.N., Bjorkhem, I., Singaraja, R.R., Di Donato, S., Lutjohann, D., Hayden, M.R., and Cattaneo, E. (2007a). Cholesterol biosynthesis pathway is disturbed in YAC128 mice and is modulated by huntingtin mutation. Hum Mol Genet *16*, 2187-2198.

Valenza, M., and Cattaneo, E. (2011). Emerging roles for cholesterol in Huntington's disease. Trends Neurosci *34*, 474-486.

Valenza, M., Leoni, V., Karasinska, J.M., Petricca, L., Fan, J., Carroll, J., Pouladi, M.A., Fossale, E., Nguyen, H.P., Riess, O.*, et al.* (2010). Cholesterol defect is marked across multiple rodent models of Huntington's disease and is manifest in astrocytes. J Neurosci *30*, 10844-10850.

Valenza, M., Leoni, V., Tarditi, A., Mariotti, C., Bjorkhem, I., Di Donato, S., and Cattaneo, E. (2007b). Progressive dysfunction of the cholesterol biosynthesis pathway in the R6/2 mouse model of Huntington's disease. Neurobiol Dis *28*, 133-142.

Valenza, M., Rigamonti, D., Goffredo, D., Zuccato, C., Fenu, S., Jamot, L., Strand, A., Tarditi, A., Woodman, B., Racchi, M.*, et al.* (2005). Dysfunction of the cholesterol biosynthetic pathway in Huntington's disease. J Neurosci *25*, 9932-9939.

Valenzuela-Fernandez, A., Alvarez, S., Gordon-Alonso, M., Barrero, M., Ursa, A., Cabrero, J.R., Fernandez, G., Naranjo-Suarez, S., Yanez-Mo, M., Serrador, J.M.*, et al.* (2005). Histone deacetylase 6 regulates human immunodeficiency virus type 1 infection. Mol Biol Cell *16*, 5445-5454.

Van Raamsdonk, J.M., Murphy, Z., Selva, D.M., Hamidizadeh, R., Pearson, J., Petersen, A., Bjorkqvist, M., Muir, C., Mackenzie, I.R., Hammond, G.L.*, et al.* (2007). Testicular degeneration in Huntington disease. Neurobiol Dis *26*, 512-520.

Van Raamsdonk, J.M., Murphy, Z., Slow, E.J., Leavitt, B.R., and Hayden, M.R. (2005a). Selective degeneration and nuclear localization of mutant huntingtin in the YAC128 mouse model of Huntington disease. Hum Mol Genet *14*, 3823-3835.

Van Raamsdonk, J.M., Pearson, J., Slow, E.J., Hossain, S.M., Leavitt, B.R., and Hayden, M.R. (2005b). Cognitive dysfunction precedes neuropathology and motor abnormalities in the YAC128 mouse model of Huntington's disease. J Neurosci *25*, 4169-4180.

Vaquero, A., Scher, M.B., Lee, D.H., Sutton, A., Cheng, H.L., Alt, F.W., Serrano, L., Sternglanz, R., and Reinberg, D. (2006). SirT2 is a histone deacetylase with preference for histone H4 Lys 16 during mitosis. Genes Dev *20*, 1256-1261.

Vaquero, A., Sternglanz, R., and Reinberg, D. (2007). NAD+-dependent deacetylation of H4 lysine 16 by class III HDACs. Oncogene *26*, 5505-5520.

Velier, J., Kim, M., Schwarz, C., Kim, T.W., Sapp, E., Chase, K., Aronin, N., and DiFiglia, M. (1998). Wild-type and mutant huntingtins function in vesicle trafficking in the secretory and endocytic pathways. Exp Neurol *152*, 34-40.

Venkatraman, P., Wetzel, R., Tanaka, M., Nukina, N., and Goldberg, A.L. (2004). Eukaryotic proteasomes cannot digest polyglutamine sequences and release them during degradation of polyglutamine-containing proteins. Mol Cell *14*, 95-104.

Verdin, E., Dequiedt, F., and Kasler, H.G. (2003). Class II histone deacetylases: versatile regulators. Trends in Genetics *19*, 286-293.

Voelter-Mahlknecht, S., and Mahlknecht, U. (2003). Cloning and structural characterization of the human histone deacetylase 6 gene. Int J Mol Med *12*, 87-93.

von Horsten, S., Schmitt, I., Nguyen, H.P., Holzmann, C., Schmidt, T., Walther, T., Bader, M., Pabst, R., Kobbe, P., Krotova, J.*, et al.* (2003). Transgenic rat model of Huntington's disease. Hum Mol Genet *12*, 617-624.

Vonsattel, J.P., and DiFiglia, M. (1998). Huntington disease. J Neuropathol Exp Neurol *57*, 369-384.

Vonsattel, J.P., Myers, R.H., Stevens, T.J., Ferrante, R.J., Bird, E.D., and Richardson, E.P., Jr. (1985). Neuropathological classification of Huntington's disease. J Neuropathol Exp Neurol *44*, 559-577.

Wacker, J.L., Zareie, M.H., Fong, H., Sarikaya, M., and Muchowski, P.J. (2004). Hsp70 and Hsp40 attenuate formation of spherical and annular polyglutamine oligomers by partitioning monomer. Nat Struct Mol Biol *11*, 1215-1222.

Walker, F.O. (2007). Huntington's disease. The Lancet *369*, 218-228.

Wang, C.E., Tydlacka, S., Orr, A.L., Yang, S.H., Graham, R.K., Hayden, M.R., Li, S., Chan, A.W., and Li, X.J. (2008a). Accumulation of N-terminal mutant huntingtin in mouse and monkey models implicated as a pathogenic mechanism in Huntington's disease. Hum Mol Genet *17*, 2738-2751.

Wang, F., Chan, C.H., Chen, K., Guan, X., Lin, H.K., and Tong, Q. (2011). Deacetylation of FOXO3 by SIRT1 or SIRT2 leads to Skp2-mediated FOXO3 ubiquitination and degradation. Oncogene.

Wang, F., Nguyen, M., Qin, F.X., and Tong, Q. (2007). SIRT2 deacetylates FOXO3a in response to oxidative stress and caloric restriction. Aging Cell *6*, 505-514.

Wang, F., and Tong, Q. (2009). SIRT2 suppresses adipocyte differentiation by deacetylating FOXO1 and enhancing FOXO1's repressive interaction with PPARgamma. Mol Biol Cell *20*, 801-808.

Wang, J., Wang, C.E., Orr, A., Tydlacka, S., Li, S.H., and Li, X.J. (2008b). Impaired ubiquitin-proteasome system activity in the synapses of Huntington's disease mice. J Cell Biol *180*, 1177-1189.

Wang, R.H., Sengupta, K., Li, C., Kim, H.S., Cao, L., Xiao, C., Kim, S., Xu, X., Zheng, Y., Chilton, B.*, et al.* (2008c). Impaired DNA damage response, genome instability, and tumorigenesis in SIRT1 mutant mice. Cancer Cell *14*, 312-323.

Warby, S.C., Doty, C.N., Graham, R.K., Shively, J., Singaraja, R.R., and Hayden, M.R. (2009). Phosphorylation of huntingtin reduces the accumulation of its nuclear fragments. Mol Cell Neurosci *40*, 121-127.

Warby, S.C., Visscher, H., Collins, J.A., Doty, C.N., Carter, C., Butland, S.L., Hayden, A.R., Kanazawa, I., Ross, C.J., and Hayden, M.R. (2011). HTT haplotypes contribute to differences in Huntington disease prevalence between Europe and East Asia. Eur J Hum Genet *19*, 561-566.

Waterham, H.R., Wijburg, F.A., Hennekam, R.C.M., Vreken, P., Poll-The, B.T., Dorland, L., Duran, M., Jira, P.E., Smeitink, J.A.M., Wevers, R.A.*, et al.* (1998). Smith-Lemli-Opitz Syndrome Is Caused by Mutations in the 7-Dehydrocholesterol Reductase Gene. American journal of human genetics *63*, 329-338.

Weiss, A., Abramowski, D., Bibel, M., Bodner, R., Chopra, V., DiFiglia, M., Fox, J., Kegel, K., Klein, C., Grueninger, S.*, et al.* (2009). Single-step detection of mutant huntingtin in animal and human tissues: a bioassay for Huntington's disease. Anal Biochem *395*, 8-15.

Werner, H.B., Kuhlmann, K., Shen, S., Uecker, M., Schardt, A., Dimova, K., Orfaniotou, F., Dhaunchak, A., Brinkmann, B.G., Mobius, W.*, et al.* (2007). Proteolipid protein is required for transport of sirtuin 2 into CNS myelin. J Neurosci *27*, 7717-7730.

Westerheide, S.D., Anckar, J., Stevens, S.M., Jr., Sistonen, L., and Morimoto, R.I. (2009). Stress-inducible regulation of heat shock factor 1 by the deacetylase SIRT1. Science *323*, 1063-1066.

Wexler, N.S., Young, A.B., Tanzi, R.E., Travers, H., Starosta-Rubinstein, S., Penney, J.B., Snodgrass, S.R., Shoulson, I., Gomez, F., Ramos Arroyo, M.A.*, et al.* (1987). Homozygotes for Huntington's disease. Nature *326*, 194-197.

Wheeler, V.C., Auerbach, W., White, J.K., Srinidhi, J., Auerbach, A., Ryan, A., Duyao, M.P., Vrbanac, V., Weaver, M., Gusella, J.F.*, et al.* (1999). Length-dependent gametic CAG repeat instability in the Huntington's disease knock-in mouse. Hum Mol Genet *8*, 115-122.

Wheeler, V.C., White, J.K., Gutekunst, C.A., Vrbanac, V., Weaver, M., Li, X.J., Li, S.H., Yi, H., Vonsattel, J.P., Gusella, J.F.*, et al.* (2000). Long glutamine tracts cause nuclear localization of a novel form of huntingtin in medium spiny striatal neurons in HdhQ92 and HdhQ111 knock-in mice. Hum Mol Genet *9*, 503-513.

White, J.K., Auerbach, W., Duyao, M.P., Vonsattel, J.P., Gusella, J.F., Joyner, A.L., and MacDonald, M.E. (1997). Huntingtin is required for neurogenesis and is not impaired by the Huntington's disease CAG expansion. Nat Genet *17*, 404-410.

Williams, A.J., and Paulson, H.L. (2008). Polyglutamine neurodegeneration: protein misfolding revisited. Trends Neurosci *31*, 521-528.

Woodman, B., Butler, R., Landles, C., Lupton, M.K., Tse, J., Hockly, E., Moffitt, H., Sathasivam, K., and Bates, G.P. (2007). The Hdh(Q150/Q150) knock-in mouse model of HD and the R6/2 exon 1 model develop comparable and widespread molecular phenotypes. Brain Res Bull *72*, 83-97.

Xie, Y., Hayden, M.R., and Xu, B. (2010). BDNF overexpression in the forebrain rescues Huntington's disease phenotypes in YAC128 mice. J Neurosci *30*, 14708-14718.

Yanai, A., Huang, K., Kang, R., Singaraja, R.R., Arstikaitis, P., Gan, L., Orban, P.C., Mullard, A., Cowan, C.M., Raymond, L.A.*, et al.* (2006). Palmitoylation of huntingtin by HIP14 is essential for its trafficking and function. Nat Neurosci *9*, 824-831.

Yang, D., Wang, C.E., Zhao, B., Li, W., Ouyang, Z., Liu, Z., Yang, H., Fan, P., O'Neill, A., Gu, W.*, et al.* (2010). Expression of Huntington's disease protein results in apoptotic neurons in the brains of cloned transgenic pigs. Hum Mol Genet *19*, 3983-3994.

Yang, S.H., Cheng, P.H., Banta, H., Piotrowska-Nitsche, K., Yang, J.J., Cheng, E.C., Snyder, B., Larkin, K., Liu, J., Orkin, J.*, et al.* (2008). Towards a transgenic model of Huntington's disease in a non-human primate. Nature *453*, 921-924.

Yang, W.M., Tsai, S.C., Wen, Y.D., Fejer, G., and Seto, E. (2002). Functional domains of histone deacetylase-3. J Biol Chem *277*, 9447-9454.

Yang, X.-J., and Seto, E. (2008). The Rpd3/Hda1 family of lysine deacetylases: from bacteria and yeast to mice and men. Nat Rev Mol Cell Biol *9*, 206-218.

Yang, X.J., and Gregoire, S. (2005). Class II histone deacetylases: from sequence to function, regulation, and clinical implication. Mol Cell Biol *25*, 2873-2884.

Yang, Y., Hou, H., Haller, E.M., Nicosia, S.V., and Bai, W. (2005). Suppression of FOXO1 activity by FHL2 through SIRT1-mediated deacetylation. EMBO J *24*, 1021-1032.

Yang, Y.H., Chen, Y.H., Zhang, C.Y., Nimmakayalu, M.A., Ward, D.C., and Weissman, S. (2000). Cloning and characterization of two mouse genes with homology to the yeast Sir2 gene. Genomics *69*, 355-369.

Yohrling, G.J., Farrell, L.A., Hollenberg, A.N., and Cha, J.H. (2003). Mutant huntingtin increases nuclear corepressor function and enhances ligand-dependent nuclear hormone receptor activation. Mol Cell Neurosci *23*, 28-38.

Yuan, Z., Zhang, X., Sengupta, N., Lane, W.S., and Seto, E. (2007). SIRT1 regulates the function of the Nijmegen breakage syndrome protein. Mol Cell *27*, 149-162.

Zala, D., Colin, E., Rangone, H., Liot, G., Humbert, S., and Saudou, F. (2008). Phosphorylation of mutant huntingtin at S421 restores anterograde and retrograde transport in neurons. Hum Mol Genet *17*, 3837-3846.

Zeitlin, S., Liu, J.P., Chapman, D.L., Papaioannou, V.E., and Efstratiadis, A. (1995). Increased apoptosis and early embryonic lethality in mice nullizygous for the Huntington's disease gene homologue. Nat Genet *11*, 155-163.

Zeron, M.M., Hansson, O., Chen, N., Wellington, C.L., Leavitt, B.R., Brundin, P., Hayden, M.R., and Raymond, L.A. (2002). Increased sensitivity to N-methyl-D-aspartate receptor-mediated excitotoxicity in a mouse model of Huntington's disease. Neuron *33*, 849-860.

Zhai, W., Jeong, H., Cui, L., Krainc, D., and Tjian, R. (2005). In vitro analysis of huntingtin-mediated transcriptional repression reveals multiple transcription factor targets. Cell *123*, 1241-1253.

Zhang, X., Yuan, Z., Zhang, Y., Yong, S., Salas-Burgos, A., Koomen, J., Olashaw, N., Parsons, J.T., Yang, X.J., Dent, S.R.*, et al.* (2007). HDAC6 modulates cell motility by altering the acetylation level of cortactin. Mol Cell *27*, 197-213.

Zhang, Y., Gilquin, B., Khochbin, S., and Matthias, P. (2006). Two catalytic domains are required for protein deacetylation. J Biol Chem *281*, 2401-2404.

Zhang, Y., Kwon, S., Yamaguchi, T., Cubizolles, F., Rousseaux, S., Kneissel, M., Cao, C., Li, N., Cheng, H.L., Chua, K.*, et al.* (2008). Mice lacking histone deacetylase 6 have hyperacetylated tubulin but are viable and develop normally. Mol Cell Biol *28*, 1688-1701.

Zhang, Y., Li, M., Drozda, M., Chen, M., Ren, S., Mejia Sanchez, R.O., Leavitt, B.R., Cattaneo, E., Ferrante, R.J., Hayden, M.R.*, et al.* (2003). Depletion of wild-type huntingtin in mouse models of neurologic diseases. J Neurochem *87*, 101-106.

Zhu, S.-W., Yee, B.K., Nyffeler, M., Winblad, B., Feldon, J., and Mohammed, A.H. (2006). Influence of differential housing on emotional behaviour and neurotrophin levels in mice. Behavioural Brain Research *169*, 10-20.

Zou, H., Wu, Y., Navre, M., and Sang, B.-C. (2006). Characterization of the two catalytic domains in histone deacetylase 6. Biochemical and Biophysical Research Communications *341*, 45-50.

Zourlidou, A., Gidalevitz, T., Kristiansen, M., Landles, C., Woodman, B., Wells, D.J., Latchman, D.S., de Belleroche, J., Tabrizi, S.J., Morimoto, R.I.*, et al.* (2007). Hsp27 overexpression in the R6/2 mouse model of Huntington's disease: chronic neurodegeneration does not induce Hsp27 activation. Hum Mol Genet *16*, 1078-1090.

Zuccato, C., and Cattaneo, E. (2007). Role of brain-derived neurotrophic factor in Huntington's disease. Prog Neurobiol *81*, 294-330.

Zuccato, C., Ciammola, A., Rigamonti, D., Leavitt, B.R., Goffredo, D., Conti, L., MacDonald, M.E., Friedlander, R.M., Silani, V., Hayden, M.R.*, et al.* (2001). Loss of huntingtin-mediated BDNF gene transcription in Huntington's disease. Science *293*, 493-498.

Zuccato, C., Liber, D., Ramos, C., Tarditi, A., Rigamonti, D., Tartari, M., Valenza, M., and Cattaneo, E. (2005). Progressive loss of BDNF in a mouse model of Huntington's disease and rescue by BDNF delivery. Pharmacol Res *52*, 133-139.

Zuccato, C., Marullo, M., Conforti, P., MacDonald, M.E., Tartari, M., and Cattaneo, E. (2008). Systematic assessment of BDNF and its receptor levels in human cortices affected by Huntington's disease. Brain Pathol *18*, 225-238.

Zuccato, C., Tartari, M., Crotti, A., Goffredo, D., Valenza, M., Conti, L., Cataudella, T., Leavitt, B.R., Hayden, M.R., Timmusk, T.*, et al.* (2003). Huntingtin interacts with REST/NRSF to modulate the transcription of NRSE-controlled neuronal genes. Nat Genet *35*, 76-83.

Zuccato, C., Valenza, M., and Cattaneo, E. (2010). Molecular mechanisms and potential therapeutical targets in Huntington's disease. Physiol Rev *90*, 905-981.

Zwilling, D., Huang, S.Y., Sathyasaikumar, K.V., Notarangelo, F.M., Guidetti, P., Wu, H.Q., Lee, J., Truong, J., Andrews-Zwilling, Y., Hsieh, E.W.*, et al.* (2011). Kynurenine 3-monooxygenase inhibition in blood ameliorates neurodegeneration. Cell *145*, 863-874.

7.0. APPENDIX

Appendix 1

Genomic sequence of the mouse *Sirt2* gene with the position and sequence of the mutation as present in the *Sirt2*KO mice. The inserted sequence (mutation) is highlighted in yellow. The mouse Sirt2 genomic sequence was obtained from NCBI under accession number: NC_000073.5.

```
   1 TTCTTGTTTC CGCTGCCGTC ACGGGACAGA GCAGTCGGTG ACAGTCCCGA
  51 GGGCCCCCAC CCCGTTCCCA TGGCCGAGCC GGACCGTGAG TTAGGGGCCC
 101 TGTTGGGAGG GTGGGAGGGT CGGGCCGCGC CGGGGCCTGG CTTTGGGCTG
 151 CAGGCCCCGG GGCCCGAGGG TAGGCTCGGT GGGGCGGGAG ACAGGATCTA
 201 CCTGAAGGGA GTGGGATTCG GAGGGGTGTT GCTAAGTGGT CCGTATTACT
 251 AGGTTGGTTG GTTTCTGGAT TGTGAAATGT AAGGGTCCGA TTGTCAAGTT
 301 CTTAATGATC GCATTTCTCG TACTTTGGCT GCTGAGGACC CTCGTTGCTA
 351 AGGACCAAAG TTACCACTAT CCCGGTTGCT AAGGTTGTCT GTTGTTAAGG
 401 GCAACTGTAG GATGGGTTCC GGGGACCCCT GTGGCCCCTT ACTATCTCAT
 451 TCCTTCAGTT CTTGTGCCTC TCCTAAACCT CCTACCTTCA CTGCATCTCC
 501 TCTCCCACAC TCAACTCTCA GCAGAAGTAT CCCTACTTAC GTCTCTTGAA
 551 AAACTTAGCC CTCCCTCATT CTCTCGACTC GCACATGCTA CCATATCCTG
 601 CTTAACTCTG AAACCTTCCT TCAGTCCAGT CTCGCCTGCT TTCTCCTCCT
 651 AAAGATTCCC CTCCTCAGCC TTTTCACGTC ACACATACCT CCACTCTAAA
 701 ATATGCCTTT TCCCATCTCC GATAGTTTTA CTACCATCCC TGACTCTGAA
 751 ATAATTAGGT TGGTGGGTCC TCTTGTCCTC CACCATTGTG AGCCCTTCTG
 801 CTTAACTCTT TCCCCGCACT GTAACCACGT CTGCTCCCCT CCTCCCCAGC
 851 CTCTGACCCT CTGGAGACCC AGGCAGGGAA GGTGCAGGAG GCTCAGGTGA
 901 GATGGGGAAG GGGTGGAGGG AAGGAGAGAC TTGGTTCCAC GTGCCGCACT
 951 GGGGGGAGGT GGCAAGGGAA GGCTTTTACC CAAGGGCCCT TGGCTTATGG
1001 CCCTGATCCC CAAGCCCATC TGGGGATTAG TACAATCTCC TGGGAGAATG
1051 GTGGCTTCTT GGGACTGTCA AGGAAAATGT ATAGCCTCAA CCCCTGGTTC
1101 CCTTCCATAT CGTCCTCGTT TCCTACTGTT GCCCATCCCA TCCTCAGCCC
1151 CTTCTGAACC TCATTTGTGC TGGACCTGAA AGAGACGGTT TTCCAGTTCA
1201 ATCCGCAAAC TCAGATCCTA TGAGGTGGGG GAAAGGACCC TATAGGGCAC
1251 GTTATAAAAG TATCGAAGCT GGGTGTGGTG CCAGCCCCCT GTAATGCCAG
1301 CACATGGGGG GGGGCAGGGG AGGGGGGAAG TGAGGTAGGA GGATGGAGAA
1351 AGGAGAGGCA GCTTGGGCCA TATGGTGAGA CCCAGTCTCA AAAAAGGAGG
1401 GAGGAAGGGA GAGAGCATAC CCCTGGAGTA CCGGGCAAAC TCTGTGGGTC
1451 AGAGATTATA GAAGATTCTA GCCAAACTCT CCCCTGGTGG AACCCACAAG
1501 CTGATCTAGG AACAAGACCA AGATATAGTC ACAGTGTCGT ATAAGTGAAG
1551 TGATAAGGGA TTTTCTTAAA TGAGATCGGA GGTGGTGTTC CATGCAGGGT
1601 ACAGGCCTGA GAGCACGAAG GGATAGTAGA TGTTTCAGTA GTTGGGTTGC
1651 TGGCGTGGTC ATTTATTGAT ACTCTGCCTG AATTTTAATG TACATGACTT
1701 CATTTAATCT TTGCAGCATC CCAGTGAAGG GAAGGCCTCT CATGGCTGTG
1751 TTACAGATGA GCAGCTTACT TGGTGAAAAC TGTTAACCCC TGTGTTCTTT
1801 GGGTAGAAAG GAAAGGGCTT GAAACTTATG GGGAAATGGG CTCCGAAAGA
1851 TGCTGCAGCT TCAGTGGAGT GTAGATGAGC CATCTCAAAG ATGTTTGAAG
1901 ACACGTGCCA AGGCCTCCGG TTCCCCCAGA GGCCAGGTTG TCCTCATATA
1951 CTCGAGGAGT GGTTCTCAAT CTTCCTAATG CTGCAACCTT TTAATGTAGC
2001 TCCAACGGTG TGGTGTCCCT CCAACCATAA AATTATTTTG TTACTACTTC
2051 ATAACTGTCC TTTTGCTACT GTTATGAACT ATAATGTAAA TATCAGATAT
2101 GTAGGATATC TGATATGGGA CCCCCCCCCC AAGAGAGGGT CGCTTGATCC
2151 CTAAAGGGAT TGTGTCCCAC AGGTTGGGAA ACAGTGTACT GGACCATGCC
2201 TACAACCACT GAATGCCAGC ATGCTCATCC TATGAGACCA CACTTCGAAG
2251 GGAGGCAGGT GCAGAAGCTG TGGTCAACAA TACCCCCATA AGAGCTGTGA
```

```
2301 CAGCCTGCTG TGGGTCTCTA GTCTCTTACT TGTCTGGCTC CCAAATGAAG
2351 GCTTAATGCC AGACTAAAAA AGGGTTTCAC AGTCAAAAGG GGTTCTCAGT
2401 GGCCAAGAAG ATGTGGGGTG TCAATTGCAG CATTATCCAG ATGGGGCAAC
2451 GCTAGCAGCA GCCTCAGTGG CTGTCAGGAG AGGGAGTCAA TGAACCACGG
2501 TTCATCATAC AATGTGTTAC TATGGAGCCA CAATAAAGAA TGAGGTGGGG
2551 GCTGGAGAGA TGGCTCAGTG GTTAAGAATT CTATTCCAGA GAACCTGAGT
2601 TCCATGTACC AGGCGCTCAC AAGTGACTAT AACTCCAGTC CCAGGGGATC
2651 TGACTCTATG GAGACTTGCA CACACATGCA CATATTCACA TAACTAAAAT
2701 AAACTAAAGA GAATGATGTA GGTCTGTGAA ACATTGTGCA GTATCTTACT
2751 CTGGCAAGAC CCAGTTCTAT AATAATGAGC AAATGCGCAA AACCTCACGC
2801 CGAGAAACCA CGTAGAGTTA TCTCTGTTTA ACTGTTGCTT GGTTTTGCTT
2851 TGGTGTTTGT TCGTTATCCA GGCTCAGGAG GCCGAAGGGG GAGGATTAGG
2901 AGTTGGAAGC CATCTTAGGT AAAACAGTAA GACTTGGACA GGCTCTTTTT
2951 AAAGCTTTTA TCTTTTTTTT TTTTTTTTTT TTTTTTTTTT TTTAGTTTCA
3001 TGTGCATTGG CATTTTGCCT GCGTGTGTGT CTGTGTGAGC GTGTCACATC
3051 CCCTAGAACT GGGGTTACAG GCAGCTCTGA TCTGCCATGT GGGTGCTGGG
3101 AATTGAAGCA GTCAGTGCTC GTAACCACTG AGCCATCTCT CCAGACCCTC
3151 TTTTTAAAAT TTTACACCTA GTTTGTTTTG TGTGTGTGTG TGTGTGTGTG
3201 TGTGTGTGTG TGTGTGTGTT TAGGATACAC ACGCCACAGT ATATGTATGG
3251 TGATCTGAGG ACAGCTATCG TCTCCTCCCA CCATGTGGGG CCTGGGAATC
3301 AAACGCAGAT TGTCAGGCTT AGCAGGCAGC CCCTTCCCCT GGTGACCCAT
3351 CATGCCAACT TATGTCATTT TTTAATATCA GTGAAGAATC ATTCTAGAGT
3401 CAGGCATGAT GGTGATGCAA TCCTGTAATC CTAGCACCTA AAACAATAAA
3451 AATAGATGGG TCAGGAATTC AAGTTCACCC TCACGTACAT ACAAGTTAGA
3501 GCCAGCCTGG GCTATGTCGG ACCCTGTCTT AAAACAATAA CAACAGAAGA
3551 ATCTTTAAAA ATAATTTAGA AAGGAGATTT GGAAGCAGAG TGTGGAAGGG
3601 AAGGTCTGGG GGCCTTTGAG CAGGGAGTTG ACTGTACTGG TCAGACTGTG
3651 TGGCATCTGC TGCAAGGCCA GCCCTGGGCT GGCCCCAGTC GGCATGTGTT
3701 GAGTGGTAGA TGGTTCTGGA AGTCCTGTTA TCTAGGCTGG GCAGTAAGCA
3751 GTAAACGTAA TGTCCCTGCC CTTGTGTGGC TGATATTGTG GCACTCAGTA
3801 GATGTTTGTG ATTTGGGGAC GGGGGAAGGA TTAAAGAAGA GAGAGGTGGA
3851 CTGTCCTCAA CAGGCCATCA TATGATCTAA GACAGAAACT GAGTCAAGGA
3901 GGCCAGGGCA GGACCCCAGG AGAGAACACG TTGAACCAGG TGGAGCTCTA
3951 GGGTTGGGAG AGGGAGTCAG TGGAAGGATG TCAGGAGGCT GGCATCCCAG
4001 TGGGTACACT GGGAATTGGC ATGAGGGTGG TGAGGTAGGG AAGCCAATGA
4051 AGGGACAGGG AGGCCACTTA GTATGGGGAC TGGGAGCAGG AGCTGGTTTG
4101 GGGAGATTCT GAGGCCACTT TGGAACATGG TTGGAGCAAG GTGGGGTCGC
4151 CCTGAGAGGC TCATGTCCGG TGTCAGAGAA GTGGCATCAC CAATGACTAG
4201 GCTGTGGTAT AGCCAGCCGA GGCACCTAGG GGCTCGCTGC TCGGCTTCAC
4251 AGCAACCTCT GAGCTATATG GACAAGTTGC GGCCCATGGG CTTGGAGGTC
4301 TATCTCGAGG TCACCTAGCA TGCATGAAGC CATGGCTTCA GGCCCTAGCA
4351 TCTTGTCAGG CTGTGATGGC CAACTGGGTA GAGTGTTGGA TGTGCTCCCA
4401 ACATCATGCC CGTAATCCCA GCTTTAGAGG GGTGGAGACA GGAAGATCAG
4451 AAGTTCAAGT TACAAAGACT TCATAGCAAG TTTGAAGCCA GCCTGGGCTA
4501 CATAAAACCC TAACTCAAAA AGCAAGCTAG GCATGGTGGC ATATGCCTTT
4551 AATCCTAGCA GTCAGAGAGA GGCAAGTGGT AATCTAGTCT ACATAGTGAG
4601 TTCTAGGCCA GCTAGGGATA TATAAAGTGA GACTCTGTCA GAAGAAAAAA
4651 GATGGGACAA GCATGCAGGT GCATGCCTTT AAACCCAGGC CACAGATCCA
4701 GGCAGATCTT CAGGAATTCC AGGTCAGCCT GGTCTGTGTA GTAAGTTTTA
4751 GGCCAGCCAG AGAGACCCCA TCTTGAAAGA AAGATAAGGC CTAGAGGAGA
4801 GCCAGGTCCT CTCTCTAAAG CAACCTTTCC CAGAGTCCTT ACACTGGCCC
4851 TGTACTTCTT CAGGGCACCT CCCAGTCAGA GCCCTACTGT ATTTGAACCA
4901 GGTTGTCACC CTTCCCATCC CTTCCCTTCC CTTCCCTTCC CTTCCCTTCC
4951 CTTCCCTTCC CTTCCCTTCC CTTCCCTTCC CCGCTAACCC CACTTCTTGG
5001 GCTTGGCCAT CCCACCCACC CCTTCCAGGA TTCAGACTCG GACACTGAGG
5051 GAGGAGCCAC TGGTGGAGAG GCAGAGAGTA AGTGTCGTCC TGGAGGAGGG
5101 CAGGGAGGTG ATCTGGGGTC TGGGATTAGA GGATGGGATT CTGGGGAGAC
5151 CCCCTCCAAG CTACCGGAGT GATAGGCAAA GCATGTAACA ATGGTTTGGG
5201 ACTGGATGCT GCTGTCTGTG GGAGACATTG GGAGTTGAGA TGTGGGAGGA
5251 GAGTGTGTGC TTGGGCCCTG GCTCGATGCC CACCTGGCGC TGTCTCTCTT
5301 GTTGTTGGCC AGTGGACTTC CTGAGGAATT TATTCACCCA GACCCTGGGC
```

```
5351 CTGGGTTCCC AAAAGGAGCG TCTTCTAGAC GAGCTGACCC TCGAAGGAGT
5401 GACACGCTAC ATGCAGAGCG AGCGCTGTGA GTCCCCAATT GCTTGGCCGC
5451 TTCTCCCATT CCTGGCCCCA GTTGACTCCA TATTTTGGGG GGTAGGAGTA
5501 GTAAGAAAGC CTGCTGTATA CACCTGTAAT CCCAAACTCT GAGCAGATTG
5551 GGAAAGGACC AGCATTTCAA GTTAGCCTCT GCTAGACTGT GTGTGTGAGG
5601 CTACCCTGAG CTACATGGGA AGTTTTCCTA AAATTCAGAA AGAAAAAAGA
5651 TGGAGGAAAC CCAACTCTTG GGATGGAGAG ATGGTTTAGT AGTTAAGAGC
5701 ACTAGCTGTT TTCCCAAAAG ACCTAGGTTG GGTTCCCAGG ACTCACATGA
5751 TGGCTTACAA CCATCTGTAA CTCCAGTTTC AGGGGATCCT ACTTATGGCC
5801 ACCATGGGCA TCAGGCATGC ATGTAGCACA CAACATTCAC GAAGGAAAAC
5851 ACCCATGTAG TTAAGAAAAA AAACAAAAAA CTCAGCTTGC TGGGGGGGGG
5901 GGTGGTGAAC GCCTTTTACC CCAGCACTCG GGAGGCAGAG GCAGGCAGAT
5951 TTCTATAGTT TGAGGCCAGC CTGGTCTGCA GAGTGAGTTC CAGGAGGTGA
6001 CTGAAGCCAG AAGATCATGA GTTTGAGGGT AACATGTGCT ACATAAGATT
6051 GTTAACTCAA AGAAAGAAAA GAGAAAGACA AGAAACCAGA ACTCTAGCCA
6101 AAAACAATAA AAAGGAGCAT GCAGACTCTT AAGCATTAAA TGTGATGGAG
6151 CCAGGCTCGA GGACATTGTT AGGACATTGT TCTCAGGCCT CACAAGTCTG
6201 TCTGCGTAGG GTGAAGGAAA GTCCAGCAGG CGGCTCCTGC TTGGGAGGGT
6251 ACCTTTGCAC TTAAGAACAA GGCCACATTG GCCCAGAAGC CCCCCCCCCC
6301 CCCCCCCGGA TGGAACTCAG CCCCTACACT CACACACCAC GCTAGGCAGG
6351 CACTCTGTCA TTGAGCTACA GCCCCAGCCC TTCCTTTCCT ACTGTTTTAT
6401 TTTGAACGCC CTGAATTTAC CCTCTAGTCC CTGAAGGTCG ATCCTCTTAC
6451 CTCAGCCTCC CACATAGCTG GGAGTACAGA GTAGCACCAC TAGGCCTGCC
6501 TTTGGGTCAC TTCCCTAGTG AATCTATTAC TGTCTTCTGA TGGGCCAGGC
6551 CTATGCCCTA GACTGGAAGT GATCAAAGCT CTGGGGTGAC TCAGGTGAGG
6601 CTAAGGAAAT TGCCACATGC TGAGCATACA TATGCTCAGC ATGCCGAGCT
6651 CATCTGCAGG CCCAGCCACT CTGGAAGCTG AGGCTAGAGC ATGTGAATTC
6701 AGAGGCAGCC TGGACTACAG AAAAAAGAGG GAAATGGAAT GATGATGGTG
6751 GCCCACACCT TTAATCCCAG CAGAGGCAGG GGGATTTCTG AGTTTGAGAT
6801 CTGCCTGGTC TACAGAGTGA GTTCCGGGAA AGCCAGGGTT ACACAGAGAA
6851 ACCCTGTCTC AAAACACGAG AGAGAGACAG AGAGAGACAG AGAGAGAGAG
6901 ACAAAGAGAG ACAGAGAGAG AGAGACAGAG AGAGAGACAG AGAGAGACAG
6951 AGAGAGACAG AGAGACTTAG GAGATTATCT CAGTCCATTA AGTGCTGGCA
7001 GCTCCCACAC AAGCAGCTCA CAAGTGCTTG TAATTCCCGG GCTGGGGAGG
7051 CAGAGGCAGG AGCCAAGCTC AGGTCCCCAT GAGACTCGTG AGACCCTGCC
7101 TTAAAATCCG TGATGGCACC AGTTGTCCTC TCACTTCCTT CCACATGTTT
7151 GCTGTGAAAT ACACGCACAA AGAGATGTGT GCACACCACC AAACAAACAA
7201 ATAACAGCCC ATATACACAC TAGGTGGATG GCCCTGGAGA AATACACACA
7251 CACACACACA CACACACACA CACACACACA CACTCGAGAG ATAAGTGATT
7301 AGAACAGGAC CCGATCTCTT GAGAGATACA GAAGTGTTTG CCATGGTATT
7351 ATTACAGGAA GCTTGTCTCA GACGTGCTGT TTAGAAGCCA GCTAGCTGGG
7401 TCACCGTGAA ATTGATATTT CTTGCTGAGG TCGAGTCACC GAAGTCTGAG
7451 AACCCAGGCC CTCGCAGTCC CCGTTGGGAA CAATGCAGCT TTGAGGGTCC
7501 TGAACAGCCC TTTGTTGAGG CCATCTTCTC CAGTTTCCCC TTGGCCCAGC
7551 TGCTCAGCGC CCTCCTTGGC AGCCGGGATG GCAGCTGAAC CTCCCTCTCC
7601 TGCCACAGGC TGGGCAGCCG GCCGCCTACA GAGCATACCC ACACAGTGGC
7651 CAGGCGACAC TGGTCCTCCC TCTTACACTC AGATCTGAGA GTCCCTGGCC
7701 CATAGGGTGC TGGTGTGGGA CGTGACATAA ATATCAACTA AGCAGACCCT
7751 TGCTGTTCGC CAGGCTCTGG GCTAAGTAGC TCACCAAGCA TCCTTGAACC
7801 TAATTATCAC GCAATAGCTG TGAGGTCTTT CTAGAAGTGA GCTGAACAGA
7851 AGAGGAAACT GAGGCACGGA GAGGTTGTGA CTTGGTGTGA ACATATGCAA
7901 GGGGCACAGT CAGGGCCCTT GAAGCTCGGT CTTGTTCTGT AGCTGTGGCA
7951 AGCTTTGAAT TTAAGATTTT CTTGCCTCAG TCTCTGGAGT TTTGGTATTA
8001 CAGTGTTACC ACACCCAGTC TCAATGCCTA CGATCTCCAG CCAGACTTGG
8051 GCCAGTAACA TCCTAAAGAA GCTGAGTGCA TAGACTGTAG CAGGCTCTCT
8101 GCTGTCATTT GTTTTTGGTT TGGTTTGGTT TTTTTTTTTT TTTTTCTAT
8151 GTAACAGACC TTGCTGGTCT GCAATTCACT TTATAGACCA CACTGGCCTC
8201 AAACTCACAG AGATCCTCCT GCCTCTGCTT CCCAAGTTCT GGGAATAAAC
8251 ACATACGCCA CCATGCCTGG TTTAAACATT ATCTTTGAGT GTGTGTGCTG
8301 GGGGTGGGTG GGTGATGTGG GCATTACTGT AGGTGCATGC ATGCTACTGT
8351 GTTTGCCAGG GGACATCTTT GAGGAGTTAT TTTTCTCGTT CTACCGTGTA
```

```
 8401 GTTTCCGGGA ATCAGGCTTA GCAGCAAGTG CCTTTACCCA CTGAGCCATC
 8451 TCGCCAGCCC CGATGGCAGA CTGACTTCTG TTCACACGTG TCCCTTAAAC
 8501 AGAACACCCC AGGGGTGCCC AATTCATGGG ATACCACACT TGTGTCTGCC
 8551 CATCAGCTGA CAGACAGATG TCGGGGCTCT GTGTGGCTGG GCTGTAGGCC
 8601 AGCCAGCAGC TGGGGCAGCA ATAGGGCCAT TTCTTCTCAG CTCTGTGCCT
 8651 GTGAATGGAT TCAATCCTAT CACCCCCTAA TAGTTCTTTA AAAACCAAGA
 8701 ACAAAGCCCC CATAAGAGTA TGAACCATGG ATCTGAAGAA GCATAATACA
 8751 CCGGAGGGGC TGGGGGCTCG GCTTGGCTCG GTTGGTGGAG TGCTTGCTTA
 8801 GTGCACAGGC CCCTAGAGTC AGTCTCCTGC ACCACACACA ACAACGGGCA
 8851 TAGCAAGGCT TGGTGGCACC CACTCCTCCC AACGCTTGCA AGGTCACTGC
 8901 GAGTTCTCAT GCTGAGACCC TGTCTCAAAG AAAGAAAAGA AAAGCTGGGC
 8951 ATGATGGCAA TGCTGGGCAC TTAAAGATGG AAGCAGGGTG ATTGGAAGTT
 9001 CAAGGTGATC CTTGGCTGGC TGCACAGTGA ATTTAATGCT TGCCTGACGT
 9051 CCATGAGATC CTGTCCAAAA CAAACAAACA AAAAAACCGT TATTTAGTGC
 9101 AATTGACTCA AAGGAGCAGA CTTTAGGCTT TTGTGTGAAC AAAGCAGGAT
 9151 GGTGAAGGGA TGTGTACAGC TAGAAACAGG TCCTAGCCAG TCATTGGAGC
 9201 TCCTGGGAGG CTGAGGAGGG AGGTACAGGA TTCCAGGCCA GCCCAGGGTA
 9251 CATAGGGAGG CACTGACTCA AAACCAGAGA AACCAGCAGA CATGCTGGTG
 9301 CACACCACAA CACCAGCACC CAAGAGGTGG AGCCAGGAGG CTCCGAAGTT
 9351 CAAGGTCAGC CTTAGCTACA TAGAAGGCTC AAGGTCAGCC TTGGCTATAT
 9401 GAAACCTTGT CTCAAATTTT CTTTTTTAAG TGTGTGTGTG TGTGTGTGTG
 9451 TGTGTGTGTA TAAGCATGAG TGTAGATGTA CAGATGCCCT CAAAGGTCAG
 9501 AGGCACAGGA TCCATGGAGC TGGAGTTAAC AGGTGGCTGT GAGCTCTGCC
 9551 TGACAGGGGT GCTGGAAATT GAACTCAGGA CCTCTGGAAA AGGAGGAGGT
 9601 GTTCTACCCA CTGAGCCATC TATGTAGCCC TCATCTGTGT GTGTGTGTGT
 9651 GTGTGTTTTG AACAAGGTTT CTCTGTGTGT CTTTGGCTGT CTTGAAACTC
 9701 ACTCTGTAGA CCAGGCTGGC CTCAAACCCA CAGAAATCTG TCTGCCTCTG
 9751 CCTCCCGAGT GCTTGGATTA AAGGTGTACA CAACTACCTT CTGACCCAAA
 9801 AGTAATTTTT TTGAAGTCTT ACAGTATTGT ACCTAGAAGA TTAGTCATTG
 9851 TCAGAATTTG GTTTGGATTG ATTGTCAAGG ACTCAAACTA GCCGTCTCTG
 9901 TACTGCCGAA CTTTGCAAGG CGTCCCCACC TCACCCCACC CCCCATCCCT
 9951 CTCCCTTCTC CTGGGTGGCT GTGTCTCCTC ACCTGAAATG TGAGGTTGCC
10001 AATGCCATCC TGCCCGGCAC CAGCAGTACG TCTAGGAGGG AAACCTTAGC
10051 ATGTGCCATC AATCCTCTGT TCCAGGCCGC AAGGTCATCT GTTTGGTGGG
10101 AGCCGGAATC TCCACGTGTA AGTTCCCCGT CCTTCAGCCA CTCCTGGGGC
10151 TGGGGGAGGC TGGAGGGGTT CGTGCACACG TGGGCAGAGC CTCTGACTGC
10201 GTTGCCTTCC TAGCCGCGGG TATCCCTGAC TTCCGCTCCC CGTCCACTGG
10251 CCTCTATGCA AACCTGGAGA AGTACCACCT TCCTTACCCA GAGGCCATCT
10301 TTGAGATCAG CTACTTCAAG GTAGACGGCT AAGATGAGGG GAGGTGGCTC
10351 CCAACTCCAG TCCTTGTCTT ACCTGGGACA TGTGGCCCTC TGCTCCTCTC
10401 TCCCACAGAA ACATCCGGAA CCCTTCTTTG CCCTTGCCAA GGAGCTCTAT
10451 CCCGGGCAGT TCAAGGTGAG GTCATCTTCT GCAGGGAGCC TGGGAAGAGT
10501 AGGCATGGAA GCAGGCTCTT TATAGGCCCT CCAGGCAAGC ATAACATGAT
10551 TAAGAACCTA GCTTCTGGGG CCAGCAGGAT GGTTCCATGG GTAAAGGTGC
10601 TTGCTACCAA ACCTAATGAC CTGAGTTCAA TCCCTGGAAT CCTCATGACT
10651 GAAGGAGAGA ACTGACTCCA TCATATTCTC TGACCTCCAC ATGTGCACTG
10701 TGGCAAGTGC ATATCCCCAG GTAGATGGTT GGATGGAGGG AGAGACAGAT
10751 GGGTGGGTAG GTAGATAGAT GGATGGATGG ATAGATGGAT GGATGGTGGG
10801 TAGATAGATG GATGGATGAT AGATAGATAG ATAGATAGAT AGATAGATAG
10851 ATAGATAGAT AGACAGATAG GTAGATGGGT AGATGGGTAG ATAGAGATAT
10901 TGTTAAAGAA AAAAGAAAAG AATTACATAA GTTCTGGCCA GATTTGATAG
10951 TTCATCCCCA TAACTGTAGC ATTTGGGAGG CAGAGACAGG AAACTTTCAA
11001 ATGCAAGGTC AGCCAAAACT ACCTATCTCA AAAGTAAAAA AAAAAATAAA
11051 AATTAAAGAT GAAAGAGGTG AAAGTGGGAG AGATGGCTCA GGGTAAAAGA
11101 GCAGATAGTA CTCTTCCAGA GGACCTGGGT TCAATTCCCA GGACCCACAT
11151 CAGGATGTTC ATAGCCCCCT GTAACTACAG CTCCGGGGAG CCTGACACCT
11201 CTGGCCTCTG TGGGCACTAG AACTCACCTC CATATACCAA CAGAGACCCA
11251 CACACATATC TGTAACTAAA AATAATTGGA ATGGTAGCTT AGCAGTTCAG
11301 TGCACTGGCT CCTCTTCCAG AGGACCTGGG TTCAATTCCC AGACCCACAT
11351 GGCAGCCTAC AGCTATCTGT AACTCCAGTT CCAGGGGATC TGACACACAC
11401 ACACACACAT GCAGACAAAA CACCAGTCAA TGCACATAAA ATAAAAATAA
```

```
11451 ATAAATCATT TAAAAAATTC CAGCTCGGGG GCCGGGCGGT GGTGGTGCAG
11501 GCCTTTAATC TCAGCACTTG GAAGGCAGAG GCAGGCAGGT TTCCGAGATC
11551 GAGGCCAGCC TGGTCTACAG AGTGAGTTCC AGGACAGCCA GGGCTATACA
11601 GAGAAACCCT GACTCGAAAA CAAACAAGCA AACAAACAAA CAAACAAACA
11651 AAAACAAGAA ACAAAACAAA AAAGAAAACA AACAAAAAAA TCCAGCTCTT
11701 GGTGAGAGGC AGGAAGATTT CTGTGAGTTT GAGGCTAGCC AATTCCAGGC
11751 TTACCTAGAG AGACCCTATC TCAAAAACCA AAAAAATAAA TAAATAGTAA
11801 AATAAACAAT TTTAAGAAAT TAAAAGAAAG GAGGAGTGGG TTGCCTGGCC
11851 CCTCGTCTCT TTATCCTGTG GCTCTGGGCC TCAGTTTACC CAACTCTAAG
11901 AAAGCTGCTG AGACTATCAG GAAGGGCTGA GACTGAAGCC TGGCTGTGAG
11951 CCTGACTCTG CAGTTTACCT ATTGGTGATG CCAAAAAGCC GCCACCATGC
12001 CCTTGCCTGG GTCTCCTCAT TTGTGGTACG GGAGAAGGCA GGCTCACCCT
12051 CACTGGGCCA CTGAGATGGG GCCATGGGGC AGAATGGGCC CACAGCATGG
12101 CCTGGGACAT TCACATCAGC ACTGTTACTC TTCTCTCAGC CAACCATCTG
12151 CCACTACTTC ATCCGCCTGC TGAAGGAGAA GGGGCTGCTG CTGCGCTGCT
12201 ACACGCAGGT AGGCGGGGCC ACGGGCAGGT GTGACCATGG GTAGGCAGGA
12251 CCTTGGGCAA GCGTGACCTT GGGTGGCAGG GCTCGAGGGC AGTAGGCCAG
12301 ATGGGTCTTG GAACACTCGG TCAGAGCTGG GCTAACACAG GCAGGCACAG
12351 GACCAGGGCT CAGCTAATTA TAGTGAATGA CCTACAATGG GCCACTTCCT
12401 CTTGGCCTCA GTTTCCCCTT TGTAAAATAG GGGACGGAAA CAGGATAGAT
12451 TGGTACTCAT TGGAATCAGG AGAAAGGTCA GAAATTCAAG GTTGCTGGAT
12501 GGTAGTGGCA TATGCCTTTA ATTCCAGTAC TCAAAAGGCA GATGCATGCA
12551 GATCTCTGTG AGTTTGAGGT CAGCCTGGTC TACATAGAAA GTTCTAGAAG
12601 AGCCAGGGCT ACACAGAGAA ACCCTGTCTT GAAAGACCAA AAAAAAAAAA
12651 ACCCAAACAA CAACAAAAAC CAAAGAAAGG TTATCATTGG CTACAAAATG
12701 AGTTTAAGGC CAACCTTCAG GATGTGAGAC TGTATCTCTA AATTAATTGA
12751 TTAGTCGATT AATTACAATA TAAACTAATA GAAGAATGTT TAAATATAAA
12801 GAAGTCAGAA CAGCTTCAAG CCCTCTCAAG TCTGCTGTGA GGTGACAGGT
12851 GACAGGACAT CCCAGACTTA CTGCAAAAGG CCTCTGTATC TGAGGGGACA
12901 CCGTCCATAC CACAGCCACT CCAAATCAGG AAAGTGACAC TGTATCGTAA
12951 GGAAGGTGGG CTTCTTATTC ATACACTTCT GAGCCTGGCC TTGGATACGG
13001 TGGCTAATGG GACACTGTGG CCACACTGAG GTTCAGACGG ATGTTCAGGC
13051 TGCTGGCTTC TATGTGTCTC TGTGCGTTTT GTGGATGTGT TGAAGTTCAG
13101 ACTGCTCTGT GTATACATGT GTGCTAAAAA ATTGTCTCAG AATACAAAGT
13151 GGCCATTACA TTACACACTT GTTATCCCAG TGCTTGGGAA GCCGAGGAAG
13201 GAGCTGGTCA TGAGTTCAAG GCCAGCCTGG GCTAATAGTG GATTTAAGGT
13251 CAGACTGGCT CCATAGCAAA CAATCTCCCC CGCCCCCCGC CCCCTCCCCC
13301 GCCCTGCCCA AGAAGAAAAA GTTAGAAAGG AAAAAGAGAG AACTCCAAAT
13351 TGTACAGAAG AGTTAATGCT TGAATACAAA TAGGTTTGAA GCTCTTGCAA
13401 TGTCAGAAAT GGCCACCAGG GGGAGGATGG GTTCAAACTT TTGGGTCCAG
13451 ATGGCTGGAG GCCCCAGCTG GGGAAGAGAC AGCTTAGTCC TTCCAGGCAC
13501 CGCCCAAGCT CAGAGTCAGC CTCATTCACA GAAAGAGGCT CAGGCCTGAT
13551 ACTAACAGCT TCCTTGAAGC CCCATACTTC CTGCTTGTTG TTGCATGTCC
13601 CTCCTGCACC CTTGTTTGCT GGCCTCTATG ACAACAGGTG TCCACCCAAG
13651 TACCAGGCCC TACCAGTGAG CCAAGCAGAC ACCGCTGCCC TCCTGGTGCC
13701 AATTCATGTG TGTGACAAGA ACAAGAGGGA CGATGAGTCA TAGACCTAGG
13751 GTGTCAGATG GGGCTGAGAC CAGCCTGAAG TTTGGAAGTC AGAGGACAAG
13801 GTGCAGGAGT CAGTCCTTCC TTTCCATCGT GTGGGTCTCA GGGATGGAGC
13851 TCAGGTCATC AGGCTTGGTG GCCTTTACCT GAGCATCTCA CTGGCTCCAC
13901 ACATAAACTT TAAAGGGAGA TTTATTTTTA TTTCATGTTT ATGGATGTTC
13951 TTCCTGCTTG TATGTCCATG ACCTATGTGT ATGCAGTGCC CACAGTAGCC
14001 AAGAGAGGCT TTAACAGATG TGTGCTGCCA TGTGGGCGCT GGGTCCCAAC
14051 CCGGGGTCTT CTGGGAGAGC ATCCAACACT CTTAACTGCT GAGCCATCCC
14101 TCCAGCCCCC ACACGTACAT TTTTGTAAAA TATCTGAAGG TGGAAAAAAA
14151 TGTTCCACTT GCCCCCTTTG TGGTCAGCTT TTTTTCCTTC GTGGCCTCTT
14201 CTCCTCAGTC ACCGTTTGAA TCACTGACCC ACTTTCTGGA ACACAGTGAC
14251 TCCGCCTCTG AGTTGTGCCG ACACAGCATC TTTGAAGCTG TGGTGCTGTT
14301 TTTAGCTCTG CACAGGAACC CATCGCTCAA GCCACTGTGG TCCCCACAGA
14351 AGAGTGGCTA TAGACCTTCA AGTTGCATAC ATGAAATTCA CCCTCCAGGA
14401 AGTTCTCTGT ATGCCCCAAA CCCAGCCTCT TGTCTGGGGA CCCCTCGATA
14451 CTCACACCAT AGAGCAGCAC CATGCTTTTT AAAATCGAAG AGTAGTCTTT
```

```
14501 TTCTTTTTTT CTTTTTCCTT TTATTTTGGG TGTGTGTCTG CTGCGTTAGT
14551 TATATAGGCC GCAGGGCTTC CGGCATGCTG GGGAAGTGCT CTACCACTGA
14601 GCCACACCCC CAGCCCAGGC AAGACCTGAG TTTGTAATCT TCTGTCTCAC
14651 CCTCCTGTAG CTGAGGTTAC AGGCTTGCTC TGCTAGCCCA GCTCTACTGT
14701 GCAGGCATTG GGTACAGGCG GCAGCCTACC ACGTCATCAT GAGGGGAAAC
14751 TGCAAACTTA CATCAGTGAT GTGCAGTAGG GTAGGTGTCA GAGGCCTGCT
14801 CCACTCAGGG TAGACCCAAC TCACGGTGGG CTTATGAGGA CAGAGCCCCA
14851 TTGCAAGGGA AGGAGCGTGT CTGTGGATAT AATCCAACAT GATCAGAGAT
14901 CTCAGGCATC TCCCTCCACC CTAGACTATG TTTCCTTTGA TCACAGAGGC
14951 TGCCGGAGGT AATTCTGTGA TCCCTTAGTT AGCTGTTTGT GTGTGTGTGT
15001 GCTGCTCACT CTCCAATGAA GGGCTTGGTA GACTGAGCCA GCGACAAAGC
15051 AGATGCAGAG TGCGGGGTGT GGCAGTGCTC CCCTGTCATC CTGGCACTCT
15101 GGAGGGAGGT TCTCCAGTTT GAGGCAGTCT CAAAAAATCA TATCCCCCCC
15151 CAAAGAAACA AATAAGTCAT TCTCTTGTTT TATTTATTCA TATTACATTA
15201 TTTAGTGTGT GTAAAGTTCA GCTGACAACT GAAGGAAGGC GTTTGCTTCT
15251 ACCATGTGAT GTCTGGGGCC CAAAGCCACG TTGCTATGTT GGTAGCAAGG
15301 ACCATTGTCA GCTGAGCCAT CTTGTCAGCC CTTACTGTGG CTTTTCCAGA
15351 CAGGTGCTAG TCTTGTCCCA GCTTGCCTGA ATCTCACCCT GTTCCTCAGG
15401 CTAGCCTCAC CTTTACAGCA GTCTAGAATT ATAGGCATGG CCTACCATGC
15451 CTGGCTTTAT TTACTTATTG CTTATTTATT TCACTTTTTT GAGGCAGGTC
15501 TTCCCATGTA GCCCTGGCTG GCCTGACATT AGCTATGTAG CCTCAGCTGA
15551 CTTTAAACTT AAAGCAGTCC TCCTACCTCA GCCTCTAATT GCAGGGCTTA
15601 TAGGCAGTCA CCACCACTGC TGACCTGATT CAGTTTATTT ATGTTAATGC
15651 TTGGCCAGAG CTGTCACATA CAAGCTACTC AGGTGGGATC CCCACAAGGA
15701 TGCCACATCT GAGGGAGACG CTGAAGATAG GTACATTTAT TGCAATAAAT
15751 GTGTGGCAAA TGGAGGGACT GTGCGTGGCT CTCTAACAAA AGAACTTCTC
15801 TGAAAATTAG AGGCAGTGAC CCAAGTTTGT AGAAGAATAT CCCATGGGCA
15851 TCCTTTAGCA ACCTTCTGTG GCCCCACTGG GGAAGCGGGC ACTTTCCATA
15901 TATCCTCACC CTTCCTCATC CCCCGCAATG CCACTTCTCA GAGCCACCAG
15951 GGCTGGCTGT CTTCCTGACC TCCCCTCCCC CTCCAGAACA TAGACACGCT
16001 GGAACGAGTG GCGGGGCTGG AGCCCCAGGA CCTGGTGGAG GCCCACGGCA
16051 CCTTCTACAC ATCACACTGT GTCAACACCT CCTGCAGAAA AGAATACACG
16101 ATGGGCTGGA TGAAAGGTGA GGCTGGACTC TGCGGGCAGG CAGGCCTCGG
16151 GCAGGCCAGG GGGAGGTAGG GGGTGGGGGG CTCTCACTGC TTGCCTGCCA
16201 TAGCCAGCCT CCAAGGGCTG GGCCCCAGTG CAGTCTGCTC CATTCTTTGG
16251 CTCTTGCTAG TCAGTGAGTT GGTTGGTTTC CACTGAGGCT AGGCTTCCCT
16301 ATGTAGCCCA GGCTGGCCTG GAGCTTGCAC TTCTGCCTCA GCCTCTCTAG
16351 TACTGAGGTT GCTTGCAGGC GTGCACTACG GTACCCAGCT GTCTTGCTTT
16401 TTATGGTAGC TGTAGAAGCC TCAAGGATTC AAGGTGACAG CAGGTCTTTG
16451 CTCCCATGCC ACCCCTCTGC TGGGCTGTCA TCCATATGAA CCGCAGAGCA
16501 CGGCCAGCCA CGTGTGGACT CCGTGTAGAC TCACGTCCTC AACGGTCACA
16551 CAGCCTGTGT CTCTGAGGTG TTTACTATCT ATCTTACATG GCAAACACGG
16601 CTACCTTCTG AGGAAGGCAT TGCACAGTGG AACCTTCCGA GACGAGGAGG
16651 CCTGTGTCTA CGTCCAACAT GGCTCCACTT GCCCCATGTG CCTACTGAAG
16701 CAAAGTGTCT AACCTCTGCT GCCACCATGT GGGTCCCAGG AACTGGACTC
16751 AGGCGCTCAG GCTTGAGGAT GGACCACCTC GCTGGCCCAG AACAGTTTAA
16801 TTTTTATTAT ATTTTTTAAA GATAGGGTCT CTAATTTCAT TAAGTTCTTG
16851 TTGGTTTAAG TTGTAGAAGT CGCAGGAGGA ACCATGGTAC ATGCCTATTA
16901 GCCTATTGCT TGGGAGAGGC AAGAGGATCA GGAGTTCAGG GTTAGCCTTG
16951 GCTACATACT AAGTTCCAGG TCAGCCTGGG CTACATGACA ACATGAAAAT
17001 AAAAACTAAT AAATTTTATA TAAGTCTTAT GTAGCTCAGC CTTCCATGTT
17051 GGACAGTGCA GCAGGAGCCT GTGGAGAGGG AAGCTGGGTG CTGTGCTGGG
17101 TAAGACAAGT GCTGGAGACA CACATGGTAG CTCACGGCTG TCACTGCTGT
17151 CACTGTCCTC ATTCATGTGA GGACACAGCA ACTGAGAGGA CAGCTAGTCC
17201 CCGCGCCTGG GTGCCAGCAC CAGTCTGTTC TGGCAGCCAT TGTGCTGAGC
17251 CTGAAGCTGC TGTGTCAACT GTGGGAATCC ATTTCTGTAT TCTTTATGCT
17301 GACTTCACAA AGCCTCTGGT GTCCCCTTGA GATCAGGACA GCTGTGGCCT
17351 TTATAGCAGG ACCCTGGAAG GTAGCTCTTC TGACAGAATG CCAGCCAGCT
17401 GCCCCCAGAC TGAGGGTTCC TGAGCAGCCC ATGTGTGCAC AGCTGGGGGT
17451 GACGGACAAT GGACATCACC CCCTTTATGT CCCTGTGGAA TCGCATCTTC
17501 CACCCACAGA ATAGCATATT TGTGCAGAAA TACCTCAGCA GCAGCCGTTA
```

```
17551 AAGCTTCGCC CTGTGACTGG CTGTATGAGT GGCTGGCGGA GTGAGCTCCA
17601 GTCCTGTGGG CTGCATGTGG CAGATGTGCT TTCAGACTCC GTGATCCATA
17651 AGTAAGAAGG AGTGTGACTT TCATAAGGGT GGTCTGTCCC ATAAGGAGTC
17701 TGTCACAGAA TCCGAGAGTG GGAAACAGTT GGGCTTGAGG TTTGATCCAA
17751 CCCAAGGCTA TCTGTATGTC CTTTCCTGAC CCAGGGCAGA TAGGACTGTC
17801 CCCAGGACCC ATTGGATGAC TCCCATTCCC CAGATGGGGG TCTGGTGGAG
17851 TCCAGGGGCA CCTGTCTGGG GCAGATGGGT TTGCCCCTGT ATATGCCCTT
17901 TCACTCACTA GCTGTGGTGC TGCCAGCCAC CCCTGGATGC CTGGAGGTGA
17951 AGGGGACGGC TCTCTAAGAA GGGAGCTCCT CTCTGTGAAG CAGGAAAGAC
18001 CACTCAGGAA ATGCCTGAGT AGTGAGCTGT GCTGTTTGTT TTGTGGCGCT
18051 GCGGATCAGA CTAGGGGACT CGGGCATTCG AGGTCAGAGG CTCTTCCACT
18101 GGGCCACACC CACAGCCCCC ATACTGGGAG ACTCAAAGCA GGCATCTCCT
18151 GCTGAGTCGT GCCCAAGCCC TCTTGGTTCC ACCGCTGAGC TAGCCTAGCT
18201 CTTGGGGTTT GTGTGCGCAT GTGTGTAGGT GTGCACATGG CATAGCATGC
18251 GTGTGCATGT CAGGGCCATC TGCAGGAGCT GCTTCTCTCC TTTTAGCATG
18301 TGGGATCTGG GGACGGAACT CAGGCCACCA GGCTTGGCAG CAGGTCCCTT
18351 TACACACTGA GCCACCTTGA AGCCTCAGCT CTTATTTTTT TGAGATGTGG
18401 TTTTGTTGTG TAGCCAAGGC TGGCCTCAAA CTCACAATTC TCCTGTTTAA
18451 TTCTCCCCCA AGCAGGCTTG CGGCATGCAC CACTGCCACC TGCCTGGGAT
18501 GCATTTCTGT TGACAGGAGG GAGGGGCAGA AGAGGGCTTC TCCAGCAGCC
18551 CTTGGGGGAG CCTCACAACT CACCCCCCCT TCCTCTTTCC CACTCAGAGA
18601 AGATCTTCTC AGAAGCAACT CCCAGGTGTG AGCAGTGTCA GAGTGTGGTA
18651 AAGCCTGGTG AGTCCTGGGC CCGGGGCTGG AGCTGGGACC CCTTCCTCCA
18701 CGGCCTCACC CCCCAATCTG GCCACTCTGC CACCTGGCCC GTCCCCTACT
18751 GTTCAGCAGA GGGTGCCCCG CCCCCCAAGC CTCAGTTGGG CCCCTGACTC
18801 CTGACTGTTC TAGCTCTGTC TCCCATATCT CCTGTCCTCT GTCCCTCTGT
18851 CCCTCTGTCC CTCTGTCTGT GTCTACCGCA GATCTGAAGC TTCTGATGGA
18901 ATTAGAACTT GGCAAAACAA TACTGAGAAT GAAGTGTATG TGGAACAGAG
18951 GCTGCTGATC TCGTTCTTCA GGCTATGAAA CTGACACATT TGGAAACCAC
19001 AGTACTTAGA ACCACAAAGT GGGAATCAAG AGAAAAACAA TGATCCCACG
19051 AGAGATCTAT AGATCTATAG ATCATGAGTG GGAGGAATGA GCTGGCCCTT
19101 AATTTGGTTT TGCTTGTTTA AATTATGATA TCCAACTATG AAACATTATC
19151 ATAAAGCAAT AGTAAAGAGC CTTCAGTAAA GAGCAGGCAT TTATCTAATC
19201 CCACCCCACC CCCACCCCCG TAGCTCCAAT CCTTCCATTC AAAATGTAGG
19251 TACTCTGTTC TCACCCTTCT TAACAAAGTA TGACAGGAAA AACTTCCATT
19301 TTAGTGGACA TCTTTATTGT TTAATAGATC ATCAATTTCG ATCCGCTCCT
19351 GGGCACCGAA CTGCGCCGCG TGTTCAGCAG GGTCGGCGTG TTCGGTGTGT
19401 CCCCCGCGGT GGGCCTCGGG GGCGGGTGCG GGGTCGGCGG GGCCGCCCCG
19451 GGTGGCTTCG GTCGGAGCCA TGGGGTCGTG CGCTCCTTTC GGTCGGGCGC
19501 TGCGGGTCGT GGGGCGGGCG TCAGGCACCG GGCTTGCGGG TCATGCACCA
19551 GGTGCGCGGT CCTTCGGGCA CCTCGACGTC GGCGGTGACG GTGAAGCCGA
19601 GCCGCTCGTA GAAGGGGAGG TTGCGGGGCG CGGAGGTCTC CAGGAAGGCG
19651 GGCACCCCGG CGCGCTCGGC CGCCTCCACT CCGGGGAGCA CGACGGCGCT
19701 GCCCAGACCC TTGCCCTGGT GGTCGGGCGA GACGCCGACG GTGGCCAGGA
19751 ACCACGCGGG CTCCTTGGGC CGGTGCGGCG CCAGGAGGCC TTCCATCTGT
19801 TGCTGCGCGG CCAGCCGGGA ACCGCTCAAC TCGGCCATGC GCGGGCCGAT
19851 CTCGGCGAAC ACCGCCCCCG CTTCGACGCT CTCCGGCGTG GTCCAGACCG
19901 CCACCGCGGC GCCGTCGTCC GCGACCCACA CCTTGCCGAT GTCGAGCCCG
19951 ACGCGCGTGA GGAAGAGTTC TTGCAGCTCG GTGACCCGCT CGATGTGGCG
20001 GTCCGGGTCG ACGGTGTGGC GCGTGGCGGG GTAGTCGGCG AACGCGGCGG
20051 CGAGGGTGCG TACGGCCCGG GGGACGTCGT CGCGGGTGGC GAGGCGCACC
20101 GTGGGCTTGT ACTCGGTCAT GGTGGCGGCT GGATCGGTCG AAAGGCCCGG
20151 AGATGAGGAA GAGGAGAACA GCGCGGCAGA CGTGCGCTTT TGAAGCGTGC
20201 AGAATGCCGG GCCTCCGGAG GACCTTCGGG CGCCCGCCCC GCCCCTGAGC
20251 CCGCCCCTGA GCCCGCCCCC GGACCCACCC CTTCCCAGCC TCTGAGCCCA
20301 GAAAGCGAAG GAGCAAAGCT GCTATTGGCC GCTGCCCCAA AGGCCTACCC
20351 GCTTCCATTG CTCAGCGGTG CTGTCCATCT GCACGAGACT AGTGAGACGT
20401 GCTACTTCCA TTTGTCACGT CCTGCACGAC GCGAGCTGCG GGGCGGGGGG
20451 GAACTTCCTG ACTAGGGGAG GAGTAGAAGG TGGCGCGAAG GGGCCACCAA
20501 AGAACGGAGC CGGTTGGCGC CTACCGGTGG ATGTGGAATG TGTGAGGCCA
20551 GAGGCCACTT GTGTAGCGCC AAGTGCCCAG CGGGGCTGCT AAAGCGCATG
```

```
20601 CTCCAGACTG CCTTGGGAAA AGCGCCTCCC CTACCCGGTA GAATATCGTG
20651 TTTTTCGGTG AGAACCTTCC ATCGCGCTTC TTCTCCTGCA TGCAGTCAGT
20701 AAGTGTCCAC TCTGGGCTGG GCCCATGTGA GGGGGACAAA GCCAGAGTAG
20751 TGGGGTCCAA GGCCTTCCTG GTTACTCCCC GCAGGACTTC TCCAAGGTGG
20801 ACCTCCTCAT CATCATGGGC ACCTCCCTGC AGGTGCAGCC CTTCGCCTCC
20851 CTCATCAGCA AGTAGGTTGA GGAGGATGGG ACTGGGTGTC AGCTCGGGAC
20901 AGGGCACTAG GGCAGATCCT GAATCTCAGC TCCCCCTTCC CAGGGCACCA
20951 CTAGCCACCC CACGGCTGCT CATTAACAAG GAAAAGACAG GCCAGGTAAG
21001 TCTGCCTCAG CTTCCCTCCC CCTCTCCTCC CCCCCTCCTT CCCTGTCCCC
21051 CTCCCCCTCC CTCCACTTTC TTTGCCCCCT TCCTCATTTG GCCACTTCCT
21101 CAGGGGACAG GGCAGGTCTC TGTCCCACCT GGAAAGCACC AGATCCTTAG
21151 ACTTGCCAGT TCAGTCAGGA GAACATGGGA GCTGGCCTGT GCACTGGGCC
21201 TCTGTCATTC TAGACTCCAC TGAGCACAGA ACAGAACCGT GCCTTGAACC
21251 TGCTGAAGCC CAAGTGCTTC CCCGGACCCA GGAGACAGTC CAGACACTAC
21301 CATTCTAGTG CCCTCTCACA TATCAAAATC TGGGGACCCT CAAGTCCCTC
21351 CTATGAAGTG GCAGAGTGTT TATATAGAGC AATCTCTGAA GATGCTAAGC
21401 TGTGTCTCCG TGACGTGTGC GATACCATGT GAACTCAGGA GACAGGCTCC
21451 CATGCCCCCC TGCCCTCTCA GACACGCCAC GGAATTTAAG ATGACCTTGA
21501 ACTCCTAGTC CTCCTGCCTC TGCCTTCCAA GTTCTGGCAT GACAAGCCTG
21551 TGCCACCACT CCTGGCTGTG TTGTTGTTTG TTTAGCAGAA GGATAAGTTG
21601 CTTGCCACGC ATGCACTAGG TCCCGAGTTT AACTGCTTGC ACCCACATAA
21651 AAATCCAGGC ATGGTGTTTG TAGTCCCACA CTGGAGAGGC AAAGATTAGT
21701 GGGTCCCTGG GGCTCACCGG GTAGCCAGTC TCACATAATC CTGAATTCCA
21751 GGCCAGTTGA GCAATGTCTC AGAAAGAATG TGTCTGGGCC GAGGCTGTAA
21801 CTCAGCGGCA GTGCTTGCCT GGCGTATGCG CGGCCCTGAG TTCAATCCTC
21851 AGCACCACCA AAGACGAAGA CGGTTATTAG TTTTGGACTA GAGAGATGGT
21901 TTACTGATTA AGACCTTCTG TCCCCAGCAC CCATGTCAGG TGGCTCACAA
21951 CTGCCTTTAA CCCCGGCTCC TGGGCATCTG ACGCCTCTCA GTCCTCTGAG
22001 CACTCACACA TAGAGAGCAC ACATGCAGTC AGATAAAAAG AAGCCAAGTG
22051 GTGGTGGTGC ACACTTTAAT TCCAGCACTT GGGAGACAGA GGCAGGTGAA
22101 TCTGAGTTTG AGACCAGCCT GGTCTCCTTA GTAAATTCCA TATTAGTCAG
22151 GACTATATAC ATATAGACAC CATCTAATCA ATCAATCAAT AACAAGTTGG
22201 CTAACTTCTA AGAAACAGTA ATTATGGTTG GCCTCTTGGT TGACCTCTAG
22251 CCTGACCTCC AGGTCCACAT GTGTACAAAT ATAGACACAT AGCCCACTAC
22301 CATACACACA CACACACACA CACACACACA CACACACTAA TTAGTAAATA
22351 GGAAAATAAG GCTAGGTATG GTGGTGCACA TCTTTTATCC CAGCACTGAG
22401 GAGGCAGAGG AAAGGTGGAT CTTTGTGAGT TCAAGGCCAG CCTGGTCTAC
22451 AGAGCAAGCC CCAGGACAGC CAGGGCTCCA CAGAGAGACC CTGTTTTAGA
22501 AATAAGCATA AGGCAGGTCT GCTGGCTCAG GGCTGTGCCC TTAGCTGTCT
22551 TCTCCCCACA GACGGACCCC TTCCTGGGCA TGATGATGGG CCTGGGAGGT
22601 GGCATGGATT TTGACTCCAA GAAGGCTTAC AGGTGAGGCT GGGCCTGGGT
22651 GAGCAGCTCG AGAAGGGTGG GTGAGGAGGG AGAGAAGACA GAAGGCCGGC
22701 TGGTCCTCAG CCTGTTCTCT TACTCCTGCT CACCCTGCAG GGACGTGGCC
22751 TGGCTGGGTG ACTGTGATCA AGGCTGCCTG GCTCTCGCTG ACCTCCTCGG
22801 ATGGAAGGTG AGGAGCTGGG CCACCCCAGC CCACCCTGAG CCCAGGCCCA
22851 TGGGGTTTAC GGTAACCTGA CTTGCGTCAA CTTTGCCCCC TACAGAAGGA
22901 ACTGGAAGAC CTTGTCCGGA GGGAGCATGC CAACATAGAT GCCCAGTCAG
22951 GGTCACAGGC CCCCAACCCC AGCACTACCA TCTCCCCTGG AAAGTCCCCA
23001 CCGCCTGCCA AGGAGGCGGC CAGGACCAAA GAGAAAGAGG AACAGCAGTA
23051 ACAGTAACCA TGACCTCCCG CAGGACAGCG GAGCCCGGCC AGCACTGGGC
23101 CCTCTTAACA TGCAGCTTGT GTGAGCTCAA AGACCCTTCG TTCTTTAACC
23151 ACGTTCTTGA AATCAGGGTC CCCAACTCAA TCCCAGAAAA GCCTAATATA
23201 CCTAGGGGCT GAGGCCTGTG CAGTCTGTAG CTGGGGCCTC TAACCACCAT
23251 AGCCTCTAAC CACCATAGCC TCTAACCACC ATAGCCTCTA ACCACCCAGG
23301 CAAGAAGCAG CCTTCCCTAA CTTCTAATTA TTCCCAGACA ACAGGCTACC
23351 CCAAAACCCC TAACAGTGCC AGAATAAGGC ATTTCTCTAT TGTTTTCAGG
23401 GGGCCTATGG CTAAATCAAA TTAACCTACC CCGCATAGGG GCTGGACTCT
23451 ACAAATAGAA CTTCACCCAA GGGGGTGGGG CCTTGTGGGA TCTCTGAGCC
23501 TGAAGGCCTG CCAACTCTCT GCCTCCAACA AAGTGGGTAC TAGGCTCCCT
23551 TTCCTGGGGA CCCACTTGCC AGCTGTTGGT GGATGAGCAA GAGACCTTGC
23601 TTATTAGAAA CAAATTAAAA AACAAAACAA AGCAACTAA
```

Appendix 2

Brain penetrance of CHDI194500 as assessed by Pharmidex Pharmaceutical Services Ltd. Reproduced with permission from the CHDI Foundation:

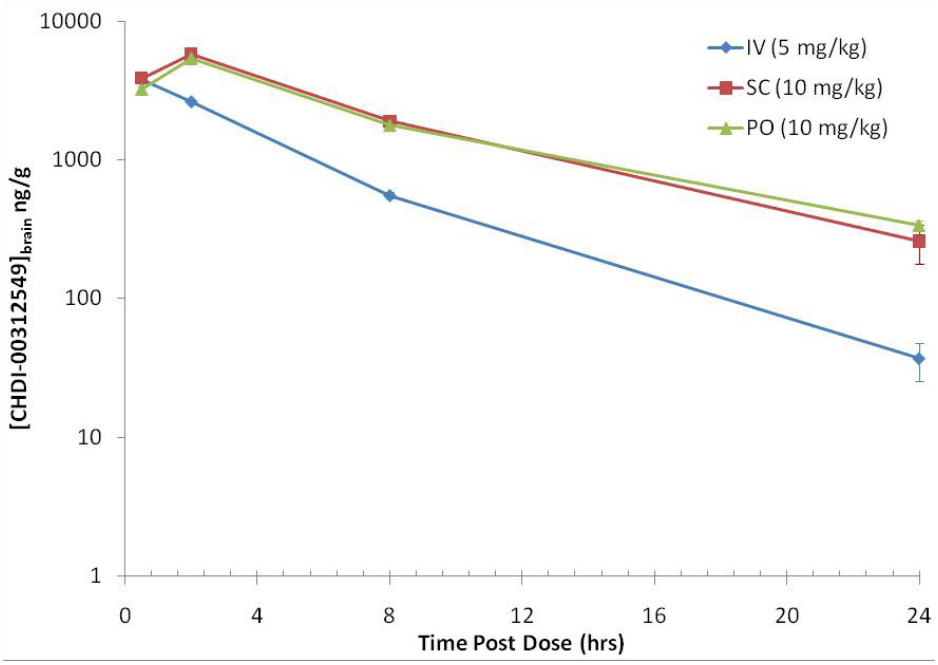

Brain penetrance of CHDI194500 following intravenous (IV), subcutaneous (SC) or oral gavage (PO). Male, 6-7 weeks old C57Bl6 mice were dosed with 5 mg/kg (IV) or 10 mg/kg (SC and PO) of CHDI194500 and brains were harvested at 0.5, 2, 8 and 24 h after compound administration. Concentration of CHDI194500 in the brain was measured by LC/MS/MS. Data obtained from CHDI Foundation in a report dated to 03/08/2009.

Determination of SIRT2 IC_{50} value CHDI194500 in an *in vitro* assay performed by Cerep. Reproduced with permission from the CHDI Foundation.

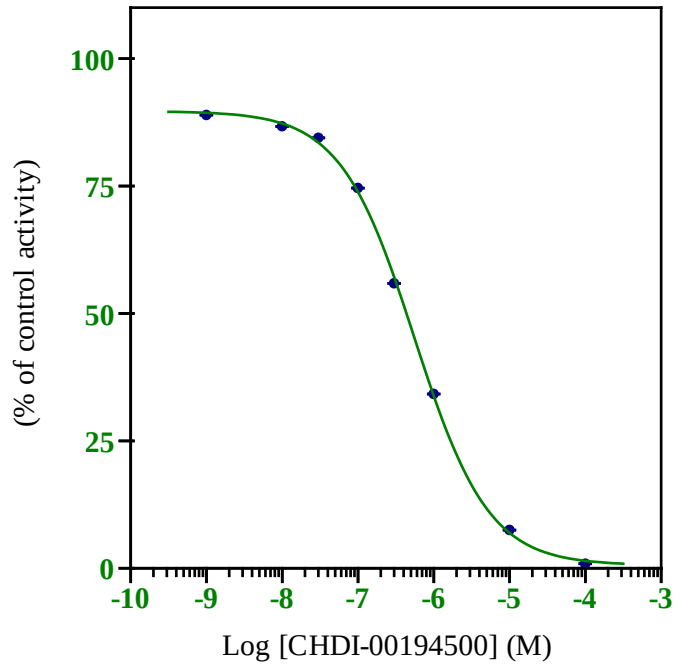

Dose-response curve showing activity of recombinant human **SIRT2** towards a fluorogenic substrate in presence of increasing CHDI19500 concentrations. 50% inhibition (IC_{50}) was achieved at concentration of **560 nM for SIRT2**. Data obtained from CHDI Foundation in a report dated to 06/08/2009.

Determination of SIRT1 IC_{50} value CHDI194500 in an *in vitro* assay performed by Cerep. Reproduced with permission from the CHDI Foundation.

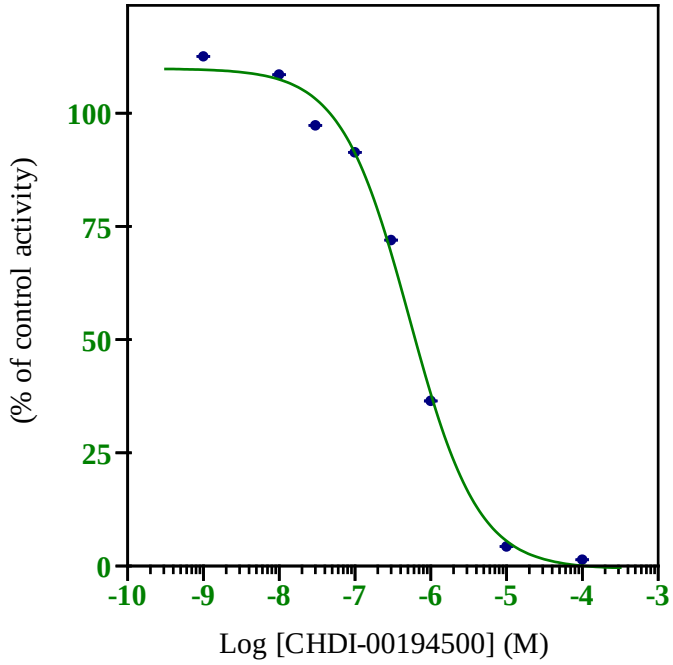

Dose-response curve showing activity of recombinant human **SIRT1** towards a fluorogenic substrate in presence of increasing CHDI19500 concentrations. 50% inhibition (IC_{50}) was achieved at concentration of **530 nM for SIRT1**. Data obtained from CHDI Foundation in a report dated to 06/08/2009.